THE UNIVERSITY
of EDINBURGH

Immune regulation induced by apoptotic cells in health and in systemic lupus erythematosus (SLE)

Joanne Elizabeth Simpson

Thesis submitted for the degree of Doctor of Philosophy

University of Edinburgh

2016

Abstract

Systemic lupus erythematosus (SLE) is a chronic autoimmune disease where failure to remove apoptotic cells, due to a defect in phagocytic cells, or deficient opsonisation, leads to secondary necrosis and the release of DNA and chromatin. The nuclear constituents from apoptotic cells are targeted by autoantibodies, which form immune complexes. Immune complex-mediated TLR9 activation of plasmacytoid dendritic cells (pDCs) and subsequent secretion of interferon (IFN-α) is thought to drive inflammation in SLE. It is currently believed that pDCs do not normally respond to apoptotic cells, as self-DNA is hidden from TLR9. However, DNA and chromatin expressed on membrane bound apoptotic bodies is essential for inducing IL-10 secreting regulatory B cells through TLR9 stimulation. The overall objective of this thesis was to understand how apoptotic cells influence immune responses in health and in patients with SLE.

Splenic mouse pDCs were activated with the synthetic TLR7 agonist R848 and TLR9 agonists CpGB and CpGA and were co-cultured with apoptotic cells, or with freeze-thawed necrotic cells. PDCs co-cultured with apoptotic cells down-regulated the expression of CD40 and CD86. When pDCs were activated by R848 or CpGB, IL-10, IFN-γ and IL-6 secretion was significantly induced in the presence of apoptotic cells. PDCs so cultured induced T cells to secrete immune-regulatory IL-10. In contrast, co-culturing apoptotic cells with pDCs activated by CpGA, augmented IFN-α secretion. These cytokine responses by pDCs were only stimulated by DNA on whole apoptotic cells; not by free nucleic acids derived from necrotic cells.

This data demonstrates that the inflammatory context in which pDCs sense whole apoptotic cells is crucial to determining the threshold of tolerance to apoptotic self. It questions the perception that pDCs see all apoptotic cells and their necrotic cellular debris as dangerous and suggests that there may be something intrinsically different about SLE apoptotic cells, which causes inflammation. SNPs near ATG5, a protein of the cell survival pathway autophagy, have been linked to SLE susceptibility, but

the role of autophagy in SLE pathogenesis is unclear. We hypothesised that dysfunctional autophagy is linked to abnormal apoptosis of SLE lymphocytes.

Western blotting revealed that ATG5-ATG12 protein complex expression was significantly reduced in SLE lymphocytes and they failed to convert LC3-I to LC3-II, the hallmark of a functioning autophagy pathway, which caused accelerated secondary necrosis. Apoptotic SLE lymphocytes had an impaired ability to stimulate IL-10 secreting regulatory B cells and they induced pro-inflammatory cytokine secretion by monocyte-derived macrophages. Phagocytosis of apoptotic SLE lymphocytes by healthy macrophages was also impaired; however this was independent of ATG5 protein expression. The novel findings of this thesis suggest SLE apoptotic lymphocytes are intrinsically pro-inflammatory, which may be caused by diminished autophagy leading to an inability of lymphocytes to correctly execute apoptosis. Furthermore, inefficient clearance of SLE apoptotic cells results from a defect in the apoptotic cell, rather than the phagocytic cell.

Lay summary

In our bodies millions of cells die naturally every day by a regulated process called apoptosis. Apoptotic cells must package their inner contents, including genetic material called DNA and chromatin, in to small membrane enclosed apoptotic bodies. This is important to ensure that apoptotic cells are quickly removed by being eaten by immune cells called phagocytes, and it is also essential for actively inducing immune cells to make proteins called anti-inflammatory cytokines, such as interleukin (IL)-10. In the complex disease systemic lupus erythematosus (SLE), it is thought that the phagocytes are unable to clear away apoptotic cells. The apoptotic cell membrane then breaks apart and the body's immune system mounts a self-inflammatory attack against the freely released DNA and chromatin.

A small population of immune cells, the plasmacytoid dendritic cells (pDCs), are key drivers of inflammation in patients with SLE. PDCs are specialised to respond to genetic material from virus infections by making lots of the pro-inflammatory cytokine interferon (IFN)-α. It is considered that pDCs do not usually respond to apoptotic cell-derived DNA and chromatin because the receptors required to do so are "hidden" inside the cell. However, in SLE, pDCs are activated to make IFN-α by self-DNA and chromatin released from apoptotic cells because it is attached to antibodies. In this thesis I wanted to find out if and how pDCs normally respond to apoptotic cells.

Here I showed that activated mouse pDCs were stimulated to secrete the anti-inflammatory cytokine IL-10, and they induced immune cells called T cells to produce IL-10, in response to DNA from whole apoptotic cells, but not from apoptotic cells that were broken apart. Whereas when pDCs were co-activated with a viral mimic, the secretion of IFN-α, but not IL-10, was increased by apoptotic cell-derived DNA. This suggests that the inflammatory environment in which pDCs sense apoptotic cells is important for determining the level of tolerance to apoptotic self. These findings also call in to question the idea that pDCs see freely released DNA as

dangerous, and it suggests that inflammation might be caused by the way that SLE cells die.

It is known that the cell survival pathway (called autophagy) is linked to SLE, but it is not clear what role autophagy plays in the disease. Here I found that SLE lymphocytes (T cells and B cells) isolated from the blood of SLE patients expressed less of the essential autophagy protein, ATG5, compared to healthy lymphocytes and this resulted in malfunctioning autophagy. As a result, SLE lymphocytes died rapidly and the cell membrane quickly began to break apart. SLE phagocytes had the same ability as healthy phagocytes to eat healthy apoptotic cells; however the ability of both healthy and SLE phagocytes to eat SLE apoptotic cells was significantly reduced. This indicates that the elimination defect in SLE may originate from the apoptotic cells, rather than as a result of dysfunctional phagocytes. Although less SLE apoptotic cells were eaten, they induced a pro-inflammatory response by the phagocytes.

The data in this thesis suggests that pDCs can generate an anti-inflammatory response to apoptotic cell-derived DNA, but this is prevented in the context of inflammatory stimuli. SLE lymphocytes die abnormally, and this appears to be caused by a defect in the autophagy pathway. Importantly, although SLE phagocytes function normally, SLE apoptotic cells fail to be removed.

Declaration

I declare that this thesis has been composed by myself and describes my own research unless where acknowledged in the text. No part of this thesis has been submitted for any other degree or professional qualification.

Signed…… **Date**…….

Joanne E. Simpson

Acknowledgements

First and foremost I would like to thank my supervisor, Mohini Gray, who for over three years has been committed to helping me succeed. Her inspiring attitude and thoughtful advice have kept me motivated throughout my PhD, even when experiments didn't go to plan! I am extremely grateful to Mohini and Dr Nicole Amft for encouraging many of their SLE patients to donate blood, and to the nurses who have taken time during the busy clinic to take the blood. Without them most of this thesis would not have been possible.

I would also like to thank Katherine Miles, who taught me in the lab, listened to my never-ending questions, and was always willing to help when I needed an extra pair of hands. Katherine also deserves thanks for doing the patient blood preps while I have been writing this thesis (sorry about the late nights!) and for providing the data in Figure 5.9. Thanks also to the past, present, and 'honorary' members of the PIG lab for making long days in the lab more bearable and for general advice.

Many thanks to Roisin MacMahon for helping with experiments in chapter three during her immunology honours project, and Prerana Hudder for determining the SELENA-SLEDAI scores of some of the SLE patients during her medical elective placement. I am appreciative of the Flow lab, Shonna, Will, and Fiona, for spending several hours at a time flow sorting the cells used in this thesis. I would like to thank Dr Simon Talbot for providing influenza virus, and Alan Ross and Kostas Kotzamanis for taking the time to show me how to propagate the murine cytomegalovirus and to help plan the experiments. Thanks also to Steve Mitchell for preparing the samples for scanning and transmission electron microscopy.

I am grateful of the Medical Research Council (MRC) for funding my PhD.

Most importantly, a huge thank you to my Mum, Dad, Adam, and Ben for their continuing support and encouragement.

Contents

List of Figures

Chapter 1 Introduction

Chapter 3 Results

Chapter 4 Results

Chapter 5 Results

List of Tables

Abbreviations

ANA	Anti-nuclear autoantibodies
AnV	Annexin V
ATP	Adenosine triphosphate
BCR	B cell receptor
BDCA	Blood dendritic cell antigen
BH	Bcl-2 homology domain
CAD	Caspase activated DNase
CARD	Caspase recruiting domain
cDC	conventional dendritic cell
CpG	Cytosine phosphate Guanine
DAMPs	Damage-associated molecular patterns
DISC	Death inducing signalling complex
DMARD	Disease-modifying antirheumatic drug
ds	Double stranded
EAE	Experimental autoimmune encephalomyelitis
EBV	Epstein Barr virus
ER	Endoplasmic reticulum
FACS	Fluorescence-activated cell sorting
FCS	Fetal calf serum
GWAS	Genome wide association studies
h	hour
HCQ	Hydroxychloroquine
HMGB1	High mobility group box 1
iBMK	Immortalised baby mouse kidney epithelial cell
IDO	Indoleamine 2,3 dioxygenase
IFN	Interferon
Ig	Immunoglobulin
IL	Interleukin
IRF	Interferon regulatory factor
ISS	Immuno-stimulatory sequences

KO	Knockout
LAP	LC3-associated phagocytosis
LC3	Microtubule-associated protein light chain 3
LPC	Lysophosphatidylcholine
LPS	Lipopolysaccharide
MACS	Magnetic-activated cell sorting
MCMV	Murine cytomegalovirus
mDC	Myeloid DC
MFG-E8	Milk fat globule EGF-factor 8
MHC	Major histocompatibility complex
min	minutes
MOI	Multiplicity of infection
MOMP	Mitochondrial outer membrane permeabilisation
MZ	Marginal zone
NAO	Nonylacridine orange
NETs	Neutrophil extracellular traps
OVA	Ovalbumin
PAMPs	Pathogen-associated molecular patterns
PBMCs	Peripheral blood mononuclear cells
pDC	Plasmacytoid dendritic cell
PDCA-1	Plasmacytoid dendritic cell antigen-1
PGN	Peptidoglycan
PI	Propidium Iodide
PS	Phosphatidylserine
PtdE	Phosphatidylethanolamine
RA	Rheumatoid arthritis
RAGE	Receptor for advanced glycation endproducts
RNP	Ribonucleoprotein
ROCK-1	Rho-associated kinase 1
ROS	Reactive oxygen species
SEM	Standard error of the mean

SLE	Systemic lupus erythematosus
Sm	Smith
SNP	Single nucleotide polymorphisms
SS	Sjogren's syndrome
ss	Single stranded
TGF-β	Transforming growth factor beta
Th	T helper cell
TIM	T cell immunoglobulin mucin domain
TLR	Toll-like receptor
TNF-α	Tumour necrosis factor alpha
Treg	Regulatory T cell
UV	Ultraviolet
WT	Wild type

Chapter 1 Introduction

The immune system has evolved a complex network of cells consisting of the innate (nonspecific) and adaptive (specific) arms, which work together to remove infectious pathogens and restore homeostasis. It is important that immune cells distinguish "self" from "non-self" to prevent destructive inflammation. The process of cell death by apoptosis is tightly regulated to ensure that the immune system does not respond aberrantly to self. For that reason, despite the presence of millions of apoptotic cells in the body at any one time, their occurrence normally goes unnoticed due to the safe packaging of self antigens onto membrane bound apoptotic bodies, their rapid disposal, and the anti-inflammatory immune response that ensues. Yet, certain chronic inflammatory disorders, such as systemic lupus erythematosus (SLE), occur in response to apoptotic cells. SLE is caused by a combination of complex genetic and environmental interactions, and it is considered that the failure to remove apoptotic cells before they become secondarily necrotic is key to driving this autoimmune disease. The current understanding of immune regulation induced by apoptotic cells in health and in SLE and conflicting ideas are discussed in more detail in this chapter.

1.1 Apoptotic cell death

1.1.1 Morphology of apoptotic cells

Apoptosis, first described by Kerr *et al.* in 1972[1], is a process of programmed cell death, which is essential for development, cell turnover, and maintaining immune homeostasis. In the 1990s it was discovered that apoptosis is an active process, requiring energy in the form of adenosine triphosphate (ATP)[2-5]. The energy-dependent morphological changes that distinguish apoptotic cells include cell shrinkage, chromatin condensation, DNA fragmentation, and maintenance of cell membrane integrity[1]. During the final stages of apoptosis the cell clusters its intracellular material, including DNA and ribonucleoproteins (RNP), on to the cell surface and subsequently dismantles, releasing these packages as small apoptotic bodies[6]. This is in contrast to necrotic cell death, where the organelles become

enlarged and the membrane becomes permeable, allowing the release of intracellular components in an inflammatory way[7].

1.1.2 Extrinsic and intrinsic apoptotic pathways

There are two mechanisms of apoptosis initiation, the extrinsic (death receptor) apoptotic pathway and the intrinsic (mitochondrial) apoptotic pathway (Reviewed in reference[8]). These pathways involve apoptosis-associated caspases that either initiate (caspases 8 and 9) or execute (caspases 3, 6, and 7) cell death. Since caspases are initially produced as proenzymes, their proteolytic function is exerted following a cascade of molecular events that trigger caspase activation (Figure 1.1).

The initiator pro-caspases contain a pro-domain, such as the caspase recruiting domain (CARD) in caspase 9 and the death effector domain (DED) in caspase 8, which interact with polyprotein complexes required for their clustering and activation[8]. The death-inducing signalling complex (DISC) is formed following ligation of the extrinsic death receptors, such as Fas receptor by FasL, or TNFR1 by TNF-α, which form a trimer leading to the recruitment of adaptor proteins FADD and TRADD, respectively, and association with pro-caspase 8[8]. Following activation of the intrinsic pathway the apoptosome is assembled when cytochrome *c* released from mitochondria binds to apoptotic protease-activating factor 1 (Apaf-1) and associates with pro-caspase 9[8].

The Bcl-2 family of proteins regulate the mitochondrial apoptosis pathway by controlling mitochondrial outer membrane permeabilisation (MOMP)[9]. These proteins interact via the Bcl-2 homology (BH) domains BH1-4. Pro-apoptotic proteins that contain only the BH3 domain, Bim, Bid, and Bad, are activated by stimuli such as DNA damage[9]. Bid is also activated by caspase 8, thereby linking death receptor pathway activation and the mitochondrial pathway[10]. The BH3-only proteins incite cell death by binding to the anti-apoptotic Bcl-2 family proteins, such as Bcl-2, Bcl-X_L, Bcl-W. This triggers the release of the sequestered activated pro-

apoptotic Bax and Bak[11,12], which induce MOMP thus permitting the escape of cytochrome *c* and committing the cell to dying.

Following maturation of the initiator caspases they cleave and activate the executioner (effector) caspases. Once activated, executioner caspases can cleave and activate other executioner caspases, hence resulting in positive feedback and maturation of all apoptosis-associated caspases irrespective of the initial stimulus[8]. Many intracellular targets linked to the unique morphology of apoptotic cells are cleaved by active caspases 3 and 7. DNA fragmentation occurs when the effector caspases cleave the inhibitor of caspase-activated DNase (CAD) thus releasing CAD and allowing it to translocate to the nucleus[13]. Chromatin condensation and cell rounding is caused by caspase-mediated cleavage of p21 activated protein kinase 2 (PAK2)[14,15]. Caspase-activated Rho-associated kinase 1 (ROCK-1) facilitates contraction of the actin-myosin cytoskeleton thus initiates cell membrane blebbing[16,17].

Another key identifier of apoptotic cells is the extracellular exposure of the membrane phospholipid phosphatidylserine (PS), which is constitutively internalised on viable cells. Transfer of PS from the cytoplasmic leaflet of the plasma membrane to the external side was initially described as a caspase-independent event[18]. However, recently it has been shown that PS exposure requires caspase-mediated inactivation of phospholipid flippase, which normally transfers PS from the outer to the inner leaflet[19].

After the transient process of cell membrane blebbing and in an independent event, apoptotic cells disassemble into apoptotic bodies, which are released from the dying corpse. It has recently been discovered that blocking pannexin channels in the membrane of T cells and monocytes results in the release of a string of apoptotic bodies, termed apoptopodia[20,21]. Interestingly the nuclear contents were excluded from the apoptopodia released from monocytes by this mechanism[21]. Breaking apart of the nuclear contents involves cytoskeleton remodelling[16,22], yet it is not known

how cells package intracellular contents, including DNA and chromatin, into membrane-bound apoptotic bodies. Furthermore, it is not completely understood why apoptotic cells release small bodies from their corpse, although it is speculated that this may increase the efficiency of apoptotic cell clearance[23].

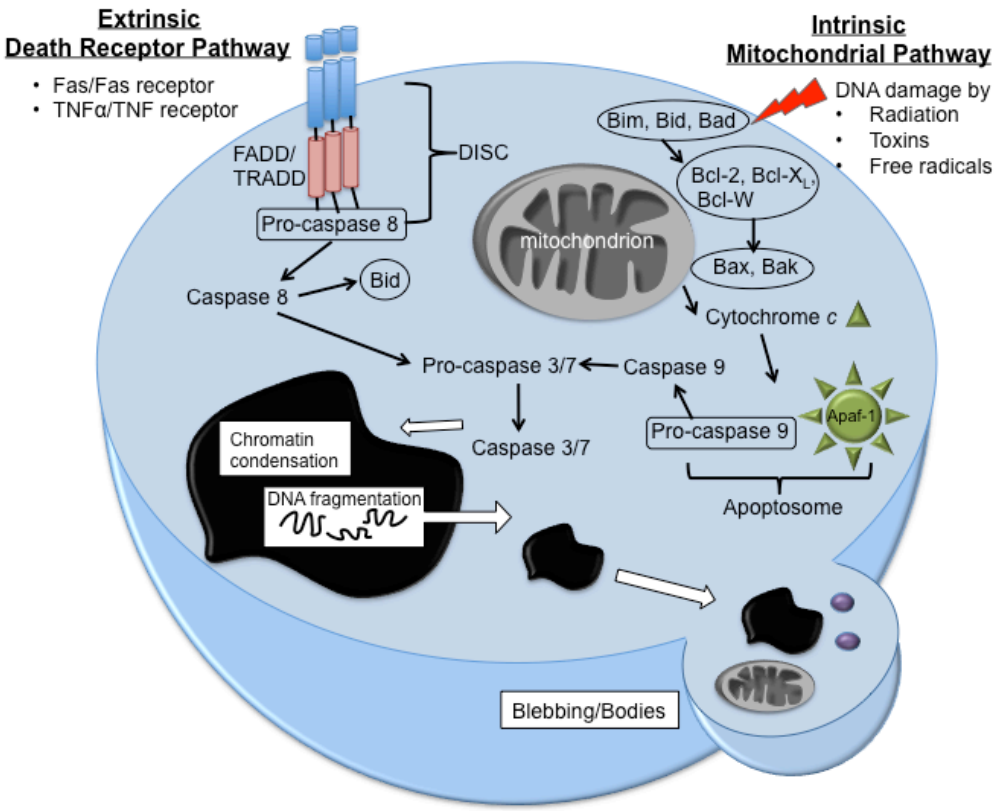

Figure 1.1. The extrinsic and intrinsic apoptosis pathways.

An overview of the caspase-activation cascade triggered following activation of death receptors (extrinsic pathway) and mitochondrial release of cytochrome *c* (intrinsic pathway). Activation of the initiator caspases 8 and 9 leads to activation of the effector caspases 3 and 7, which cleave many proteins to induce chromatin condensation, DNA fragmentation, and membrane blebbing.

1.1.3 **Apoptotic cells regulate the immune response**

1.1.3.1 Phagocytosis of apoptotic cells

Around a billion cells die by apoptosis in the body each day, yet apoptotic cells are rarely seen in healthy tissue histology[24] because professional phagocytes, such as macrophages, and local phagocytes, such as neighbouring epithelial cells, rapidly remove apoptotic cells from the environment. Apoptotic cells actively promote their own clearance, in addition to inducing a non-phlogistic response by the phagocytes that engulf them. This is essential for maintaining self-tolerance.

Apoptotic cells release "find-me" factors and produce "eat-me" signals in order to be located and recognised by professional mononuclear phagocytes[25] (Figure 1.2). The "find-me" chemotactic factors include the nucleotides ATP and UTP[26], the lipids lysophosphatidylcholine (LPC)[27] and sphingosine-1-phosphate (S1P)[28], and the classical chemokine CX_3CL1 (fractalkine)[29]. Apoptosis effector caspases mediate the release of LPC from the membrane through activation of phospholipase A2[27], ATP/UTP through pannexin-1 membrane channels[30], and CX_3CL1[29]. These attractants then signal through G-protein coupled receptors on the phagocytes; the nucleotides signal through $P2Y_2$[26], LPC ligates G2A[27], and CX_3CL1 acts through its receptor CX_3CR1[29].

Neutrophils are also professional phagocytes and they are the critical first line innate defence for mounting an inflammatory attack against invading pathogens[31]. However, although neutrophils can respond to the "find-me" chemoattractants, they are rarely found at sites of apoptotic cells *in vivo*[7]. This is because apoptotic cells also secrete the "keep out" signal, lactoferrin, an anti-inflammatory protein that binds to specific receptors on neutrophils[32]. Thus, apoptotic cells preferentially attract monocytes and macrophages to avoid inflammatory responses.

After the appropriate phagocytes are recruited, apoptotic cells are tethered to their surface then engulfed. This is facilitated by the "eat-me" signals that decorate the

apoptotic cell surface. There are many "eat-me" signals (Reviewed in references[25,33,34]) including the expression of oxidised low-density lipoprotein (oxLDL)-like sites, which bind to the scavenger receptor CD36[33]. The most commonly studied "eat-me" signal is PS, which can be recognised by phagocytes directly through T cell immunoglobulin mucin domain (TIM)-4, or stabilin 2[25]. PS is also indirectly recognised via bridging molecules, such as milk fat globule EGF-factor 8 (MFG-E8), or Gas-6, which bring the apoptotic cells to appropriate engulfment receptors on phagocytes, such as $\alpha_v\beta_{3/5}$, and MER, respectively[25]. Furthermore, complement proteins and antibodies opsonise apoptotic cells to mediate phagocytosis. For example, binding of the classical complement pathway protein C1q to the apoptotic membrane[35-37], or to IgM that has bound to the membrane[38] triggers phagocytosis through the C1q receptor, the CD91-calreticulin complex[33]. Although PS is essential for apoptotic cell uptake, knockout mouse studies have demonstrated that the combination of PS with other "eat-me" components is required to initiate phagocytosis[25].

An additional measure to flag up that apoptotic cells should be phagocytosed is the loss of "don't eat me" signals that are expressed on viable cells. This includes the loss CD47, which normally interacts with macrophages by binding signal regulatory protein-α (SIP-α), and inactivation of CD31, which subsequently binds to phagocyte-expressed CD31[7].

Following receptor-mediated uptake, phagocytes must degrade the apoptotic cell cargo by step-wise maturation of phagosomes involving acidification and fusion with lysosomes (reviewed in reference[39]). It has recently been demonstrated that apoptotic cell opsonins regulate the intracellular processing of phagocytosed apoptotic cells[40,41]. C3 delays phagosome maturation by prolonging apoptotic cells in endosomes and consequently enhances antigen loading on to major histocompatibility complex (MHC) class II for presentation to $CD4^+$ T cells[40]. Whereas, MFG-E8 mediates phagosome trafficking to lysosomes thus avoiding

apoptotic fragments outwith lysosomes being cross-presented by MHC class I to $CD8^+$ T cells[41].

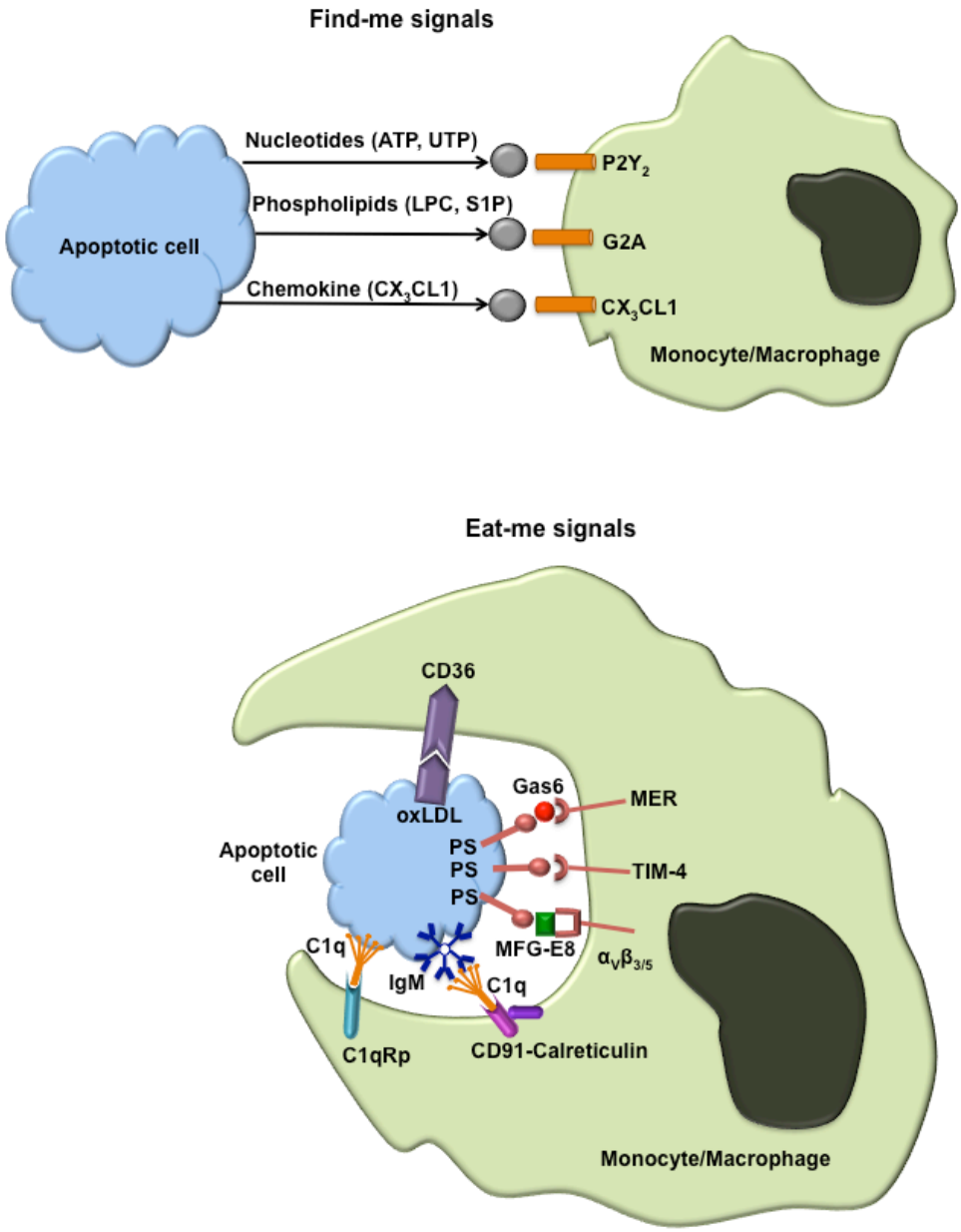

Figure 1.2. "Find-me" and "eat-me" signals that mediate apoptotic cell phagocytosis.

An overview of the chemotactic factors released by apoptotic cells to attract mononuclear professional phagocytes. The phagocytes then engulf the apoptotic cells following interactions directly with the ligands displayed on the apoptotic cell surface, such as phosphatidylserine (PS) and oxLDL-like sites, or indirectly via adaptor proteins, such as Gas-6, MFG-E8, IgM, and C1q, that have bound to the apoptotic cell surface. Adapted from Gregory and Pound (2010)[42].

1.1.3.2 Anti-inflammatory responses induced by apoptotic cells

Apoptotic cells induce an anti-inflammatory phenotype in macrophages, which is reported to require cell contact and is independent of phagocytosis[43]. Contact with apoptotic cells inhibits the synthesis of pro-inflammatory cytokines, for example tumour necrosis factor (TNF)-α and interleukin (IL)-1β, in response to inflammatory stimuli, such as lipopolysaccharide (LPS)[44,45]. This is likely to occur following the secretion of anti-inflammatory transforming growth factor (TGF)-β secretion[46]. TGF-β is a multifunctional cytokine, which is initially secreted in latent form through association with two proteins, latent TGF-β-binding protein and latency-associated protein. It is activated in response to apoptotic cell interactions with the α_V containing integrins during phagocytosis.

Through binding to TGF-β receptor II (TGF-βRII), TGF-β regulates the proliferation and differentiation of many innate and adaptive immune cells, including promoting the survival of natural regulatory T cells[47]. Additionally, TGF-β inhibits the expression of the co-stimulatory molecules CD86 and CD40 [48], which are normally upregulated on phagocytes following the uptake and processing of antigens onto MHC. Consequently, T cells that recognise apoptotic cell-derived peptide-MHC complexes in the absence of co-stimulation are induced into an anergic state, or into regulatory T cells (Tregs)[48].

Macrophages located in the marginal zone (MZ) of the spleen are stimulated to secrete the anti-inflammatory tryptophan catabolising enzyme indoleamine 2,3 dioxygenase (IDO) by apoptotic cells being filtered from circulating blood[49]. Furthermore, although apoptotic (and necrotic) human neutrophils are commonly found at sites of inflammation, these dying cells release anti-inflammatory alpha-defensins to inhibit pro-inflammatory macrophages[50]. This mechanism is important for restoring the inflammatory environment back to normal, as indicated by alpha-defensins reducing the severity of a mouse model of peritonitis[50].

Apoptotic cells also interact with non-phagocytic cells to induce regulation. For example, the innate-like, weakly self-reacting MZ and B1 B cells express high levels of TIM-1[51], a PS-binding glycoprotein from the same family as TIM-4. In mice, when apoptotic cells bind to TIM-1 this induces anti-inflammatory signalling resulting in the secretion of IL-10 [52], which has been shown to reduce the severity of experimental autoimmune encephalomyelitis (EAE), the mouse model of multiple sclerosis[53]. TIM-1 potentially has regulatory function in human B cells too[54]. IL-10-secreting MZB and B1 B cells are also induced following TLR9 activation by apoptotic cell derived DNA[55]. Regulatory B cells induced in this way protect mice from developing severe collagen-induced arthritis (CIA) through the induction of IL-10 secreting antigen specific $CD4^+$ T cells[55,56].

IL-10 is a potent immunosuppressive cytokine, which signals through a heterodimeric receptor (IL-10Rα and β). It acts by down regulating inflammatory cytokine production by many cell types including T helper cells, monocytes, and neutrophils, and it inhibits antigen presentation by monocytes and DCs[57].

1.1.4 **Apoptotic cells prevent autoimmunity**

In a healthy immune system, the response to apoptotic cells maintains homeostasis during the extensive turnover of cells and resolves inflammation to minimise tissue damage. The anti-inflammatory reaction induced by apoptotic cells is not always beneficial to the host, as apoptotic cells can promote tumour progression[58]. Nevertheless, the importance of the immunosuppressive response is clearly demonstrated when the removal of apoptotic cells is faulty. This causes chronic inflammation in the lungs of patients with chronic obstructive pulmonary disease (COPD)[59], whereas the excess of apoptotic cells in genetically susceptible people causes SLE, an autoimmune disease affecting multiple tissues and organs. In this thesis I was particularly interested in comparing immune regulation induced by apoptotic cells from healthy donors and patients with SLE.

1.2 Systemic lupus erythematosus

1.2.1 Symptoms and serology

SLE is a chronic multisystem autoimmune disease with a female to male ratio of 9:1, predominantly affecting females of childbearing age. The symptoms and organ presentation can vary greatly between patients, ranging from mild, such as the characteristic butterfly rash across the face, alopecia, and joint pain and swelling, to more severe where inflammation causes potentially life-threatening damage to the kidneys, heart, or brain.

Autoreactive B cells secrete anti-nuclear IgG autoantibodies (ANA), which are characteristic of SLE and are detected in sera during diagnostic tests. ANA include anti-dsDNA, chromatin, RNP, Smith (Sm; recognise the core units of small nuclear RNP), Ro and La antibodies. Although anti-DNA and anti-Sm antibodies are specific to SLE, anti-Ro and anti-La antibodies are commonly found in Sjogren's syndrome (SS), a closely related autoimmune disease affecting the exocrine glands, which can develop in combination with SLE. The anti-phospholipid antibodies, lupus anti-coagulant and anti-cardiolipin, are also found in approximately half of SLE patients, which may cause thrombosis and complications during pregnancy. Furthermore, the presence of antibodies specific for the first component of the classical complement pathway, anti-C1q antibodies, has long been associated with lupus nephritis[60-62].

The aetiology of SLE is still unknown, but the onset of disease is most likely caused by a combination of genetic and environmental factors[63]. Environmental factors that are linked to SLE include exposure to ultraviolet (UV) light and virus infections [63]. For example, antibodies generated against Epstein-Barr virus (EBV) derived protein EBV nuclear antigen (EBNA)-1 cross-react with the autoantigens Ro and Sm[64], indicating a role for molecular mimicry in SLE. The concordance rate of SLE in monozygotic twins is ten-fold higher than dizygotic twins[65], suggesting that there is a genetic cause. Genome-wide association studies (GWAS) have identified more than 50 genes associated with SLE (reviewed in reference[66]). These can be sub-divided

into groups of genes associated with lymphocyte activation (including PTPN22, STAT4, and BANK1), cross-talk between leukocytes (such as HLA-DR2, HLA-DR3, and OX40L), innate immune signalling (such as IRAK1 and IRF7), and removal of apoptotic cells (in particular C1q and FcRs)[66]. Recently, single nucleotide polymorphisms (SNPs) in genes associated with the autophagy pathway, including Atg5, have been linked to SLE[67] and the relevance of this will be discussed later in this chapter (section 1.4).

1.2.2 **Treatment of SLE**

Like many other autoimmune diseases there is no cure for SLE, therefore drugs are used to control the aberrant inflammation. Depending on how severe the symptoms are, SLE patients are currently treated with non-steroidal anti-inflammatory drugs (NSAIDs), corticosteroids, disease modifying anti-rheumatic drugs (DMARDs), such as hydroxychloroquine (HCQ) and methotrexate, and/or immunosuppressants, such as azathioprine, and mycophenolate mofetil. These available treatments are useful for controlling SLE symptoms by non-specifically dampening the inflammatory immune response. Due to the complex and heterogeneous nature of this autoimmune disease, it has proved difficult to develop new specific therapies.

Recently, belimumab has become the first FDA approved drug since the 1950s, and currently the only approved biologic therapy, for SLE treatment[68] following the results of two independent, but similarly designed phase III, double-blind, placebo-controlled trials[69,70]. Belimumab is a monoclonal antibody that targets B lymphocyte stimulator (BLyS; also termed B cell activating factor, BAFF), an essential factor for B cell survival and maturation. Therefore, neutralisation of soluble BLyS by belimumab induces the reduction in B cells, potentially eliminating autoreactive B cells, which rely more greatly on BLyS for survival[71]. Belimumab-treated SLE patients with active disease showed a significant improvement in clinical symptoms and fewer disease flares compared to those treated with placebo[69,70]. Belimumab therapy additionally resulted in a greater number of SLE patients being able to reduce their steroid dosage[69,70]. However, more than 40% of the SLE patients in the

clinical trials failed to respond to BLyS neutralisation[72] indicating that B cells are not the main influence of disease activity in a high proportion of cases. Furthermore, it remains to be investigated if belimumab is beneficial, or even safe, to treat patients with lupus nephritis or central nervous system lupus, as this subset of patients with severe SLE was excluded from the phase III trials.

Other promising biologics mainly targeting pro-inflammatory cytokines involved in SLE pathogenesis are discussed in section 1.2.4. Nevertheless, it would be ideal to specifically address the underlying cause of the disease, but this is not clearly known.

1.2.3 The current paradigm of SLE pathogenesis

1.2.3.1 Apoptotic cells are the primary antigen source in SLE

It is well established that apoptotic cells encompass the source of autoantigens to which SLE autoantibodies are targeted. Nuclear components, including DNA and RNP, and negatively charged phospholipids, such as PS, are exposed in clusters on the surface of apoptotic cells and bodies[6,73,74] and are the ligands for ANA and anti-phospholipid antibodies, respectively. Additionally, C1q bound to the surface of apoptotic cells is the ligand for anti-C1q antibodies[75]. Therefore, it is not surprising that apoptosis-inducing events, such as virus infection and exposure to sunlight, are associated with flares of disease symptoms.

Apoptotic cells are considered to become immunogenic in SLE due to the failure to rapidly remove the dying cells; therefore they eventually break apart, increasing the exposure of the accumulated nuclear components to the immune system[76]. It is reported that macrophages from SLE patients have an impaired ability to phagocytose apoptotic neutrophils[77] and apoptotic T cells[78]. The phagocyte defect may be caused by genetic alterations in phagocytic receptors. For example SNP rs1143679 in integrin-alpha(M) (ITGAM; CD11b), a component of complement receptor (CR)3 (CD11b/CD18), is a strong genetic risk factor (odds ratio 1.76) associated with SLE[67,79,80]. Heterozygous expression of this SNP, which is most

common in SLE patients, impairs CR3-mediated uptake of iC3b opsonised particles, including apoptotic cells by professional phagocytes[81].

Mouse models of SLE complement the reports that phagocytosis is dysfunctional in patients. Peritoneal macrophages from MRL/Mp and New Zealand black/white (NZB/W) F1 mice have defective phagocytosis of sterile inflammation-induced accumulation of apoptotic neutrophils[82]. Yet, clearance of IgG1 opsonised mouse RBCs was efficient, indicating that the defect was specific to the phagocytosis of apoptotic cells[82]. Conversely, the accumulation of systemically injected apoptotic cells in wild type mice is reported to induce the non-pathogenic generation of anti-ssDNA and anti-cardiolipin IgG antibodies, but not anti-dsDNA or other ANA[83]. This provides evidence that an accumulation of apoptotic cells is required in combination with disease-modifying genes in order for SLE to develop.

In addition to intrinsic defects in the phagocytic cells, the loss of opsonisation is also associated with impaired removal of apoptotic cells in SLE. The development of glomerulonephritis and an excess of apoptotic bodies in mice deficient in C1q demonstrates the importance of efficient removal of apoptotic cells by phagocytosis to prevent inflammation[84]. The severity of autoimmunity was influenced by C1q-deficiency on a 129/C57BL6 background[84], which express SLE susceptibility loci on chromosome 1[85]. This further supports the need for genetic risk factors to allow the break in tolerance to self-nucleic acids. In fact, although very rare, the majority of individuals who have inherited deficiencies in early components of the classical complement pathway, in particular C1q, develop SLE (reviewed in reference[86]).

Innate-like B cells (B1a and MZB subsets) express self-reactive BCRs and are activated to secrete natural IgM antibodies with specificities for apoptotic cell surface components, such as dsDNA, independently of T cell help[57]. In health, despite being self-reactive, innate-like B cells maintain tolerance to apoptotic cells through the secretion of anti-inflammatory IL-10 (discussed in section 1.1.3.2) and the protective role of natural IgM antibodies bound to apoptotic cells, which recruit

C1q thus promoting phagocytosis[38,57]. Self-tolerance is breached in SLE due to failure at conventional B cell tolerance checkpoints (reviewed[87]). Circulating $CD27^{high}$ plasma cells, which become autoreactive following somatic hypermutation, are elevated in SLE[88]. It is then assumed that reduced disposal of apoptotic cells, such as in the absence of C1q, causes the increased exposure of intracellular antigens, which are immunogenic to the autoreactive B cells[89].

1.2.3.2 Immune complexes in SLE

In the absence of effective removal, apoptotic cells become secondarily necrotic thereby switching what should be an anti-inflammatory response to an inflammatory response. Secondary necrosis is considered to result in the inflammatory release of danger associated molecular patterns, such as DNA and chromatin[90]. Furthermore, the binding of IgG autoantibodies to their nuclear autoantigens released from the broken apart apoptotic cells results in the formation of immune complexes, which are found circulating in SLE patient blood and are considered to drive inflammation.

Immune complexes deposit in the skin, joints and organs, where they cause inflammation through activation of the classical complement cascade. The C1 complex is activated when C1q binds to IgG in the immune complex and subsequently initiates activation of the C1r and C1s. The C1s enzyme then cleaves C2 and C4 into fragments that generate the C3 convertase (C4bC2a), which cleaves C3 to produce C3a and C3b. C3b acts as an opsonin, thus renders antigen susceptible to phagocytosis, and it also forms the C5 convertase by interacting with C4bC2a to cleave C5 into C5a and C5b[91]. C3a and C5a mediate inflammation by increasing vascular permeability and recruiting inflammatory macrophages, neutrophils and lymphocytes to the site of immune complexes[91]. The final step of the complement cascade is the formation of the membrane attack complex[92], a disruptive pore in the plasma membrane which is initiated by sequential binding of C5b to C6, C7, C8 and up to 16 C9 molecules[91]. Immune complex deposition in the glomeruli of the kidney is particularly detrimental, as this leads to nephritis and may result in irreversible

kidney damage. A low level of C3 and/or C4 in SLE patients is characteristic of an activated complement cascade and active disease[92].

RNP-IgG immune complexes also drive inflammation in SLE by activating neutrophils through FcγRIIa and TLR7 to undergo NETosis, a specific form of caspase-independent, reactive oxygen species (ROS)-dependent cell death[93]. NETotic neutrophils extrude DNA and decondensed chromatin mixed together with granular proteins such as the antimicrobial peptide LL37, in large web-like structures called neutrophil extracellular traps (NETs)[94]. Although these structures are an important component of innate immunity for entrapping and destroying pathogens[95], in recent years it has been discovered that NETs play a pathogenic role in SLE. NETs are normally destroyed by serum DNase1, yet this mechanism to rapidly remove a source of self-antigens does not function in some SLE patients and anti-dsDNA autoantibodies form immune complexes with the NETs, which deposit in kidney glomeruli[96]. Hence impaired clearance of NETotic neutrophils provides an additional source of immune complexes in SLE.

Previous investigations revealed that a circulating component of SLE patient blood was acting as an endogenous inducer of IFN-α secretion by plasmacytoid dendritic cells (pDC)[97]. The inducer of IFN-α could be mimicked by binding anti-dsDNA IgG antibodies to CpG-DNA[98]. It is now known that nucleic acids in complex with autoIgG made by B cells, or LL37 released by NETotic neutrophils activate pDCs to secrete IFN-α. FcγRII-mediated endocytosis is required for the induction of pDC IFN-α secretion by apoptotic cell-derived nucleic acids found in immune complexes with IgG[99-101]. Immune complexes also induce pDCs to secrete IL-6[93] and other pro-inflammatory cytokines including TNF-α and IL-12[102]. It is specifically SLE immune complexes that induce activation of pDCs due to the presence of self-DNA and RNP, as immune complexes found in the serum of other rheumatic diseases, such as RA, do not induce this response[101].

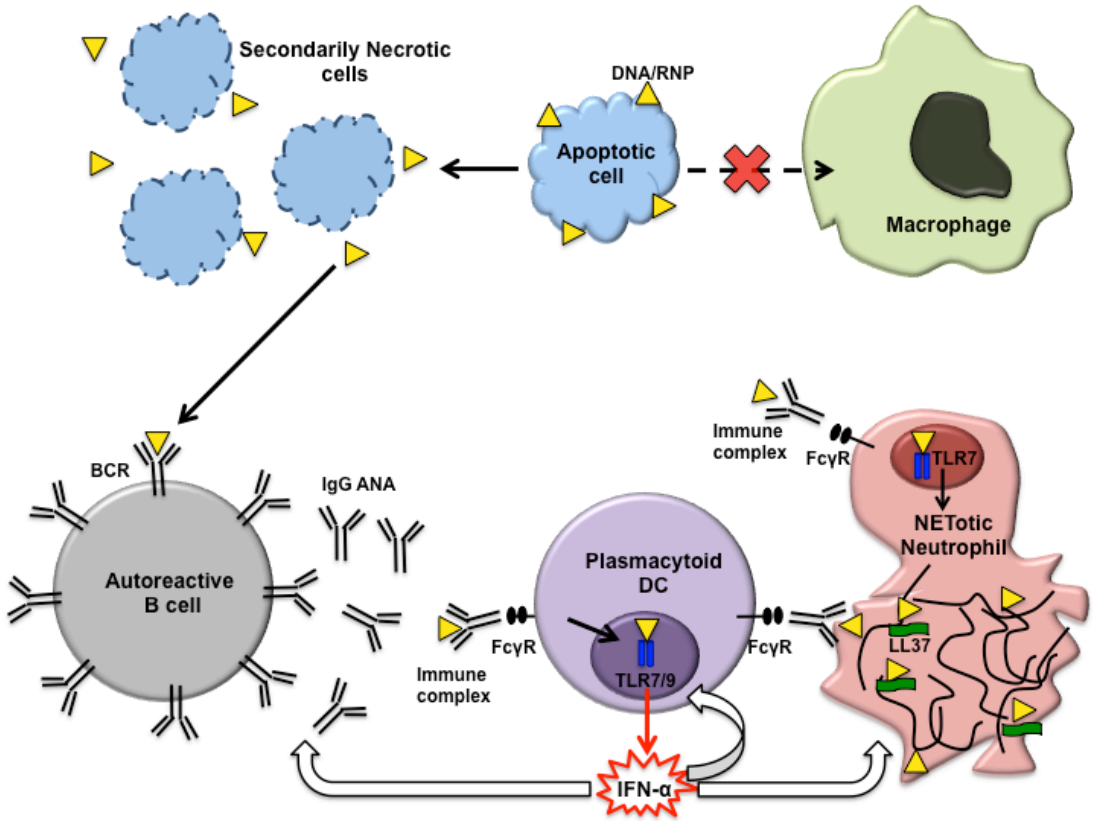

Figure 1.3. The current paradigm of SLE pathogenesis.

It is currently considered that impaired phagocytosis caused by dysfunctional phagocytes and loss of opsonisation results in the accumulation of apoptotic cells, which progress to secondary necrosis. The intracellular components that are normally clustered on the surface of apoptotic cells are released following secondary necrosis. Autoreactive B cells, which have escaped self-tolerance checkpoints, are stimulated by nuclear contents released from secondarily necrotic cells and differentiate into IgG antinuclear autoantibody (ANA)-secreting plasma cells. The binding of the ANA to nuclear antigens forms immune complexes, which stimulate pDCs to secrete IFN-α. This requires Fc receptor-mediated uptake to allow the self-nuclear components to reach TLR7 and TLR9. By the same mechanism, immune complexes also induce neutrophils to undergo NETosis thus releasing more self DNA available for ANA to bind, or already in complex with LL37, further driving IFN-α secretion by pDCs.

1.2.3.3 Are apoptotic cells really a danger signal?

It is accepted that the failure of phagocytes to quickly and efficiently remove apoptotic cells is detrimental due to the accumulation of secondary necrotic cells. Though it seems counterintuitive why a cell that has invested energy into dying by

apoptosis would naturally progress to becoming pro-inflammatory. However the data that supports this is inferred from studies that report on the pro-inflammatory nature of late apoptotic/necrotic cells utilising tumour cells[103], which are likely to express a fundamentally different complement of danger signals to primary cells. In addition studies using primary necrotic cells, that have not first undergone programmed cell death will release the danger signal high mobility group box 1 (HMGB1), in contrast to secondarily necrotic primary cells, in which HMGB1 is tightly associated with chromatin[104].

In fact it was published many years ago that late apoptotic cells fail to induce inflammatory responses[105,106], and early and late apoptotic cells induce the same signalling in macrophages, which is distinct from necrotic cells[107]. MZB and B1 B cells are induced to become anti-inflammatory in response to DNA expressed on early and late apoptotic cells, even in the presence of inflammatory PAMPs, such as LPS and PGN[55]. Therefore, it is unlikely that apoptotic cells and secondary necrotic cells are inflammatory in a healthy immune system. Perhaps in SLE, cells undergoing apoptotic death act as a danger stimuli due to an intrinsic defect caused by the underlying complex genetic nature of the disease.

1.2.4 IFN-α and the type I IFN signature

A high serum level of IFN-α compared to healthy individuals is reported in some SLE patients and this has been associated with disease activity[108]. However, elevated serum IFN-α is also found in healthy first degree relatives of SLE patients indicating that it might be a heritable trait that increases SLE susceptibility[108]. Nevertheless, it is considered that the immunomodulatory effects exerted by IFN-α are central to the pathogenesis of SLE. This is supported by reports of the development of reversible SLE symptoms in some patients administered with long-term IFN-α therapy to fight against viral infections and certain forms of malignancies[109,110].

There are 12 functional subtypes of IFN-α, which is part of the type I IFN family also including IFN-β, IFN-ε, IFN-κ and IFN-ω[108]. All type I IFNs signal through the

same receptor composed of two subunits, IFNAR1 and IFNAR2, yet they induce distinct biological responses due to different binding affinities[111]. IFNAR signals through Janus kinase (Jak)1 and tyrosine kinase (Tyk)2 with the subsequent formation of the signalling transducer and activation of transcription (STAT)1-STAT2 heterodimer. This is recruited to the nucleus where it binds to interferon regulatory factor (IRF)9 thus forming the IFN-stimulated gene factor 3 (ISGF3) complex, which induces the transcription of hundreds of IFN-inducible genes by interacting with IFN-stimulated response elements. A subset of patients with severe SLE have a type I IFN "signature", which is defined by up-regulated expression of IFN-α-induced genes in peripheral blood mononuclear cells (PBMC)[112,113].

However, the type I IFN signature in the autoimmune setting is not unique to SLE, as it is also correlated with disease activity and autoantibody levels in the closely related disease SS (reviewed in reference[114]). Furthermore, a small study has reported that an elevated baseline of type I IFN-induced genes in the peripheral blood of rheumatoid arthritis (RA) patients is associated with non-responders to rituximab therapy[115]. Conversely, the type I IFN signature in RA neutrophils indicates a good response to inhibitory TNF-α therapy[116]. Gene expression meta-analysis of SLE, SS, and RA studies found that these three connective tissue diseases share common type I IFN-induced genes[117]. Therefore, it suggests that the type I IFN signature may represent active disease activity.

IFN-α is an important anti-viral pleiotropic cytokine, which acts by directly interfering with virus replication and survival, in addition to linking innate and adaptive immunity. IFN-α induces the differentiation of monocytes into inflammatory antigen-presenting DCs[118], promotes B cell survival by inducing BAFF expression, and stimulates the differentiation of B cells into plasmablasts[119]. IFN-α also feeds back on neutrophils further driving NETosis and the release of immune complexes[93]. Therefore there is a positive feedback loop developed between immune complexes and IFN-α synthesis.

During virus infections, the IFN signature is normally transient due to tight regulation of IFN-α responses[120]. However, in SLE it is considered that chronic inflammation is driven by the excessive production of IFN-α by immune complex activation of pDCs and inadequate regulation due to genetic variations in components of IFN-α production, such as the transcription factor IRF7, and signalling, for example Tyk2[108].

Mouse models of SLE demonstrate that the role of IFN-α in disease pathogenesis is inconclusive. MRL$^{lpr/lpr}$ mice that do not express IFNAR1 develop worse disease[121], indicating that IFN-α signalling is protective. Conversely, deficiency of the IFNAR prevents autoantibody production and limits the severity of glomerulonephritis in the genetically susceptible SLE prone NZB mice[122], and the pristane-induced SLE-like disease[123]. Although pristane-induced SLE is the only model with an associated IFN signature[124], it is intriguing that the major source of IFN-α production in this model is not pDCs, but inflammatory (Ly6C^{high}) monocytes responding in a TLR7-dependent and immune complex-independent way[125].

Inhibiting IFN-α signalling either by targeting IFN-α or the IFNAR with biologics has been the subject of recent clinical trials (reviewed in reference[126]). A phase I clinical trial of the anti-IFN-α monoclonal antibody, sifalimumab, reported that it did not significantly improve clinical activity compared to placebo[127]. Similarly, a phase II trial of rontalizumab, a humanised antibody to IFN-α, failed to meet its primary and secondary endpoints[128]. Conversely, the anti-IFN-α humanised antibody AGS-009, resulted in partial reduction in type I IFN-induced genes during a small phase I trial[126]. The anti-IFNAR1 monoclonal antibody MEDI-546, almost completely inhibited the expression of type I IFN-induced genes in systemic sclerosis patients and is currently undergoing trials in SLE[126]. An additional mechanism is to broadly target IFN-α using an IFN-α kinoid, which is a complex of recombinant IFN-α and the immunogenic protein keyhole limpet haemocyanin[129]. In a recent phase I/II trial, IFN-α kinoid successfully induced T cell-dependent production of neutralising IFN-α antibodies and the reduction in the type I IFN signature, but did not benefit clinical

disease activity[129]. Long-term depletion of IFN-α may increase the risk of viral infections.

The disappointing results reported from clinical trials targeting IFN-α might be explained by a recent study, which found that the IFN signature associated with SLE is extremely complex and is not solely induced by IFN-α, but also by IFN-β and the type II IFN, IFN-γ[130]. Therefore, future studies will have to take into account the previously unidentified contribution of IFN-γ to SLE pathogenesis.

1.2.4.1 Other inflammatory cytokines in SLE

In addition to IFN-α, other inflammatory cytokines including IL-6, IL-17, and IL-18 are elevated in SLE patient serum and also contribute to the inflammatory pathogenesis. IL-6 is most commonly thought of as pro-inflammatory, yet in certain situations it exerts anti-inflammatory responses. For example, although IL-6 promotes inflammatory arthritis, it also induces IL-10 secreting regulatory B cells to subsequently dampen the inflammation[131]. In the context of SLE, IL-6, which is secreted by pDCs following TLR stimulation, may stimulate IgG autoantibody secretion by plasma cells differentiated by IFN-α[119]. In the MRL$^{lpr/lpr}$ mouse model of SLE, the absence of IL-6 delays the development of severe renal disease, indicating that IL-6 may be a promising therapeutic target[132], although the results of two recent phase II clinical trials using anti-IL-6 monoclonal antibodies, sirukumab and PF-04236921, have showed varying outcomes, with the severe risk of infection a major challenge[133].

The role of IL-17 in SLE has gained interest in the last few years due to reports that it is elevated in SLE serum, though there is currently no evidence to suggest that it correlates with disease activity[134]. CD4$^+$ T helper (Th)17 cells and double negative CD3$^+$ T cells, which are both elevated in SLE patient PBMCs, may be the source of IL-17 in SLE (Reviewed[134]). Differentiation of human Th17 cells requires IL-6, TGF-β, and IL-1β, whilst their maturation into pro-inflammatory cells is induced by IL-23[135]. Interestingly, TLR7-stimulated pDCs secrete IL-1β and IL-23, in addition

to IFN-α and IL-6, which promotes Th17 differentiation and maturation[136]. Furthermore, a pDC depletion study has reported that they regulate Th17-mediated inflammation in EAE by an unknown mechanism[137].

An additional source of IL-17 might be released from NETotic neutrophils in SLE skin lesions[138]. This is the predominant mechanism of IL-17 release in psoriasis[139], an autoimmune disease, which like SLE, is driven by immune complex-mediated induction of IFN-α by pDCs[140]. IL-17 plays a role in the immune response against extracellular pathogens by stimulating the secretion of antimicrobial peptides, pro-inflammatory cytokines, and chemokines to attract neutrophils. These functions, in addition to IL-17 stimulating autoreactive B cells to differentiate into antibody secreting plasma cells may contribute to inflammation in SLE[134]. IL-17 targeted therapy has not been investigated in SLE. However, blocking this cytokine with anti-IL-17 monoclonal antibodies (secukinumab and ixekizumab), or anti-IL-17 receptor monoclonal antibody (brodalumab) has been successful in other autoimmune diseases, in particular psoriasis[134].

Unlike IL-6 and IL-17, the secretion of the pro-inflammatory cytokines IL-1β and IL-18 requires two activation steps: the first signal (NFκB activation) stimulates the production of precursor proteins whilst the second signal (inflammasome stimulation) activates the caspase 1-mediated cleavage of the precursors to make active IL-1β and IL-18[141,142]. Inflammasomes are multiprotein innate immune receptors composed of NOD-like receptors (NLRs; such as NLRP3), or absent in melanoma (AIM)2, which contain a pyrin domain (PYD). The PYD interacts with apoptosis-associated speck-like protein containing CARD (ASC), which subsequently recruits and activates caspase 1[142].

There is an emerging role of the inflammasome in SLE pathogenesis (reviewed[143]). In a healthy immune system, C1q bound to phagocytosed apoptotic cells represses NLRP3 inflammasome activation[144]. Whereas in SLE, C3a released during immune complex-mediated complement activation (discussed in section 1.2.3.2), may

enhance NLRP3 activation in stimulated monocytes by mediating ATP release[145]. Additionally, healthy monocytes are stimulated to produce IL-1β in response to NLRP3 inflammasome activation by nuclear constituents, including U1-small nuclear ribonucleoprotein[146] and self-DNA[147], which form immune complexes with SLE autoantibodies. LL37 extruded in NETs also stimulates IL-1β and IL-18 secretion by SLE macrophages by activating NLRP3, with IL-18 subsequently triggering more NETosis[148]. A pathogenic role of inflammasomes in SLE is indicated by reports that disease is reduced in experimentally-induced SLE mouse models deficient in caspase-1 [149] and IL-1β[150].

1.3 Plasmacytoid dendritic cells

PDCs are considered to be the key source of elevated IFN-α in SLE. PDCs are a small population (<1%) of lineage-negative, bone-marrow derived circulatory cells of the innate immune system[151]. Human pDCs can be distinguished by their expression of blood dendritic cell antigen (BDCA)-2, BDCA-4, CD4, FcγRII, CD123 (IL-3Rα) and MHC Class II[151]. Mouse pDCs do not express CD123, but do express plasmacytoid DC antigen (PDCA)-1, B cell marker B220, and at low levels CD11c[151]. PDCs were originally identified as natural interferon-producing cells (IPC) due to their rapid secretion of vast quantities of Type I IFN[152]. Additionally, pDCs were also initially termed plasmacytoid T cells, as these $CD4^+$ cells were found in abundance in the T cell rich regions of lymphoid organs[153]. In 1999, investigations of these cells converged when IPC were found to be equivalent to plasmacytoid T cells[154].

Human and mouse pDC populations develop from both the myeloid and lymphoid pathways, with the latter expressing Ig heavy chain V-J rearrangements[155,156]. PDC development is under the control of the transcription factor E2-2[157,158], which is induced by Fms-like tyrosine kinase 3 (Flt-3) and STAT3 signalling[102]. Immature pDCs have a B cell morphology, but upon maturation, they develop a similar morphology to conventional dendritic cells (cDC)[159], yet these dendritic cells are functionally distinct. Mature cDCs are professional antigen presenting cells, as they

have the unique ability to present antigen to prime naïve $CD4^+$ T cells[160]. Conversely, activated pDCs are professional type I IFN secreting cells, but have a limited ability to prime $CD4^+$ T cells compared to cDCs[102,161]. This is likely due to the continuous turnover of MHC class II-peptide in pDCs, unlike activated cDCs which accumulate MHC class II complexes expressing the same antigen[162]. Furthermore, the continual loading of MHC class I with intracellular antigens renders pDCs efficient at priming anti-viral $CD8^+$ cytotoxic T cells[163].

1.3.1 Plasmacytoid DCs are specialised to sense nucleic acids

Toll-like receptors (TLR) are a family of ten human and twelve mouse germline-encoded, transmembrane pattern recognition receptors (PRR), which have extracellular leucine rich repeats (LRR) specific for various conserved pathogen-associated molecular patterns (PAMPs)[164,165]. Most of these receptors are expressed on the cell surface membrane. However, viral and bacterial nucleic acid-specific receptors, TLR3, TLR7/8, and TLR9, are distinguished from other TLRs by their location on intracellular membranes[166,167]. These intracellular receptors respectively recognise double-stranded (ds)RNA, single-stranded (ss)RNA, and cytosine-phosphate-guanine (CpG) sequences in DNA[168]. Unlike other immune cells, immature pDCs selectively express TLR7 and TLR9.

Upon stimulation with the appropriate ligand, TLRs dimerise and TLR7 and TLR9 translocate from the endoplasmic reticulum (ER) to endosomes with help from the ER membrane protein UNC93B[169] and chaperone protein gp96[170]. Acidification of the endosome and proteolytic cleavage of TLR7 and TLR9 is required for receptor activation and interactions between the cytosolic Toll-IL-1 resistance (TIR) domains of the TLR and the TIR-containing signalling adaptor protein, MyD88[165,171]. TLR/MyD88 association activation induces the phosphorylation of IL-1 receptor-associated kinase (IRAK)4, which activates TNF receptor associated factor (TRAF)6. This MyD88-dependent signalling pathway is shared with all TLRs, except TLR3, which is TRIF-dependent, and upon activation ultimately leads to

NFκB-mediated secretion of pro-inflammatory cytokines, such as TNF-α and IL-6. Activation of intracellular TLRs in pDCs induces an additional signalling pathway, whereby MyD88-dependent activation of IRAK1 and TRAF3 results in IRF7-mediated transcription of IFN-α and other type I IFNs (Figure 1.4).

Unlike most PAMPs, which are pathogen-specific, nucleic acids are also components of mammalian cells. Tolerance to self-DNA was initially considered to occur by TLR9-specificity for unmethylated CpG motifs found in microbial DNA, but not methylated CpG motifs in mammalian DNA[161]. This view was challenged when it was reported that the deoxyribose backbone was important for TLR9 activation[172]. Re-localisation of chimeric TLR9 to the cell surface revealed endosome acidification is important for distinguishing microbial DNA from self-DNA[166]. Therefore, it is currently considered that intracellular compartmentalisation of TLR7 and TLR9 is vital for maintaining tolerance to self, as this enables regulation of the source of ligands that can reach the TLR[166].

The specialised ability of pDCs to respond to nucleic acids and rapidly secrete IFN-α is owed to the selective expression of TLR7 and TLR9 and constitutive expression of IRF7[173]. Although other cells can make IFN-α in response to virus infections this response is limited compared to the rapid and vast secretion of IFN-α by pDCs. PDCs are therefore important in the first line of defence against systemic virus infections, such as murine cytomegalovirus (MCMV) and herpes simplex virus (HSV)-1 while the other cells come in to play later in infection[102]. The importance of pDC-derived IFN-α to provide protection against virus infections is demonstrated when this response is lost, such as severe influenza A infection in IRF7-deficient humans[174]. Conversely, the 129 mouse strain develops detrimental influenza virus-induced inflammation caused by excessive IFN-α secretion by pDCs[175], indicating that this key anti-viral response is pathogenic on the autoimmune 129 genetic background. The nucleic acid-induced IFN-α response that is specialised for anti-viral immunity associates pDCs with the loss of tolerance to self-nuclear components and pathogenesis in SLE patients.

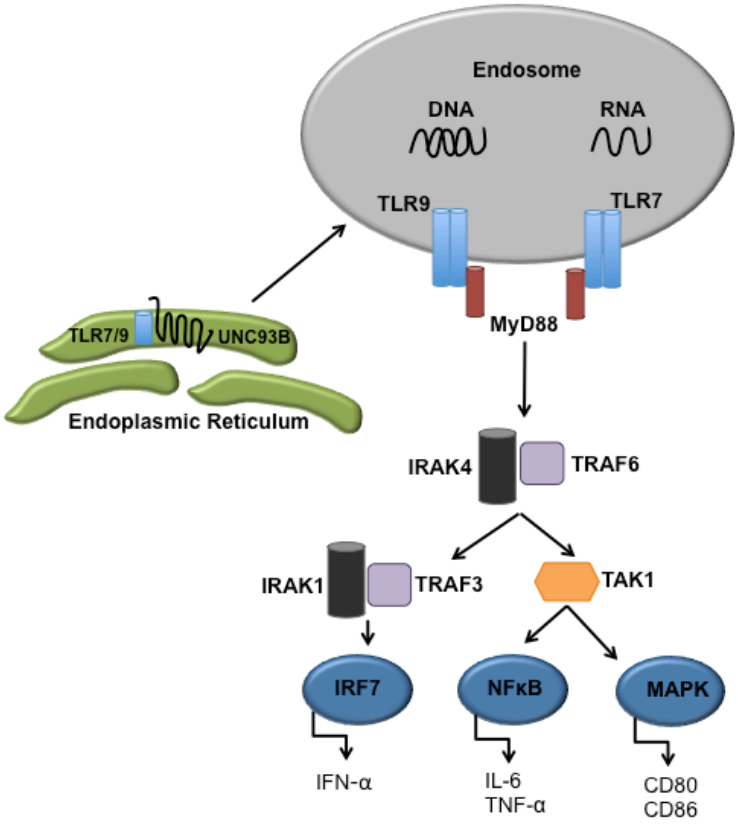

Figure 1.4. Toll-like receptor 7 and 9 signalling in plasmacytoid DCs.

An overview of the signalling pathways that stimulate the transcription of IFN-α, pro-inflammatory cytokines, and activation markers following TLR7 and TLR9 engagement in pDCs. Adapted from Gilliet et al. (2008)[161]

1.3.2 **Plasmacytoid DCs are tolerogenic**

PDCs are primarily recognised for playing a central role in anti-viral IFN-α responses, yet evidence suggests that they are also important in promoting tolerance. Immature pDCs always induce tolerance, whilst activated pDCs can induce tolerance or immunity depending on the environmental context[162]. PDCs help regulate central tolerance in the thymus; in humans this is reported to occur through the induction of IL-10 secreting FoxP3^{+} natural Tregs by activated thymic pDCs[176,177], whereas in mice the recruitment of antigen-presenting peripheral pDCs induces deletion of self-reactive T cells[178].

Peripheral T cell tolerance to tumour cells, alloantigens, and allergens is also regulated by pDCs through IL-10 producing Tregs[179,180] most commonly induced by pDC expression of IDO[181-184]. Following activation, pDCs upregulate the expression of inducible co-stimulator ligand (ICOS-L), which also drives IL-10 secreting Tregs[185]. Furthermore, peripheral T cell tolerance to self-antigens in the autoimmune setting of RA may be regulated by mouse and human pDCs through IDO-induced IL-10 secreting Tregs[186,187]. Yet, although the inflammatory response of pDCs to apoptotic cell-derived self nucleic acids has been described in the context of autoimmune disease, it is not fully understood if pDCs induce tolerance to apoptotic cells in a healthy immune setting. Research using a mouse model of apoptotic cell-induced allogeneic hematopoietic cell engraftment reported macrophage-derived TGF-β was necessary for pDCs to indirectly induce immune suppression to apoptotic cells[188]. However there are no reports that direct pDC-apoptotic cell interactions are immunoregulatory.

The expression of TLR7 and TLR9, which are responsible for potent IFN-α production in response to nucleic acids from viruses and SLE immune complexes, may indicate that pDCs should ignore apoptotic cells to maintain homeostasis in health. However, it has previously been demonstrated that pDCs induce regulation in response to stimulation through TLR9 using the synthetic ligand CpGB by promoting naïve T cell differentiation in to $Foxp3^+$ Tregs [189]. This has been supported by additional evidence that pDCs promote TLR9-dependent, IDO-mediated T cell suppression and differentiation into Tregs [181,190]. Additionally, recent evidence established that DNA complexes on the surface of apoptotic cells stimulate TLR9-dependent differentiation of IL-10-secreting regulatory B cells[55]. Therefore, it is conceivable that DNA expressed by apoptotic cells may activate pDCs through TLR9 to trigger a regulatory response, perhaps by upregulating the expression of IDO.

This suggests there are two distinct pathways of TLR9 activation depending on the source of ligand; a protective inflammatory response can be generated in response to pathogens, whereas tolerance to self-DNA is maintained. The concept of a regulatory role for TLR9 is further supported by evidence that TLR9-deficient lupus-prone mice develop accelerated disease[191]. On the other hand, TLR7-deficient mice are protected from generating severe SLE[191]. TLR9 was shown to regulate the antibody and IFN-α response produced by TLR7 ligation[192,193]. This suggests that TLR7 and TLR9 play opposing roles in SLE. Additionally, lupus-prone BXSB mice that carry the Y-linked autoimmune acceleration (*Yaa)* gene have augmented progression of SLE-like disease.[194] The *Yaa* gene was discovered to cause duplication and overexpression of TLR7[195], due to translocation of the telomeric end of the X chromosome to the Y chromosome. Similarly, elevated expression of TLR7 in humans is associated with increased risk of SLE in males, further implicating this receptor in the loss of tolerance to self [196].

1.3.3 Do plasmacytoid DCs sense apoptotic DNA in a healthy immune system?

The current paradigm of SLE suggests that the stabilisation of self nucleic acids in immune complexes facilitates their delivery to TLR7 and TLR9 thus breaching tolerance[161]. However, the induction of IL-10-secreting regulatory B cells by apoptotic cells is dependent on TLR9 stimulation by DNA and chromatin exposed on the apoptotic cell membrane[55]. This occurs in response to antigen recognition and internalisation by self-reactive BCRs, which triggers the redistribution of TLR9 from the ER to endosomes[55]. Hence it is likely that TLR7 and TLR9 traffic to endosomes as a means to function optimally[197], rather than as a mechanism to avoid interacting with mammalian chromatin. Despite the important role of pDCs in tolerance (section 1.3.2), there is currently no evidence to suggest that in health they sense apoptotic cell-derived DNA and chromatin in a similar regulatory way to B cells. The main issue is how, in a healthy person, who does not have IgG ANA, would self-DNA reach intracellular TLR9 in pDCs?

The same question arises as to how pDCs sense viral DNA and RNA, since they are rarely infected by viruses[198] and they do not require productive viral replication to make IFN-α. However, pDCs respond to other infected cells. Direct contact with hepatitis C virus (HCV)-infected hepatocytes, but not free virus, induces IFN-α secretion by human pDCs[199] resulting from the release of exosomes containing HCV RNA[200]. Similarly, contact with hepatitis A virus (HAV)-infected cells, or HAV enveloped within host cell membrane, but not free virions, stimulates human pDCs to produce IFN-α, though this occurs via uptake by as yet unidentified PS receptors[201]. It is also interesting that human pDCs can phagocytose fragments from HIV-infected apoptotic cells, which are then cross-presented to T cells[202], but it was not determined if IFN-α was also induced.

Therefore, pDCs sense virus nucleic acids from infected cells, indicating that the same antibody-independent mechanisms could be used to sense self-DNA on apoptotic cells. However, it is essential that if this occurs in health IFN-α is not produced. In fact, human pDCs express inhibitory cell surface receptors including the type II C-type lectin receptor BDCA-2 and immunoglobulin-like transcript (ILT)7, which associate with immunoreceptor-based tyrosine activation motif (ITAM)-containing γ-chain of FcεRI[161]. Mouse pDCs express Siglec-H, which is associated with ITAM-containing adaptor DAP12[161]. Activation of these receptors stimulates a BCR-like signalosome including LYN, SYK, B cell linker (BLNK), and B cell adaptor protein (BCAP), which regulates TLR7 and TLR9 signalling to inhibit IFN-α secretion[203-205]. These regulatory receptors might function to control the threshold of TLR activation, hence prevent an inflammatory response by pDCs exposed to self-DNA.

PDCs also express on their surface the receptor for advanced glycation end-products (RAGE)[206], which recognises the ligands HMGB1[207], C1q[208], and PS[209]. Contradicting studies report that free HMGB1 inhibits TLR9-mediated IFN-α production by pDCs[206], whereas HMGB1-DNA complexes augment IFN-α secretion[210]. Nevertheless, although it is published that human pDCs endocytose

apoptotic bodies[211] it has not been determined if pDCs can phagocytose apoptotic bodies via uptake by RAGE, or even low level expression of TIM-1[212].

1.4 Autophagy

In addition to impaired phagocytosis of apoptotic cells it is emerging that autophagy may play a role in SLE.

1.4.1 The autophagy pathway

The term autophagy (from the Greek auto "self" and phagy "to eat") was founded by Christian de Duve over 50 years ago and it describes a mechanism that functions to promote cell survival and maintain tissue homeostasis[213]. Three types of autophagy exist: microautophagy, macropautophagy, and chaperone-mediated autophagy. The common link between these pathways is the transport of a cell's own long-lived cytoplasmic proteins and organelles to the lysosome for degradation and recycling. Microautophagy involves lysosomal membrane invagination to directly engulf cell components (reviewed in reference[214]), whereas chaperone-mediated autophagy selectively tags proteins, which then cross the lysosome membrane to be degraded (reviewed in reference[215]). The main autophagy pathway is macroautophagy (herein referred to as autophagy), which is characterised by cytoplasmic constituents enclosed in double membrane vesicles that fuse with lysosomes[213]. This catabolic process is constitutively active at basal levels in most cell types, and is upregulated in response to need.

Cell stress, such as nutrient or energy depletion, induces non-selective autophagy of cytosolic components, which are degraded and recycled to provide the cell with essential nutrients. Selective, or cargo-specific, autophagy occurs to remove specific organelles that are damaged or in excess by degradation in the autophagosome. Several selective autophagy pathways are known, including ribophagy to remove ribosomes, xenophagy to eliminate pathogens, and mitophagy to selectively degrade mitochondria. Mitophagy occurs during the development of red blood cells to remove all mitochondria and to selectively remove mitochondria from sperm in a

fertilised egg to allow for inheritance of maternal mitochondrial DNA. It is also an essential quality control process required to maintain normal cell homeostasis by removing damaged or excessive mitochondria.

Autophagy involves a complex pathway of many proteins, which work together during the three stages of the process, initiation, elongation and closure, and maturation (Figure 1.5). The pathway is initiated when inhibition of the mammalian target of rapamycin (mTOR) causes dephosphorylation and activation of components of the ULK complex (consisting of ULK1 and ULK2 interacting with FIP200, autophagy-related (ATG)13 and ATG101), and the beclin-1-associated protein, AMBRA1[216,217]. The ULK complex activates the beclin1 complex (composed of beclin-1, ATG14 and the class III PI3K Vps34), which is essential for promoting activation of Vps34[218]. Vps34 phosphorylates phosphatidylinositol generating PI_3P, a phospholipid crucial for generating the isolation membrane called the phagophore[213], which is formed from one of multiple membranes sources, such as the ER[219,220], plasma membrane[221], and mitochondrial outer membrane[222].

The next step of elongation and closure of the membrane involves two ubiquitin-like conjugation systems. Firstly, the E1-like enzyme ATG7 activates ATG12, which is then transferred to the E2 enzyme ATG10 before finally conjugating to ATG5[213]. ATG5-ATG12 dimerise and subsequently ATG5 interacts with a dimer of ATG16, enabling ATG5-ATG12 to associate with the phagophore membrane[213]. In the second pathway, LC3-I is conjugated to the membrane lipid phosphatidylethanolamine (PtdE) to form LC3-II. This involves activation of cytosolic LC3 by ATG4 to make LC3-I, which then associates with ATG3 to be lipidated by PtdE. The ATG12-ATG5-ATG16 conjugate acts as an E3-ligase by promoting the transfer of LC3 from ATG3 to PtdE[223]. LC3-II forms a stable interaction with the outer and inner membrane, which mediates the recruitment of cargo and is essential for membrane closure thus forming the complete autophagosome.

Autophagosomes then fuse with lysosomes, a process that is mediated by several molecules including PLEKHM1, an adaptor protein that binds to LC3 on the autophagosome, and the small GTPase, Rab 7, on the lysosome[224]. This recruits the homotypic fusion and protein sorting (HOPS) complex which also interacts with the SNARE, syntaxin (Stx)-17[225,226]. The final step of the pathway is the degradation of the cargo and inner membrane, including LC3-II, by the lysosomal hydrolases in the autolysosome.

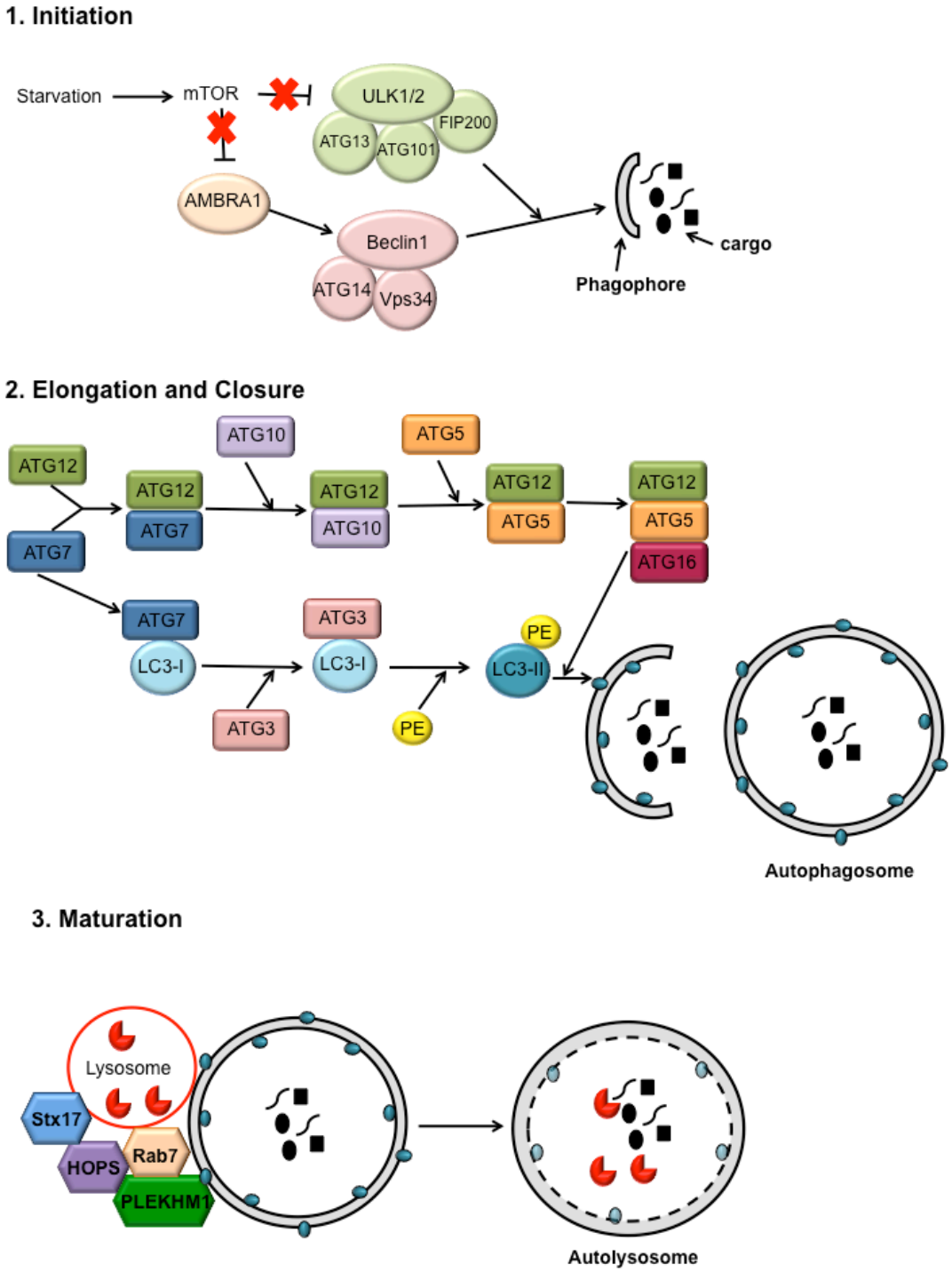

Figure 1.5. The autophagy pathway.

1. Initiation of the autophagy pathway involves generating the isolation membrane (phagophore) to enclose the cargo. 2. The double membrane is then elongated and fused, forming the autophagosome. This requires the conversion of LC3-I to LC3-II by binding of phosphatidylethanolamine (PE). 3. The cargo is degraded following fusion of the autophagosome with lysosomes to form the autolysosome.

1.4.2 **Role of autophagy in systemic lupus erythematosus**

Autophagosomes were first hypothesised to be linked to SLE by Weissmann in 1964 when he suggested that SLE lysosome membranes were more fragile than healthy individuals[227]. In recent years it has become clear that there is an association between deregulated autophagy and SLE. It is published that SLE $CD4^+$ T cells from $MRL^{lpr/lpr}$ and NZB/W F1 SLE-prone mice and a small number of SLE patients contain more autophagosmes compared to healthy controls[228]. This corresponds with data from a human study, which found elevated autophagy in SLE $CD19^+$ B cells in addition to $CD4^+$ T cells[229]. Bone marrow-derived B cells from NZB/W F1 mice expressed a particularly elevated number of autophagosomes, even in young mice that had not yet developed disease[229]. These findings suggest that autophagy is intrinsically deregulated in SLE lymphocytes to promote the survival of autoreactive T cells and B cells[228,229]. Conversely, it has been reported that $CD4^+$ T cells from SLE patients are resistant to both SLE serum- and starvation-induced autophagy, as indicated by reduced LC3-II[230].

GWAS analyses have identified several SNPs linked with SLE susceptibility in and near autophagy-associated gene Atg5[67,231,232], which encodes an essential component of the autophagy pathway that is required for LC3-I conversion to LC3-II (discussed in section 1.4.1). Another risk factor for SLE is SNPs near the gene encoding damage-regulated autophagy modulator (DRAM)-1[233], a lysosome membrane protein that is activated by tumour suppressor p53 and induces both autophagy and apoptosis[234]. However, the effect of these SNPs is currently not described.

Although the published literature is still limited, it is clear that autophagy is deregulated in SLE patients. The cause of this appears to be unknown and the link between autophagy and apoptosis in SLE cells has not been addressed. A key unanswered question is, how does dysfunctional autophagy affect SLE pathogenesis?

1.4.3 **Cross-talk between autophagy and apoptosis**

Autophagy has largely been seen as a survival mechanism by cells to avoid cellular apoptosis through the removal of damaged proteins and organelles, yet similarities exist between the autophagy and apoptosis processes. Autophagy and apoptosis both function to preserve homeostasis, either within the cell or in the whole organism, respectively. Whilst autophagy is concerned with the packaging and delivery of effete organelles to the lysosomal pathway of the same cell, following apoptosis the packaging of intracellular components into apoptotic bodies allows for the delivery of cellular corpses to the lysosomal pathway of the phagocytes that ingest them. The presence of autophagosomes in dying cells has been noted for many years[235], though it was taken to indicate either a last attempt to survive, or a form of non-apoptotic cell death characterized by a lack of caspase activation and DNA fragmentation[236].

It is now recognised that the autophagy and apoptosis pathways share regulatory elements (reviewed in[237]). The proteins Bcl-2 and Bcl-X_L not only function to inhibit apoptosis, they also have the capacity to prevent autophagy by sequestering Beclin-1 [238]. Pro-apoptotic BH3-only proteins, including Bid and Bad, are also pro-autophagic by breaking apart the interactions between Bcl-2, or Bcl-X_L and beclin-1, leading to activation of the PI3K, Vps34[237]. Likewise, autophagy proteins function in apoptosis induction, such as non-conjugated ATG12, which interacts with and inhibits anti-apoptotic proteins[239]. In apoptotic cells, the autophagy pathway is inhibited by caspase-mediated cleavage of autophagy proteins[240-242]. However, this converts the function of the autophagy proteins into pro-apoptotic proteins. For example caspase-activated calpain-cleaved ATG5 translocates to the mitochondria, where it induces apoptosis through inhibition of anti-apoptotic Bcl-X_L[243]. Additionally, intracellular DISC-mediated activation of apoptotic caspase 8 can occur on the autophagosome membrane [244,245].

In addition to regulating the initiation of apoptosis, autophagy also influences how other cells respond to apoptotic cells. The activation of autophagy prior to apoptotic cell death is important for the release of the "find me" signals, LPC and ATP[246],

which subsequently recruit phagocytes. In addition a number of recent studies have identified the importance of autophagy proteins in the heterophagy of apoptotic corpses by phagocytes[247-249]. Binding of PS to the TIM-4 receptor stimulates autophagy proteins, such as ATG5, ATG7, and LC3-II, expressed by the phagocytic cells to mediate the lysosomal degradation, but not uptake, of apoptotic cells[247]. This process, termed LC3-associated phagocytosis (LAP), is distinct from the canonical autophagy pathway since a double membrane is not formed and it proceeds independently of ULK1[247,250]. Therefore, autophagy proteins are connected with the anti-inflammatory removal of apoptotic cells, which was discussed in section 1.1.3.

1.4.4 **Autophagy regulates inflammation**

Autophagy also plays a role in eliminating infectious bacteria and viruses by LAP[251], or indeed by the canonical autophagy pathway, xenophagy[252]. PDCs are stimulated to make IFN-α in response to certain ssRNA viruses by autophagy-recruited endosomes containing TLR7; the antiviral response is inhibited in autophagy-deficient pDCs[253]. TLR9 is also recruited to autophagosomes following FcγR engagement in pDCs stimulated by DNA-IgG immune complexes[254] and B cell receptor cross-linking in B cells simultaneously stimulated by CpG DNA[255]. Therefore, the autophagy machinery potentially contributes to SLE pathology by enabling TLR signalling, though it remains to be investigated if the autophagy proteins are involved in IFN-α secretion induced by TLR7 activation by self-RNA/RNP-containing immune complexes.

Conversely, the over activation of IFN-α production in response to cytosolic DNA is suppressed by autophagy proteins, for example ATG5-ATG12 and ULK1, which inhibit signalling of the cytosolic DNA receptors retinoic acid-inducible gene (RIG)-1 and stimulator of IFN genes (STING), respectively (reviewed in reference[256]). Aberrant NLRP3 inflammasome activity is additionally prevented via the removal of damaged mitochondria by mitophagy to prevent the release of endogenous agonists, such as mitochondrial ROS and DNA[257]. Autophagy machinery also degrades the components of activated NLRP3 and AIM2 inflammasomes[258]. Furthermore,

autophagy is required in combination with superoxide production for neutrophils to undergo NETosis[259].

In addition to the important role of autophagy proteins in regulating innate immune responses to infection, they also influence adaptive immunity[256]. For example, the loading of pathogen antigens onto MHC class II for presentation to T cells is reported to require the autophagy machinery[260,261]. Equally, autophagy is essential for processing self-antigens onto MHC class II, which is critical in the thymus to avoid the development of T cells with self-reactive receptors; mice with *Atg5*-deficient thymi develop autoimmune colitis[262]. Autophagy also plays a role in humoral immunity by regulating the development of plasma cells and secretion of antibodies[229,263]. Thus, autophagy is intricately involved in the immune system.

1.5 Hypothesis

In summary, SLE is a complex and heterogeneous inflammatory disease driven by the loss of tolerance to apoptotic cell-derived nuclear constituents. This goes against the anti-inflammatory response that is normally induced by apoptotic cells. In a healthy immune system it is currently considered that pDCs do not respond to self nucleic acids due to the intracellular compartmentalisation of TLR7/9. However, the IgG ANA produced by autoreactive B cells in SLE generate immune complexes with nucleic acids released from apoptotic cells that have become secondarily necrotic due to failure in phagocytosis mechanisms. These immune complexes enable their transport into pDCs thus stimulating IFN-α production through TLR7/9 activation. Yet it is known that in health, stimulation of innate-like B cell TLR9 by apoptotic DNA/chromatin induces IL-10 secretion and immune regulation. Although a tolerogenic role of pDCs is defined, it has not been described if pDCs in health can respond directly to apoptotic DNA in a similar way as innate-like B cells.

Many defects have been associated with SLE, including impaired function of phagocytes, loss of apoptotic cell opsonisation, and unchecked development of autoreactive B cells. More recently, genetic and cellular defects in autophagy have

emerged as potentially contributing to SLE. Autophagy was originally discovered as a pathway to promote cell survival, but it is now known to play a significant role in regulating apoptosis, apoptotic cell removal, and innate and adaptive inflammation. However, it is not clear how, or if, the published autophagy defects are related to cell death in SLE.

The over-arching hypothesis of this thesis was, in health apoptotic cells induce regulatory immunity through pDCs whereas in SLE there is an intrinsic defect in the apoptotic lymphocytes that contributes to inflammatory immunity. To address this hypothesis, the results chapters assessed the following specific aims:

1. Establish if apoptotic cells induce cytokine secretion by TLR-stimulated pDCs in healthy subjects.
2. Analyse the cell death kinetics of SLE lymphocytes.
3. Determine if dysfunctional autophagy in SLE lymphocytes causes inflammatory cell death.

Chapter 2 Materials and Methods

2.1 Ethical approval

All work involving mice was covered by Dr Mohini Gray's Project Licence granted by the UK Home Office under the Animals (Scientific Procedures) Act 1986. Locally, this was approved by the University of Edinburgh Ethical Review Committee. Permission was granted by the Lothian SAHSC BioResource (Ref QF-TGU-A-SAMREQA) to collect samples of blood from consenting adults. Samples of healthy donor blood were collected from the CIR blood resource approved by AMREC (Ref 15-HV-013).

2.1.1 Mice

Wild type Balb/c and DO11.10 TCR mice, and wild type C57BL/6 and C57BL/6 background TLR9$^{-/-}$ and C1q$^{-/-}$ mice were bred and maintained under pathogen-free conditions at the animal facilities at the University of Edinburgh, UK. DO11.10 mice were kindly provided by Professor Jürgen Schwarze (University of Edinburgh, UK). TLR9$^{-/-}$ mice were generously provided by Professor Shizuo Akira (Hyogo College of Medicine, Nishinomiya, Japan). C1q$^{-/-}$ mice were a kind gift from Professor Marina Botto (Imperial College London, UK). In all experiments mice were age and sex matched and used aged 6-12 weeks

2.1.2 Patients

SLE patients were recruited from the Western General Hospital, Edinburgh following informed consent and ethical approval. The mean age of the patients was 47 (range 19 – 77), with a female:male (F:M) ratio of 7.2:1. Patient characteristics and the figure number(s) where the samples were used are listed in appendix A table A.1. Prerana Hudder calculated the safety of estrogens in lupus erythematosus national assessment – SLE disease activity index (SELENA-SLEDAI) scores where the patient details were available to her during her medical elective. Healthy controls were recruited from the Centre for Inflammation Research, University of Edinburgh,

and non-SLE patient controls were recruited from the Western General Hospital, Edinburgh following informed consent and ethical approval. The mean age of controls was 40 (range 19 – 77) with a F:M ratio of 3.9:1. Characteristics of the non-SLE patients are listed in appendix A table A.2.

2.2 Media

2.2.1 Mouse cell culture media

IMDM (Gibco) supplemented with 10% FCS, 100 U/ml penicillin, 100 μg/ml streptomycin, and 2 μM 2–mercaptoethanol was used in the majority of experiments. Where cells were purified from C1q-deficient mice, the culture medium was X-VIVO™ 15 (Lonza) supplemented with 100 U/ml penicillin, 100 μg/ml streptomycin.

2.2.2 Human cell culture media

RPMI (Gibco) supplemented with 10% FCS, 2 mM L-glutamine, 100 U/ml penicillin, and 100μg/ml streptomycin. Human monocytes and macrophages were cultured in IMDM (Gibco) supplemented with 100 U/ml penicillin, 100μg/ml streptomycin, and 10% serum (pooled from ten healthy donors).

2.2.3 Starvation media

HBSS containing calcium and magnesium (Life Technologies) and supplemented with 100 U/ml penicillin, and 100μg/ml streptomycin.

2.3 Cell isolation and purification

2.3.1 Peripheral blood mononuclear cells (PBMCs)

40 ml of venous blood from healthy donors and SLE patients was collected into 50ml Falcon tubes (BD Biosciences) containing 4ml 3.8% sodium citrate to prevent clotting. The blood was centrifuged at 350xg for 20 min at room temperature prior to aspirating the top layer consisting of platelet-rich plasma in to 10ml glass tubes. 200μl 1M calcium chloride was added per 10ml and the plasma was incubated in a 37°C water bath for a minimum of 1 h. The serum was removed from the platelet plug and was retained to include in cell culture medium, or it was stored at -30°C.

6ml of 6% Dextran 500 (Pharmacosmos) was added to the remaining blood cell layer then filled to 50 ml with NaCl. Following sedimentation of the red blood cells for 20 min at room temperature, the leukocyte-rich top layer was aspirated in to a new 50ml Falcon tube and centrifuged at 350xg for 6 min at room temperature. A stock of 90% Percoll (GE Healthcare) was used to create a gradient in a 15ml Falcon tube (BD Biosciences) by layering 3ml 81%, 3 ml 68%, and 3ml 55% percoll (containing cells from the leukocyte-rich layer). The Percoll gradient was centrifuged at 720xg for 20 min then the peripheral blood mononuclear cells (PBMCs, top layer) was collected, washed and counted. PBMCs that were not used immediately in an experiment were frozen at $10x10^6$/ml in FCS containing 10% DMSO and stored in liquid nitrogen. Neutrophils (bottom layer) were also collected, washed, and counted.

To generate macrophages, PBMCs ($2x10^6$/ml) were cultured for 1 h in serum-free human monocyte medium in a 24-well plate (Corning) to allow the monocytes to adhere to the plastic. The non-adherent cells (lymphocytes) were then removed and replaced with human monocyte medium containing 10% healthy donor serum. The monocytes were cultured for seven days, or where stated three days, and the medium was removed and replaced half way through the culture period.

2.3.2 **CD19$^+$ B cells**

Single-cell suspensions of mouse spleen and human PBMCs were incubated with 5µl (mouse), or 10µl (human) anti-CD19 microbeads (Miltenyi Biotec) in 45µl (mouse), or 40µl (human) autoMACS buffer (Miltenyi Biotec) per 10^7 cells for 15 min at 4^oC. The cells were then washed in autoMACS buffer and centrifuged at 300xg for 10 min. While the cells were being washed, an LS column (Miltenyi Biotec) attached to a quadroMACS magnet (Miltenyi Biotec) was rinsed with 3ml autoMACS buffer. The cells were resuspended in 500µl autoMACS buffer per 10^8 cells and allowed to flow through the LS column followed by three washes with autoMACS buffer, with the CD19-negative cells collected in a 15ml greiner tube for further use. To collect the CD19-positive cells, the column was removed from the magnet and flushed through with 5ml autoMACS buffer using the plunger provided with the column.

2.3.3 **Plasmacytoid dendritic cells**

Mouse plasmacytoid dendritic cells (pDCs) were enriched from single-cell suspensions of red cell lysed spleen by depleting B cells using anti-mouse CD19 microbeads (Miltenyi Biotec), as described in 2.4.2, and were further sorted using a FACSAria cell sorter (BD Biosciences) to generate a highly purified population. To block non-specific binding of antibodies the CD19-negative splenocytes were resuspended at $40x10^6$ per ml and incubated with anti-mouse CD16/CD32 antibody (BioLegend) for 10 min at 4^oC. The cells were then stained with anti-mouse PDCA-1, B220, Ly6C, CD3, and CD11b antibodies described in Table 2.1 for 20 min at 4^oC and then immediately flow sorted.

Where stated, human pDCs were enriched by negative selection using the pDC isolation kit II (Miltenyi Biotec). PBMCs were incubated with 400µl autoMACS buffer and 100µl of Non-pDC biotin antibody cocktail II per 10^8 cells for 10 min at 4^oC. The cells were then washed in autoMACS buffer and centrifuged at 300xg for 10 min. The pellet was then resuspended in 400µl autoMACS buffer and incubated with 100µl Non-pDC MicroBead cocktail II per 10^8 cells for 15 min at 4^oC. While the cells were being washed and centrifuged at 300xg for 10 min an LS column (Miltenyi Biotec) attached to a quadroMACS magnet (Miltenyi Biotec) was rinsed with 3ml autoMACS buffer. The cells were resuspended in 500µl autoMACS buffer and passed through the LS column followed by three washes with autoMACS buffer, with the non-pDCs attaching to the column and the pDC-positive population passing through into a 15ml greiner tube.

Where applicable, human pDCs were flow sorted to high purity using a FACSAria cell sorter (BD Biosciences). To block non-specific binding of antibodies to the PBMCs, the cells were resuspended at $10x10^6$ per 100µl and incubated with 20µl of FcR blocking reagent (Miltenyi Biotec) for 10 min at 4^oC. The cells were then washed and resuspended at $40x10^6$ per ml in FACS buffer (PBS, 1% FCS) and stained with anti-human CD304, CD123, CD19, CD3, and CD14 antibodies described in Table 2.1 for 20 min at 4^oC.

Staining protocol	Antibody (clone)	Fluorochrome	Isotype	Source	Dilution
Mouse pDC flow sort	Anti-PDCA-1 (927)	APC	Rat IgG2bκ	BioLegend	1:200
	Anti-B2.20 (RA3-6B2)	PerCP	Rat IgG2aκ	BioLegend	1:200
	Anti-Ly6C	PE	IgM κ	BD Biosciences	1:400
	Anti-CD3 (145-2C11)	FITC	Armenian Hamster IgG	BioLegend	1:200
	Anti-CD11b (M1/70)	BV421	Rat IgG2bκ	BioLegend	1:200
Human pDC flow sort	Anti-CD304 (AD5-176)	PE	Mouse IgG1	Miltenyi Biotec	1:200
	Anti-CD123 (AC145)	FITC	Mouse IgG2a	Miltenyi Biotec	1:200
	Anti-CD19 (HIB19)	PerCPCy5.5	Mouse IgG1	BioLegend	1:400
	Anti-CD3 (UCH1)	APC	Mouse IgG1	BioLegend	1:400
	Anti-CD14 (MEM-15)	PEDy647	Mouse IgG1	ImmunoTool	1:400

Table 2.1. Fluorescently conjugated antibodies used to flow sort pDCs.

2.3.4 $CD4^+$ T cells

$CD4^+$ T cells were sorted from mouse spleen and lymph nodes and human PBMCs using 5µl (mouse), or 10µl (human) anti-CD4 microbeads (Miltenyi Biotec) in 45µl (mouse), or 40µl (human) MACS buffer per 10^7 cells for 15 min at 4^oC. The cells were isolated using magnetic separation as described in 2.3.2.

2.4 Cell lines

The NIH 3T3 (mouse embryonic fibroblast) and the C127 (mouse mammary epithelial) cell lines, which were kindly provided by Professor Peter Ghazal (DIPM, University of Edinburgh), were maintained in culture flasks in DMEM (Gibco)

supplemented with 10% FCS, 2 mM L-glutamine, 100 U/ml penicillin, 100 µg/ml streptomycin at 37°C 5% CO_2. The wild type (WT) and A*tg5*$^{-/-}$ immortalised baby mouse kidney epithelial (iBMK) cell lines were gifted from Professor Eileen White (Rutgers Cancer Institute of New Jersey), and were maintained in culture flasks in DMEM/F-12 + GlutaMAX™ (Gibco) supplemented with 10% FCS, 100 U/ml penicillin, and 100 µg/ml streptomycin at 37°C 5% CO_2.

These adherent cell lines were passaged every 3-4 days when they were 70-80% confluent. To split the cells, the media was removed and replaced with PBS to wash the cells. The washed cells were incubated in Trypsin-EDTA (ThermoFisher Scientific) for 5 min at 37°C to detach them from the flasks. Double the volume of culture medium (containing 10% FCS) was then added to neutralise enzymatic activity of trypsin. The cells were transferred into a 50ml Greiner tube and centrifuged at 300xg for 5min. After discarding the supernatant, the cell pellet was gently resuspended in culture medium and added at a ratio of 1:10 to new flask containing fresh medium.

2.5 Viruses

The Influenza A virus (H1N1) used in this thesis was derived from frozen stocks of known titre generated by Dr Simon Talbot (DIPM, University of Edinburgh).

Murine cytomegalovirus (MCMV) was kindly provided by Prof Peter Ghazal (DIPM, University of Edinburgh). To prepare a seed stock of MCMV to use in this thesis, twenty 15cm culture dishes (Corning) of 3T3 cells were grown to 70-80% confluence in DMEM + 10% FCS + 2 mM L-glutamine (without pen/strep). On the day of infection, 3T3 cells were detached and pooled into a single tube, centrifuged at 300xg for 5 min, then resuspended in 5ml of media. After counting the cells they were infected with MCMV at a multiplicity of infection (MOI) 0.001 by incubating for 1 h at 37°C 5% CO_2 and gently mixing the tube every 15 min. 5ml of media was added to make up to total volume 10ml of infected cells, which was split evenly between two 500 ml bottle of media. After mixing well, 25ml of cells in media was

pipetted in to 15cm plates (40 plates in total) and incubated at 37^{o}C 5% CO_2 for 4 days, when the infected cells had become rounded. The cells were then harvested using a cell scraper and pooled into 250ml centrifuge tubes.

To concentrate the MCMV bulk stocks, the supernatant was centrifuged at 7,500xg at 4^{o}C for 20 min in a high-speed centrifuge (Beckman). The supernatant was poured into new 250ml centrifuge tubes and kept on ice while the pellets were resuspended in a total of 10ml medium. The cell pellet was disrupted using a 40ml glass homogeniser then centrifuged at 3,600xg at 4^{o}C for 20 min to remove cell debris. The supernatant was added to the 250ml tube kept on ice and the pellet was discarded. To pellet the virus stock, the supernatant was centrifuged at 35,000xg at 4^{o}C for 3 h with no brake. After discarding the supernatant the pellets were resuspended in residual fluid and pooled. The virus suspension was disrupted using a 25ml glass homogeniser and then it was slowly pipetted onto 20% Sorbitol (Sigma-Aldrich) in 30ml tubes (10 parts sorbitol for 1 part virus suspension). This was centrifuged at 35,000xg at 4^{o}C for 3 h and the supernatant was aspirated. 500µl of ice-cold 20% Sorbitol was added to resuspend the virus pellet and then topped up to 2ml, homogenised, aliquoted, and stored at -80^{o}C.

To determine the viral titre of the MCMV stock, a plaque assay was performed. 3T3 cells were cultured to 80-90% confluence by adding $4x10^4$ cells per ml per well in a 12-well plate (Corning). The medium was removed and the concentrated virus was added at dilutions 0, 10^{-2}, 10^{-3}, 10^{-4}, 10^{-5}, 10^{-6}, 10^{-7}, and 10^{-8}. After incubating at 37^{o}C 5% CO_2 for 1 h, the cells were overlaid with 1ml 2.5% agarose (Invitrogen) to immobilise newly produced virions and placed back in the incubator for 4 days. 1% formalin solution was added to the cells and they were fixed by incubating overnight at 4^{o}C. The formalin was poured off and the wells washed with tap water to remove the agarose media plugs and then the plaques were stained overnight with 0.1% toluidine blue solution. Using a light microscope, the number of visible plaques per well was counted.

2.6 Induction of apoptosis

To generate apoptotic thymocytes, single-cell suspensions of murine thymi were exposed to UVB-irradiation (100 mJ/cm^2) then incubated in mouse medium at 37^{o}C 5% CO_2 for 4 h prior to coculture. Mouse CD19$^+$ B cells were induced to become apoptotic by the same method described for thymocytes. Apoptotic human lymphocytes were generated either by UVB-irradiation (100 mJ/cm^2), or by LEAF™ purified anti-human CD95 (FAS) antibody, 10µg/ml (BioLegend) followed by 4 h incubation at 37^{o}C 5% CO_2. Necrotic cells were generated from apoptotic cells by performing five cycles of freezing on -80^{o}C dry ice and thawing in 37^{o}C water bath. C127 cells were induced to become apoptotic by UVB-irradiation (100 mJ/cm^2) and iBMK cells became apoptotic after 6 h culture in starvation medium.

The proportion of apoptotic cells was measured by flow cytometry by staining 0.5x10^6 cells in 50µl of the cell membrane impermeable DNA-intercalating stain propidium iodide (PI) and surface expression of PS using Annexin V (AnV) conjugated to FITC or AF647 (1:200; BioLegend). The 20 min staining period and subsequent wash steps were performed in AnV binding buffer pH 7.4 (Table 2.2).

Reagent	Concentration
HEPES	10mM
NaCl	140mM
KCl	5mM
$MgCl_2$	1mM
$CaCl_2$	2.5mM

Table 2.2. Annexin V Binding Buffer.

2.7 In vitro cultures

Cells were treated with the following TLR ligands: TLR7 ligand R848, 1µg/ml (InvivoGen); mouse TLR9 ligands, CpGB 10µg/ml for pDCs and 1µg/ml for B cells (CpG ODN 1826, Eurofins MWG Operon) and, CpGA 20 µg/ml (CpG ODN 1585, InvivoGen); human TLR9 ligands, CpGA 3µg/ml (CpG ODN 2216, InvivoGen) and

CpGB, 2μM (CpG ODN 2206, Eurofins MWG Operon); TLR4 ligand LPS, 5ng/ml (human) and 5μg/ml (mouse, Sigma-Aldrich); mouse TLR2 ligand PGN 10μg/ml (InvivoGen).

Where stated, the following components were added to culture medium: DNase, 50μg/ml (Roche, UK. Added each day of the culture period); Box A from HMGB1, 20μg/ml (IBL International); $OVA_{323-339}$, 4μg/ml (Albachem).

2.7.1 Mouse cell cultures

PDCs (10^4), or $CD19^+$ B cells ($2x10^5$), were co-cultured with apoptotic thymocytes (10^6), or apoptotic $CD19^+$ B cells ($2x10^5$) and where stated $CD4^+$ WT or OVA-T cells (10^5), in 96-well round bottom plates in mouse medium at 37°C 5% CO_2 for the duration of the assay. In transwell experiments, pDCs ($4x10^4$) were cultured in the lower part of the transwell and apoptotic cells ($4x10^6$) located in the upper transwell insert (permeable membrane 0.4μm pore size) in 24-well plates.

2.7.2 Human cell cultures

PBMCs (10^6) were co-cultured with healthy $CD4^+$ T cells (10^6), whereas $CD19^+$ B cells ($2x10^5$) were co-cultured with healthy or SLE apoptotic lymphocytes ($0.5x10^6$) in 96-well round bottom plates in human cell culture medium at 37°C 5% CO_2 for the duration of the assay. Day seven macrophages were co-cultured with healthy or SLE apoptotic lymphocytes (10^6) in 96-well flat bottom plates in IMDM (10% healthy serum) at 37°C 5% CO_2 for the duration of the assay.

2.8 Flow Cytometry

All antibody staining and wash steps were performed in FACS buffer (PBS, 1% FCS) unless otherwise stated. Single stain controls of each fluorochrome and isotype controls were used to determine appropriate compensation and gating, respectively. Samples were analysed using the LSR Fortessa (BD Biosciences) or the FACSCalibur (BD Biosciences) and analysed using FlowJo Software (version 10.0).

2.8.1 Mouse pDC activation markers

Mouse pDCs ($1x10^4$) were incubated in 50µl FACS buffer containing anti-mouse CD40, CD86, and MHC Class II antibodies described in Table 2.3. After 20 min at 4^oC, the cells were washed and resuspended in 300µl of FACS buffer to be analysed immediately.

2.8.2 Intracellular IL-10 cytokine staining

Cells were taken on day three and day seven of culture and re-suspended at $1x10^6$ per ml in fresh medium with added PMA, 20ng/ml (Sigma-Aldrich) and Ionomycin, 1µg/ml (Sigma-Aldrich). After 1 h, brefeldin A, 1µg/ml (Sigma-Aldrich) was added to block secretion of cytokines and the cells were incubated for an additional 3 h. The cells were then surface-stained (PDCA1-APC and B220-Percp), followed by fixation and permeabilisation (BD Biosciences) before intracellular cytokine staining with PE rat anti-mouse IL-10 (1:100; BD Pharmingen) or PE rat IgG2b isotype control (1:100; BD Pharmingen).

2.8.3 IL-10 secretion assay

The mouse IL-10 secretion assay was performed in accordance with the manufacturer's instructions (Miltenyi Biotec) with a few minor changes. On day seven of culture, cells were washed and re-suspended in mouse medium containing IL-10 catch reagent and incubated on ice for 5 min. The cells were then continuously rotated for 4 h at 37^oC prior to washing and staining with PE-conjugated mouse IL-10 detection antibody (Miltenyi Biotec) and anti-mouse CD4-FITC (1:100; BioLegend).

2.8.4 TLR9$^{-/-}$ mouse T cells and B cells

$1x10^6$ WT and TLR9$^{-/-}$ mouse splenocytes were incubated with anti-mouse CD16/CD32 antibody (1:400; BioLegend) for 10 min at 4^oC to block non-specific binding. The cells were then stained in 100µl with anti-mouse CD3, CD19, CD21, and CD23 antibodies described in Table 2.3 for 20 min at 4^oC, washed and then analysed on the flow cytometer.

2.8.5 **HMGB1 staining**

UV-irradiated thymocytes ($0.5x10^6$) were resuspended in 50µl and incubated with anti-HMGB1 antibody (1:100; ThermoFisher Scientific) for 20 min at 4°C. After washing the thymocytes, they were incubated in 50µl with secondary antibody goat anti-rabbit IgG AF647 (1:200; Life Technologies) for 20 min at 4°C. The cells were washed and analysed immediately.

2.8.6 **Intracellular TLR9 staining**

The human pDC/TLR9 kit (Imgenex) was used in accordance with the manufacturer's protocol to assess TLR9 expression in pDCs within PBMCs. 10µl of human lineage marker antibody mix (anti-CD3, CD14, CD16, CD19, CD20, and CD56 antibodies conjugated to FITC, and anti-HLA-DR antibody conjugated to PerCPCy5.5) and 5µl of anti-CD123 conjugated to AF647 was added to $1x10^6$ PBMCs in 100µl for 20 min at 4°C. The cells were washed twice in cold 1x staining buffer and centrifuged for 10 min at 1,200xg. After removing the supernatant and resuspending the pellet, 300µl of 1x fixation buffer was added and the cells were briefly vortexed and incubated for 20 min at 4°C. To wash, 2ml of 1x permeabilisation buffer was added and the cells were centrifuged for 10 min at 1,200xg. The supernatant was removed and the pellet resuspended in 1ml 1x permeabilisation buffer for 10 min at 4°C, then washed with 2ml of 1x permeabilisation buffer. 5µl of anti-human TLR9 antibody conjugated to PE was added to the cells in 100µl residual buffer. The cells were vortexed to mix, incubated for 25 min at 4°C then washed twice with 2ml of 1x permeabilisation buffer. The samples were stored overnight in 300µl of 1x staining buffer at 4°C in the dark and were analysed the following morning.

2.8.7 **Human inflammatory cytokines**

Quantification of human IL-6, IL-12p70, TNF-α, and IL-1β protein in supernatant was measured in a single sample using the cytometric bead array (CBA) human inflammatory cytokines kit (BD Biosciences). In a 96-well plate, 50µl per well of capture beads were added to all wells and 50µl of a serial two-fold dilution of cytokine standard (0-5,000 pg/ml) and 50µl of sample supernatant were added in

duplicate wells. The human inflammatory cytokine PE detection reagent was added to all wells at 50µl. The plate was incubated in the dark for 3 h and then centrifuged at 300xg for 5 min to pellet the beads. After carefully aspirating the supernatant, the wells were washed twice with 250µl of wash buffer. The pellets were resuspended in 100µl of wash buffer and acquired on the FACSArray (BD Biosciences).

2.8.8 Human B and T cell subsets

To assess B cell and T cell subsets in healthy and SLE PBMCs non-specific binding of antibodies was blocked by resuspending $1x10^6$ cells in 50µl and incubating with 10µl of FcR blocking reagent (Miltenyi Biotec) for 10 min at 4^oC. The cells were then washed and resuspended at $1x10^6$ cells in 100µl FACS buffer (PBS, 1% FCS) and stained for B cells with anti-human CD20, CD38, CD24, CD27, IgD, IgM, and CD1c antibodies, or T cells with anti-human CD3, CD4, and CD8 antibodies described in Table 2.3. After 20 min at 4^oC, the cells were washed and resuspended in 300µl FACS buffer to analyse immediately.

2.8.9 Mitochondrial membrane integrity

Human lymphocytes ($0.5x10^6$) were incubated in 50µl with nonylacridine orange (NAO) at a final concentration of 100nM at 37^oC for 15 min in the dark. The cells were then washed twice, resuspended in 300µl, and analysed immediately.

2.8.10 Caspase 3 and caspase 7 activation

Apoptosis in human lymphocytes was detected using the FAM-FLICA® *in vitro* Caspase-3/7 Detection kit (ImmunoChemistry Technologies), which fluorescently labels activated caspase 3 and caspase 7. Cells were resuspended at $2x10^6$ per ml and 290µl was pipetted into a FACS tube with 10µl of 30X FLICA solution. After 15 h, the cells were washed twice with 2ml of 1X apoptosis wash buffer by centrifuging at 230xg for 6 min. The cells were resuspended in 300µl of 1X apoptosis wash buffer and analysed immediately.

2.8.11 Autophagy detection

Autophagic vacuoles in healthy and SLE lymphocytes were analysed using the Cyto-ID® Autophagy detection kit (Enzo Life Sciences). $1x10^6$ cells were resuspended in

250µl 1X assay buffer and 250µl Cyto-ID green stain (1µl of Cyto-ID green detection reagent diluted in 1ml 1X assay buffer). The samples were mixed well and incubated at 37°C in the dark for 30 min, then washed twice with 1ml 1X assay buffer and centrifugation at 300xg for 5 min. The cells were resuspended in 300µl of 1X assay buffer and analysed immediately.

Staining protocol	Antibody (clone)	Fluorochrome	Isotype	Source	Dilution
Mouse pDC activation	Anti-CD40 (3/23)	PECy7	Rat IgG2aκ	BioLegend	1:200
	Anti-CD86 (GL-1)	BV421	Rat IgG2aκ	BioLegend	1:200
	Anti-MHC Class II (M5/114.15.2)	PECy5	Rat IgG2bκ	eBioscience	1:400
Intracellular IL-10	Anti-IL10	PE	Rat IgG2b	BD Biosciences	1:100
Mouse T & B cells	Anti-CD3 (145-2C11)	FITC	Armenian Hamster IgG	BioLegend	1:200
	Anti-B2.20 (RA3-6B2)	Percp	Rat IgG2aκ	BioLegend	1:200
	Anti-CD19 (6D5)	PE	Rat IgG2aκ	BioLegend	1:200
	Anti-CD21 (8d9)	APCe780	Rat IgG2aλ	eBioscience	1:200
	Anti-CD23 (B3B4)	PECy7	Rat IgG2aκ	BioLegend	1:200
HMGB1	Anti-HMGB1	Unconjugated	Rabbit IgG	Thermo Fisher	1:100
Human B cell subsets	Anti-CD20 (2H7)	Pacific Blue	Mouse IgG2bκ	BioLegend	1:125
	Anti-CD38 (HIT2)	BV605	Mouse IgG1κ	BioLegend	1:30
	Anti-CD24 (ML5)	FITC	Mouse IgG2aκ	BioLegend	1:40

	Anti-CD1c (L161)	Percp Cy5.5	Mouse IgG1κ	BioLegend	1:40
	Anti-IgM (polyclonal)	Texas Red	Goat	AbD Serotec	1:50
	Anti-CD27 (M-T271)	APC	Mouse IgG1κ	BD Biosciences	1:10
	Anti-IgD (IA62)	APC Cy7	Mouse IgG2aκ	BioLegend	1:40
Human T cells	Anti-CD3 (UCHT1)	BUV395	Mouse IgG1κ	BD Biosciences	1:40
	Anti-CD4 (OKT4)	Percp	Mouse IgG2b	BioLegend	1:40
	Anti-CD8	PE	Mouse IgG2aκ	ImmunoTool	1:50

Figure 2.3. Antibodies used for staining cells for flow cytometric analysis.

2.9 Cytokine ELISA

The concentration of human and mouse IL-10 and IL-6, mouse IFN-γ and IL-12, and human TNF-α and IL-1β (R&D Systems), and human IFN-α (eBioscience) were measured using standard ELISA with minor changes to the manufacturer's protocol. 96-well EIA/RIA plates (Corning) were coated overnight at room temperature with capture antibody and then washed three times with PBS (0.05% Tween-20) and patted on paper towel to remove excess fluid. The wells were blocked for 1 h at room temperature by adding 150µl ELISA block (1% BSA, 5% sucrose, 0.2% azide in PBS). After washing and drying the wells, a two-fold serial dilution of standard protein was performed in duplicate and cell culture supernatants were added to wells in triplicate in a final volume of 50µl per well. Dilutions of the standard and samples were performed in 1X reagent diluent (R&D Systems). The plates were incubated at room temperature for 1.5 h, then washed and incubated with 50µl of the detection antibody for 1 h at room temperature. After washing and drying the wells, 50µl of streptavidin horseradish peroxidase (HRP; 1:200) was added for 30 min at room temperature. The wells were then washed and dried prior to adding 50µl SureBlue™ Reserve TMB Microwell Peroxidase substrate (KPL Inc.). When the top standard

turned dark blue (10-15 min), the enzymatic reaction was stopped by adding 50µl 0.6N sulphuric acid.

The VeriKine mouse IFN-α ELISA kit, which detects all 13 IFN-α subtypes, was used to quantify the concentration of IFN-α in accordance with the manufacturer's protocol (PBL Interferon Source). A seven-point standard curve (6.25-400 pg/ml) was created by two-fold serial dilution in Sample Buffer and culture supernatant samples were diluted appropriately in Sample Buffer. Per well, 100µl of standard or sample were added to wells from the pre-coated microtiter plate followed by 50µl Antibody Solution. The plates were sealed and incubated at room temperature for 1 h with shaking at 450rpm and then incubated for a further 24 h at 4°C without shaking. After washing the wells four times with Wash Solution, 100µl of HRP solution was added per well and the plate was incubated at room temperature for 2 h with shaking at 450rpm. The wells were then washed four times and 100µl of TMB solution was added per well for 15 min followed by 100µl of Stop solution.

The Human IL-18 Instant ELISA (eBioscience) was used to detect human IL-18 in accordance with the manufacturer's instructions. In duplicate, two-fold serial dilutions of standard (78-5,000 pg/ml), or 100µl dH_2O plus 50µl of sample were added to pre-coated microwell strips. Following incubation at room temperature for 3 h with shaking at 400rpm, the wells were washed six times with PBS (0.05% Tween-20) then incubated with 100µl TMB substrate solution. When the highest standard turned dark blue, 100µl of Stop Solution was added immediately per well.

Absorbance values were read at 450nm on a Synergy HT plate reader (Biotech, Winnoski, U.S.A) using Gen5 (version V.1.01.14) software from BioTek. Absorbance readings from the standard curve were used to calculate the appropriate cytokine concentration of samples using GraphPad Prism software version 6.0.

2.10 Intracellular calcium flux

$CD19^+$ WT and $C1q^{-/-}$ cells were resuspended at $10x10^6$ per ml in cation-free HBSS (PAA Laboratories) and incubated with 2μM fura-2/AM for 30 min at 37°C. The cells were washed twice and incubated in cation-free HBSS for 10 min for optimal de-esterification then resuspended at $2x10^6$ per ml in HBSS with divalent cations. Changes in fluorescence upon addition of 10μg/ml anti-mouse IgM (Southern Biotec) were determined using the LS5OB luminescence spectrometer (Perkin Elmer) with dual wavelength excitation (340nm and 380nm) and emission at 510nm, and FLWinLab Software. To obtain the maximal fluorescence (R_{max}), 10% Triton X-100 was added to induce cell lysis and subsequent release of intracellular calcium. When this fluorescence became constant, the minimal fluorescence (R_{min}) was obtained by adding 250mM of the calcium chelator EGTA. The concentration of intracellular Ca^{2+}, $[Ca^{2+}]_i$ was calculated from the relationship $[Ca^{2+}]_i = Kd.(R - R_{min})/(R_{max} - R).b$, where R is the ratio of fluorescence obtained at 340nm and 380nm in the cuvette before calibration, R_{max} is the fluorescence ratio under saturating intracellular Ca^{2+}, R_{min} is the fluorescence ratio in the absence of Ca^{2+}, Kd is the dissociation constant for fura-2/AM (taken as 224nm at 37°C), and b is the fluorescence ratio at 340nm of cells in the absence and presence of Ca^{2+}.

2.11 Purification of serum IgG

IgG was purified from the serum of four SLE patients and three healthy blood donors using 100μl Protein G Sepharose beads (Sigma-Aldrich) per sample. Protein G beads were washed three times in 1ml PBS and centrifuged at 10,000xg for 5 min prior to mixing with 1ml of serum. Following continuous rolling for 30 min at room temperature the tubes were centrifuged at 10,000xg for 5 min and the serum discarded. IgG-Protein G beads were washed three times as before. 500μl 0.1M glycine (pH 2.7) was added to dissociate the beads from IgG, then the pH was neutralised with 1M Tris HCl (pH 9.0). The IgG-containing supernatant was added to dialysis high retention seamless membrane tubing (Sigma-Aldrich) and submerged in 5L of PBS with constant stirring at 4°C for 24 h, with the PBS replaced three times.

Centricon 100kDa centrifugal filter devices (Millipore) were used to concentrate the IgG antibody.

Total protein was quantified using DC protein assay reagents (Bio-Rad Laboratories). The protein standard was generated by diluting BSA (Europa Bioproducts) in PBS to 5mg/ml (top standard) and doing a two-fold dilution series in a 96-well plate (Corning). In triplicate wells, 5µl of sample or standard was added followed by 25µl of working reagent A (20µl of reagent S per 1 ml reagent A) and 200µl of reagent B. The plate was incubated for 15 min at room temperature on a plate shaker. Absorbance was read at 750nm using the Synergy HT plate reader and Gen5 software (version V.1.01.14). Absorbance readings from the protein standard were plotted against the known protein concentrations and the resulting line equation was used to calculate the protein concentration of the samples.

Additionally, the concentration of total IgG antibody was quantified by the Human IgG total Ready-SET-Go® ELISA (Affymetrix eBioscience) in accordance with the manufacturer's protocol. Capture antibody was added to 96-well EIA/RIA plates (Corning) and incubated overnight at 4°C. The wells were washed twice with wash buffer (PBS + 0.05% Tween-20) and patted on paper towel to remove excess fluid then 250µl of blocking buffer was added per well for 2 h at room temperature. After washing the wells, two-fold serial dilutions of the standards with assay buffer A was performed in duplicate and serum samples diluted 1:100,000 in assay buffer A were added to wells in triplicate. The plate was incubated at room temperature for 2 h on a microplate shaker at 400 rpm. 100µl of detection antibody was added to the washed wells and incubated at room temperature for 1 h on a microplate shaker at 400 rpm prior to washing and adding 100µl of Substrate Solution per well. After 15 min, adding 100µl Stop Solution to each well terminated the reaction and the plate was then read at 450nm using the Synergy HT plate reader and Gen5 software (version V.1.01.14).

2.12 TdT-mediated dUTP Nick-End Labeling (TUNEL)

Fragmented DNA in human lymphocytes was detected by confocal microscopy using the DeadEnd™ Fluorometric TUNEL system (Promega). $1x10^6$ cells were added to 96-well round-bottom plates (Corning) and fixed in 200µl 4% PFA for 25 minutes at 4^oC. The cells were then washed twice with PBS and centrifuged at 300xg for 5 min at room temperature. To permeabilise the cells they were incubated with 200µl 0.2% Triton-X 100 in PBS for 5 min. After washing twice with PBS, 200µl of equilibration buffer was added to the wells and incubated for 10 min at room temperature. The plate was centrifuged at 230xg for 6 min and the buffer was removed and replaced with TdT incubation buffer (per reaction: 180µl equilibration buffer, 20µl nucleotide mix, and 4µl rTdT enzyme) for a further 60 min in the dark at 37^oC. Adding 2x SSC buffer for 15 min at room temperature terminated the reaction. The cells were washed three times prior to counterstaining with DAPI (1:10,000), and adhered to slides by cytospin (300xg for 3 min). Coverslips were attached to the slides using ProLong gold antifade reagent (Invitrogen). Images were acquired on a Leica TCS SP5 (Leica Microsystems) confocal laser scanning microscope with a fixed stage inverted microscope DMI6000CS, equipped with a HCX PL APO 63x/1.33 NA oil immersion objective. Images were acquired using LAS AF software (Leica Microsystems) and fluorescence was measured using ImageJ software.

2.13 Scanning Electron Microscopy

The cells were fixed in a solution of 3% glutaraldehyde in 0.1 M sodium cacodylate buffer (pH 7.3) for 2 h. They were then washed in 3 x 10 min changes of 0.1 M sodium cacodylate buffer. Stephen Mitchell (Electron Microscopy Facility, School of Biological Sciences, University of Edinburgh, UK) prepared the fixed samples for viewing as follows: cells were post-fixed in 1% osmium tetroxide in 0.1 M sodium cacodylate buffer for 45 min. A further 3 x 10 min washes were performed in 0.1 M sodium cacodylate buffer. Dehydration in graded concentrations of acetone (50%, 70%, 90%, and 3 x 100%) for 10 min each was followed by critical point drying using liquid carbon dioxide. After mounting on aluminium stubs with carbon tabs

attached, the samples were sputter coated with 20nm gold palladium. The cells were then viewed using a Hitachi S-4700 scanning electron microscope.

2.14 Transmission Electron Microscopy

Cells were fixed in 3% glutaraldehyde in 0.1M Sodium Cacodylate buffer, pH 7.3, for 2 h then washed in three 10 min changes of 0.1M Sodium Cacodylate. Stephen Mitchell (Electron Microscopy Facility, School of Biological Sciences, University of Edinburgh, UK) prepared the fixed samples for viewing as follows: Cells were post-fixed in 1% Osmium Tetroxide in 0.1M Sodium Cacodylate for 45 min, then washed in three 10 min changes of 0.1M Sodium Cacodylate buffer. These samples were then dehydrated in 50%, 70%, 90% and 100% normal grade acetones for 10 min each, then for a further two 10-miN changes in analar acetone. Samples were then embedded in Araldite resin. Sections, 1µm thick were cut on a Reichert OMU4 ultramicrotome, stained with Toluidine Blue, and viewed in a light microscope to select suitable areas for investigation. Ultrathin sections, 60nm thick were cut from selected areas, stained in Uranyl Acetate and Lead Citrate. The cells were viewed in a Philips CM120 Transmission electron microscope and images were taken on a Gatan Orius CCD camera.

2.15 Western Blotting

2.15.1 Cell lysis

A stock of 2X RIPA buffer (Table 2.4) was diluted to 1X immediately prior to use by mixing 500µl 2X RIPA buffer with 300µl dH_20 and 200µl Complete mini protease inhibitor cocktail (Roche, Sigma-Aldrich). 50µl 1X RIPA buffer was added to each cell pellet following washes in cold PBS and centrifuging at 300xg for 5 min. The pellet was then vortexed and incubated on ice for a total of 30 min, vortexing every 10 min. The lysate was centrifuged at 12,000xg for 15 min at 4^{o}C and the supernatant was pipetted in to a new tube and stored at -20^{o}C.

Reagent	Concentration
Tris (pH 7.4)	20mM
NaCl	200mM
EDTA	2mM
EGTA	2mM
SDS	0.2%
Sodium deoxycholate	1%
Triton-X 100	2%
Glycerol	20%

Table 2.4 2X RIPA Buffer

2.15.2 Quantification of protein concentration

Cell lysates were thawed slowly on ice and then quantified using the DC protein assay reagents (Bio-Rad Laboratories) as described in section 2.11. The protein standard was generated by diluting BSA (Europa Bioproducts) in RIPA buffer to 5mg/ml (top standard) and doing a two-fold dilution series in a 96-well plate.

2.15.3 SDS-PAGE and Transfer

20µg of protein samples were prepared for gel electrophoresis by adding 5x Laemmli buffer to obtain a 1x dilution. To further denature proteins, the samples were heated to 95^{o}C for 5 min followed by brief centrifugation. The samples were loaded onto a 12% gel (Table 2.5 and 2.6) alongside SeeBlue Plus2 pre-stained protein standard (Invitrogen) for determination of band molecular weight. The gel tank (Bio-Rad) was filled with running buffer (25mM Tris, 192mM glycine, 0.1% SDS in dH_2O) and run at 170V for 5 min, or until the samples had moved out of the wells, then 130V for approximately 90 min. Proteins were then transferred onto a PVDF membrane (GE Healthcare) using the semi-dry transfer method. Membranes were pre-soaked in methanol before being equilibrated in transfer buffer (25mM Tris, 192mM glycine, 10% methanol in dH_2O). Gels were rinsed in transfer buffer and layered on top of the membrane and the gel/membrane was sandwiched between blotting paper in a Trans-Blot semi-dry (Bio-Rad). After running at 30V for 45 min, membranes were blocked in 1x TBST (20 mM Tris, 150 mM NaCl. 0.1% Tween-20; pH 7.4) containing 5% milk for 1 h at room temperature. Membranes were immunoblotted overnight at 4^{o}C in 1x TBST/5% milk with the relevant antibodies stated in the results chapter at

dilutions stipulated in Table 2.7. The membranes were washed 4x for 15 min in 1x TBST then incubated in goat anti-rabbit HRP-conjugated secondary antibody (1:3000; Santa Cruz Biotechnology) for 45 min at room temperature with rotation. After washing for 2 h with 1x TBST replaced every 15 min, the blots were developed with WestFemto enhanced chemiluminescent substrate (ThermoFisher Scientific).

Reagent	Volume (mL) for one gel
dH_20	3.3
30% acrylamide mix	4.0
1.5 M Tris (pH 8.8)	2.5
10%SDS	0.1
10% ammonium persulfate	0.1
TEMED	0.004

Table 2.5. 12% Resolving Gel

Reagent	Volume (mL) for one gel
dH_20	2.7
30% acrylamide mix	0.67
1.0 M Tris (pH 6.8)	0.5
10%SDS	0.04
10% ammonium persulfate	0.04
TEMED	0.004

Table 2.6. 5% Stacking Gel

Antibody	Host	Source	Dilution
Anti-ATG5	Rabbit	Abcam	1:2000
Anti-LC3B	Rabbit	MBL International	1:1000
Anti-ATG3	Rabbit	Abcam	1:1000
Anti-β–actin	Rabbit	Abcam	1:5000

Table 2.7. Antibodies used for western blotting

2.16 RNA extraction

2.16.1 Chloroform/Isopropanol Method

$1x10^6$ cells cells were washed in PBS and centrifuged at 300xg for 5 min. 100µl TRI Reagent (Ambion) was added to the cell pellet, which was then mixed by gently pipetting to lyse the cells and incubated at room temperature for 5 min. 30µl chloroform (Sigma-Aldrich) was added per 100µl TRI Reagent and the tubes were vortexed for 15 sec, incubated on ice for 5 min, and then centrifuged at 12,000xg for 15 min at 4°C. The upper aqueous phase containing RNA was carefully collected and transferred to a new tube. To precipitate RNA, 50µl isopropanol (Sigma-Aldrich) was added per 100µl TRI Reagent originally used, and 1µl glycogen (Invitrogen) was added to enhance RNA sedimentation. The samples were subsequently incubated for 10 min at room temperature and then centrifuged at 12,000xg for 10 min at 4°C. The supernatant was carefully removed and 100µl of 75% ethanol was added to the remaining RNA pellet. After briefly vortexing and incubating for 10 min at room temperature, the samples were then centrifuged at 5000xg for 5 min at 4°C. The supernatant was removed and the RNA pellet was air-dried for 15 min on ice. To DNase treat the RNA, the pellet was resuspended in 8µl RNase-free water, mixed with 1µl RQ1 DNase 10X reaction buffer and 1µl RQ1 RNase-Free DNase (Promega) then incubated for 30 min at 37°C. The reaction was stopped by adding 1µL RQ1 Stop Reaction Buffer (Promega) and incubating for 10 min at 65°C. 30µl RNase-free water (Ambion) and 55µl isopropanol was then added to the RNA and incubated for 10 min at room temperature. The RNA was centrifuged at 12,000xg for 15 min at 4°C. After removing the supernatant 100µl 75% ethanol was added, the sample was incubated for 15 min at room temperature, and centrifuged at 12 000xg for 5min, 4°C. The ethanol was removed and the pellet was air-dried for 15 min on ice. RNA was re-suspended in 15µl RNase-free water. RNA concentration was measured by the NanoDrop 1000 spectrophotometer (Thermo Scientific).

2.16.2 Qiagen RNeasy Mini Kit Method

$2x10^6$ cells were washed in PBS and centrifuged at 300xg for 5 min then the pellet was lysed in 250µl TRI Reagent (Ambion), as described in 2.16.1. 30µl chloroform

(Sigma-Aldrich) was added per 100µl TRI Reagent and the tubes were vortexed for 15 sec, incubated at room temperature for 2-3 min, and then centrifuged at 12,000xg for 15 min at 4°C. The upper aqueous phase containing RNA was carefully collected and transferred to a new collection tube. Per 100µl of aqueous phase, 350µl of cold buffer RLT and 250µl of cold 100% ethanol were added. The sample was vortexed, pipetted into an RNeasy Mini column with a 2ml collection tube, and centrifuged at 12,000xg for 15 sec at room temperature. After discarding the flow through, on-column DNase digest was performed as follows. 500µl of buffer RW1 was pipetted in the column and centrifuged at 12,000xg for 15 sec. The column was then added to a new collection tube and DNase 1 mix (10µl DNase with 70µl of buffer RDD) was pipetted directly onto the centre of the column for 15 min at room temperature. 500µl of buffer RW1 was added to the column and centrifuged at 12,000xg for 15 sec. The collection tube was changed and 500µl of buffer RPE was pipetted in the column and centrifuged at 12,000xg for 15 sec. The flow through was then discarded and 500µl of buffer RPE was pipetted in the column and centrifuged at 12,000xg for 2 min. To remove the last drops of buffer the column was added to a new collection tube and centrifuged at maximum speed for 2 min with open an open lid. To recover the RNA in the flow through, 12µl RNase-free H_2O was pipetted directly onto the centre of the column, incubated for 2 min at room temperature, and centrifuged at 12,000xg for 1 min. RNA concentration was measured by the NanoDrop 1000 spectrophotometer (ThermoScientific), and stored at -80^{o}C.

2.17 Quantitative real-time PCR (qPCR)

2.17.1 Reverse transcription of RNA to cDNA

RNA was reverse transcribed to cDNA using the High Capacity cDNA reverse transcription (RT) kit (Applied Biosystems/Life Technologies). 1µg RNA was made up to 10µl with nuclease-free H_20 (Ambion) in 0.6 ml thin-walled PCR tubes (Thermo Fisher Scientific) and 10µl 2x RT master mix (Table 2.8) was added. The tubes were placed in the iCycler Thermal Cycler (Bio-Rad) and reverse transcription was performed using the following conditions: annealing at 25^{o}C for 10 min,

extension at 37°C for 120 min, denaturing at 85°C. The cDNA samples were stored at -20°C until required.

Component	Volume per sample (µl)
10x RT Buffer	2.0
25x dNTP mix (100mM)	0.8
10x RT Random Primers	2.0
MultiScribe Reverse Transcriptase	1.0
RNase Inhibitor	1.0
Nuclease-free H_20 (Ambion)	3.2

Table 2.8. 2X Reverse Transcription master mix

2.17.2 qPCR using Taqman assay

20ng of cDNA in a final volume of 10µl was pipetted into duplicate wells in a MicroAmp Fast Optical 96-well plate (Applied Biosystems). Per well, 15µl of reaction mastermix (12.5µl 2X Taqman Universal PCR Mastermix, 1.25µl 20X Taqman probe, 1.25µl Nuclease-free H_20) was added. Taqman probes were used for analysis of human ATG5 (Hs00169468_m1), ATG3 (Hs00223937_m1), Calpain-1 (Hs00559804_m1), and Calpain-2 (Hs00965097_m1). In separate wells, the relative gene expression between cDNA samples was quantitated using the endogenous control gene 18S rRNA. Per well, 2µl of diluted cDNA was added and mixed with 23µl of reaction mastermix (12.5µl 2X Taqman Universal PCR Mastermix, 1.25µl 20X Eukaryotic 18s rRNA (FAM/MGB) probe, 9.25µl Nuclease-free H_20). The plates were sealed with MicroAmp® Optical adhesive film (Life Technologies) and centrifuged at 300xg for 30 sec. Plates were run on a 7900HT Fast-real time system using SDS software version 2.4.1 (Applied Biosystems) with PCR amplification cycle: 50°C 2 min 1x cycle, 95°C 10 min 1x cycle, 95°C 15 sec and 60°C 1 min 40x cycles.

Resulting threshold cycles (C_T) values were obtained from the amplification plot. The data was analysed using delta-delta C_T, which normalises the fold difference in samples to the fold difference in the respective 18S reference gene.

2.18 SNP Genotyping

SNP genotyping was performed on genomic DNA from controls (*n*=23 healthy and *n*=15 control patients) and SLE patients (*n*=42). The donors were matched for age (control 45 [24-77]; SLE 47 [21-71]) and sex F:M (control 5.3:1; SLE 6:1).

2.18.1 Isolation of DNA from whole blood

200µl of whole blood extracted from healthy donors, SLE patients, and patient controls was pipetted in to a 0.5ml eppendorf tube and snap-frozen on dry ice. The frozen blood was stored at -80^{o}C until used. Genomic DNA was isolated from the blood using the FlexiGene DNA kit (Qiagen). The frozen blood was thawed quickly in a 37^{o}C water bath and transferred to a 1.5ml eppendorf tube. 500µl Buffer FG1 was added to the blood and mixed by inversion of the tube then centrifuged at 10,000xg for 20 sec. After discarding the supernatant the tube was inverted on to a clean sheet of absorbent paper towel for 2 min. A mixture of 100µl Buffer FG2 and 1µl Qiagen Protease was prepared, which was added per sample and immediately vortexed for 5 sec. The tube was centrifuged briefly and then placed in a heating block at 65^{o}C for 5 min to digest the protein. 100µl isopropanol (100%) was added and the sample was mixed by inversion until the DNA precipitated. Following centrifugation at 10,000xg for 5 min the supernatant was discarded and 100µl ethanol (70%) was added and the tube was vortexed for 5 sec. The tube was centrifuged at 10,000xg for 5 min and the supernatant discarded. After inversion on to a clean sheet of absorbent paper towel for 5 min, the DNA was air-dried for 5 min and the DNA was dissolved in 200µl Buffer FG3 at 65^{o}C for 1 h. The DNA was quantified using the NanoDrop 1000 spectrophotometer (ThermoScientific).

2.18.2 Analysing DNA integrity by Agarose Gel Electrophoresis

Integrity of gDNA was checked on 2% agarose gels following isolation from blood. To make the agarose gel, 1.2g agarose was dissolved in 1X TAE buffer (40mM Tris, 20mM Acetate and 1mM EDTA) by heating the mixture and adding GelRed™ nucleic acid gel stain (1:10,000; Biotium). When it had cooled the gel was poured into a mini-sub cell GT tank (Bio-Rad) with a 15-lane comb. 10µl of gDNA sample

was mixed with 2µl blue/orange 6X loading dye (Promega) and loaded in to the lanes alongside Quickload 100bp DNA ladder (New England BioLabs). The gel tank was filled with 1X TAE buffer and run at 80V for 1 h and then imaged using a U:Genius3 (Syngene).

2.18.3 Taqman SNP Genotyping Assay

13.75µl of reaction mix (12.5µl 2X Taqman Genotyping Mastermix and 1.25µl 20X predesigned SNP genotyping assay) was pipetted into each well in MicroAmp Fast Optical 96-well plate (Applied Biosystems). gDNA was diluted to 10ng in nuclease-free H_2O to a final volume of 11.25µl and then added to wells in duplicate. The plates were sealed with MicroAmp® Optical adhesive film (Life Technologies) and briefly centrifuged. Each assay contained two Taqman MGB probes with different reporter dyes at the 5' end to distinguish the two alleles (Allele 1/Allele 2) at the SNP site. VIC dye was linked to allele 1 and FAM dye was linked to allele 2. The following SNPs were analysed **(allele 1/allele 2)**:

ATG5 rs573775

CCATGCTCACAGCCCTCTGGCCCCA**(A/G)**TGAAACAGTAAATGCTTCCACTTGG

ATG5 rs6568431

CACTTCAGTCAGCTAGGAAAGATAC**(A/C)**CTTTTGGCAGGGTGCGGTGGCTCAC

DRAM-1 rs4622329

ACATGTCTTCTTTTTATGGGCAAGA**(A/G)**TGTCTCCAGTTCACTTGGGTTTTTC

ATG16L-1 rs2241880

CCCAGTCCCCCAGGACAATGTGGAT**(A/G)**CTCATCCTGGTTCTGGTAAAGAAGT

Plates were run on a 7900HT Fast-real time PCR system using SDS software version 2.4.1 (Applied Biosystems). An allelic discrimination pre-read run was performed to record the background fluorescence of each well. The amplification run was performed using the thermal profile: 2 min at 50°C, 10 min at 95°C followed by 40X cycles each of 15 sec at 95°C and 1 min at 60°C. An allelic discrimination post-read run then recorded the fluorescence of each well and subtracted the pre-read run

values to obtain the fluorescence that was caused by the PCR amplification. Taqman Genotyper Software was used to analyse the raw data.

2.19 Phagocytosis Assays

For visualisation of apoptotic cells, healthy and SLE lymphocytes, and non-adherent iBMK cells were re-suspended at $10x10^6$ cells per ml in serum-free IMDM and labelled with cell membrane tracker (CM) green, or orange, 1μg/ml (Invitrogen), for 15 min at 37°C. Fluorescently labelled cells were washed in serum-containing medium and induced to become apoptotic by UV irradiation ($100mJ/cm^2$) at $1x10^6$ cells per ml. Apoptotic cells were used in the phagocytosis assay at a ratio of 5:1 (apoptotic cell: macrophage). Zymosan A (*S. cerevisiae*) bioparticles conjugated to AF594 (Molecular Probes, Life Technologies) were used in the phagocytosis assay at a ratio of 8:1 (zymosan: macrophage) as described previously[247]. After 1 h at 37°C 5% CO_2 macrophages were washed twice with PBS to remove apoptotic cells and zymosan bioparticles that had not been phagocytosed.

2.19.1 Confocal microscopy

For measuring phagocytic index by confocal microscopy, macrophages on coverslips were fixed with 4% PFA for 20 min, stained with DAPI (1:10,000) for 5 min and mounted on to slides using ProLong gold antifade reagent (Invitrogen). Images were acquired on a Leica TCS SP5 (Leica Microsystems) confocal laser scanning microscope with a fixed stage inverted microscope DMI6000CS, equipped with a HCX PL APO 63x/1.33 NA oil immersion objective. Images were acquired using LAS AF software (Leica Microsystems) and analysed using ImageJ software. The phagocytic index was defined as the product of the percentage of macrophages positive for phagocytosis and the number of apoptotic cells/zymosan bioparticles per macrophage, as previously described[45].

2.19.2 Flow cytometry

To detect phagocytosis by flow cytometry, macrophages were detached from the well by adding 500μl Accutase® cell detachment solution for 15 min at room temperature. HMDMs were stained with anti-human CD14 AF647 clone HCD14

(BioLegend) and BMDMs were stained with anti-mouse F4/80 APC clone BM8 (eBioscience; performed by Katherine Miles) for 20 min at 4^{o}C then acquired using the LSR Fortessa (BD Biosciences).

2.20 LC3-associated phagocytosis (LAP) assays

Healthy and SLE monocytes were cultured on coverslips at 2x10^{6}/ml for three days, as described in section 2.3.1. CM-green labelled healthy donor CD4^{+} lymphocytes were UV irradiated (100mJ/cm^{2}) at 1x10^{6} per ml, and incubated overnight (500µl per well in a 24-well plate) to become apoptotic. The apoptotic CD4^{+} lymphocytes were counted and added to the macrophages on coverslips at 1.5x10^{6} per well in 250µl for 60 min. All healthy and SLE day macrophages were fed CD4^{+} lymphocytes from the same healthy donor. The zymosan bioparticles were added as described in section 2.19. After the incubation period, coverslips were washed twice with PBS to remove free apoptotic cells and zymosan bioparticles. To permeabilise the macrophages and release non-membrane bound LC3, the coverslips were incubated in digitonin, 100µg/ml (Sigma-Aldrich) in PBS containing 1% PFA for 2 min on ice. After washing in TBS (20mM Tris/100mM NaCl) + 0.01% Tween-20, the macrophages were fixed in 4% PFA (Sigma-Aldrich) for 20 min at room temperature. The coverslips were briefly washed then incubated in TBS containing 1% BSA, 0.3M glycine, and 0.05% Tween-20 for 30 min at room temperature to block non-specific antibody binding. 250µl of primary polyclonal antibody, anti-LC3, (1:300; MBL International) in TBS/1% BSA was added to coverslips in 24-well plates overnight at 4°C. The coverslips were washed for five repeats of 5 min then incubated for 1 h at room temperature with secondary antibody, goat anti-rabbit AF647 (1:400; Life Technologies) for macrophages cultured with apoptotic cells, and goat anti-rabbit AF488 (1:400; Life Technologies) for macrophages cultured with zymosan bioparticles. The coverslips were washed for five repeats of 5 min then stained with DAPI (1:10,000) for 5 min and mounted on to slides using ProLong gold antifade reagent (Invitrogen). Images were obtained by confocal microscopy as described in section 2.6.1.

2.21 Statistical analysis

All statistical analysis was performed using GraphPad Prism 6. Where appropriate, results are reported as the mean of *n* experiments ± standard error of the mean (SEM). Comparisons between two groups were assessed by Student's *t*-test and for data containing more than two groups the analysis of variance (ANOVA). A paired *t*-test was performed if the comparison was between matched samples (*i.e*. untreated compared to treated). SNP genotype frequencies and distribution between controls and SLE patients was tested using 3 x 2 contingency tables and the χ^2 test, and the allele frequencies were tested using the Fisher's exact test stating odds ratio (OR) and 95% confidence interval (95% CI). *P* values less than 0.05 were considered significant to reject the null hypothesis.

Chapter 3 Apoptotic cells induce differential cytokine secretion by activated pDCs

3.1 Introduction

The innate immune pDC is best known for its ability to secrete large amounts of type I IFN in response to viral infection[152]. The selective expression of TLR7 and TLR9, and constitutive expression of IRF7, leads to the rapid production of type I IFN and downstream effector molecules, which ensures that pDCs are rarely infected themselves with virus[198]. Rather, they sense virally infected host cells, many of which have undergone apoptosis[201,264]. Following infection-induced apoptosis, complexes containing viral particles and host nucleic acids are expressed on the surface of apoptotic cells and smaller apoptotic bodies[265].

Once engulfed within the pDC, viral particles are trafficked to endosomes where they encounter TLRs. Here single stranded RNA is recognised by TLR7, whilst double-stranded DNA stimulates TLR9. Synthetic immuno-stimulatory oligonucleotide sequences (ISS) include the TLR9 ligands CpGA, CpGB and the TLR7 ligand R848. CpGA forms multimeric complexes that are held up in the early endosomes, stimulating MyD88-IRF7 and leading to type I IFN secretion[266,267]. In contrast, monomeric CpGB homes to the late endosomal lysosomal pathway, stimulating MyD88-NF-κB and the secretion of IL-6, TNF-α and pro-inflammatory chemokines[268,269]. This size-mediated intracellular trafficking is believed to explain the differential effect on cytokine production[102].

To carry out immune surveillance, pDCs circulate through the blood entering secondary lymphoid organs via high endothelial venules, where they gather in the T cell regions and the marginal zone of the spleen[270]. They are also recruited to damaged tissues where they encounter apoptotic cells within an inflammatory milieu[102,140]. PDCs are therefore in a prime position to interact with either healthy or

infected apoptotic cells being filtered from the blood into the splenic marginal zone, or dying at sites of infection and inflammation[271]. However, it is generally believed that pDCs only recognise late apoptotic/secondarily necrotic cell derived nucleic acids in association with high-titre autoantibodies found in SLE[272], or bound to the antimicrobial peptide LL37, released from NETotic neutrophils[93,273]. Receptor-mediated uptake of these immune complexes by pDCs then leads to the secretion of IFNα following TLR7/9 activation[98-101,272].

Although the nuclear antigens associated with SLE are expressed on the surface of apoptotic cells during the normal process of programmed cell death[6,73,274], the intracellular location of TLR7 and TLR9 is thought to shield the pDC from mammalian nucleic acid under normal conditions[166]. However immature pDCs can endocytose antigens from infected[275] and apoptotic cells[276], suggesting that they should be able to interact with and endocytose chromatin complexes expressed by apoptotic cells. Furthermore, TLR9-activated pDCs promote immune tolerance via the generation of regulatory T cells[189]. Currently the literature draws conflicting conclusions on the response of pDCs to apoptotic cells.

Aims

The main hypothesis of this chapter was that pDCs respond to primary apoptotic cells, but immunity or tolerance is promoted depending on the context in which they are recognised. This was evaluated using the following aims:

- Compare the cytokine response of highly purified pDCs co-cultured with synthetic TLR7/9 ligands and apoptotic, or necrotic primary cells.
- Establish if the co-recognition of apoptotic cells and virus enhances IFN-α production by pDCs.
- Assess how pDCs recognise apoptotic cells and what is required for inducing IL-10 secretion.

3.2 Results

3.2.1 Apoptotic cells do not stimulate pDCs *in vitro.*

PDCs are likely to encounter healthy apoptotic cells *in vivo*, so I first asked if they sensed apoptotic cells as a danger signal. In the absence of other stimuli, highly purified murine splenic pDCs (Appendix B Figure 1) were co-cultured for up to three days with apoptotic thymocytes. In the presence of apoptotic cells, pDCs did not upregulate expression of activation markers CD40, CD86 and MHC Class II (Figure 3.1.A). They also did not secrete cytokines, including IL-10, IL-6, IFN-γ, IL-12, or IFN-α (Figure 3.1.B), even though 30% of apoptotic cells had started to become secondarily necrotic within 24 hours (Figure 3.1.C).

3.2.2 PDCs that have interacted with apoptotic cells produce IL-10 or IFN-α depending on the TLR stimulus.

PDCs rapidly die *in vitro* unless survival is maintained by additional activation[277,278]. I included the TLR7 ligand R848 in the co-culture with apoptotic cells, which upregulated the pDC activation markers CD86, CD40 and MHC Class II, and promoted pDC survival (Figure 3.2A-D). The combination of apoptotic cells and R848 induced the pDCs to secrete significantly more IL-10, IL6, and IFN-γ (Figure 3.3.A-C), but not IL-12, or IFN-α (Figure 3.3.D-E) three days (and seven days, Figure 3.3.Aii) following co-culture. A similar pattern of cytokine secretion was seen when pDCs were stimulated with the TLR9 ligand CpGB (Figure 3.3.A-E), which was shown to bind to the surface of apoptotic cells (Appendix B Figure 2.Ai). In contrast, IL-10, IL6, IFN-γ, and IL-12 were not enhanced when pDCs were cultured with apoptotic cells and the synthetic TLR9 ligand CpGA (Figure 3.3.A-D), which also interacted with the apoptotic cell surface (Appendix B Figure 2.Bi); whereas IFN-α secretion was significantly augmented (Figure 3.3.E). To determine if this effect was specific to apoptotic thymocytes, TLR-activated pDCs were also co-cultured with apoptotic splenic B cells, which yielded similar results (Figure 3.3.F-G). Apoptotic cells that were cultured alone with TLR ligands were not stimulated to produce cytokines. The time points and concentration of synthetic TLR ligands were selected based on initial time courses and dose responses (Appendix B Figure 3).

It is currently believed that pDCs do not produce IL-10 in response to TLR stimuli alone[279], though it has not been investigated how TLR-stimulated pDCs respond to apoptotic cells. I confirmed that IL-10 was being generated by pDCs in co-culture using intracellular IL-10 staining. Following three days of co-culture with apoptotic cells and R848, a mean of 12.5% pDCs expressed IL-10 protein and this was still evident seven days later in a mean of 9% of the pDCs (Figure 3.4.A-B). Intracellular IL-10 was not detected in R848-stimulated pDCs in the absence of apoptotic cells (Figure 3.4.A), or in more than 2% of the apoptotic cells (Figure 3.4.C).

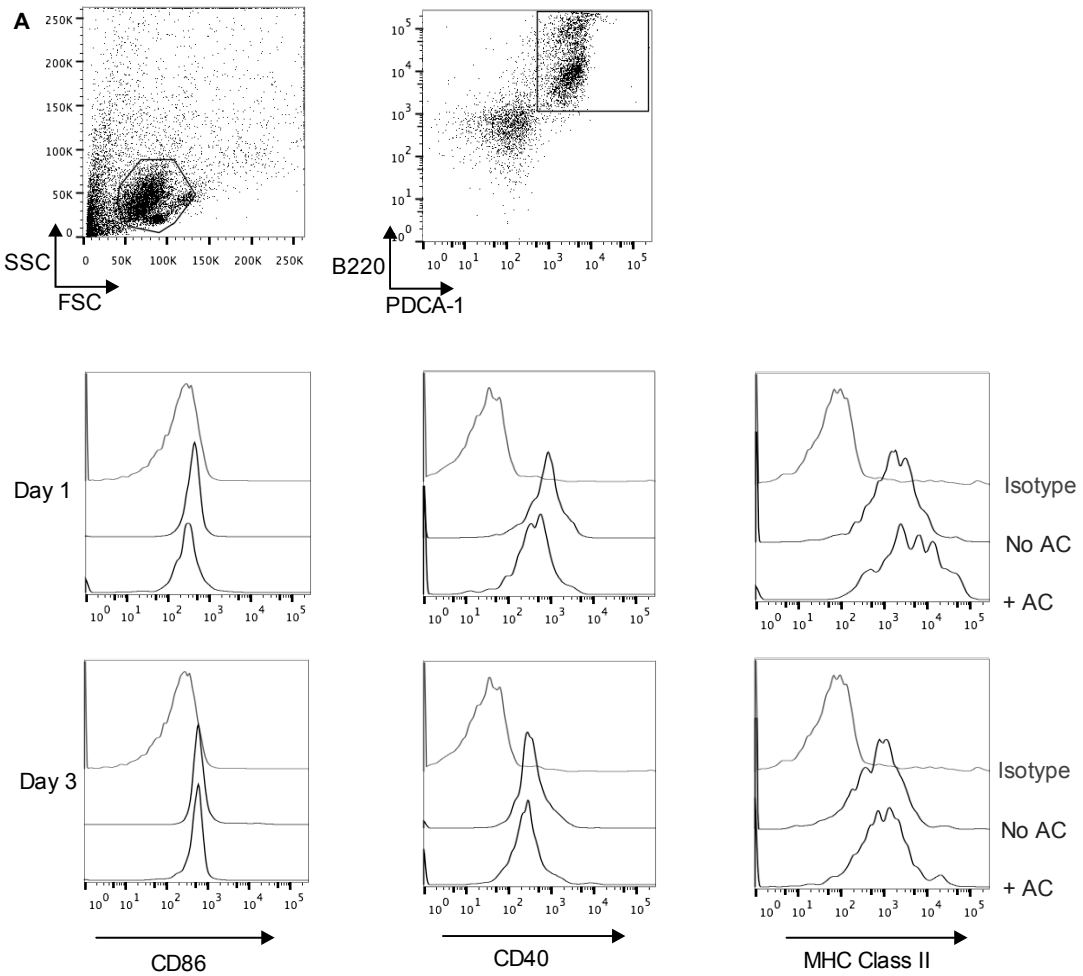
A
SSC
FSC
B220
PDCA-1
Day 1
Day 3
Isotype
No AC
+ AC
CD86
CD40
MHC Class II

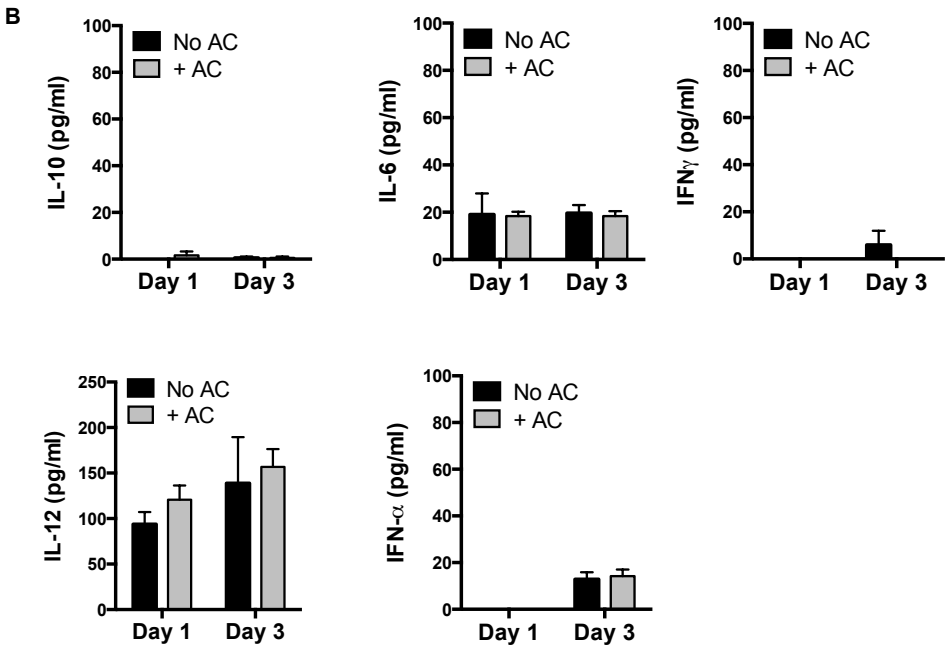
B
IL-10 (pg/ml)
IL-6 (pg/ml)
IFNγ (pg/ml)
IL-12 (pg/ml)
IFN-α (pg/ml)
No AC
+ AC
Day 1
Day 3

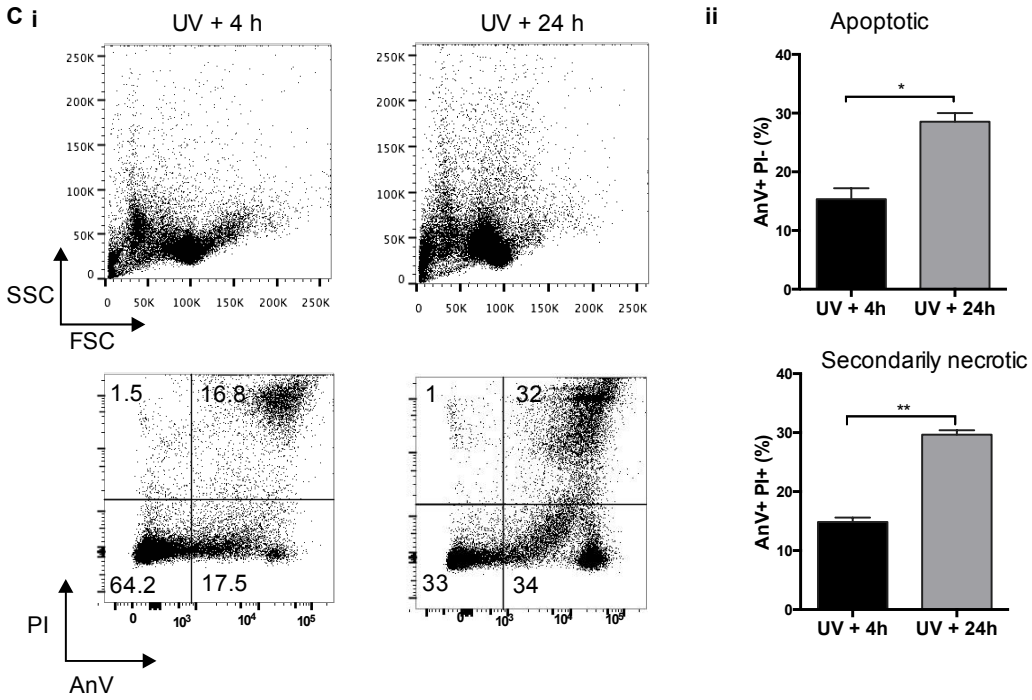

Figure 3.1. Apoptotic cells do not stimulate pDCs *in vitro*.

Beginning on the previous page, (**A**) pDCs were cultured alone (No AC) and with 10^6 UV-irradiated apoptotic thymocytes (+ AC) for one and three days. The cells were harvested and analysed by flow cytometry using the markers PDCA1 and B220 to select for pDCs, and the activation markers CD86, CD40, and MHC Class II. (**B**) The secretion of IL-10, IL-6, IFN-γ, IL-12, and IFN-α by pDCs cultured alone (No AC, black bar) and with 10^6 UV-irradiated apoptotic thymocytes (+ AC, grey bar) was measured in cell supernatants after one and three days in culture. (**Ci**) Representative FACS plots showing annexin V and propidium iodide staining of thymocytes 4 h and 24 h after UV irradiation. (**Cii**) The mean proportion of apoptotic ($AnV^+ PI^-$) and secondarily necrotic (AnV^+PI^+) thymocytes 4 h (black bar) and 24 h (grey bar) after UV irradiation. Error bars represent SEM of three independent experiments. Statistical significance was determined by *t* test. * P= 0.0303; ** P=0.0052.

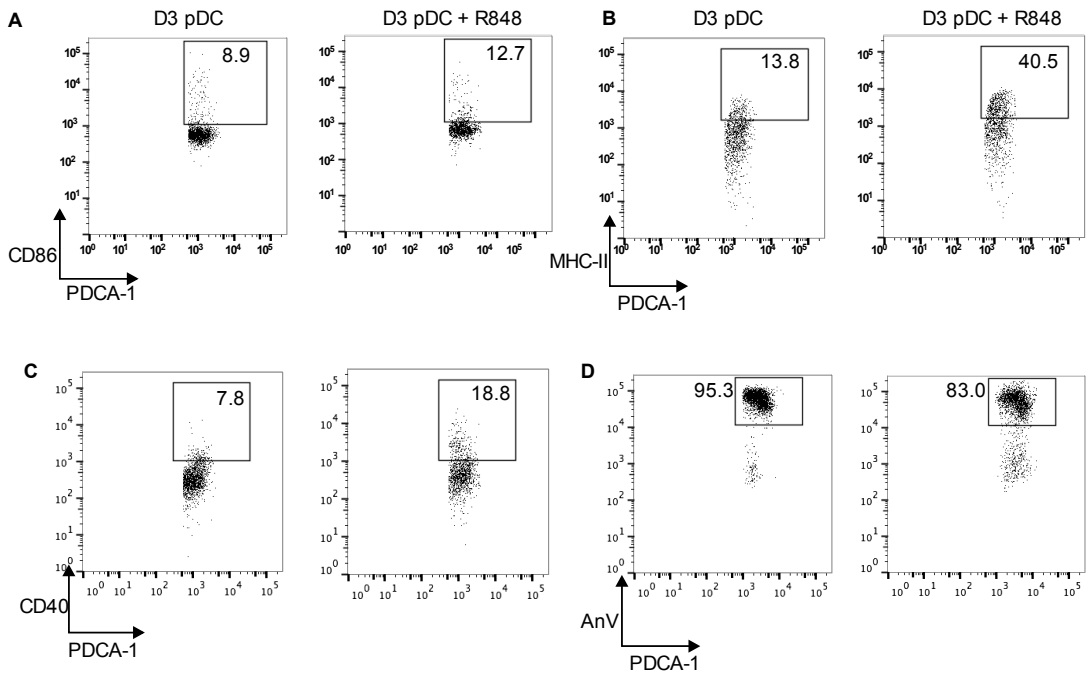

Figure 3.2. TLR7 stimulation by R848 induces pDC activation and survival

PDCs were cultured for three days alone (D3 pDC) and with R848 (D3 pDC + R848) and then analysed by flow cytometry for the expression of (**A**) CD86, (**B**) MHC Class II, (**C**) CD40, and (**D**) annexin V (AnV). FACS plots represent one of three independent experiments.

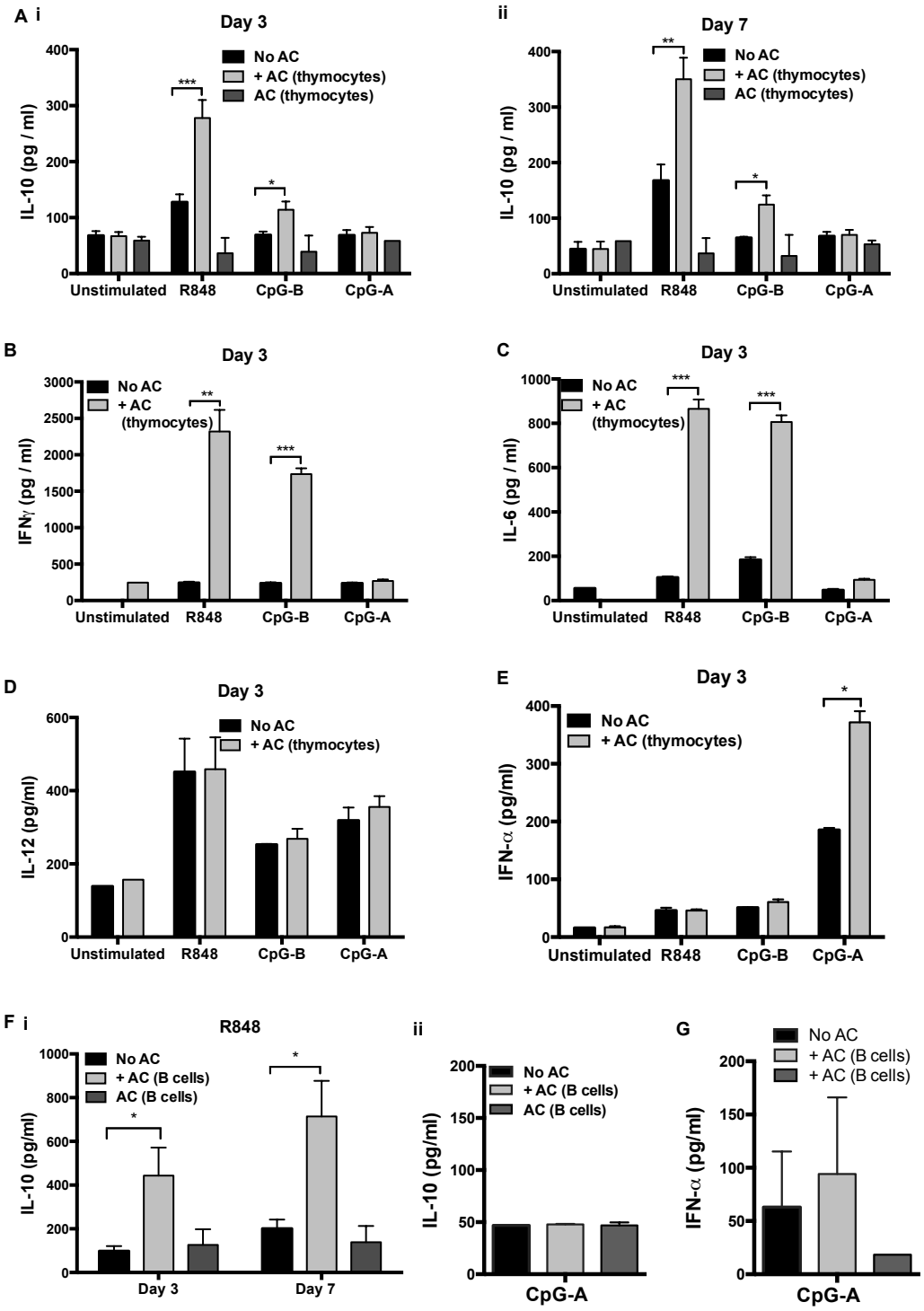

Figure 3.3. Apoptotic cells induce pDCs to produce IL-10, or IFN-α depending on the TLR stimulus.

pDCs were unstimulated, or stimulated with R848 (1μg/ml), CpGB (10μg/ml), and CpGA (20μg/ml) and were cultured alone (No AC, black bar), or with 10^6 apoptotic thymocytes (+ AC, light grey bar). Apoptotic (AC) thymocytes were cultured alone unstimulated, or stimulated with R848, CpGB, and CpGA, which did not result in

cytokine production. IL-10 protein was measured in cell supernatants by ELISA after (**Ai**) three days and (**Aii**) seven days in culture. (**B**) IFN-γ, (**C**) IL-6, (**D**) IL-12, and (**E**) IFN-α protein production were also quantified by ELISA after three days in culture. (**Fi**) IL-10 was measured in the cell supernatants three days and seven days after pDCs stimulated with R848 were cultured alone, or with $2x10^5$ apoptotic (AC) B cells. CpGA-stimulated pDCs were cultured with and without apoptotic B cells for three days then (**Fii**) IL-10 and (**G**) IFN-α were quantified in cell supernatant. Data are the mean of three to eight independent experiments. Error bars represent SEM. Statistical significance was determined by *t*-test, comparing cytokine responses by pDCs with and without apoptotic cells. * $p < 0.05$; ** $p < 0.01$; *** $p < 0.001$.

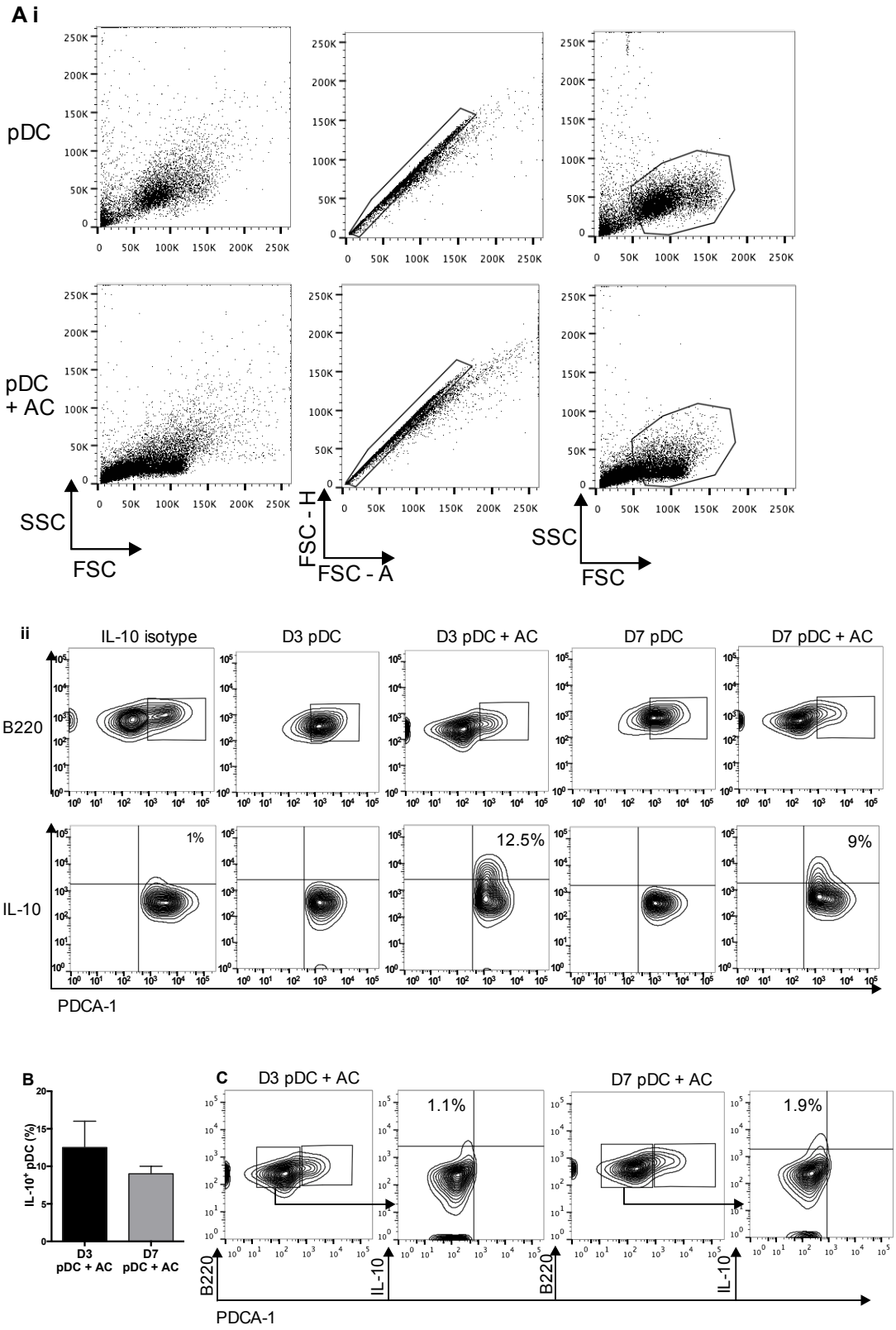

Figure 3.4. TLR-stimulated pDCs secrete IL-10 after co-culture with apoptotic cells.

(**A**) PDCs stimulated with R848 and cultured alone (pDC) or with apoptotic B cells (pDC + AC) for three days (D3) and seven days (D7) were harvested and stained for intracellular IL-10. (**i**) FACS plots showing the gating strategy to select single cells. (**ii**) FACS plots showing the gating strategy of selecting IL-10-positive pDCs. FACS plots are representative of three independent experiments. (**B**) The mean percentage of IL-10 secreting pDCs ($PDCA1^+$ $B220^+$ $IL\text{-}10^+$) following culture with apoptotic B cells. Error bars represent SEM. (**C**) Representative FACS plots of intracellular IL-10 in apoptotic B cells ($B220^+$ $PDCA1^-$) cultured with R848 and pDCs for three and seven days.

3.2.3 PDCs respond to direct contact with whole apoptotic, but not necrotic cells.

It has been reported that pDCs secrete IFN-α in response to nuclear material released from necrotic cell lines that is in a complex with autoantibodies[272]. I asked if necrotic debris derived from primary cells could also induce pDCs to secrete IFN-α. In contrast to whole apoptotic cells, necrotic primary cells did not enhance IFN-α production by CpGA-stimulated pDCs (Figure 3.5.A). Additionally, IL-10 production was not induced by pDCs activated with R848 or CpGB if the apoptotic cells were made necrotic by freeze-thawing (Figure 3.5.B-C). This shows that TLR-activated pDCs only respond to intact primary apoptotic cells.

To determine if this occurred through direct pDC-apoptotic cell contact, I separated pDCs and apoptotic cells in culture using a transwell insert. Flow cytometric analysis of the supernatant revealed that components of apoptotic cells less than 0.4μm in size (here called 'bodies', as previously described[20]), but very few viable and apoptotic cells could pass through the transwell insert into the well below (Figure 3.6.A). Preventing direct cell contact for 72 h significantly inhibited one third of apoptotic cell-induced IL-10 production and 80% IFN-α production by pDCs stimulated with CpGB (Figure 3.6.B) and CpGA (Figure 3.6.C), respectively.

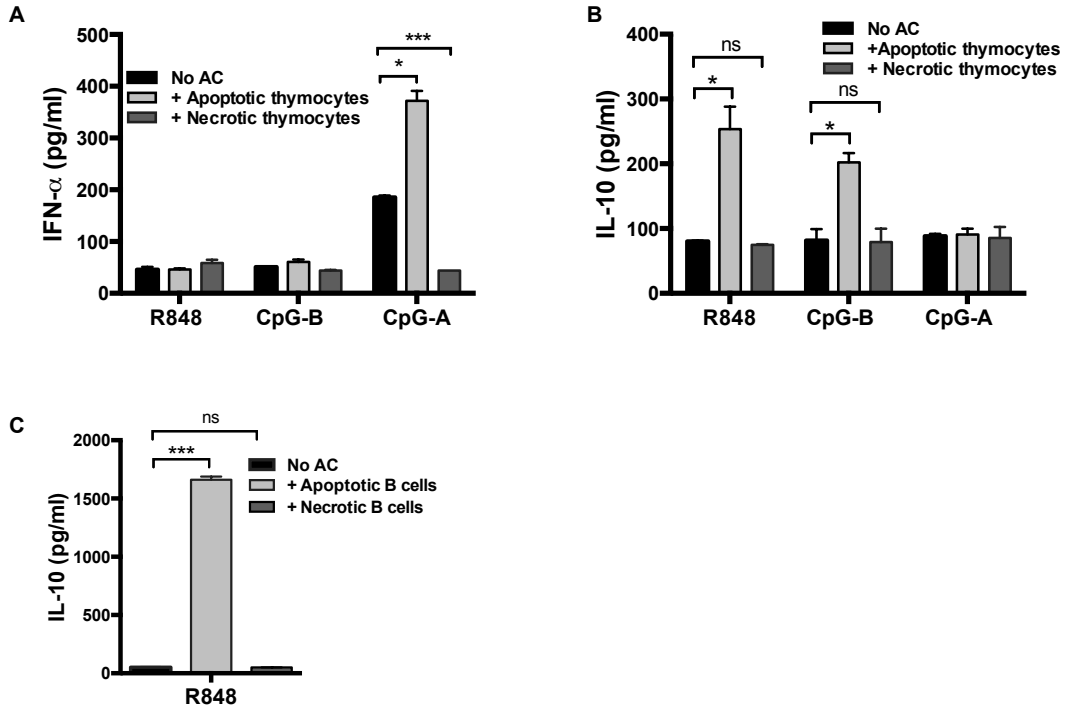

Figure 3.5. PDCs do not respond to necrotic primary cells.

(**A**) IFN-α and (**B**) IL-10 production were measured three days after R848, CpGB, and CpGA-stimulated pDCs were co-cultured alone (black bar) and with apoptotic (light grey bar), or necrotic (dark grey bar) thymocytes. (**C**) IL-10 production was measured three days after pDCs were co-cultured with R848 and apoptotic (light grey bar), or necrotic (dark grey bar) B cells. Data is the mean of three independent experiments with error bars representing SEM. Statistical significance was determined by one-way ANOVA, comparing cytokine responses by pDCs with and without apoptotic cells or necrotic cells. (**A**) $^{*}P$=0.0111 and $^{***}P$=0.0006; (**B**) R848 $^{*}P$=0.0382 and CpGB $^{*}P$=0.0332; (**C**) $^{***}P$=0.0001.

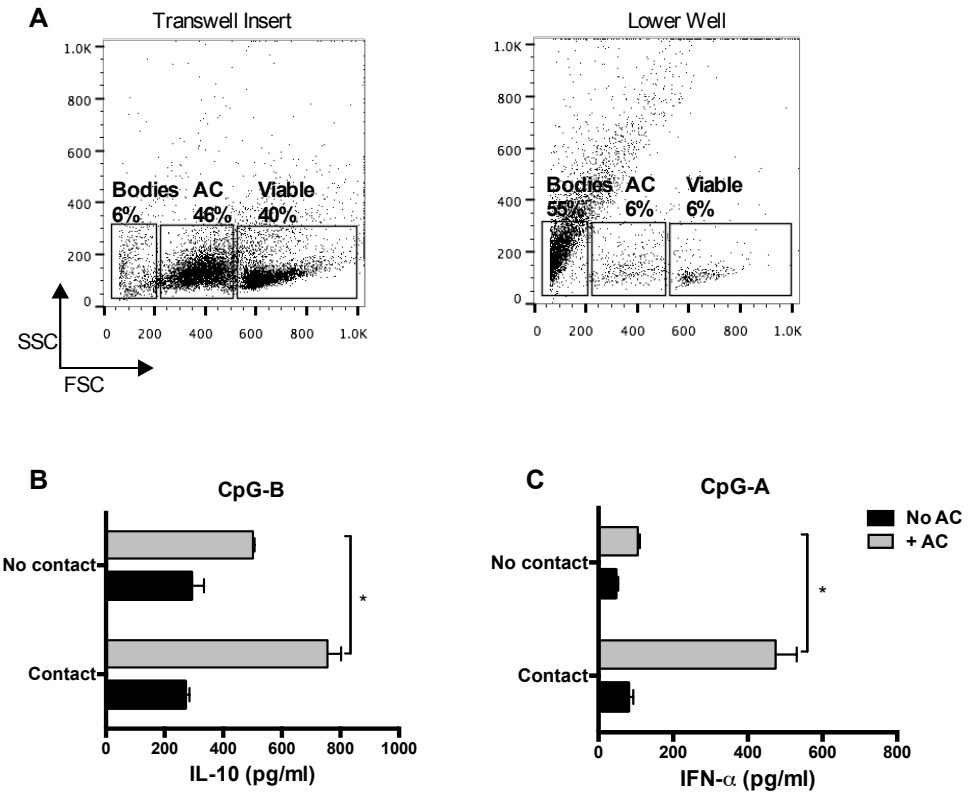

Figure 3.6. Direct contact with apoptotic cells induces IL-10 and IFN-α secretion by pDCs.

(**A**) Representative FACS plots showing the proportion of viable cells, apoptotic cells (AC) and bodies (determined by size and granularity, and excluding cell debris) remaining in the transwell insert and found in the well below after UV-irradiated thymocytes were cultured in the transwell for 24 h. $4x10^4$ pDC were stimulated with (**B**) CpGB and (**C**) CpGA and cultured with and without $4x10^6$ apoptotic cells (AC) in the presence (no contact) or absence (contact) of a transwell insert. After 3 days in culture, (**B**) IL-10 ($^*P$=0.0324) and (**C**) IFN-α ($^*P$=0.0232) in supernatants was measured by ELISA. Results represent mean plus or minus SEM of three independent experiments.

3.2.4 PDCs fail to respond to apoptotic cells in the presence of virus.

I wanted to determine if viral antigens mimic the pDC stimuli provided by CpGA and subvert apoptotic cell induced IL-10 secretion to stimulate IFN-α secretion. However, pDCs were not stimulated to secrete IFN-α following culture with the dsDNA virus, murine cytomegalovirus (MCMV) released from infected 3T3 cells, even in the presence of apoptotic cells (Figure 3.7.A). The ssRNA influenza A virus

also failed to induce IFN-α secretion and the pDCs did not respond to thymocytes that had been incubated with influenza for 1 h prior to initiation of apoptosis by UV irradiation (Figure 3.7.Bi). Less than 2% of thymocytes were infected by influenza virus, as indicated by surface expression of virus protein markers hemagglutinin (HA) and $M2^{280}$ (Figure 3.7.Bii-iii). Therefore I hypothesised that for pDCs to respond, the TLR ligands provided by virus and apoptotic cell nucleic acids need to be expressed on the same intact membrane. For that reason, it would be more physiological to use cells that were naturally infected by the viruses.

MCMV and influenza virus both successfully infect epithelial cells, but it was important to check if apoptotic epithelial cell lines could induce IL-10 regulation since I wanted to ask if virus infection subverts IL-10. The C127 (mouse mammary epithelial) cell line was induced to undergo apoptosis by UV irradiation and after 6 h the majority of non-adherent cells were early apoptotic (AnV^+PI^-; Figure 3.8.Aii), whereas after 18 h incubation most of the non-adherent cells were necrotic (AnV^-PI^+; Figure 3.8.A.iii). Nevertheless, pDCs cultured with apoptotic C127 cells (UV + 6h) and R848 did not produce IL-10 (Figure 3.8.B). I also found that starvation-induced apoptotic iBMK cells did not stimulate IL-10-secreting B cells (Figure 3.8.C). This indicated that apoptotic cell lines do not induce the same regulatory phenotype as apoptotic primary cells and could not be used in my assays.

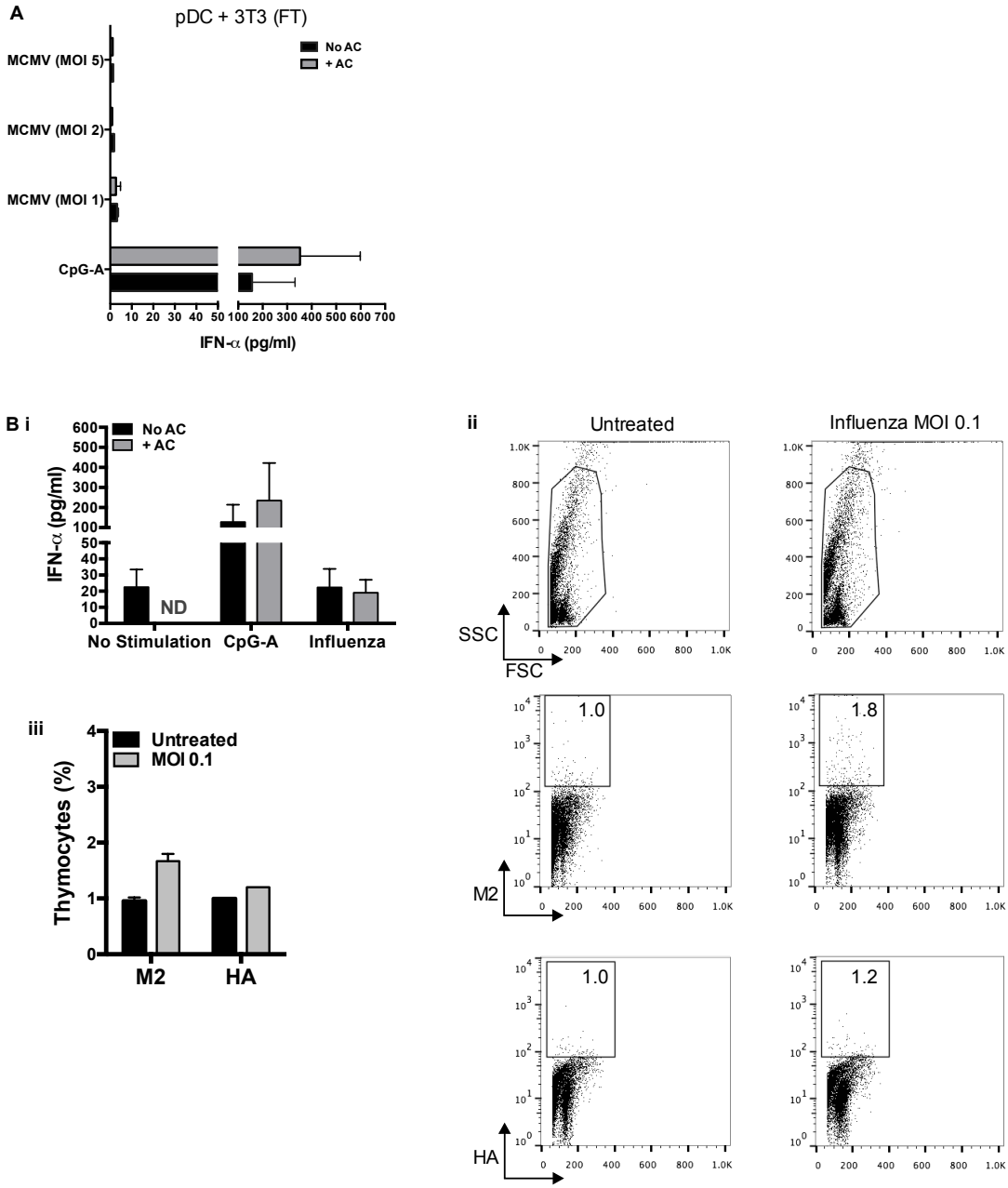

Figure 3.7. PDCs were not stimulated to secrete IFN-α when co-cultured with virus and apoptotic cells.

(**A**) IFN-α in supernatant was measured 24 h after pDCs were cultured without apoptotic cells (No AC) and with apoptotic cells (+ AC) in the following conditions: with 3T3 cells and CpGA, or 3T3 cells infected overnight with MCMV at a multiplicity of infection (MOI) 1, 2, and 5 then freeze-thawed (FT) to release free virus. (**Bi**) pDCs were cultured alone (No Stimulation), with CpGA with and without apoptotic cells, and with UV-inactivated influenza virus (MOI 0.1) either directly (No AC) or via infected thymocytes induced to become apoptotic cells (+ AC). (**Bii-iii**) Influenza virus infection rate was measured by detecting M2 protein using 14C2 monoclonal antibody (anti-mouse IgG AF647 secondary antibody) and

hemagglutinin (HA; anti-mouse IgG AF555 secondary antibody). Results are expressed as the mean of (**A-Bi**) three and (**Bii-iii**) two independent experiments with error bars presenting SEM. Not determined (ND).

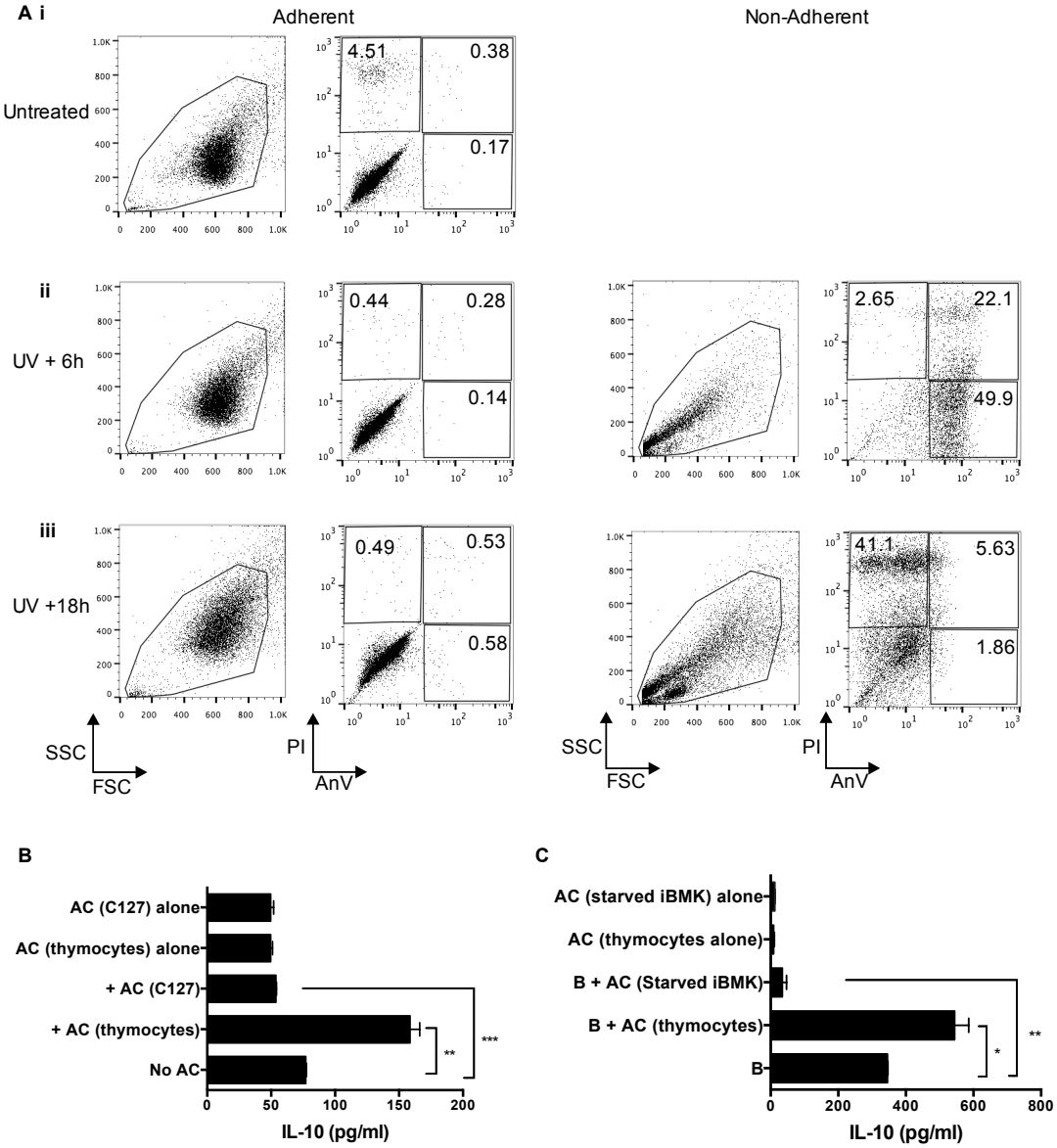

Figure 3.8. Apoptotic epithelial cell lines do not induce IL-10 secretion

Representative FACS plots showing the proportion of apoptotic adherent and non-adherent C127 cells was analysed by annexin V and PI staining of (**Ai**) untreated cells and UV irradiated cells after (**Aii**) 6 h, and (**Aiii**) 18 h. (**B**) IL-10 was measured in culture supernatants three days after pDCs were cultured with R848 alone (No AC), and with apoptotic thymocytes, or apoptotic C127 cells that had been UV irradiated and incubated for 6 h. $^{**}P$=0.0043; $^{***}P$=0.0004. (**C**) IL-10 was measured in culture supernatants three days after $CD19^{+}$ B cells were cultured with R848 alone

and with apoptotic thymocytes, or apoptotic iBMK cells that had been incubated in starvation media for 6 h. The results present the mean of three independent experiments and SEM. $^{*}P$=0.412; $^{**}P$=0.0016.

3.2.5 Cytokine production by pDCs is dependent on apoptotic cell-derived DNA complexes

Cells that have undergone apoptosis express nuclear DNA-containing chromatin complexes on the cell surface membrane and released apoptotic bodies[6]. It was previously shown that apoptotic cell-derived DNA complexes are essential for apoptotic cell-mediated induction of IL-10-secreting regulatory B cells[55]. To establish if DNA expressed by apoptotic cells was also important for stimulating IL-10 secretion from pDCs, DNA was enzymatically removed from the apoptotic cell surface using DNase, as previously reported[55]. This did not affect the proportion of thymocytes that became apoptotic (AnV^+ PI^-) or secondarily necrotic (AnV^+ PI^+) (Figure 3.9.A), and it did not affect binding of CpG to the surface of apoptotic cells (Appendix B Figure 2.Aii and Bii). Removing apoptotic DNA complexes abolished the production of IL-10 from apoptotic cell/CpGB-stimulated pDCs (by day seven, Figure 3.9.B) and apoptotic cell/R848-stimulated pDCs (Figure 3.9.C). It also significantly reduced secretion of IL-6 and IFN-γ (Figure 3.9.D-E).

I then asked if removing the DNA complexes that promote IL-10 secretion resulted in the pDCs sensing the apoptotic cells as inflammatory. However, IFN-α production was not enhanced when R848-stimulated pDCs were co-cultured with DNase-treated apoptotic cells (Figure 3.9.F). In fact, IFN-α production by CpGA-stimulated pDCs was also inhibited when apoptotic DNA complexes were removed (Figure 3.9.F). This confirms the importance of both the apoptotic cell expressed endogenous nucleic acid containing complexes on an intact membrane, and the synthetic TLR ligand presented to the pDCs.

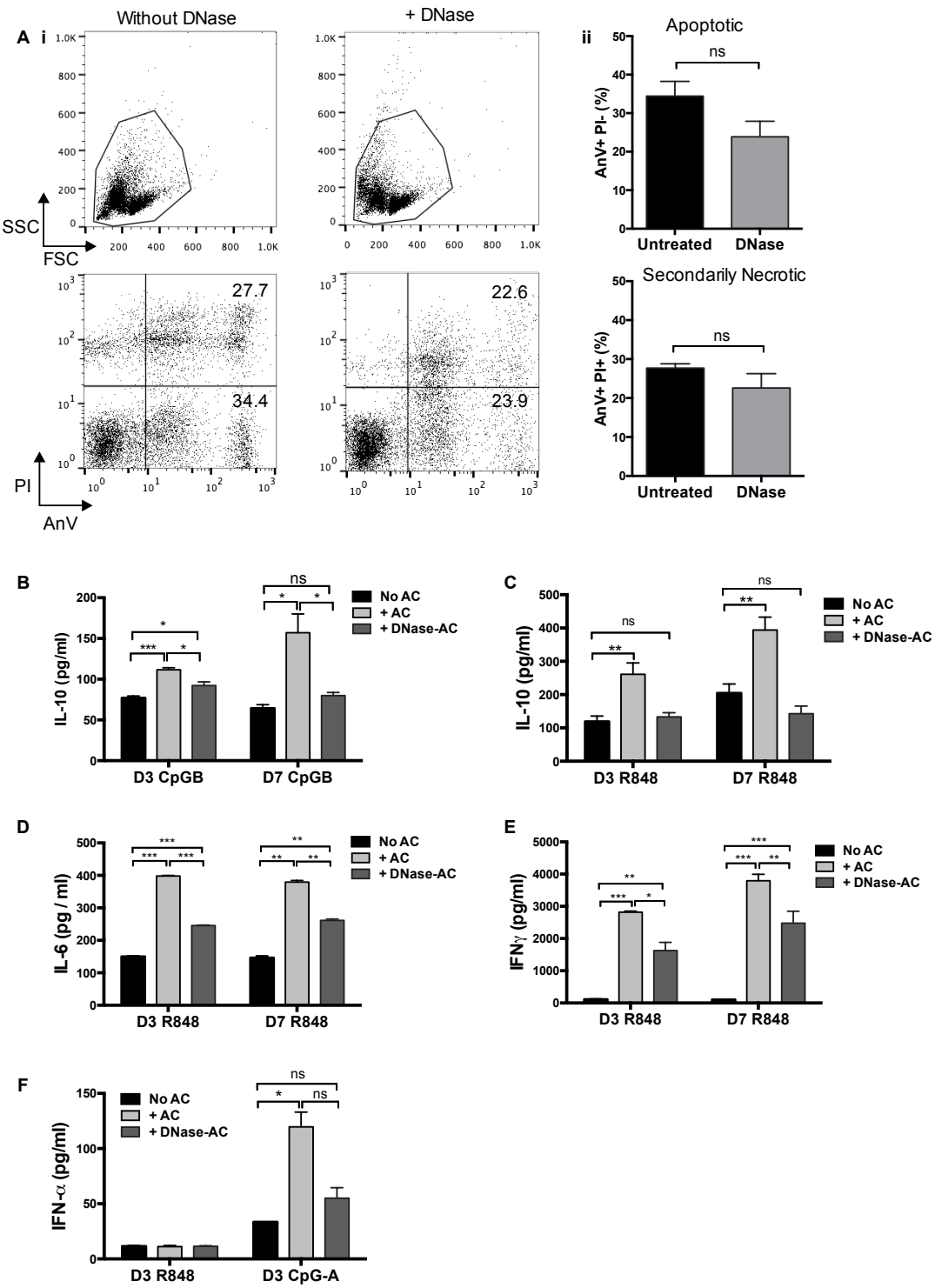

Figure 3.9. CpGB and R848-induced cytokine production by pDCs is dependent on apoptotic cell-derived DNA complexes.

(**Ai**) Representative FACS plots showing AnV and PI staining of UV-irradiated untreated thymocytes and DNase-treated thymocytes. (**Aii**) The mean proportion of apoptotic (AnV^+ PI^-) and secondarily necrotic (AnV^+ PI^+) untreated (black bar) and

DNase-treated (grey bar) UV-irradiated thymocytes from three independent experiments. (**B**) IL-10 was measured in the cell supernatant three and seven days after pDCs were cultured with CpGB alone (No AC, black bar) and with 10^6 apoptotic cells (+ AC, light grey bar), or DNase-treated apoptotic cells (+ DNase-AC, dark grey bar). (**C**) IL-10, (**D**) IL-6, and (**E**) IFN-γ were measured in the cell supernatant three and seven days after pDCs were cultured with R848 alone (No AC, black bar) and with 10^6 apoptotic cells (+ AC, light grey bar), or DNase-treated apoptotic cells (+ DNase-AC, dark grey bar). (**F**) IFN-α production was measured three days after pDCs were cultured with R848, or CpGA in the presence and absence of apoptotic cells (+ AC, light grey bar), or DNase-treated apoptotic cells (+ DNase-AC, dark grey bar). Data is shown as the mean of three to eight independent experiments, with error bars representing SEM. Statistical significance was determined by one-way ANOVA. $^{*}P < 0.05$; $^{**}P < 0.01$; $^{***}P < 0.001$; ns (not significant).

3.2.6 TLR9 expression is required to sustain IL-10 production by pDCs.

In addition to stimulating anti-viral immunity, TLR9 ligands also drive pDC dependent T cell regulation[189]. Furthermore, TLR9 expressed by innate-like B cells plays an essential tolerogenic role, inducing regulatory B cells in mice and humans, in response to apoptotic cell-derived DNA[55]. Therefore, I was interested to determine if apoptotic DNA-dependent induction of IL-10 secretion by pDCs occurred through TLR9.

As expected, IL-10 and IFN-α secretion was not detected in TLR9-deficient pDCs co-cultured with apoptotic cells and the TLR9 agonists CpGB (Figure 3.10.A) and CpGA (Figure 3.10.B), respectively. However following three days of co-culture with apoptotic cells and R848, WT and TLR9-deficient pDC secreted equivalent amounts of IL-10 (Figure 3.10.C), suggesting that TLR9 stimulation by the apoptotic cell expressed chromatin complexes was not required to induce TLR7-stimulated pDCs to secrete IL-10 by day three. Whilst WT pDCs had significantly increased the production of IL-10 from a mean of 261pg/ml to 394pg/ml by day seven, IL-10 reduced from a mean of 230pg/ml to 176pg/ml in TLR9-deficient pDCs (Figure 3.10.C). This indicates that TLR9 signalling was required to augment IL-10 secretion induced by R848/apoptotic cells. A similar pattern was also seen for the production of IL-6 (Figure 3.10.D) and IFN-γ (Figure 3.10.E) on day three and day seven.

Additional support for a regulatory role for TLR signalling is seen in TLR9 deficient lupus-prone mice, where despite the reduction in anti-DNA antibody titres, TLR7-mediated disease is exacerbated; suggesting TLR9 negatively regulates TLR7 activation[191,192,281-283]. Hence it may be expected that pDCs activated through TLR7 (via R848) in the absence of TLR9 would secrete IFN-α when co-cultured with apoptotic cells. However, this was not seen (Figure 3.10.F).

I consistently found that after flow sorting spleen, I obtained an average of one third of the number of TLR9-deficient pDCs compared to WT pDCs (Figure 3.11.A). However, the proportion of pre-sorted splenic pDCs was equivalent in WT and TLR9-deficient mice (Figure 3.11.B). Additionally, although there was no significant difference in the proportion of T cells (Figure 3.11.B) and whole B cells (Figure 3.11.C), the TLR9-deficient spleen contained a lower proportion of MZB cells (Figure 3.11.C).

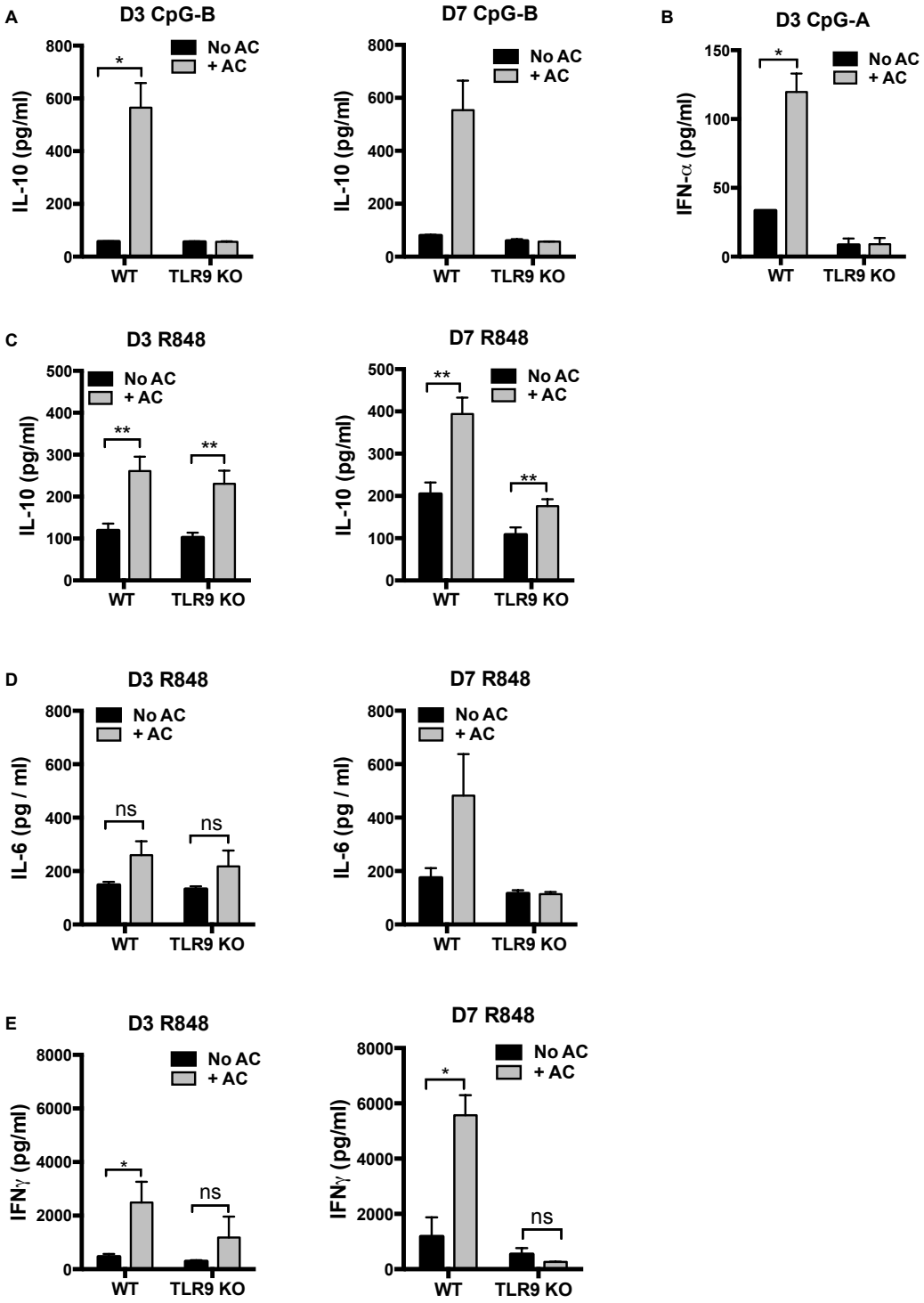

(Figure 3.10 continued overleaf)

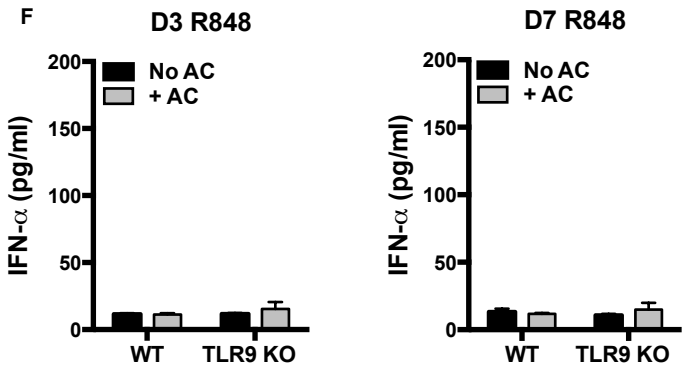

Figure 3.10. IL-10 production by pDCs is sustained through TLR9.

Beginning on the previous page, (**A**) PDCs isolated from wild type (WT) C57BL/6 and TLR9-knockout (TLR9 KO) mice were cultured with CpGB alone (No AC, black bar) and with apoptotic cells (+ AC, grey bar). IL-10 protein was measured by ELISA after three days (D3) and seven days (D7) in culture. (**B**) WT and TLR9 KO pDCs were cultured with CpGA alone and with apoptotic cells. IFN-α protein in culture supernatants was measured after three days. (**C**) IL-10, (**D**) IL-6, (**E**) IFN-γ, and (**F**) IFN-α production was measured three and seven days after WT and TLR9 KO pDCs were cultured with R848 alone and with apoptotic cells. Data is shown as the mean of three to eight independent experiments, with error bars representing SEM. Statistical significance was determined by *t*-test. $^{*}P < 0.05$; $^{**}P < 0.01$; $^{***}P < 0.001$; ns (not significant).

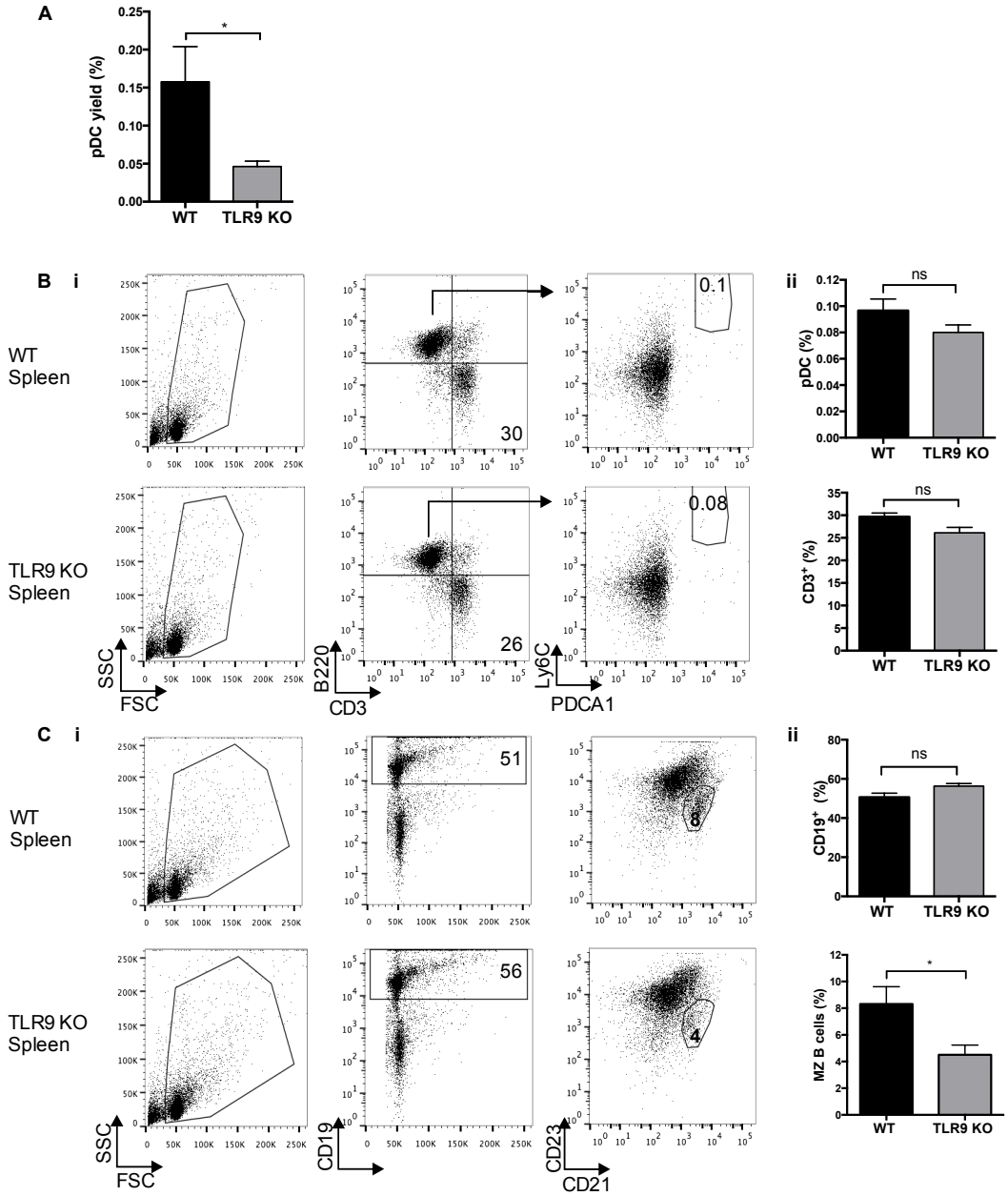

Figure 3.11. Fewer pDCs were purified from TLR9 KO spleen following flow sorting.

(**A**) The percentage of WT (black bar) and TLR9 KO (grey bar) pDCs isolated following flow sorting was calculated as a percentage of the original whole spleen cell count. (**Bi**) Spleens from wild type (WT) and TLR9-deficient (TLR9 KO) mice were analysed by flow cytometry to detect T cells ($CD3^+$) and pDCs ($B220^+$ $PDCA1^+$ $Ly6C^+$). (**Bii**) The mean proportion of pDCs (top) and T cells (bottom) in WT (black bar) and TLR9 KO (grey bar) spleen. (**Ci**) Total B cells ($CD19^+$) and marginal zone B cells (MZB; $CD19^+$ $CD21^{high}$ $CD23^{low}$) in WT and TLR9 KO spleen were analysed by flow cytometry. (**Cii**) The mean proportion of total B cells (top) and MZB cells (bottom) in WT (black bar) and TLR9 KO (grey bar) spleen. Data is

shown as the mean of (**A**) eight and (**B-C**) three independent experiments, with error bars representing SEM. Statistical significance was determined by *t* test. $^{*}P$= (**A**) 0.0329; (**Cii**) 0.0487; ns (not significant).

3.2.7 Antagonising HMGB1-RAGE interaction did not significantly inhibit apoptotic cell-induced IFN-α.

HMGB1 is a non-histone nuclear protein, which functions by binding to and bending DNA thereby increasing interactions with transcription factors[284]. HMGB1 released from necrotic cells acts as an alarmin by promoting inflammation[104,285]. It has also been reported that HMGB1 is released from late apoptotic cells[286,287] and more recently it was shown to be expressed on apoptotic blebs[288]. Consistent with this, I found that HMGB1 expression was highest in late apoptotic/secondarily necrotic (82.3% AnV^+ PI^+) and necrotic (56.6% AnV^- PI^+) thymocytes, compared to live (3.4% AnV^- PI^-) and early apoptotic cells (9.3% AnV^+ PI^-) where the plasma membrane remained intact (Figure 3.12.A).

PDCs express the HMGB1 receptor, RAGE, but not TLR2 or TLR4[206]. Following interactions with HMGB1, RAGE associates with TLR9, which is important for mediating IFN-α production induced by DNA-containing immune complexes from SLE patients[210]. The complex formed by HMGB1 and CpGA also augments IFN-α production by pDCs through this mechanism[210]. Therefore, I assessed if HMGB1 was involved in apoptotic cell-induced IFN-α secretion by CpGA-stimulated pDCs.

IFN-α secretion by pDCs cultured with CpGA was enhanced by a mean of 45% when apoptotic cells were added to the culture; but this was limited to a mean of 13% when binding of HMGB1 to RAGE was inhibited using the non-activating antagonist, box A from HMGB1 (Figure 3.12.B). However, the difference in IFN-α secretion between untreated and box A-treated cultures did not reach significance. Including box A in the culture medium did not inhibit IL-10 production by pDCs co-cultured for three days with R848 and apoptotic cells (Figure 3.12.C).

3.2.8 **Apoptotic cells promote pDC-induced regulation.**

PDCs are also known to promote immunological tolerance by inducing IL-10-secreting Tregs cells via IDO and ICOS-L[181-183,185]. I repeated preliminary experiments generated during my MSc project in the Gray lab, which showed that seven days after culture OVA-specific T cells co-cultured with both pDCs and apoptotic cells resulted in a significant increase in IL-10 protein to approximately 6000 pg/ml compared to T cells cultured with pDCs alone (2700 pg/ml) and apoptotic cells alone (3700 pg/ml) (Appendix B Figure 4.A). This suggests that the interaction of pDC with apoptotic cells may additionally induce IL-10 secretion by T cells; however IL-10 secretion was not mediated by IDO expression, as shown by using the competitive inhibitor, 1-methyl-DL-tryptophan (1MT) (Appendix B Figure 4.B).

Using these results, I hypothesised that apoptotic cells would drive TLR7-stimulated pDCs to adopt a regulatory phenotype. To test this, I co-cultured apoptotic cells, R848 and pDCs with $CD4^+$ T cells for seven days. This resulted in a significant increase in IL-10 in the culture medium (3500 pg/ml) compared to T cells co-cultured with R848 individually with pDCs (710 pg/ml), or apoptotic cells (110 pg/ml) (Figure 3.13.A). Using an IL10-secretion assay, I confirmed that this increase in IL-10 originated from the T cells, because while R848-activated pDC induced a mean of 7% of T cells to secrete IL-10, this was augmented more than 7 fold in the presence of apoptotic cells (Figure 3.13.B).

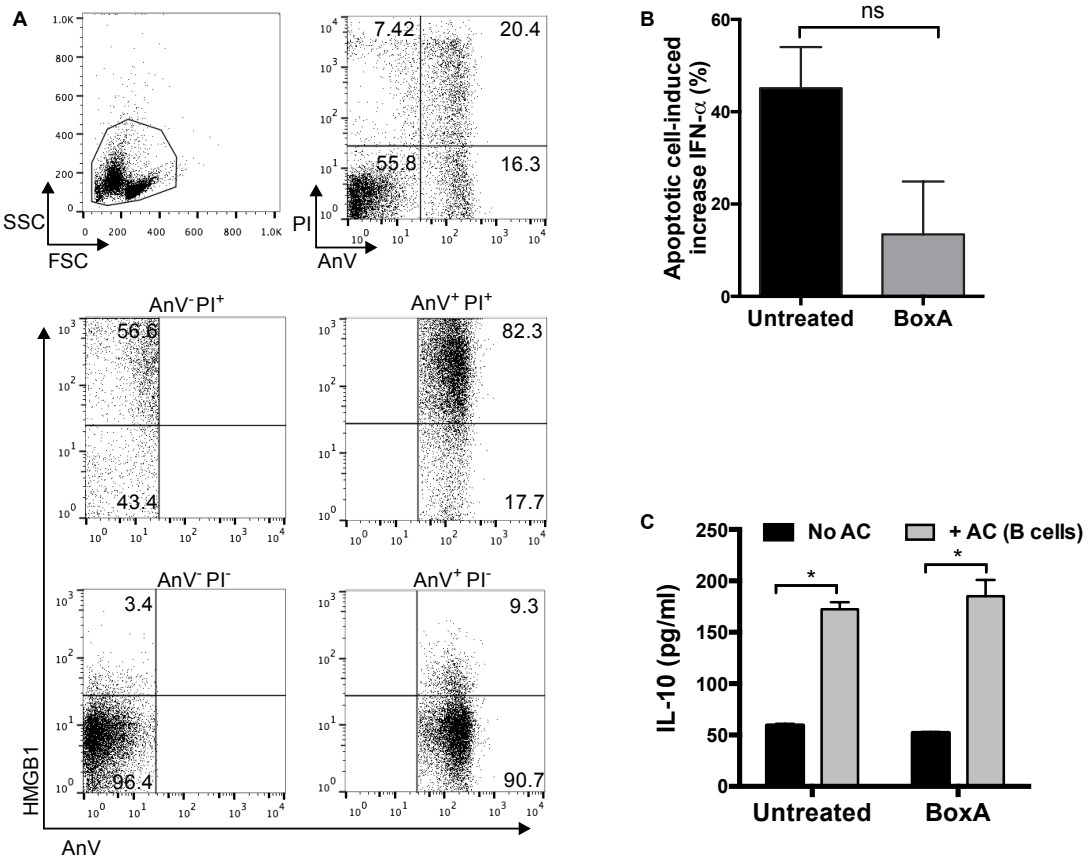

Figure 3.12. Antagonising HMGB1-RAGE interaction did not significantly inhibit apoptotic cell-induced IFN-α production.

(**A**) UV-irradiated thymocytes, were analysed by flow cytometry to detect anti-HMGB1 antibody (goat anti-rabbit IgG AF647 secondary antibody) binding to the four different AnV and PI populations. (**B**) The percentage increase in IFN-α production induced by co-culture of CpGA-stimulated pDC with apoptotic cells in untreated medium (black bar), or medium treated with box A (grey bar). ns (not significant). (**C**) IL-10 production by pDCs cultured with R848, with (grey bar) and without (black bar) apoptotic cells in untreated medium ($^{*}P$=0.0321), or medium treated with box A ($^{*}P$=0.0142). Results are (**B**) the mean and (**C**) representative of three independent experiments. Statistical significance was determined by *t*-test.

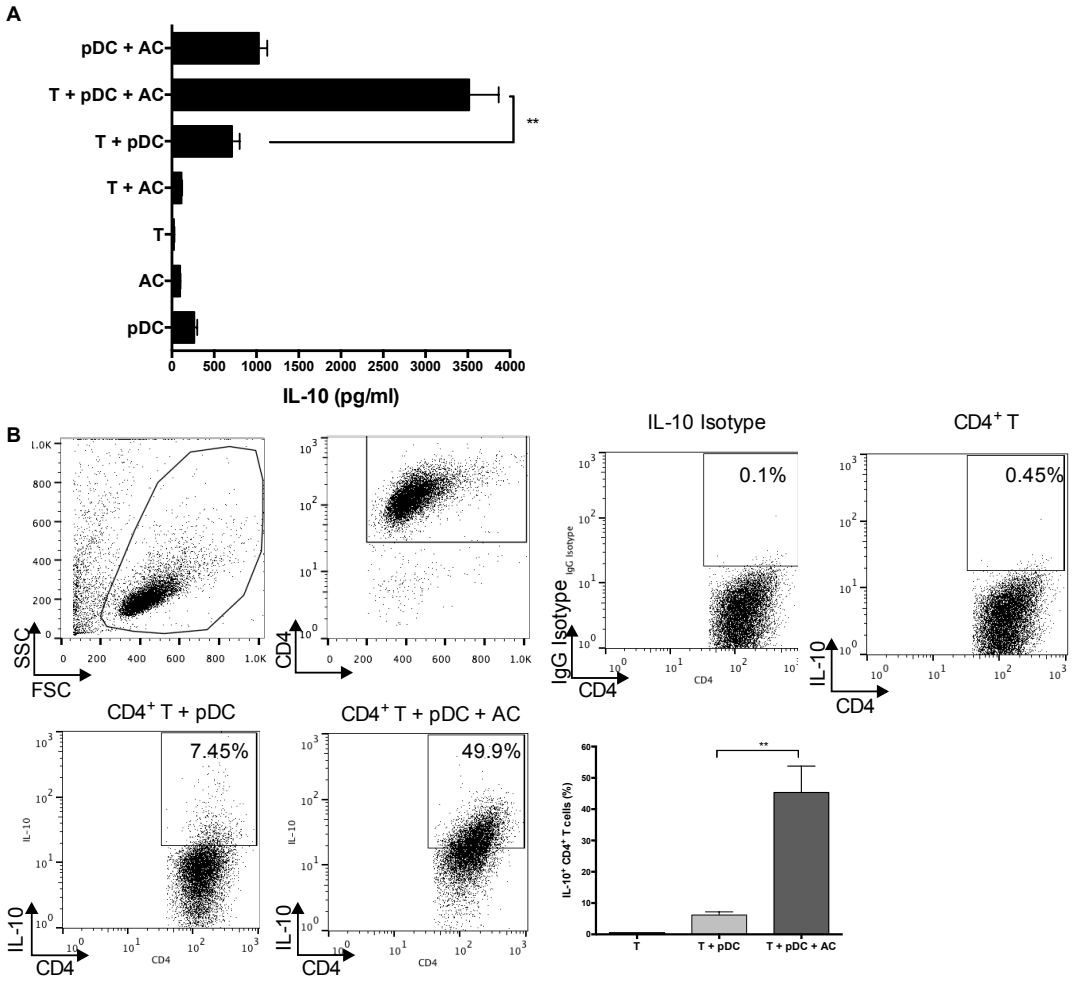

Figure 3.13. PDCs co-cultured with apoptotic cells induce IL-10 secretion by CD4$^+$ T cells.

(**A**) CD4$^+$ T cells were cultured with R848 (1μg/ml), pDCs and apoptotic B cells in various combinations. After seven days, IL-10 production was measured by ELISA. (**B**) CD4$^+$ T cell IL-10 production was quantified by IL-10 secretion assay. Data is shown as the mean of three independent experiments (**A**) or as a representative plot from 1 of 3 independent experiments (**B**). Statistical significance was determined by one-way ANOVA. (A)$^{**}P$=0.0015; (B)$^{**}P$=0.0099.

3.2.9 IL-10 secretion is enhanced in B cells, but not pDCs, isolated from C1q-deficient mice.

The lack of complement protein C1q is a major risk factor for developing SLE[86], as C1q binds directly to the apoptotic cell membranes allowing other complement components to bind and mediate clearance by phagocytosis[36,37,289]. Additionally, C1q inhibits CpG and immune complex-mediated IFN-α production by pDCs[290-292], and it

maintains B cell tolerance to intracellular antigens[89]. Therefore, because C1q is associated with regulating immune responses to apoptotic cells, I was interested to assess if the IL-10 response to wild type apoptotic cells was altered when pDCs and B cells were generated in a C1q-deficient environment.

All experiments were performed in the absence of serum that would provide C1q. Here I show that, although IL-10 secretion by OVA-specific T cells was induced by pDCs purified from C1q KO mice and cultured with apoptotic cells and OVA peptide, the concentration of IL-10 produced was significantly impaired in comparison to co-culture with WT pDC (Figure 3.14.A). However, there was no significant difference in CpGB/apoptotic cell-induced IL-10 secretion by pDCs purified from WT and C1q KO mice (Figure 3.14.B).

Conversely, apoptotic cells induced the production of more than double the concentration of IL-10 by B cells from C1q KO mice that were cultured with the TLR9 ligand CpGB, TLR7 ligand R848, TLR2 ligand PGN, and TLR4 ligand LPS (Figure 3.14.Ci-iv). IL-10 secretion by the TLR-stimulated B cells isolated from C1q KO mice was also significantly enhanced in the absence of apoptotic cells (Figure 3.14.Ci-iv). To determine if B cells from C1q KO mice responded more greatly to apoptotic cells due to a regulatory role played by C1q to dampen BCR activity during development, I measured BCR-mediated calcium flux. I observed no difference in calcium flux following stimulation of B cells from WT and C1q-deficient mice with anti-IgM (Figure 3.14.D).

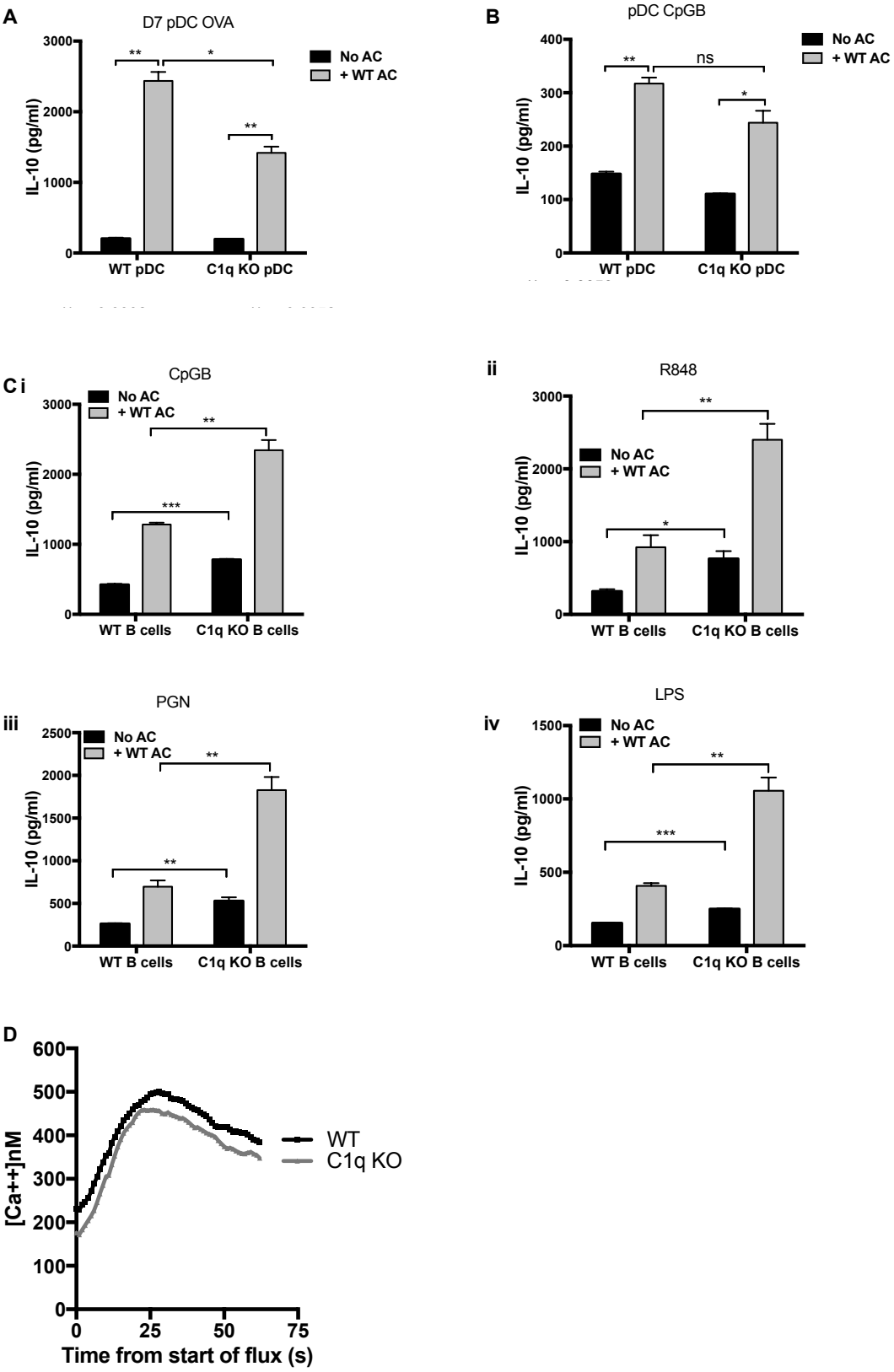
A
D7 pDC OVA
IL-10 (pg/ml)
No AC
+ WT AC
WT pDC
C1q KO pDC
B
pDC CpGB
ns
C i
CpGB
WT B cells
C1q KO B cells
ii
R848
iii
PGN
iv
LPS
D
[Ca++]nM
Time from start of flux (s)
WT
C1q KO

Figure 3.14. IL-10 secretion is enhanced in B cells, but not pDCs, isolated from C1q-deficient mice.

On the previous page, (**A**) IL-10 was measured seven days after OVA-specific T cells were cultured with OVA-peptide and pDCs from WT, or C1q KO mice, with (grey bar) and without (black bar) WT apoptotic thymocytes. (**B**) IL-10 was measured three days after pDCs purified from WT and C1q KO mice were cultured with CpGB alone (black bar) and with WT apoptotic thymocytes (grey bar). (**C**) IL-10 was measured three days after $CD19^+$ B cells purified from WT and C1q KO mice were cultured without apoptotic cells (black bar), and with WT apoptotic thymocytes (grey bar) and (**i**) CpGB, (**ii**) R848, (**iii**) PGN, and (**iv**) LPS. (**D**) Intracellular calcium flux in B cells isolated from WT and C1q KO mice responding to IgM was quantified using a spectrofluorimeter. Results are presented as the mean and SEM of three independent experiments. Statistical significance was determined by *t*-test. $^*P < 0.05$; $^{**}P < 0.01$; $^{***}P < 0.001$; ns (not significant).

3.3 Discussion

Immune complexes composed of autoantibodies and nucleic acids derived from apoptotic cells are considered to drive SLE pathogenesis through TLR7/9 mediated IFN-α production by pDCs. However, the ability of pDCs from healthy subjects to maintain tolerance to apoptotic cells via IL-10, or induce pro-inflammatory IFN-α has not been clearly defined. This *in vitro* study shows that apoptotic cells and necrotic debris alone was insufficient to stimulate pDCs. Chromatin complexes expressed on the surface of late apoptotic cells, but not nuclear complexes released from necrotic cells directly affected pDC function only when they were presented with a second signal, provided in this study by ISS-ODNs.

Depending on the TLR ligand used to co-activate the pDCs, IL-10 or IFN-α was produced, demonstrating that the type and the context of cell death influences pDC responses. CpGA, which localised to the surface of apoptotic cells, prevented IL-10 secretion induced by apoptotic DNA. The addition of CpGA may have mimicked the response to a virally-infected apoptotic cell, as it is known that infection-induced apoptosis results in the arrangement of autoantigens and viral antigens in clusters on small apoptotic blebs[265]. This might ensure that an adequate anti-viral response is induced, as it has been shown that IFN-α secretion by pDCs is enhanced by virus-

infected myeloid (m)DCs compared to free virus, although this was independent of mDC DNA[264].

As pDCs did not respond to apoptotic cells in the presence of free virus and they required direct contact with apoptotic cells to elicit optimal cytokine responses, it suggests that pDCs sample ligands that are co-expressed on an intact (apoptotic) cell membrane. Immature pDCs can endocytose and cross-present viral antigens from apoptotic cells[202,275], therefore they should be able to interact with and endocytose chromatin complexes expressed by apoptotic cells or bodies. The RAGE antagonist, box A from HMGB1, limited apoptotic cell-induced IFN-α production by pDCs. Although the inhibition was not statistically significant, it suggests that activation of RAGE is involved in inflammatory pDC recognition of apoptotic cells.

A link to various viruses and autoimmune diseases including SLE, Sjögren's syndrome[293] and type I diabetes has been known for some time[294]. Viral infection has been associated with both increased and decreased susceptibility to autoimmunity[294]. Thus CpGB and R848 might mimic viruses that induce IL-10 to inhibit the immune system, such as measles virus[295] and HIV[296]. The nature of the apoptotic cell cargo may alter the way that self nucleic acids are recognised by pDCs. Consequently, viral infection would shape the outcome of the innate and adaptive immune response to autoantigens co-expressed on apoptotic cells, by inducing pDCs to secrete either IL-10 or IFN-α.

It is currently considered that pDCs only respond to apoptotic cell-derived chromatin when it is in a complex with IgG autoantibodies and thus delivered to TLR9 through receptor-mediated uptake[99,100]. In comparison, I show that both IL-10 and IFN-α cytokine production by pDCs was inhibited when DNA was removed from the apoptotic cell membrane. Therefore, pDCs can indeed respond to apoptotic cell expressed self-DNA, but only when they receive a second signal provided by the TLR ligand. This might demonstrate that only activated pDCs have the capacity to take up apoptotic cell material. However, the source of apoptotic cells is likely to be

important in determining the response elicited from pDCs. Previous studies show enhanced IFN-α when apoptotic or necrotic cells derived from tumour cell lines are used[100,272], and I found that they failed to promote anti-inflammatory IL-10 secretion by pDCs and B cells. This suggests that apoptotic cell lines may be intrinsically pro-inflammatory. It is also possible that, since pDCs, which have a similar diameter as lymphocytes at 8-10μm[297], are not classed as professional phagocytic cells they might have a limited ability to take up large components, such as apoptotic epithelial cells and their apoptotic bodies.

PDCs potentially respond to DNA-containing complexes expressed on apoptotic cells rather than DNA per se, as DNase, and freeze-thawing, may break apart interactions between DNA and other nuclear components. For example, the DNA-binding protein HMGB1, which becomes oxidised during apoptosis, has been shown to be important for inducing tolerance to apoptotic cells[298], in addition to promoting IFN-α secretion in response to SLE DNA complexes, or CpGA[210]. However, although inhibiting the HMGB1 receptor RAGE demonstrated that apoptotic cell-induced IL-10 production occurs independently of RAGE, it is potentially required for apoptotic cell-induced IFN-α. Nevertheless, this was not necessarily via HMGB1, as RAGE has many ligands including the components important for apoptotic cell recognition and uptake, C1q[299] and phosphatidylserine[300]. Therefore, repeating the experiments utilising a specific HMGB1 antagonist would distinguish if HMGB1 plays a role in apoptotic cell recognition, or if further investigation into the other RAGE ligands is required.

IL-10 secretion by pDCs occurred within 72 hours of co-culture with apoptotic cells and was maintained for up to seven days, provided pDCs also expressed TLR9. In the absence of TLR9, long-term (seven days) apoptotic cell-induced IL-10 production by R848-stimulated pDCs was diminished, indicating that TLR7 cooperates with TLR9 to maintain the regulatory response. It is possible that continuous TLR9 signals by environmental stimuli, such as apoptotic cells, may be required to promote cell survival, as fewer TLR9-deficient pDCs were yielded

following the harsh process of flow sorting. Furthermore, MZB cells, which express high levels of TLR9, were reduced in TLR9-deficient spleen. In support of this, it has also been shown that anti-apoptotic gene expression is upregulated at early time points (up to 4 h) in CpGB stimulated pDCs[301], and *in vivo* studies have identified two temporal and functionally distinct peaks of gene expression in B cells following TLR9 stimulation [302]. The later peak, which begins five days after stimulation, upregulates genes involved in the DNA damage response [302], which will ultimately prevent cell death. Further work is required to elucidate the cell death kinetics of TLR9-deficient pDCs.

In recent years it has become clear that cytosolic DNA receptors also play an important role in stimulating type I IFN production in response to sensing microbial DNA and inefficiently cleared apoptotic DNA, with STING being the principal adaptor protein in many of these pathways (reviewed[303]). Additionally, human pDCs express MyD88-dependent cytosolic DNA receptors DExD/H-box helicases DHX9 and DHX36, which specifically sense CpGB and CpGA, respectively, and induce cytokine responses akin to TLR9[304]. Therefore, while CpG/R848 provide a signal through TLR9/TLR7, apoptotic DNA may be sensed by cytosolic receptors. It is currently not known how the apoptotic cells signal in pDCs to induce IL-10. This will be discussed further in chapter six.

It is reported that pDCs do not secrete IL-10 in response to synthetic TLR ligands[279] or apoptotic cells, though these stimuli have been shown to induce IL-10 by regulatory B cells in a TLR9 dependent manner[55]. Again contact with whole apoptotic cell membranes was required. Only a small proportion of pDCs were IL-10-positive following stimulation with R848 and apoptotic cells, which suggests that there perhaps a specific subset of pDCs that secrete IL-10 in response to apoptotic cells. Similarly, apoptotic cell-induced IL-10-secreting regulatory B cells originate from the MZB and B1a B cell subsets[55], yet not all of these innate-like B cells secrete IL-10. Consequently, regulatory B cells are currently defined by function rather than cell surface markers[57,305]. It is not known from the results in this chapter

if the same pDCs that produce IL-10 can then switch to make IFN-α, or if the different responses occur in functionally distinct pDC subsets.

PDCs develop from both common myeloid progenitors (CMP) and common lymphoid progenitor (CLP) pathways and studies have shown that pDCs derived from CLP produce less IFN-α in response to CpGA stimulation compared to pDCs from CMP [155,306]. However this is likely associated with reduced survival of CLP-derived pDCs[155]. Cell surface markers have also been attributed to pDCs with distinct functions; $CD9^{pos}$Siglec-H^{low} pDCs secrete IFN-α whereas $CD9^{neg}$Siglec-H^{high} pDCs do not[307]. Hence pDCs with low IFN-α secreting ability might represent a specific subset of regulatory pDCs. Co-staining for intracellular IL-10 and IFN-α along with these markers would assess this.

PDCs play an important role in influencing adaptive immune responses and are ideally placed to interact with T cells in secondary lymphoid organs. Antigen presentation by pDCs is known to be important for reducing the severity of autoimmune arthritis, by limiting effector T cell activation[186]. Human pDCs can also ingest microvesicles from apoptotic cells and present the antigen to T cells[211]. Here I showed that pDCs co-cultured with R848 and apoptotic cells induced $CD4^+$ T cells to secrete IL-10. Although it remains to be determined if this occurred via secretion of IL-10 by the pDC, or through cell-to-cell contact with the T cells, it again confirms that TLR7-stimulated pDCs do not automatically induce a pro-inflammatory response to apoptotic cells.

Apoptotic cell-induced IL-10 secretion by OVA-specific $CD4^+$ T cells, but not by TLR9-stimulated pDCs, was reduced when pDCs were isolated from C1q-deficient mice. In contrast, I found that B cells derived from C1q-deficient mice were hyper-responsive to stimulation by TLR ligands and apoptotic cells, as measured by increased production of IL-10. Katherine Miles (Gray lab) has now shown a similar phenotype in B cells, in particular MZB cells that lack the complement receptor CD21 (unpublished data). These results imply that complement proteins function during innate-like B cell development to dampen TLR-mediated responses to

apoptotic DNA. However, although C1q inhibits TLR7/9-mediated IFN-α production by pDCs[290-292], it does not appear to influence their regulatory response to apoptotic cells. Yet, perhaps signals from C1q-apoptotic cell complexes during the maturation of pDCs *in vivo* alters their function such that they have a greater capacity to induce IL-10 secretion by antigen-specific T cells. It has been shown that T cell cytokine secretion is enhanced by C1q-primed cDCs[308]

In summary, this chapter demonstrates that pDCs do not respond to dying cells unless they are co-activated by a TLR stimulus, which would be crucial *in vivo* to ensure that pDCs do not respond inappropriately to apoptotic or secondarily necrotic cells outwith an inflammatory milieu. The combined TLR/apoptotic cell stimulus determines the final pDC response to apoptotic cells, either inducing anti-inflammatory IL-10 and augmentation of T cell secretion of IL-10, or the production of pro-inflammatory IFN-α. The combination of infectious TLR9 ligands that induce IFN-α and apoptotic cells may be sufficient to break tolerance to self, leading to autoimmunity in genetically susceptible people. Understanding how pDCs respond to apoptotic cells could potentially lead to new selective therapeutic targets to reduce aberrant inflammation in autoimmune diseases, such as SLE, or promote immune reactivity to tumour associated apoptotic cells, which is discussed further in chapter six.

Chapter 4 The role of apoptotic cells in driving SLE

4.1 Introduction

It has been known for many years that peripheral blood lymphocytes from SLE patients are more susceptible to undergoing apoptosis (annexin V^+)[230,309] and have a faster rate of apoptosis than healthy donor lymphocytes[310]. The cause has been attributed to increased activation induced cell death of SLE T cells and B cells[311-313], which potentially explains lymphopenia[309], a characteristic used during the classification of SLE[314]. It is unclear how elevated cell death is related to disease activity, with some studies reporting a correlation of lymphocyte apoptosis with active SLE[309,315] and other studies finding no such association[230].

It is not clear if accelerated lymphocyte death initiates or perpetuates SLE pathogenesis. Secondary necrosis is considered to occur due to impaired removal of the apoptotic cells, which subsequently break apart releasing nuclear contents that bind to the autoantibodies. There is limited data to suggest that SLE lymphocytes are intrinsically susceptible to becoming necrotic.

The current paradigm indicates that in health, pDCs tend to ignore early and late apoptotic cells unless the apoptotic nuclear components, such as DNA or RNP, are stabilised in immune complexes with auto-IgG, or LL37[272,316-318], which are found circulating in SLE patient serum. Yet, in chapter three I observed that whole apoptotic cells, but not necrotic cells, augmented IFN-α production by mouse pDCs co-exposed to CpGA. It is not known if healthy human pDCs also make IFN-α in response to activation by CpGA/apoptotic cells and if this response is exacerbated in pDCs from SLE patients. Furthermore, it has not been addressed if SLE apoptotic cells are capable of stimulating an immune regulatory response prior to breaking apart.

Aims

In this chapter I hypothesised that in the presence of CpGA, apoptotic cells would enhance IFN-α secretion by healthy donor and SLE patient pDCs. It was also hypothesised that lymphocytes from SLE patients die abnormally, and this would result in the failure of SLE apoptotic cells to promote anti-inflammatory immune responses. The following aims were used to test the hypothesis:

- Establish if healthy and SLE pDCs make IFN-α in response to culture with CpGA/apoptotic cells.
- Determine the cell death kinetics of lymphocytes from healthy donors and SLE patients.
- Investigate if apoptotic SLE lymphocytes are efficient at inducing IL-10 secreting regulatory B cells.

4.2 Results

4.2.1 Purifying human pDCs results in reduced CpGA-mediated IFN-α production.

First I compared CpGA-mediated IFN-α production by pDCs enriched by different mechanisms to determine what method gave the best response. PDCs were either flow sorted to high purity (>95%, Figure 4.1.A), as described in the materials and methods (page 41), or enriched to 44% of the cell population by MACS using negative selection (Figure 4.1.B). Additionally, I also looked at pDCs in PBMCs since it is reported that CpGA exclusively activates pDCs within the mixed population of leukocytes present in PBMCs[319]. This was confirmed using pDC-depleted (pDC^{-ve}) PBMCs (Figure 4.1.D). The PBMCs were depleted of $CD19^{+}$ B cells as an additional control to remove the other most common human leukocytes that constitutively express TLR9[320]. I found that pDCs in culture with CD19-depleted PBMCs secreted the highest concentration of IFN-α in response to 72 h CpGA stimulation compared to pDCs enriched by MACS, and purified by FACS (Figure

4.1.D), even though they represent less than 1% of the PBMC population (Figure 4.1.C). For that reason, I decided to use CD19-negative PBMC in future assays.

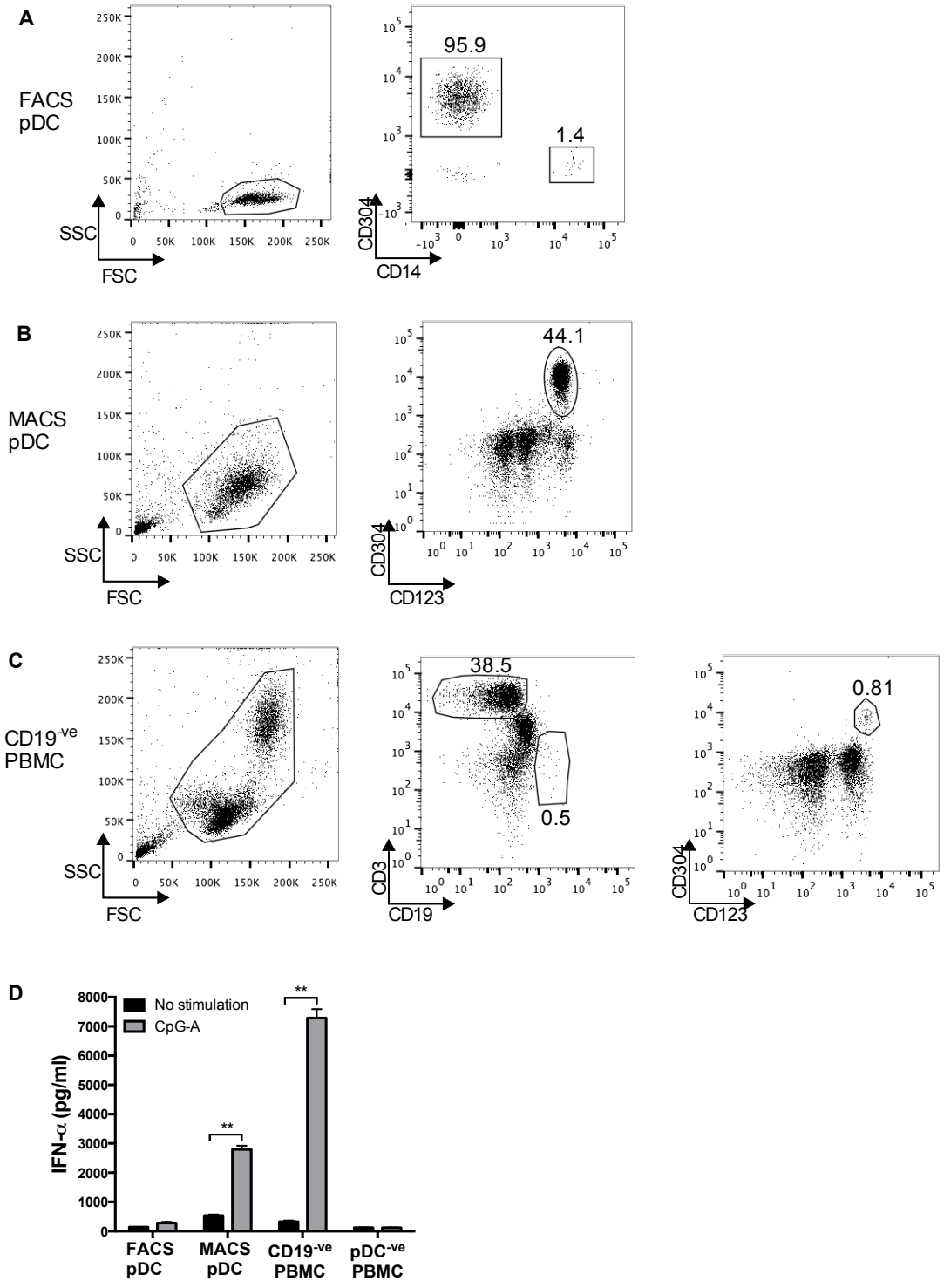

Figure 4.1. IFN-α secretion is greatest by human pDCs that have not been sorted.

On the previous page, (**A**) PBMCs were flow sorted (FACS) to isolate pDCs ($CD304^+$) that were more than 95% pure and contained 1.4% contaminating $CD14^+$ monocytes. (**B**) The purity of pDCs ($CD304^+$ $CD123^{high}$) was assessed by flow cytometry following negative selection by magnetic cell sorting (MACS). (**C**) The proportion of pDCs ($CD304^+$ $CD123^{high}$) in PBMCs that were depleted of $CD19^+$ B cells was detected by flow cytometry. (**D**) IFN-α was measured in culture supernatant by ELISA 72 h after 10^4 pDCs sorted by FACS and MACS, and pDCs within 10^6 CD19-negative PBMCs were cultured alone (no stimulation, black bar) and with CpGA (grey bar). 10^6 pDC-negative PBMCs were cultured in the same way. Results are presented as mean with error bars representing SEM of three independent experiments. Statistical significance was assessed by *t* test; $^{**}P<0.01$.

4.2.2 Human pDCs stimulated with CpGA respond to whole apoptotic cells, but not necrotic cells, by secreting IFN-α

I wanted to investigate if IFN-α secretion by healthy human pDCs was enhanced by co-activation with CpGA and apoptotic cells, as was shown in mouse pDC (chapter 3, page 74). CD19-negative PBMCs containing pDCs were cultured for 72h in order to keep the assays comparable to the mouse pDC cultures in chapter three, and after checking that CpGA-induced IFN-α secretion was not significantly elevated at an earlier time point (Appendix C Figure 1A). Similar to mouse pDCs, apoptotic cells failed to enhance IFN-α production by human pDCs in the absence of additional TLR stimulation, or in the presence of CpGB (Figure 4.2.A). Nevertheless, when the pDCs were activated with CpGA (3μg/ml chosen after dose response analysis, Appendix C Figure 1B), IFN-α secretion was significantly augmented by co-activation with apoptotic cells (Figure 4.2.A).

Additionally, like mouse pDCs, healthy human pDCs were only stimulated to enhance IFN-α production when they were co-cultured with CpGA/apoptotic cells, but not by CpGA/necrotic cells generated by breaking apart the membrane of the apoptotic cells by freeze-thaw cycles (Figure 4.2.B).

Since the majority of published studies have shown that pDCs only respond to necrotic cell material that has formed immune complexes with IgG, or $LL37^{272,316,321}$, I was interested to determine if adding SLE patient anti-DNA and anti-RNP IgG

autoantibodies to the culture medium enhanced IFN-α production by pDCs. In contrast to previous reports, I found that IgG purified from both healthy donors and from SLE patients inhibited CpGA-mediated IFN-α secretion even in the presence of apoptotic cells (Figure 4.2.C) and necrotic cells (Figure 4.2.D). Furthermore, SLE IgG did not enhance IFN-α production by high purity pDCs co-cultured with CpGA and apoptotic cells (Figure 4.2.E).

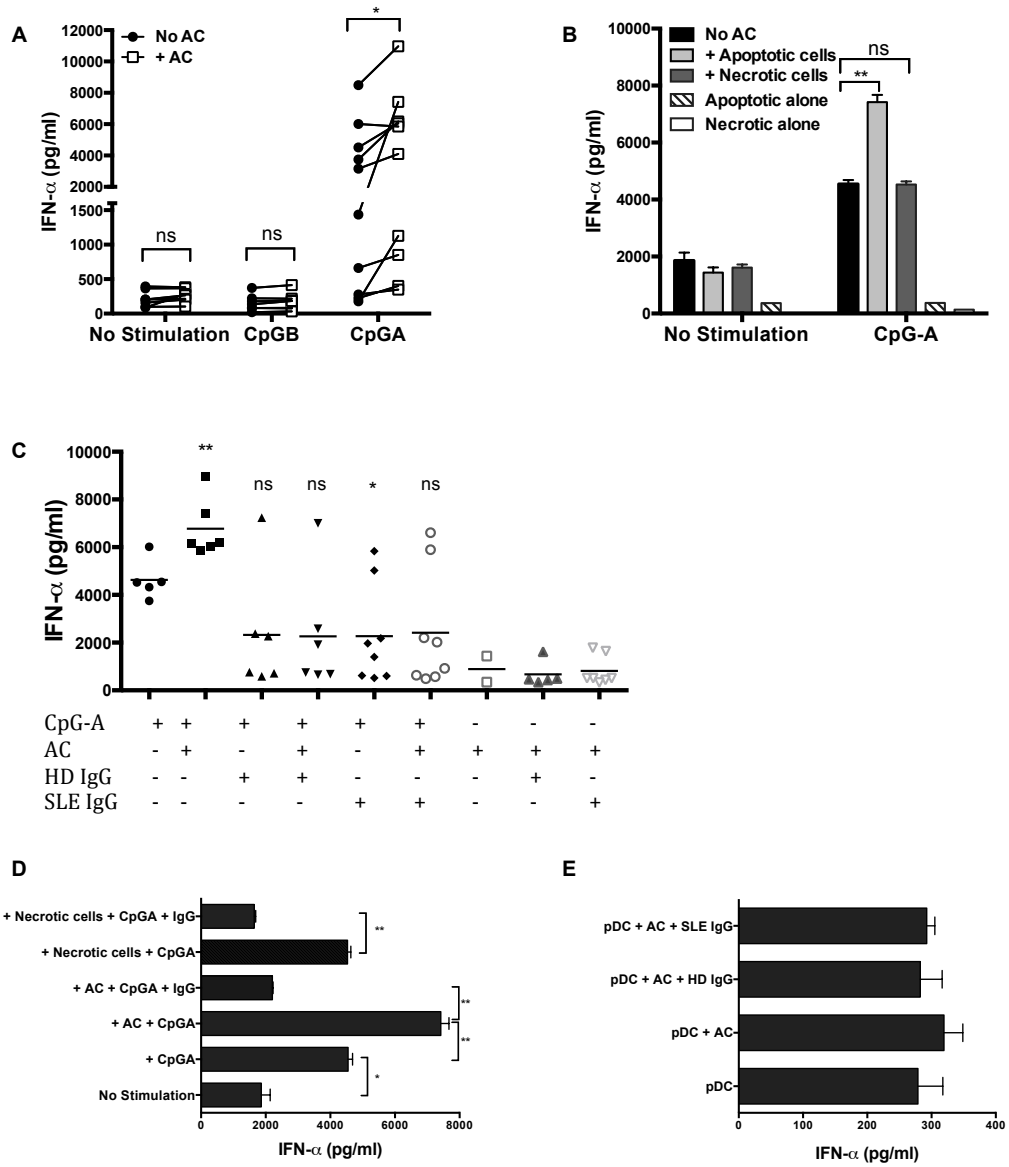

Figure 4.2. Apoptotic cells, but not necrotic cells, or IgG, augment IFN-α production by human pDCs.

Beginning on the previous page, (**A**) IFN-α production by CD19-negative PBMCs was measured by ELISA 72 h after they were cultured alone (•) or with 10^6 UV-irradiated apoptotic $CD4^+$ T cells (□) in media alone (no stimulation), and with CpGB, or CpGA. *n*=10 donors. Statistical significance was assessed by *t* test; *P*=0.0325 (**B**) IFN-α production by CD19-negative PBMCs was measured by ELISA 72 h after CD19-negative PBMCs were cultured without stimulation and with CpGA either alone (No AC, black bar), with 10^6 UV-irradiated apoptotic $CD4^+$ T cells (light grey bar), or 10^6 freeze-thawed necrotic $CD4^+$ T cells (dark grey bar). Apoptotic cells and necrotic cells were also cultured in the absence of PBMCs. Data is represented as the mean with error bars showing SEM of three independent experiments. Statistical significance was determined by Student's *t* test; $^{**}P$=0.0099. (**C**) CD19-negative PBMCs were cultured in various combinations with and without apoptotic cells, CpGA, and IgG antibodies (10μg/ml) purified from healthy donor (HD) or SLE serum. After 72 h, IFN-α in culture supernatants was measured by ELISA. Results are from five to eight independent experiments. Statistical significance was measured by two-way ANOVA; $^{*}P$-0.0346; $^{**}P$=0.0086*;* ns non-significant. (**D**) CD19-negative PBMCs were cultured with CpGA in the presence and absence of apoptotic cells (AC), necrotic cells, and SLE patient IgG antibodies for 72 h then IFN-α was measured in the culture supernatants. Data is represented as the mean with error bars showing SEM of three independent experiments. $^{*}P<0.05$; $^{**}P<0.01$. (**E**) Flow sorted pDCs were cultured with CpGA alone, and with apoptotic cells (AC) with and without healthy donor (HD), or SLE IgG autoantibodies. Data is represented as the mean with error bars showing SEM of three independent experiments.

4.2.3 SLE PBMCs contain fewer pDCs and fail to respond to CpGA.

I postulated that SLE pDCs would be primed to respond to apoptotic cells by secreting a higher concentration of IFN-α than healthy donor pDCs, due to the potential increased contact with apoptotic cells in an inflammatory milieu in SLE. However, CD19-depleted SLE PBMCs stimulated with CpGA secreted a mean of ten times less IFN-α compared to healthy CD19-depleted PBMCs, and this was not enhanced by co-culture with apoptotic cells (Figure 4.3.A). Furthermore, I found no difference in the concentration of IFN-α in serum (Figure 4.3.B), despite published findings that IFN-α is elevated in the serum of SLE patients[322]. Detection of other cytokines revealed that after 72 h stimulation with CpGA, both healthy and SLE CD19-depleted PBMCs secreted significant amounts of IL-6 (Figure 4.3.C), but not IL-12 (Figure 4.3.D), TNF-α (Figure 4.3.E), or IL-1β (Figure 4.3.F).

Since I was using CD19-depleted PBMCs in the assays I wanted to check that I was stimulating an equivalent number of healthy and SLE pDCs in the culture wells. Flow cytometry analysis revealed that SLE PBMC contained a significantly lower proportion of pDCs ($CD304^{+}$ $CD123^{high}$; mean 0.2%) compared to healthy PBMC (mean 0.5%; Figure 4.3.Gi-ii). Nevertheless, there was no significant correlation (Spearman) between the proportion of pDCs in SLE PBMCs and the concentration of IFN-α secreted in response to CpGA (Figure 4.3.Giii). The proportion of pDCs in healthy donor PBMCs also did not correlate with IFN-α (Figure 4.3.Giv). HCQ, a DMARD commonly used to treat SLE, is reported to work by interacting with DNA and RNA, which subsequently prevents them from binding to TLR9 and TLR7, respectively[323]. Therefore, as an additional control, non-SLE patients who were on HCQ therapy were included in the control group. Furthermore, half of the SLE PBMCs used for IFN-α analysis were from patients that were not receiving HCQ therapy at the time of blood donation, including the outlier in the SLE group (Patient Number 6) who had a high proportion of pDCs, but low IFN-α secretion.

In chapter three I showed fewer flow-sorted pDCs were yielded from TLR9-deficient spleen (Figure 3.11 Page 89) suggesting a link between TLR9 expression and pDC numbers. Therefore, I was interested to assess TLR9 expression by SLE pDCs. Using intracellular staining, I found that the proportion of pDCs expressing TLR9 (Figure 4.4.A-Bi) and the intensity of TLR9 staining (Figure 4.4.Bii) was the same in SLE as in health. As a negative control, I confirmed that the pDC-negative populations did not express TLR9 (Figure 4.4.Ai-ii).

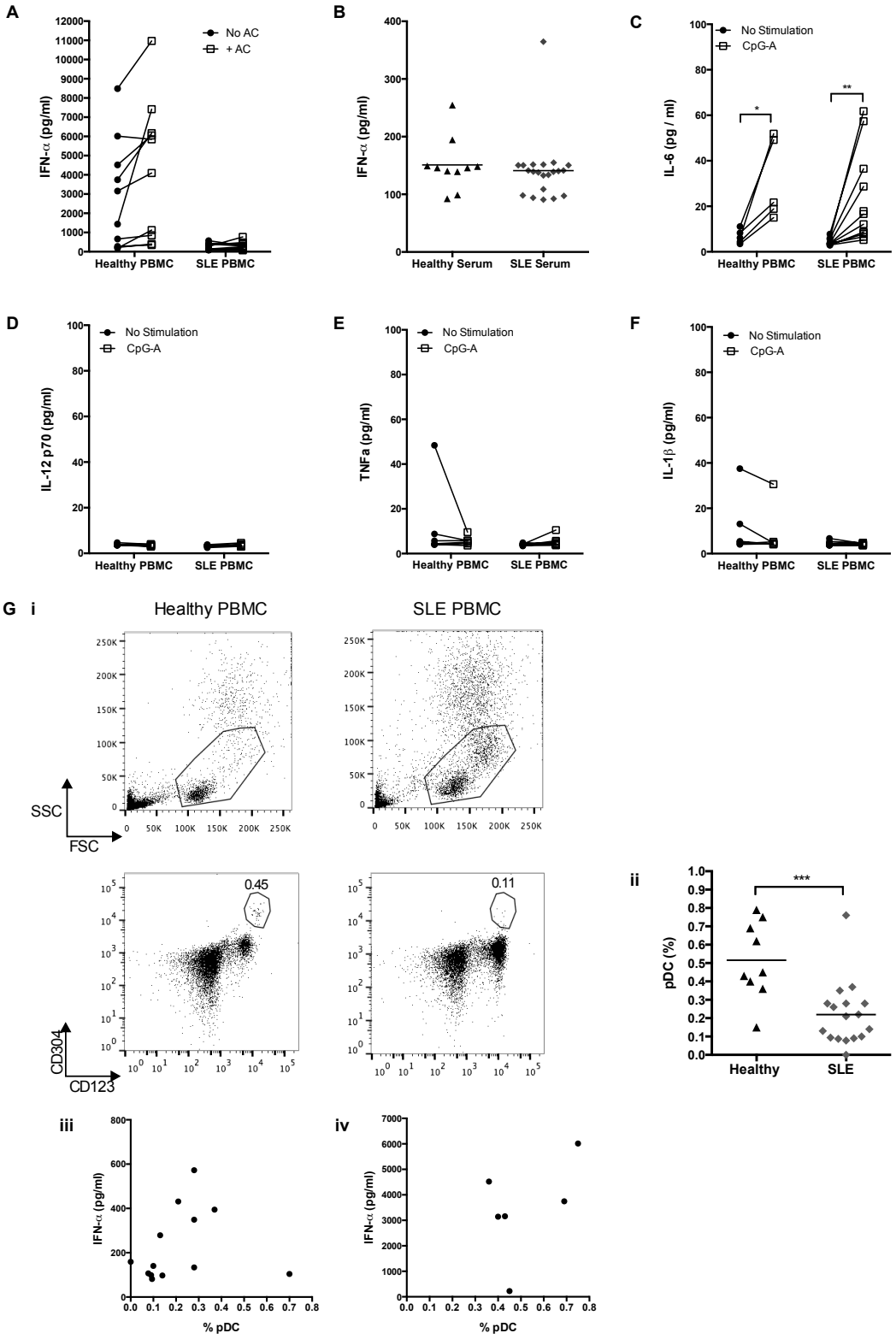

Figure 4.3. SLE patients have a lower proportion of peripheral pDCs and make less IFN-α in response to CpGA.

On the previous page, (**A**) IFN-α in culture supernatant was measured 72 h after CD19-depleted PBMCs from healthy donors and SLE patients were cultured with CpGA alone (No AC, •), or with apoptotic $CD4^+$ T cells (+ AC, □). n = 10 (healthy) and 12 (SLE) (**B**) The concentration of IFN-α in healthy donor and SLE patient serum was quantified by ELISA. n = 10 (healthy) and 21 (SLE). (**C**) IL-6, (**D**) IL-12p70, (**E**) TNF-α, and (**F**) IL-1β was measured by the CBA inflammatory human cytokine kit 72 h after healthy and SLE PBMC were cultured without stimulation (•), or with CpGA (□). (**C-D**) n = 5 (healthy) and 10 (SLE). (**Gi**) Representative flow cytometry plot and (**Gii**) quantification of the proportion of pDCs ($CD123^{high}$ $CD304^+$) in healthy and SLE PBMCs. n = 9 (healthy) and 17 (SLE). IFN-α concentration secreted by (**Giii**) SLE (n = 13) and (**Giv**) healthy (n = 6) PBMCs after 72 h CpGA stimulation plotted against the proportion of pDCs within the PBMCs. Each data point represents one donor. Statistical significance was determined by (**B**) paired t-test; $^*P = 0.015$; $^{**}P = 0.009$, and (**Gii**) unpaired t-test; $^{***}P = 0.0008$. Spearman correlation co-efficient, (**Giii**) r = 0.3702; $P = 0.2140$, (**Giv**) r = 0.2571; $P = 0.6583$.

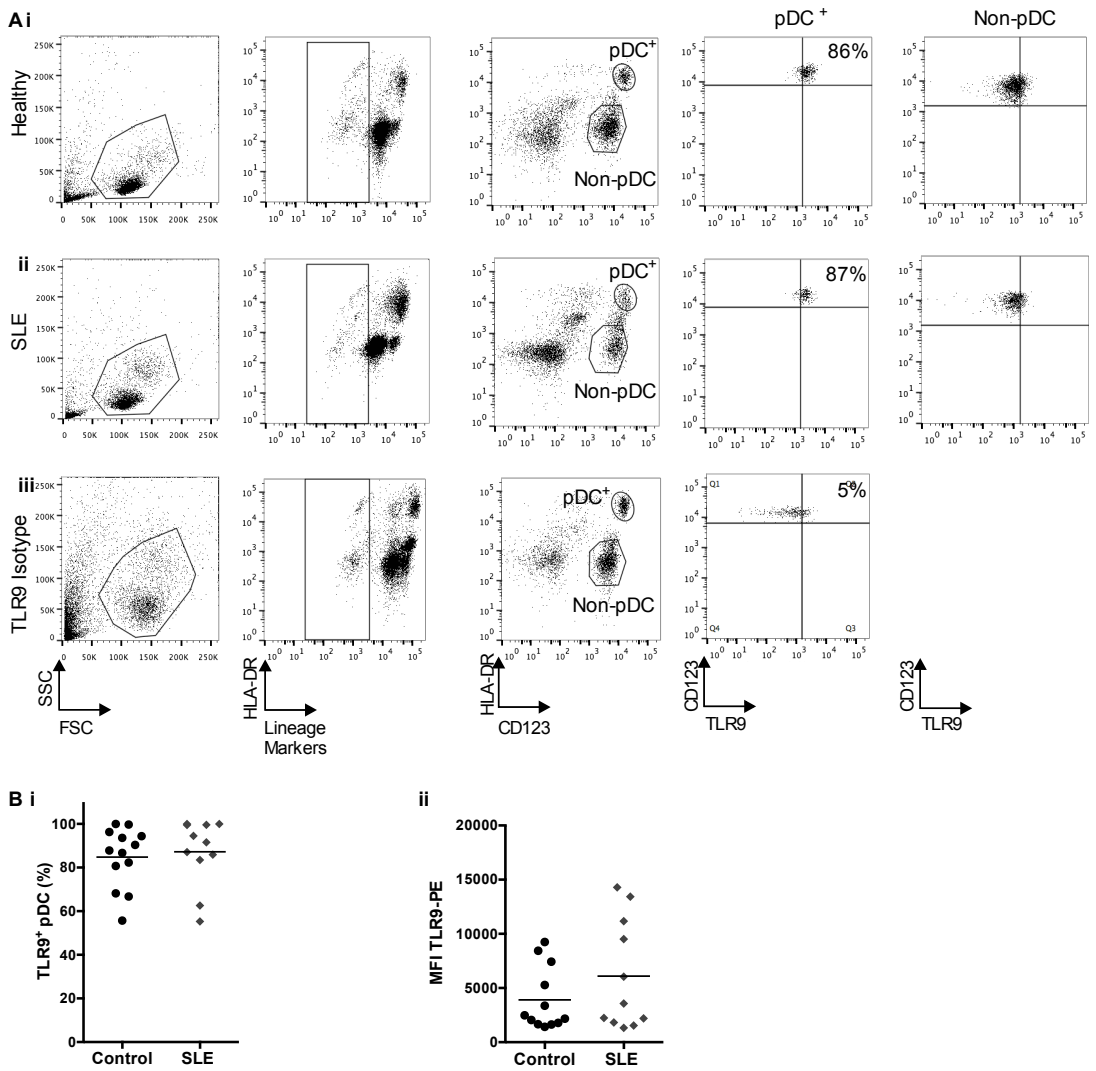

Figure 4.4. SLE and control pDCs express TLR9.

Beginning on the previous page, (**A**) Intracellular TLR9 expression in peripheral pDCs (Lineage$^-$ HLA-DR$^+$ CD123^{high}) and pDC-negatives (Lineage$^-$ HLA-DR$^-$ CD123$^+$) was assessed by flow cytometry of (**i**) control PBMCs and (**ii**) SLE PBMCs. (**iii**) The TLR9 isotype control antibody was used to set the gates. (**B**) Intracellular TLR9 expression in pDCs was quantified as (**i**) the proportion of TLR9-positive pDCs and (**ii**) as the MFI of TLR9-PE. There was no significant difference between control and SLE as determined by unpaired *t* test. n = 12 (control) and 11 (SLE).

4.2.4 SLE B cells make IL-10 in response to CpGB.

Since SLE pDCs did not respond well to TLR9 stimulation by CpGA, I was interested to determine if TLR9 stimulation was also affected in B cells. I stimulated B cells for 72 h with CpGB (2μM chosen following dose response; Appendix C Figure 1C) and found that, compared to unstimulated B cells, IL-10 secretion was enhanced by more that 100% in SLE CD19$^+$ B cells and a mean of 87% control CD19$^+$ B cells (Figure 4.5.A). The difference between IL-10 secretion by SLE and control B cells was not statistically significant. In addition, TLR9 stimulation of whole PBMCs that contained SLE B cells also resulted in increased IL-10 secretion (Figure 4.5.B). However, co-culturing CpGB-stimulated SLE PBMCs with apoptotic cells further augmented IL-10 secretion by a mean of only 8% compared to a mean of 44% increase in control PBMCs (Figure 4.5.C).

I next wanted to determine if the limited apoptotic cell-mediated IL-10 response by SLE PBMC occurred due to differences in the B cell populations in SLE, compared to controls (healthy donors and non-SLE patients). Consistent with the published literature[324], I found that the CD24^{hi}CD38^{hi} 'transitional' B cell population was increased in SLE patients compared to controls (Figure 4.6.A-C), although the difference did not reach statistical significance. Whereas, the IgD$^+$ CD27$^-$ 'naïve, IgD$^-$ CD27$^+$ 'switched memory', and IgD^{low}CD27$^+$ CD1c$^+$ IgM$^+$ 'marginal zone' B cell populations were reduced in SLE (Figure 4.6.C).

There was no significant difference in the percentage of $CD20^+$ and $CD19^+$ B cells (Figure 4.6.Di and 4.6.Dii, respectively) in the control and SLE lymphocyte populations. However, SLE lymphocytes contained a lower proportion of $CD3^+$ T cells (mean 52%) compared to healthy lymphocytes (mean 70%; Figure 4.7.B). The expression of both $CD3^+$ $CD4^+$ T cells and $CD3^+$ $CD8^+$ T cells were significantly reduced in SLE by 51% and 45%, respectively (Figure 4.7.C). This is in contrast to published data that showed SLE patients had the same percentage of $CD4^+$ and $CD8^+$ T cells as healthy donors[230].

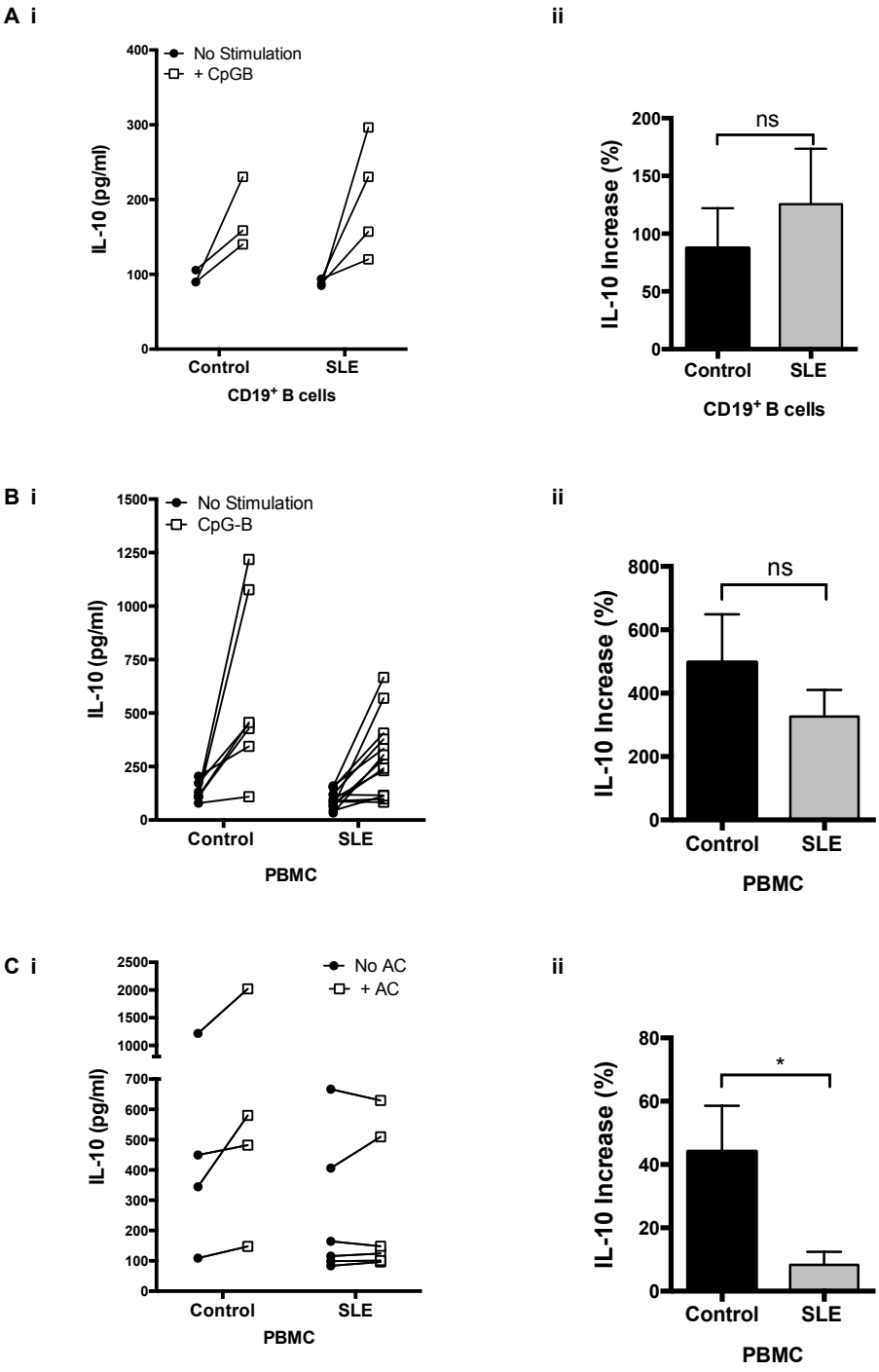

Figure 4.5. SLE B cells make IL-10 in response to TLR9 stimulation by CpGB, but not apoptotic cells.

(**A**) Control and SLE $CD19^+$ B cells were cultured without stimulation (•), or with TLR9 stimulation by CpGB (□). After 72 h (**i**) IL-10 concentration in supernatant was measured and (**ii**) the percentage increase in IL-10 secretion following TLR9 stimulation was determined. n = 3 (control) and 4 (SLE). (**B**) Control and SLE PBMCs were cultured without stimulation (•), or with TLR9 stimulation by CpGB

(□). After 72 h (**i**) IL-10 concentration in supernatant was measured and (**ii**) the percentage increase in IL-10 secretion following TLR9 stimulation was determined. n = 7 (control) and 13 (SLE). (**C**) Control and SLE PBMCs were cultured with CpGB alone (No AC, •), or with apoptotic $CD4^+$ T cells (+ AC, □). After 72 h (**i**) IL-10 concentration in supernatant was measured and (**ii**) the percentage increase in IL-10 secretion following co-culture with apoptotic cells was determined. n = 4 (control) and 6 (SLE). Statistical significance of the difference in the percentage increase in IL-10 secretion by control and SLE cells was analysed by unpaired t-test; (**Aii** and **Bii**) No significant difference (ns); (**Cii**) $^*P = 0.0214$.

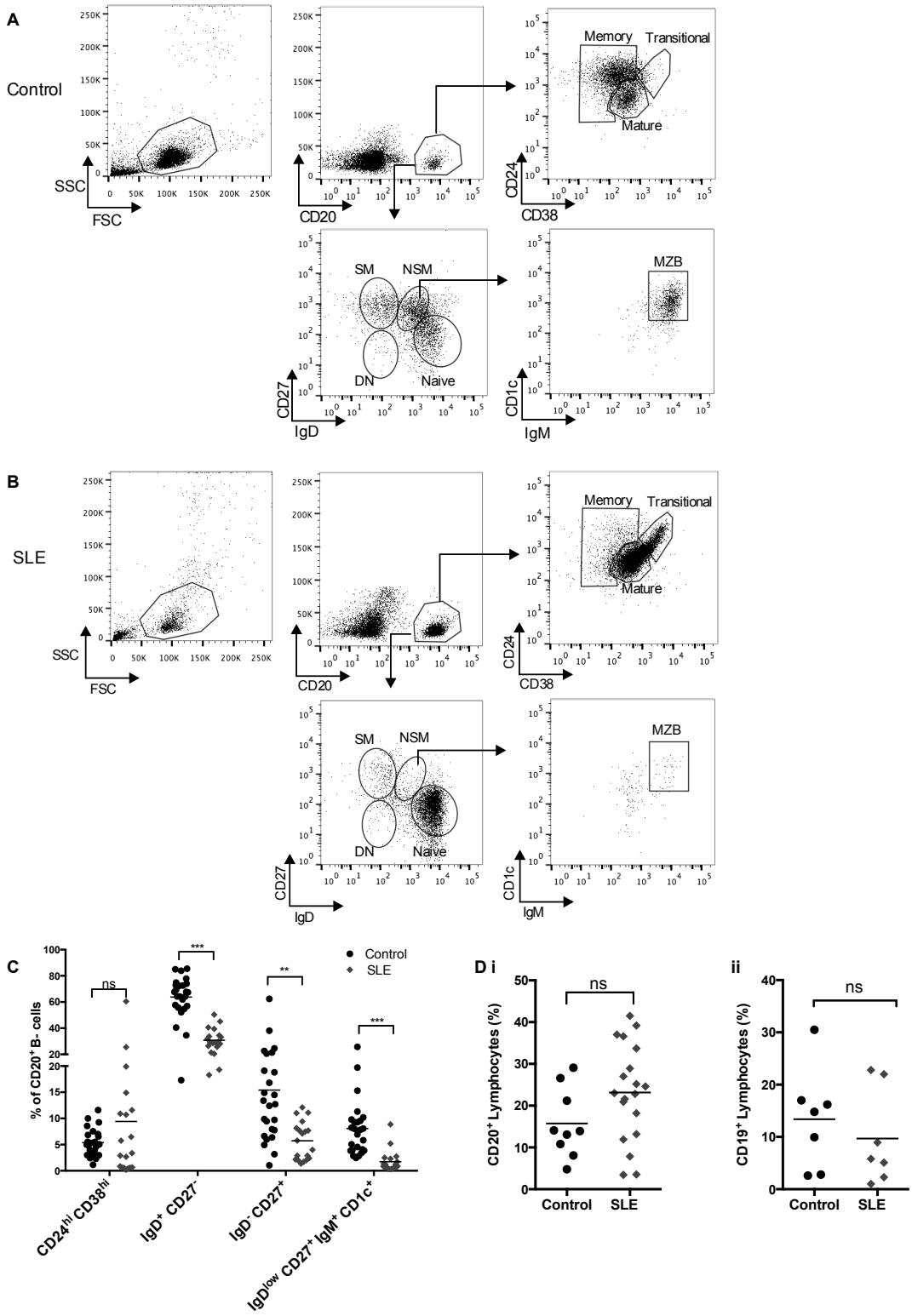

Figure 4.6. SLE patients have a lower proportion of naïve, switched memory, and marginal zone B cells.

The proportion of (**A**) control and (**B**) SLE $CD20^+$ B cells that were transitional ($CD38^{high}$ $CD24^{high}$), naïve (IgD^+ $CD27^-$), switched memory (IgD^- $CD27^+$), and

marginal zone (MZB, IgD^{low} $CD27^{+}$ IgM^{+} $CD1c^{+}$) was assessed by flow cytometry and (**C**) quantified. (**D**) The percentage of (**i**) $CD20^{+}$ and (**ii**) $CD19^{+}$ control and SLE lymphocytes. Each data point represents one donor; (**C**) n = 25 (control) and 19 (SLE) (**Di**) n = 9 (control) and 19 (SLE); (**Dii**) n = 7 (control) and 7 (SLE). Statistical significance was determined by unpaired t-test; no significance (ns); $^{**}P < 0.01$; $^{***}P < 0.0001$.

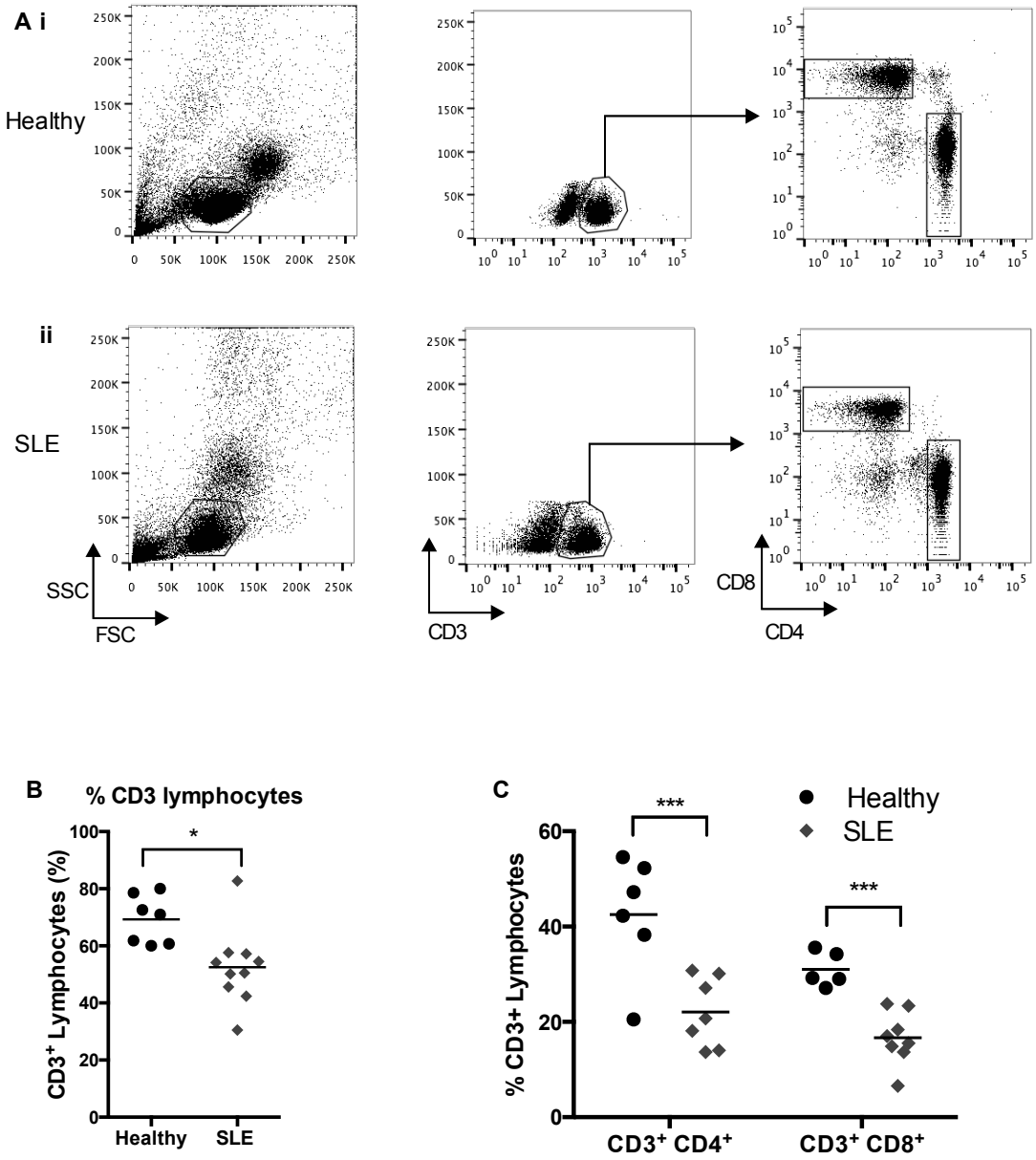

Figure 4.7. SLE patients have a lower proportion of $CD4^{+}$ and $CD8^{+}$ T cells.

(**A**) CD3, CD4, and CD8 expressing (**i**) healthy and (**ii**) SLE lymphocytes were analysed by flow cytometry. (**B**) The percentage of CD3-positive healthy and SLE lymphocytes was quantified. n = 7 (healthy) and 10 (SLE). $^{*}P$ = 0.0109. (**C**) The percentage of $CD3^{+}$ $CD4^{+}$ (n = 6 (healthy) and 7 (SLE); $^{***}P$ = 0.003) and $CD3^{+}$

$CD8^+$ T cells (n = 5 (healthy) and 8 (SLE); $^{***}P = 0.003$) in healthy (•) and SLE (◆) lymphocytes was quantified. Statistical significance was determined by unpaired t-test.

4.2.5 SLE lymphocytes are more susceptible to dying following initiation of apoptosis.

As discussed at the beginning of this chapter, lymphopenia in SLE patients may be caused by the lymphocytes becoming apoptotic at a faster rate than lymphocytes from healthy donors. I wanted to further assess cell death, but due to the low numbers of leukocytes obtained from SLE patient blood I decided to look at the whole lymphocyte population obtained in the non-adherent cell fraction after adhering the monocytes to plastic. This did not affect the proportion of T cells and B cells within the lymphocyte population (Appendix C Figure 2). However, it should be noted that the non-adherent population that I have called lymphocytes in this chapter and in chapter five likely contains contaminating monocytes due to the impaired ability of SLE monocytes to adhere to plastic[78].

I measured apoptosis by flow cytometry using AnV and propidium iodide (PI), which were gated as shown by the representative FACS plots (Figure 4.8.Ai-ii). AnV is a phospholipid binding protein that identifies cells in the early stage of apoptosis when PS is transferred from the inner leaflet to the outside of the plasma membrane. Late apoptotic/necrotic cells are detected by co-staining with cell membrane impermeable DNA-intercalating dyes, such as PI, which are excluded from early apoptotic cells due to an intact cell membrane.

Here I found that SLE lymphocytes were already dying immediately following isolation from the blood. At this stage (0 h) a mean of 19% of SLE lymphocytes were AnV single positive (Figure 4.8.Bi) and 7% were double positive for AnV and PI, indicating secondary necrosis (Figure 4.8.Bii). Consistent with published reports, SLE lymphocytes were induced to become apoptotic at an accelerated rate. A mean of 23% SLE lymphocytes were AnV single positive 2 h following initiation of the intrinsic apoptotic pathway by UV irradiation and this was enhanced to 40% after 4

h, compared to 14% (2 h) and 24% (4 h) of healthy control lymphocytes (Figure 4.8.Bi). Activating the extrinsic apoptotic pathway by Fas ligation with anti-CD95 antibody (also known as Fas) for 4 h also resulted in a mean of 40% SLE lymphocytes and 25% healthy lymphocytes becoming AnV single positive (Figure 4.8.Bi). Healthy donor lymphocytes did not progress to secondary necrosis 4 h after induction of apoptosis with UV (4%) or anti-CD95 antibody (4%) (Figure 4.8.Bii), as expected. However, a mean of 22% UV irradiated, and 13% anti-CD95 antibody treated SLE lymphocytes were AnV and PI double positive after 4 h (Figure 4.8.Bii).

The surface of lymphocytes was assessed using scanning electron microscopy to quantify cells that were designated as looking viable, apoptotic (indicated by the protrusion of apoptotic bodies), and necrotic (indicated by the appearance of a compromised membrane) (Figure 4.8.Ci-ii). Immediately following isolation, 40% of 50 SLE lymphocytes counted per sample were in a necrotic state, whereas less than 20% of healthy lymphocytes were necrotic or apoptotic (Figure 4.8.Di). After 4 h of apoptosis induction using anti-CD95, 50% of healthy lymphocytes had started to generate apoptotic bodies, with only 10% showing necrotic cell phenotype (Figure 4.8.Dii). Conversely, more than half of SLE lymphocytes plasma membrane appeared necrotic following 4h anti-CD95 treatment, while 28% remained viable and 18% had the appearance of apoptotic bodies (Figure 4.8.Dii).

4.2.6 **Apoptosis is not accelerated in SLE neutrophils.**

It is also known that an increase in circulating apoptotic neutrophils[77,325] and neutropenia are commonly associated with SLE[326]. Therefore, I asked if SLE neutrophils, like lymphocytes, were also dying at an accelerated rate. Neutrophils have a short lifespan and naturally die rapidly in culture[327]. Peripheral human neutrophils isolated from blood by a percoll gradient can be sorted to high purity using their size (FSC) and granularity (SSC)[328]. I analysed neutrophils by flow cytometry using FSC/SSC gating to determine the rate of spontaneous cell death after 2 h, 4 h, and 12 h in culture, which revealed that a similar proportion of SLE

neutrophils were AnV-positive at these time points compared to healthy neutrophils (Figure 4.9).

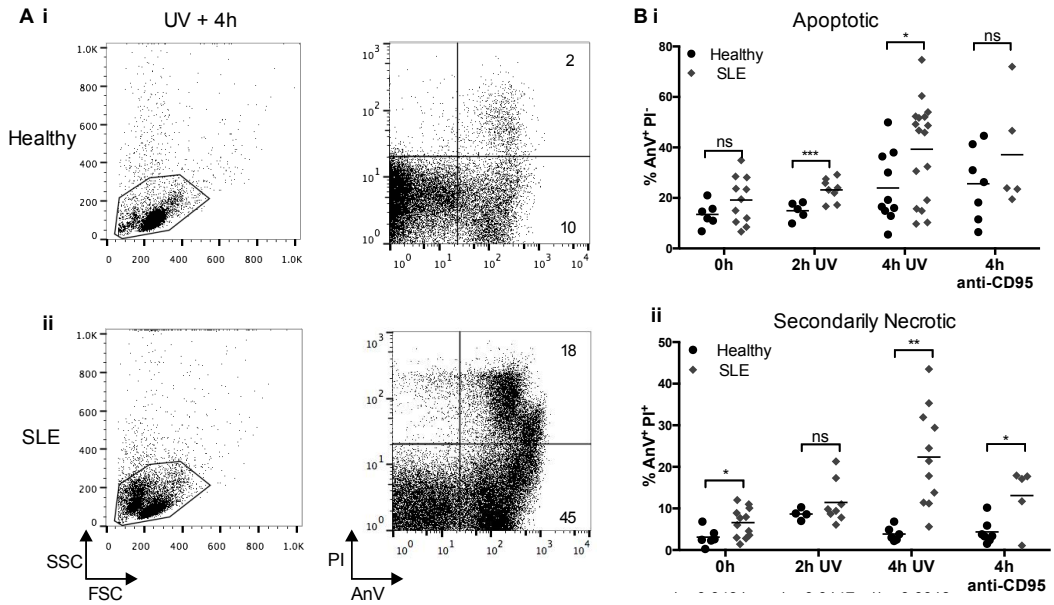

Figure 4.8. SLE lymphocytes are more susceptible to becoming secondarily necrotic.

(Continued overleaf)

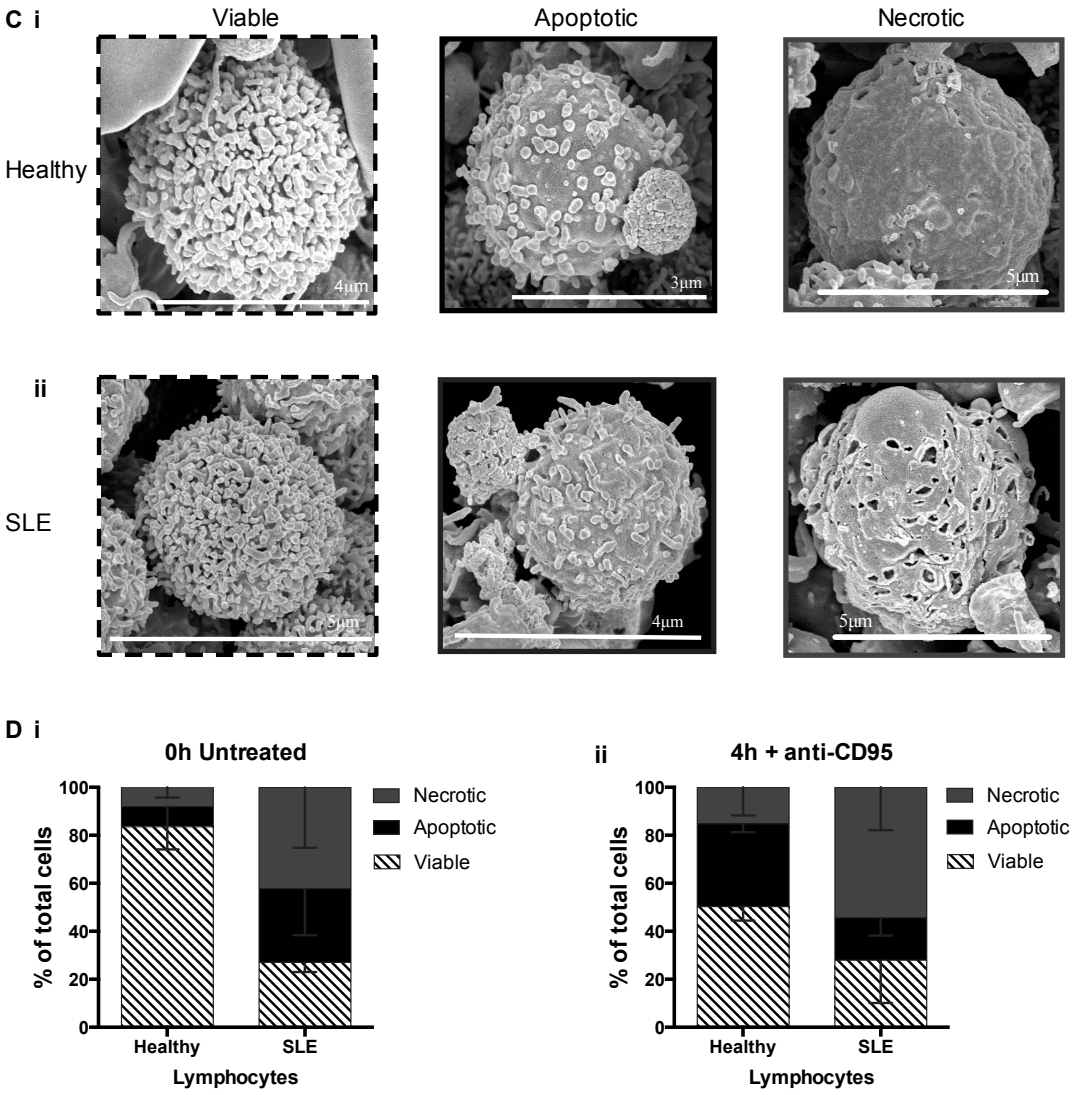

Figure 4.8. SLE lymphocytes are more susceptible to becoming secondarily necrotic.

On the previous page, (**A**) Representative flow cytometry plot showing the gating strategy for measuring apoptosis by AnV and PI staining of (**i**) healthy and (**ii**) SLE lymphocytes. (**B**) The percentage of healthy (•) and SLE (◆) lymphocytes that were (**i**) early apoptotic (AnV^+ PI^-) and (**ii**) secondarily necrotic (AnV^+ PI^+) at 0 h, 2 h and 4 h post-UV irradiation, and 4 h after anti-CD95 treatment. n = 5-10 (healthy) and 5-17 (SLE). (**C**) Representative scanning electron microscopy images showing (**i**) healthy and (**ii**) SLE lymphocytes that were classified as viable, apoptotic, and necrotic. (**D**) The proportion of healthy and SLE lymphocytes that looked viable, apoptotic, and necrotic was quantified at (**i**) 0 h and (**ii**) 4 h after anti-CD95 treatment. n = 2. Statistical significance was quantified by unpaired t-test; no significance (ns); $^{*}P < 0.05$; $^{**}P < 0.01$; $^{***}P < 0.0001$.

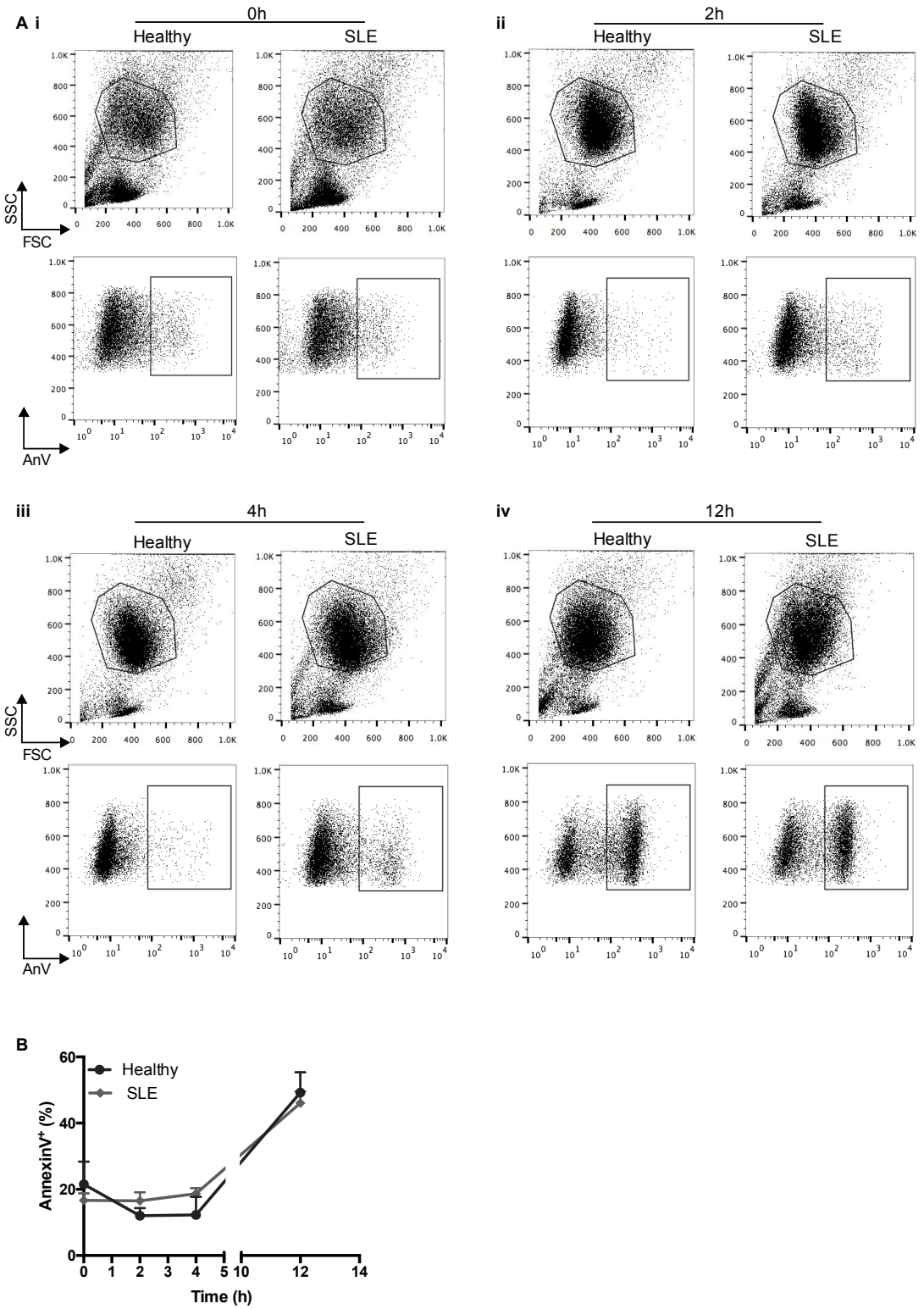

Figure 4.9. SLE neutrophils die spontaneously at the same rate as healthy neutrophils.

(**A**) Representative flow cytometry plots showing the gating strategy for measuring apoptosis by AnV staining of healthy and SLE neutrophils that were cultured for (**i**) 0

h, (**ii**) 2 h, (**iii**) 4 h, and (**iv**) 12 h. (**B**) The percentage of the healthy (•) and SLE (◆) neutrophil population that was AnV-positive at 0 h, 2 h, 4 h, and 12 h was quantified. Each data point represents the mean of four donors with error bars showing SEM.

4.2.7 Caspase-activated DNA fragmentation is impaired in apoptotic SLE lymphocytes.

I measured activation of the apoptosis executioner caspases to determine if the high proportion of necrotic SLE lymphocytes (AnV^+ PI^+; Figure 4.8.Bii) was caused by activation of the apoptotic cell death pathway. This was achieved using a fluorescence assay to detect the conversion of pro-caspases 3 and 7 in to active caspases 3 and 7 (optimisation Appendix C Figure 3), which confirmed that SLE lymphocyte cell death did indeed occur in response to normal activation of caspases (Figure 4.10).

The effector caspases trigger processes required for chromatin condensation and DNA fragmentation[329]. I assessed DNA fragmentation in untreated (Figure 4.11.A) and anti-CD95 treated lymphocytes (Figure 4.11.B) by confocal microscopy and found that the mean fluorescence intensity of TUNEL-positive nuclei was significantly lower in the SLE lymphocytes (Figure 4.11.D).

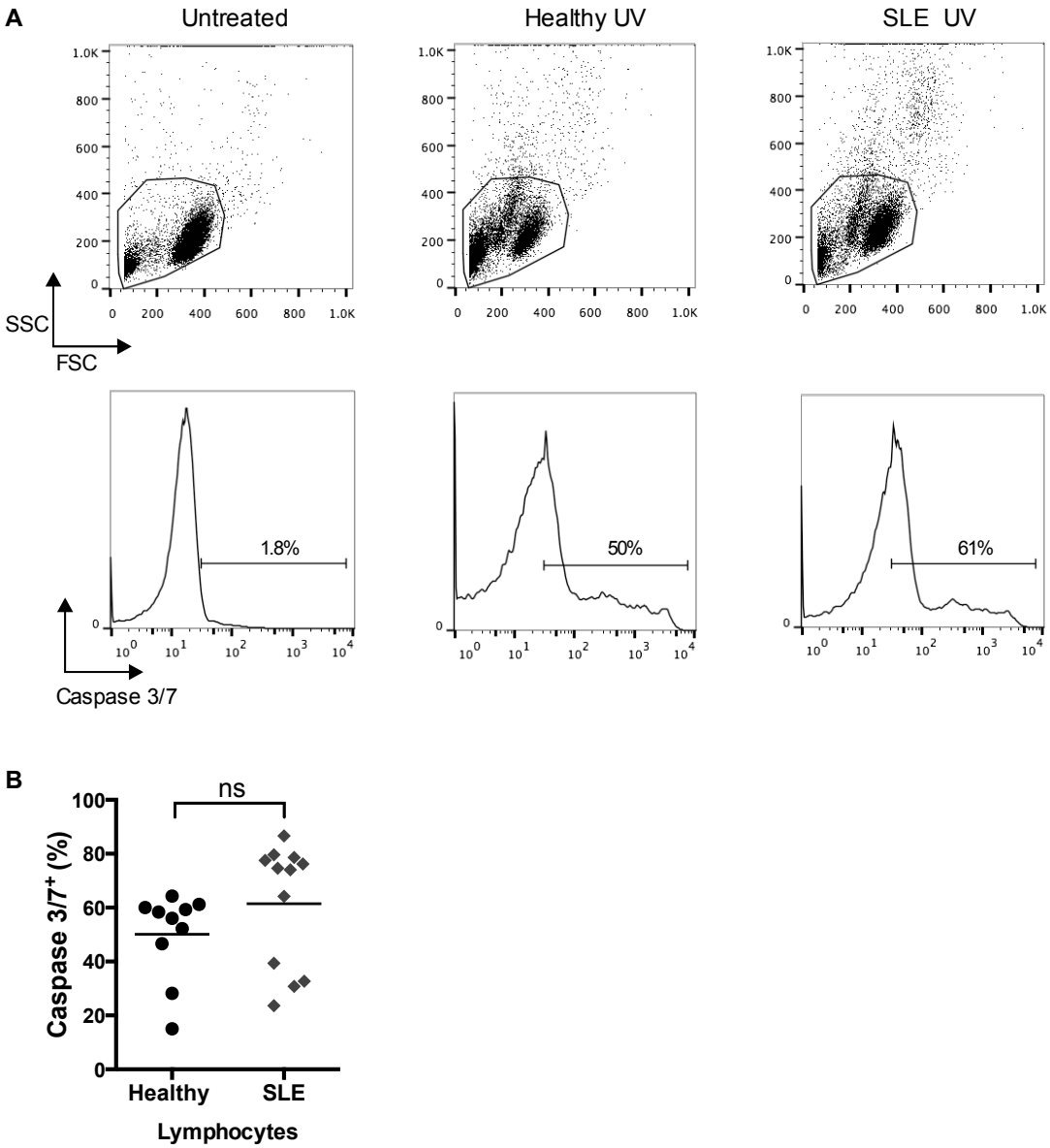

Figure 4.10. Caspase 3 and 7 are activated in healthy and SLE lymphocytes after UV irradiation.

(**A**) Representative histograms showing the gating strategy of activated caspase 3/7-positive lymphocytes using untreated healthy lymphocytes as a negative control. (**B**) The proportion of caspase 3/7-positive healthy and SLE lymphocytes was quantified after UV irradiation to induce apoptosis. n = 10 (healthy) and 12 (SLE). Statistical significance was determined by unpaired t-test. ns (not significant).

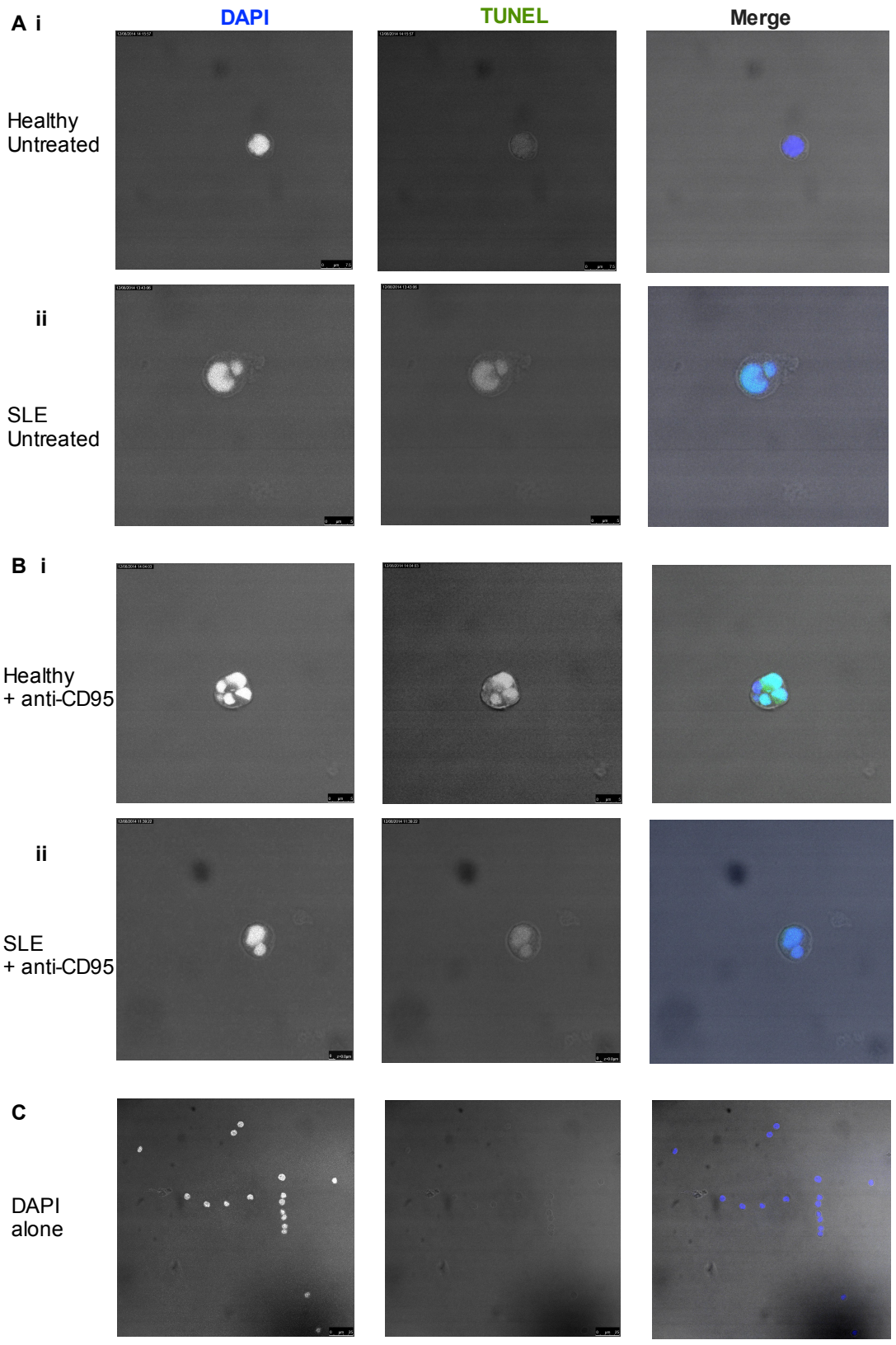
A i
DAPI
TUNEL
Merge
Healthy
Untreated
ii
SLE
Untreated
B i
Healthy
+ anti-CD95
ii
SLE
+ anti-CD95
C
DAPI
alone
D
TUNEL Fluorescence Intensity
100
80
60
40
20
0
***
Healthy
SLE

Figure 4.11. The fluorescent intensity of TUNEL-positive nuclei in SLE lymphocytes was reduced compared to healthy lymphocytes.

Beginning on the previous page, (**A**) Untreated and (**B**) 4 h anti-CD95 treated (**i**) healthy and (**ii**) SLE lymphocytes were fixed and stained using the TUNEL assay to detect DNA fragmentation (green) and DNA (DAPI, blue) then assessed by confocal microscopy. (**C**) Non-specific fluorescence of DAPI into TUNEL-positive channel was assessed. Scale bar: (**Ai**) 7.5μm; (**Aii-Bii**) 5μm; (**C**) 25μm. (**D**) The mean fluorescence intensity of TUNEL-positive nuclei in anti-CD95 treated lymphocytes from three independent donors was measured in at least 30 fields of view (per donor) using ImageJ software. Statistical significance was determined by unpaired *t*-test. $^{***}P = 0.0004$.

4.2.8 SLE lymphocytes have an excess of mitochondria.

I next assessed mitochondria, since they play a central role in the apoptosis pathway. Cardiolipin is an important lipid component of the inner mitochondrial membrane. Apoptotic stimuli triggers elevated ROS resulting in the oxidation of cardiolipin, which then accumulates on the outer mitochondrial membrane and permits the formation of membrane pores[330]. The subsequent release of cytochrome *c* induces the apoptotic caspase cascade[5]. NAO is a fluorescent marker that binds to non-oxidised cardiolipin, and consequently was originally used to determine mitochondrial mass[331]. However, NAO fluorescence is reduced when cardiolipin is oxidised, therefore it is now also used to detect loss of mitochondrial membrane integrity, which occurs during the very early stages of apoptosis initiation[332].

The proportion of cells that had lost NAO fluorescence after 4 h culture in media alone (untreated), or following apoptosis induction by UV irradiation, or anti-CD95 was measured by flow cytometry (Figure 4.12.Ai). Compared to healthy lymphocytes, approximately double the proportion of SLE lymphocytes was NAO-negative 4 h after culture in media alone and after UV-irradiation (Figure 4.12.Aii). 4 h anti-CD95 treatment resulted in the greatest difference between healthy and SLE lymphocytes, with a mean of three times more NAO-negative SLE lymphocytes compared to healthy lymphocytes (Figure 4.12.Aii).

Transmission electron microscopy of $CD19^+$ B cells and $CD4^+$ T cells fixed immediately following isolation from the blood showed an accumulation of structures that resemble mitochondria in cells derived from SLE patients (Figure 4.12.Bi and Ci). Healthy donor B cells contained a mean of 1.4 mitochondria whereas SLE B cells had a mean of 6.4 mitochondria (Figure 4.12.Bii). Similarly, healthy T cells contained a mean of 2.1 mitochondria and SLE T cells had a mean of 5.9 mitochondria (Figure 4.12.Cii).

4.2.9 Apoptotic SLE lymphocytes have an impaired ability to induce regulatory B cells.

Apoptotic cells normally instruct the immune system to prevent inflammation. For example, dying cells regulate immunity through apoptotic DNA-dependent induction of IL10-secreting regulatory B cells[55,56]. I hypothesised that, because AnV single positive early apoptotic cells were more numerous in SLE lymphocytes following UV irradiation (Figure 4.8.Bi), they should be able to enhance IL-10 secretion by CpGB-stimulated healthy donor B cells. However, compared to the response induced by healthy apoptotic lymphocytes (mean 1,312 pg/ml), IL-10 secretion was significantly impaired when B cells were co-cultured with apoptotic SLE lymphocytes (mean 728 pg/ml; Figure 4.13A). IL-6 production was also limited, although this was not statistically significant (Figure 4.13B). I was also surprised to find that apoptotic lymphocytes from SLE patients failed to augment CpGA-induced IFN-α production by healthy pDCs, although this did not reach statistical significance (Figure 4.13.C)

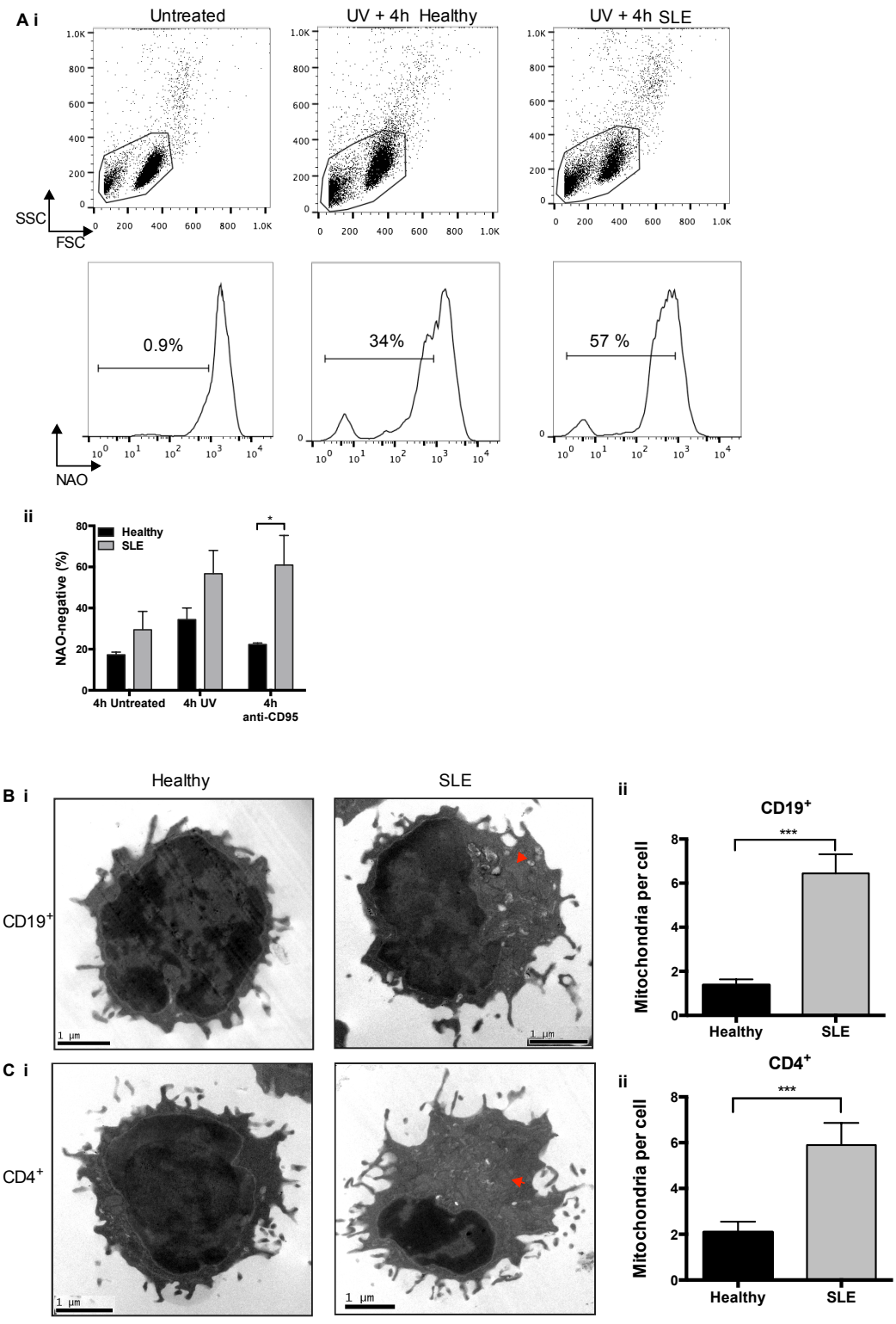

Figure 4.12. SLE lymphocyte mitochondria lose membrane integrity more rapidly and are in higher abundance than healthy lymphocyte mitochondria.

(**Ai**) Representative flow cytometry plots showing the selection of the NAO negative gate using healthy lymphocytes that were stained with NAO, but were not induced to

become apoptotic (untreated), as a negative control. (**Aii**) The percentage of NAO-negative healthy (black bar, $n = 5$) and SLE (grey bar, $n = 5$) lymphocytes 4 h after culture in media (4 h untreated), following UV irradiation (4 h UV), and after anti-CD95 antibody treatment (4 h anti-CD95). (**Bi**) Untreated healthy and SLE $CD19^+$ B cells were imaged by transmission electron microscopy. (**ii**) The mean number of mitochondria (indicated by the red arrow head) per B cell was quantified. (**Ci**) Untreated $CD4^+$ T cells were imaged by transmission electron microscopy. (**ii**) The mean number of mitochondria (indicated by the red arrow head) per T cell was quantified. Scale bar: 1μm Statistical significance was determined by unpaired *t*-test; $^*P = 0.018$; $^{***}P < 0.001$.

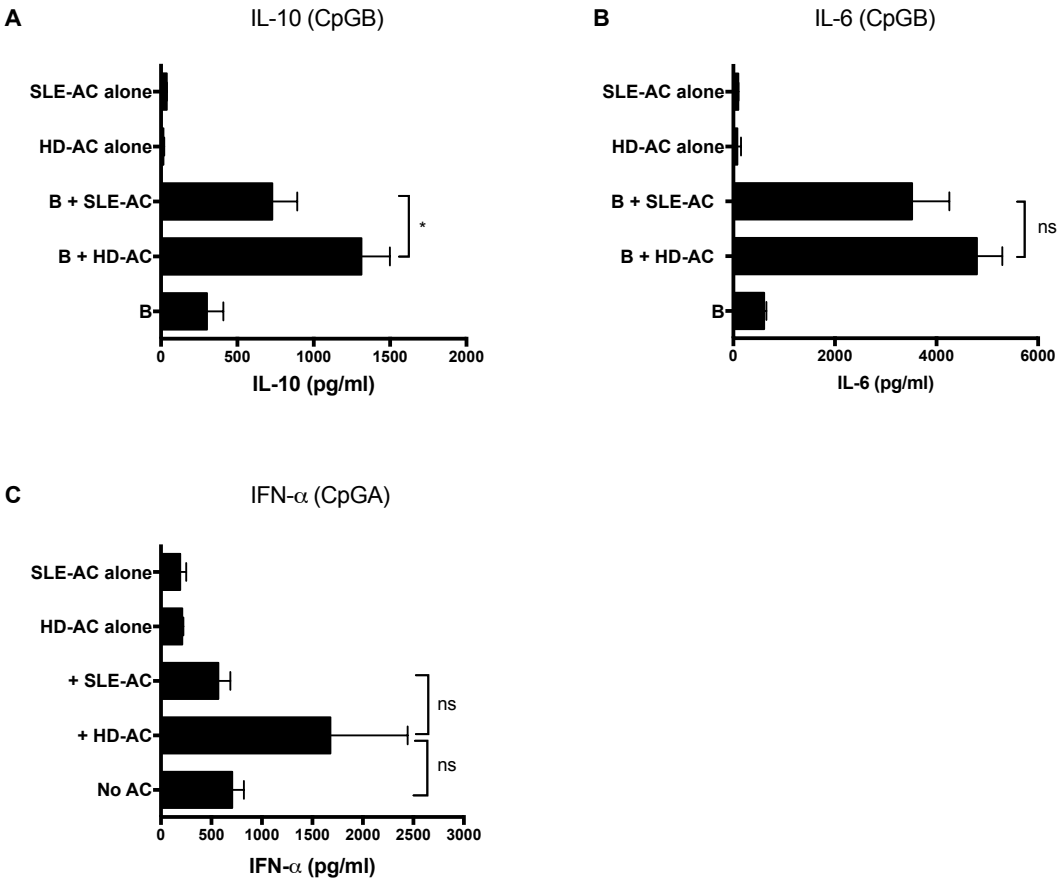

Figure 4.13. Apoptotic SLE lymphocytes have an impaired ability to induce cytokine secretion by healthy B cells and pDCs.

(**A**) IL-10 and (**B**) IL-6 production was quantified by ELISA 72 h after healthy B cells were cultured with CpGB alone, and CpGB plus $0.5x10^6$ healthy donor apoptotic lymphocytes (B + HD-AC), or $0.5x10^6$ SLE apoptotic lymphocytes (B + SLE-AC). Healthy and SLE apoptotic cells were cultured with CpGB alone as a negative control. (**C**) IFN-α production was quantified 72 h after CD19-negative healthy PBMCs were cultured with CpGA alone (No AC), and with 10^6 healthy donor apoptotic lymphocytes (+ HD-AC), or 10^6 SLE apoptotic lymphocytes (+

SLE-AC). Graphs are the mean of (**A-B**) nine and (**C**) three independent experiments with error representing SEM. The significant difference in cytokine production induced by healthy apoptotic lymphocytes compared to SLE apoptotic lymphocytes was analysed by *t*-test; $^{*}P = 0.0346$.

4.3 Discussion

In this chapter I set out to investigate if healthy human pDCs respond to apoptotic cells in a similar way to mouse pDCs and if SLE lymphocytes die abnormally. I have revealed that, in the absence of SLE IgG autoantibodies, apoptotic cells augment CpGA-induced IFN-α secretion by healthy human pDCs, but IFN-α production in response to TLR9 stimulation was impaired in SLE pDCs. I also found that SLE lymphocytes had a high propensity to becoming secondarily necrotic. Furthermore, apoptotic SLE lymphocytes had a reduced ability to modulate responses by healthy B cells and pDCs. These findings are important when considering the role of pDCs and apoptotic cells in SLE pathogenesis.

I was interested to find that apoptotic cells, but not necrotic cells, induced healthy donor pDCs to secrete IFN-α only when they were co-exposed to CpGA, which is consistent with the mouse pDC data presented in chapter three. This novel finding increases our understanding of how human pDCs respond to apoptotic cells in an inflammatory environment. It expands our view that pDCs 'ignore' apoptotic cell-derived nucleic acids in homeostatic conditions, but this is disrupted by an intervening inflammatory stimulus, such as FcγRIIa activation by immune complexes[101,272], or TLR9 activation by CpGA.

It has been published that small DNA-containing membrane microparticles (DNA-MMP) released from apoptotic cells, but not necrotic cells, were endocytosed by healthy human pDCs independently of FcγRII and induced TLR9-dependent IFN-α secretion[333]. This study supports my finding of antibody-independent uptake and stimulation of human pDCs by self-apoptotic cell components. However, the authors reported IFN-α production using apoptotic MMPs alone, which contradicts my need

to co-activate the pDCs with a synthetic TLR9 ligand in order for whole apoptotic cells to augment IFN-α secretion.

The accepted paradigm is that pDCs only respond to late apoptotic/necrotic cells following a two-signal stimulation: 1) IgG autoantibodies engaging FcγRIIa followed by, 2) entry of immune complexes in to pDCs and engaging TLR7/9[100,101,272]. I also had to provide a second signal (CpGA activation of TLR9) in order for primary apoptotic cells to become immunogenic. Yet, in contrast to the published findings using late apoptotic/necrotic cell lines, I found that IFN-α secretion was inhibited by IgG purified from anti-DNA^+ RNP^+ SLE patient serum even in the presence of free DNA/RNA released from necrotic primary cells. This again highlights the difference between apoptotic cell lines and primary cells, as discussed in chapter three.

However, studies have shown that monocytes regulate immune complex and bacterial DNA-induced IFN-α production by human pDCs in PBMC cultures[321,334]. Therefore, it is important to take in to consideration the regulatory network of cells that pDCs will encounter *in vivo*. Nevertheless, I did not see an IgG-mediated increase when the pDCs were purified from PBMCs; although they potentially had not survived in culture long enough to respond. FcγRIIa is also a negative regulator of CpGA-induced IFN-α production when it is triggered in the absence of immune complexes by high concentrations (>5mg/ml) of 'free' IgG[100]. Therefore, although I only used 10μg/ml of IgG antibodies in the assays (in accordance to previous studies[93]), it is possible that the SLE IgG autoantibodies failed to form a complex with healthy donor apoptotic and necrotic DNA/RNA thus they acted by directly inhibiting pDC IFN-α through FcγRIIa.

The number of pDCs found circulating in SLE patients has not been consistently reported. It is now known that the human pDC marker BDCA-2 that was used in previous studies to show a reduction in peripheral pDCs in SLE[335,336] is downregulated following TLR7/9 activation[337]. Therefore it is not clear if the

perceived reduction was due to the SLE pDCs being activated. In this chapter I confirmed that pDCs were reduced in SLE PBMCs using the markers CD304 and CD123. Conversely, it has also been reported that the percentage of BDCA-4 $(CD304)^+$ peripheral blood pDCs in SLE patients was not significantly different[336] or higher than healthy donors[338].

Despite being reduced, perhaps due to mobilisation to sites of inflammation[339], SLE pDCs were not completely depleted (>0.1%) and they expressed normal levels of TLR9 protein. Nevertheless, SLE PBMCs failed to make a good IFN-α response to CpGA even in the presence of apoptotic cells. This complements published findings that SLE PBMC made less IFN-α in response to DNA-containing immune complexes, or HSV-1[336]. It could be considered that SLE pDCs were potentially hyporesponsive to TLR9 stimulation *in vitro* due to the induction of TLR9 tolerance by immune complexes during circulation, which has been described in lupus-susceptible mice[340]. Addtionally, the SLE pDCs might not have survived the *in vitro* cell culture.

While I saw low IFN-α production by SLE PBMCs, it was apparent that not all responses to TLR9 activation were defective, as demonstrated by equivalent CpGA-induced IL-6 secretion by both healthy and SLE PBMCs. IL-6 and IFN-α secreted by pDCs along with 'help' via CD40 signalling induce the differentiation of virus-specific and autoreactive antibody secreting plasma cells[119,341]. Like IFN-α, IL-6 is elevated in SLE serum and it is emerging as a new potential therapeutic target for treating SLE patients, as discussed in chapter one and reviewed in reference[126]

PDCs are associated with SLE pathogenesis due to their natural ability to make IFN-α in response to nucleic acids. Although it is not known how SLE pDCs respond to TLR9 and apoptotic cells within patients, the lack of an increase of IFN-α in this in vitro study questions the significance of pDC activity in SLE. Additionally, IRF5 SNPs, which are related to the IFN-α pathway and are associated with SLE susceptibility[342] actually reduce the ability of pDCs to secrete IFN-α in response to

RNA immune complexes, or CpGA[343] even though IFNα-induced gene upregulation was elevated by serum from patients with these SNPs[344]. Specific depletion of pDCs in the BXSB lupus mouse model indicate that pDCs are necessary for initiating disease through activation of T cells, B cells and mDCs, and autoantibody production, but the IFN-α signature in blood was not affected[345]. Other cells, in particular neutrophils in circulation and bone marrow are emerging as an additional source of IFN-α production in SLE[346,347].

In the second part of this chapter I confirmed that SLE lymphocytes (enriched from PBMCs by adhering monocytes to culture wells) were more susceptible to becoming apoptotic, but I also found that they became significantly more secondarily necrotic at an early time point. The lack of the appearance of apoptotic bodies imaged by scanning electron microscopy and less intense, more diffuse DNA fragmentation suggests that SLE lymphocytes were dying abnormally even though the apoptotic effector caspases 3 and 7 were activated. Intriguingly, chromatin fragmentation in apoptotic renal cells is reduced in lupus-prone mouse models[348], and caspase-activated DNase-deficiency, which results in the inability to correctly fragment nuclear DNA during apoptosis, leads to increased anti-DNA/chromatin antibodies[349]. I speculate that the apoptosis pathway is initiated, but it is unable to successfully proceed; therefore the dying cells break apart instead. Pharmacological caspase inhibitors, such as zVAD-fmk, would confirm if the apoptotic caspase cascade elicited the increased number of necrotic SLE lymphocytes, or if this occurred independently of the effector caspases.

Although enhanced Fas-expression due to lymphocyte activation might explain why Fas-mediated apoptosis was enhanced using anti-CD95 (Fas) antibody in SLE lymphocytes, I found that rapid cell death was also induced by activation of the intrinsic death pathway by UV irradiation. This suggests that SLE lymphocytes are intrinsically susceptible to becoming secondarily necrotic. Using NAO fluorescence, I observed that a higher proportion of SLE lymphocytes had disrupted mitochondrial integrity, which complements reports that SLE T cells have increased mitochondrial

membrane polarisation and less ATP[350,351]. Furthermore, mouse B cells co-stimulated through the BCR and TLR7 have depleted ATP, loss of mitochondrial membrane potential and showed necrotic morphology[352]. It was discovered many years ago that when intracellular ATP concentration is low, apoptosis switches to necrosis, although this did not result in externalisation of PS[2 3]. Therefore, malfunctioning mitochondria might be key to explaining why SLE lymphocytes do not survive.

In addition, dynamin-related protein 1 (Drp1) expression is reduced in SLE T cells[353]. Drp1 is required for mitochondrial fission and mitophagy, an autophagy process first termed a decade ago[354], which is essential for regulating mitochondrial quality. Mitochondrial mass is increased in autophagy-deficient peripheral T cells and this is associated with elevated apoptosis[355]. I hypothesise that dysfunctional mitophagy might be associated with the abnormal accumulation of structures resembling mitochondria I observed in SLE T and B cells. Whether SLE mitochondria are inflammatory is not known and this will be discussed in more detail in chapter six in the context of the other work reported in this thesis.

Enriched SLE apoptotic lymphocytes were impaired at regulating both anti-inflammatory IL-10 secretion by B cells and pro-inflammatory IFN-α secretion by pDCs; further supporting the hypothesis that apoptosis is abnormal is SLE lymphocytes. To induce these immune responses it is essential that healthy B cells and pDCs recognise apoptotic DNA/chromatin expressed on intact apoptotic cell membranes[55] (chapter 3 page 84). Human pDCs are unable to phagocytose large components, such as whole apoptotic cells[356], but they can internalise apoptotic bodies[211], which express the DNA and chromatin[357]. However, the membrane of apoptotic SLE lymphocytes rapidly breaks apart and apoptotic bodies are less frequent. These novel findings indicate that apoptotic DNA/chromatin from SLE patients may not be presented, or recognised in the same way as in health. Whilst pDCs recognised healthy apoptotic lymphocytes independently of SLE IgG, it remains to be investigated if it is required for the recognition of SLE apoptotic

lymphocytes. The potential role of SLE DNA in disease pathogenesis will be discussed in chapter six.

Looking from the other perspective, I showed that healthy apoptotic cells failed to augment IL-10 secretion by SLE B cells (within PBMCs) even though they responded well to TLR9 stimulation by CpGB. This was potentially due to SLE patients expressing fewer peripheral MZB cells, which play an important role in regulating tolerance to self-DNA/chromatin complexes expressed on apoptotic cells[55,57]. Immature transitional B cells were higher in SLE patient blood, as previously reported[324,358], but they have reduced IL-10 production and immune regulatory function in response to CD40 stimulation[324]. More recently, another immature B cell population ($CD27^{-}CD38^{int}IgD^{+}$) from SLE patients has been reported to have impaired CD40-induced IL-10 secretion and regulation of T cells[359]. Therefore, the combination of both dysfunctional B cells and abnormal apoptotic cells may contribute to impaired immune regulation in SLE.

In summary, the findings of this chapter demonstrate that we may need to re-assess how healthy pDCs respond to apoptotic cells and the role of pDC-derived IFN-α in SLE pathogenesis. It also suggests that, in addition to activation-induced cell death, the elevated number of apoptotic lymphocytes found circulating in SLE is likely caused by an intrinsic abnormality, which predisposes them to dying abnormally. The inability of SLE lymphocytes to survive and induce immune regulation is further investigated in chapter five.

Chapter 5 The role of autophagy in apoptosis and SLE

5.1 Introduction

The rapid removal of apoptotic cells by neighbouring cells and professional phagocytes is vital for maintaining homeostasis[33]. It is widely accepted that inefficient clearance of apoptotic cells is central to driving inflammation in SLE patients due to an accumulation of secondarily necrotic cells and the abnormal exposure of apoptotic chromatin. The impaired removal of apoptotic cells has been attributed to intrinsic defects in the phagocytic function of SLE macrophages[77,78], which might be caused by reduced Fc-receptor mediated uptake[360]. Additionally, C1q deficiency is a very strong risk factor for developing SLE, which is believed to be due to the loss of apoptotic cell opsonisation and subsequent phagocytosis[361].

However the nuclear antigens associated with SLE are normally expressed on the surface of apoptotic cells and smaller apoptotic bodies[362,363]. Membrane-bound apoptotic bodies contain nuclear antigens, such as DNA, that are safely packaged and more easily phagocytosed. They promote immune regulation, such as stimulating the generation of IL10-secreting regulatory B cells[55,364] and pDCs (chapter 3). Yet the accumulation of apoptotic cells cannot be the only explanation for an increased tendency towards autoimmunity. For example, mice deficient in the apoptotic "eat-me" signals mannose-binding lectin[365] and CD14[106] do not develop autoimmunity, despite an accumulation of apoptotic cells. However, SLE lymphocytes are more susceptible to apoptosis and do so at an accelerated rate (chapter 4), which indicates that there is additional intrinsic defect in the apoptotic cells that triggers inflammation in SLE patients.

A number of recent studies have identified an important role for autophagy proteins in the heterophagy of apoptotic corpses by phagocytes[247-249]. Autophagy proteins,

such as ATG5, ATG7, and LC3-II, are required to mediate the lysosomal degradation, but not uptake, of apoptotic cells in the non-canonical autophagy mechanism, LAP[247,250]. The activation of autophagy prior to apoptotic cell death is also important for the release of "find me" signals to recruit phagocytes, such as LPC and ATP[246]. Additionally, although autophagy has largely been seen as a survival mechanism by cells to avoid cellular apoptosis, it is now clear that the autophagy and apoptosis pathways share many regulatory elements (discussed in chapter 1 section 1.4.3). For example, Bcl-2 not only functions as an anti-apoptotic protein, but also prevents autophagy via its inhibitory interaction with Beclin-1 [238], whereas calpain-cleaved ATG5 translocates to the mitochondria, where it induces apoptosis through inhibition of anti-apoptotic BCL-X_L[243].

Variants in the autophagy-related genes ATG5[67,231] and DRAM-1 [233], are associated with SLE, but the function of autophagy in the pathogenesis of SLE is unclear. On one hand the induction of autophagy has been reported to be defective in SLE $CD4^+$ T cells [230,366]. Conversely, in comparison to healthy control cells, SLE T cells have been shown to contain more vacuoles[228] and $LC3^+$ punctae, which are also increased in SLE B cells [229]. Nevertheless, it has not been investigated if autophagy defects in SLE patients cause accelerated apoptosis, or impaired phagocytosis.

I hypothesised that the reduced ability of SLE lymphocytes to survive and to correctly execute apoptosis (discussed in Chapter 4) is caused by defective autophagy.

Aims

The focus of this chapter was to evaluate the link between autophagy and aberrant apoptosis in SLE using the following aims:

- Establish if autophagy proteins are defective in SLE lymphocytes.
- Assess if autophagy defects are associated with known SNPs.
- Determine if the autophagy proteins play a role in phagocytic uptake of apoptotic cells.

- Analyse the response of macrophages to apoptotic SLE lymphocytes compared to apoptotic healthy lymphocytes.

5.2 Results

5.2.1 The Atg5$^{-/-}$ iBMK cell line undergoes accelerated secondary necrosis.

I was interested to determine if autophagy proteins, in particular ATG5, play a role in controlling apoptotic cell death, since it is known that autophagy is associated with SLE susceptibility[67,231,232] and SLE lymphocytes become apoptotic at an accelerated rate, rapidly progressing to secondary necrosis (Chapter 4 Figure 4.8). Therefore, I examined the death kinetics of Atg5$^{-/-}$ iBMKs compared to wild type (Atg5$^{+/+}$) iBMKs over 6 h, following the induction of apoptosis with UV irradiation.

The adherent cells were viable, indicated by AnV and PI staining, thus only the non-adherent cells at each time point were collected, counted, and analysed by flow cytometry. While deficiency of ATG5 protein (Figure 5.2.A) did not affect the proportion of Atg5$^{-/-}$ iBMKs that were early apoptotic (AnV^{+} PI^{-}) compared to Atg5$^{+/+}$ iBMKs (Figure 5.2.B), it did result in approximately double of the Atg5$^{-/-}$ iBMKs becoming secondarily necrotic (AnV^{+} PI^{+}) at 6 h following UV treatment (Figure 5.2.B). Although the result did not reach statistical significance, this implies that ATG5, which is required for functional autophagosome formation, is necessary to control the rate that cells die by apoptosis.

It is still unknown why autophagy should continue to function in cells committed to apoptosis (reviewed in[367]); it is mostly considered that autophagy is inhibited following caspase-mediated cleavage and inactivation of autophagy proteins[240-242], which would disregard a crucial role. Nevertheless, I still see ATG5 protein expression in late apoptotic/secondarily necrotic cells (Appendix D Figure 1).

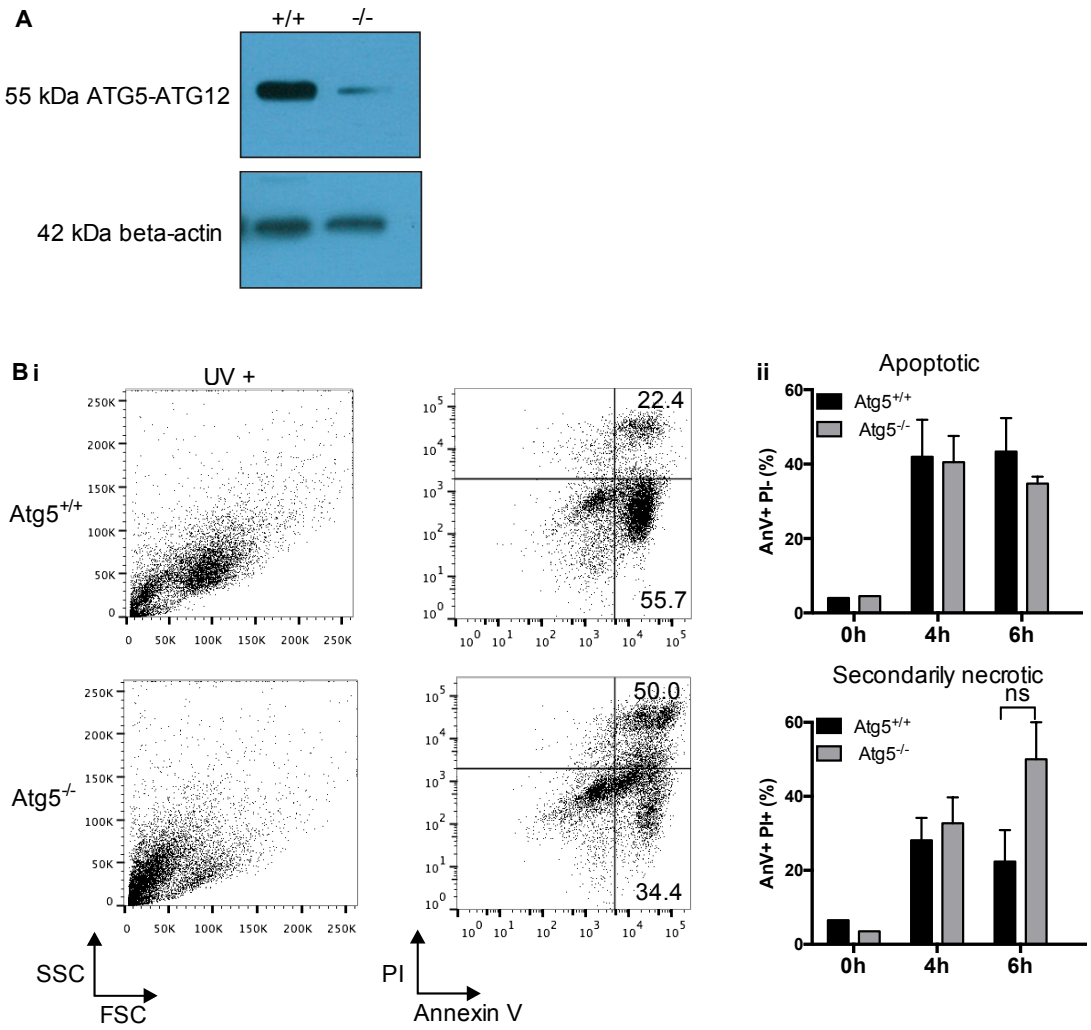

Figure 5.1 Atg5$^{-/-}$ iBMK cells become more secondarily necrotic than WT iBMK cells after UV irradiation.

(**A**) Western blot to show that Atg5$^{-/-}$ iBMK cells have less 55kDa ATG5-ATG12 protein complex compared to WT (Atg5$^{+/+}$) iBMK cells. β-actin was probed as a loading control. (**Bi**) Representative FACS plots of Atg5$^{+/+}$ (top) and Atg5$^{-/-}$ (bottom) iBMK cells to show annexin V (AnV) and propidium iodide (PI) staining after the induction of apoptosis with UV irradiation. (**Bii**) The mean percentages of AnV^{+} PI^{-} (top) and AnV^{+} PI^{+} (bottom) Atg5$^{+/+}$ (black bar) and Atg5$^{-/-}$ (grey bar) iBMKs at 0 h, 4 h, and 6 h after UV irradiation pooled from three independent experiments. Error bars represent SEM. Statistical significance was determined by *t*-test. ns (not significant).

5.2.2 ATG5 protein expression is reduced in SLE lymphocytes

Despite the association of ATG5 SNPs with SLE, the role of autophagy in the pathogenesis of SLE is unclear. Furthermore, it is not established how, or if, the expression and function of the ATG5 protein is altered in lymphocytes from SLE patients. For that reason, I measured ATG5 protein in lymphocytes isolated from controls (healthy donors and non-SLE patients) and SLE patients. ATG5 constitutively forms a complex with ATG12, which is irreversible due to the isopeptide bond[368]. Therefore, the anti-ATG5 antibody detects the 55kDa ATG5-ATG12 complex, with very little 33 kDa 'free' ATG5 found.

Western blotting revealed a two-fold reduction of ATG5-ATG12 protein expression in untreated SLE lymphocytes compared to controls (Figure 5.2.Ai), which was more clearly seen when ATG5 protein density was normalised to β-actin (Figure 5.2.Aii) The ubiquitin protein ligase (E3)-like enzyme activity of ATG5-ATG12 is exerted through the association with and activation of ATG3[223]. Therefore, I was interested to determine if expression of ATG3 protein was also reduced in SLE lymphocytes. However, there was no significant difference in protein expression of ATG3 in SLE patient lymphocytes compared to control lymphocytes (Figure 5.2.B). I also found no significant difference in ATG5-ATG12 protein expression in untreated monocyte-derived macrophages from healthy donors and SLE patients (Figure 5.2.C). Both the lymphocytes and macrophages are not highly pure populations due to the adherence method used to enrich for them.

Analysis of the expression of other upstream autophagy proteins was not possible due to the limited amount of protein lysate generated from the number of SLE lymphocytes available.

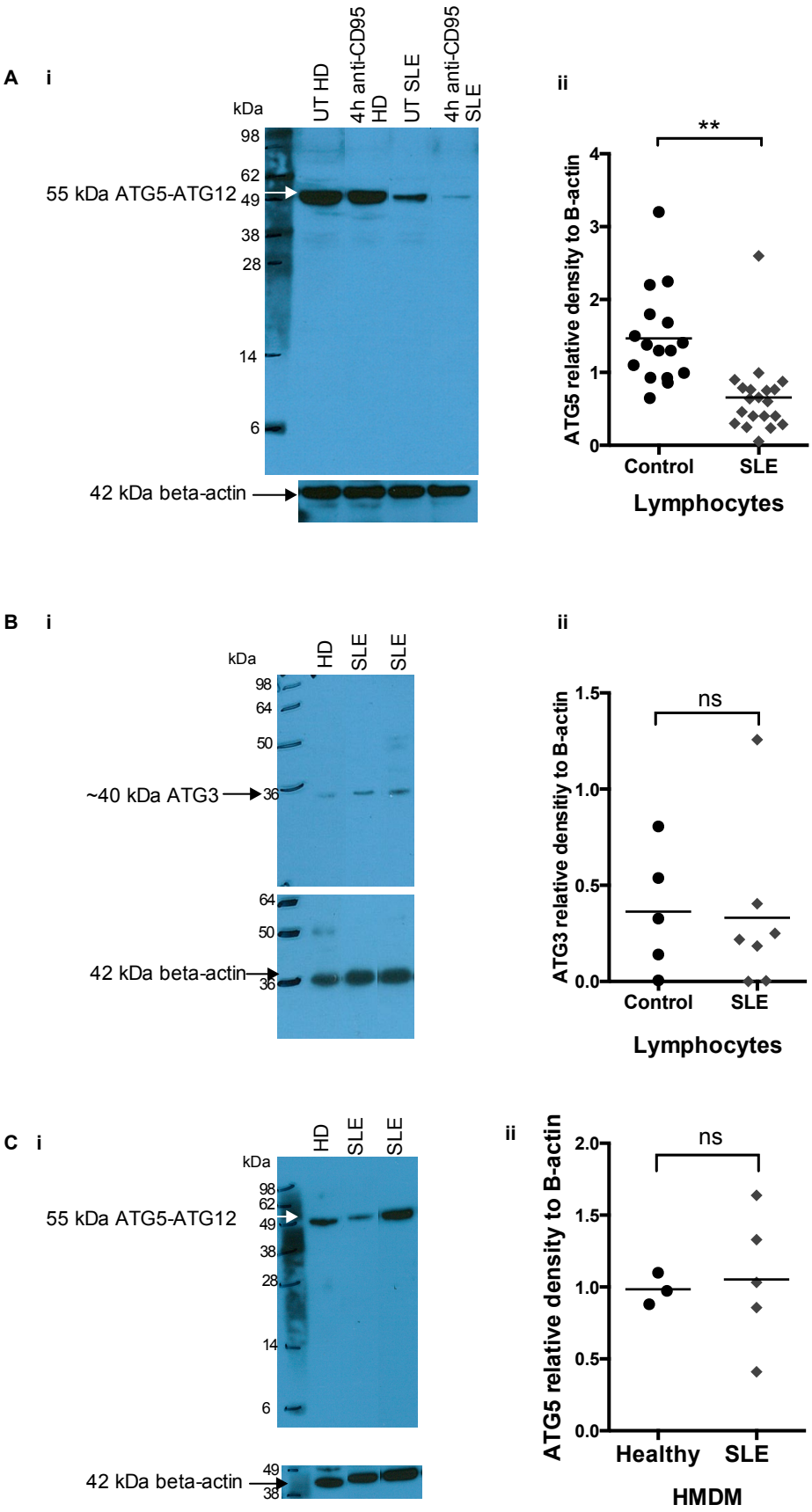
A i
UT HD
4h anti-CD95 HD
UT SLE
4h anti-CD95 SLE
kDa
98
62
49
38
28
14
6
55 kDa ATG5-ATG12
42 kDa beta-actin
ii
**
ATG5 relative density to B-actin
4
3
2
1
0
Control
SLE
Lymphocytes
B i
HD
SLE
SLE
kDa
98
64
50
36
~40 kDa ATG3
64
50
36
42 kDa beta-actin
ii
ns
ATG3 relative densitiy to B-actin
1.5
1.0
0.5
0.0
Control
SLE
Lymphocytes
C i
HD
SLE
SLE
kDa
98
62
49
38
28
14
6
55 kDa ATG5-ATG12
49
38
42 kDa beta-actin
ii
ns
ATG5 relative density to B-actin
2.0
1.5
1.0
0.5
0.0
Healthy
SLE
HMDM

Figure 5.2. ATG5-ATG12 protein expression is reduced in SLE lymphocytes.

Beginning on the previous page, (**Ai**) Western blot showing less 55kDa ATG5-ATG12 protein expression in SLE lymphocytes compared to healthy donor (HD) lymphocytes that were untreated (UT) and treated with anti-CD95 for 4 h. β-actin was probed as a loading control. (**Aii**) The ATG5-ATG12 band density was normalised to β-actin band density using ImageJ software. ** $P = 0.0038$. (**Bi**) Western blot to show that there is no difference in ATG3 protein expression in HD and SLE lymphocytes. β-actin was probed as a loading control. (**Bii**) ATG3 band density was normalised to β-actin band density using ImageJ software. There was no statistically significant difference (ns) between controls and SLE. (**Ci**) Western blot to show that there is no difference in ATG5-ATG12 protein expression in HD and SLE human monocyte derived macrophages (HMDM). β-actin was probed as a loading control. (**Cii**) The ATG5-ATG12 band density was normalised to β-actin band density using ImageJ software. There was no statistically significant difference (ns) between controls and SLE. The difference in the protein ladder markers is because (**Ai**) is a pre-cast gel (Novex® Life Technologies), whereas (**Bi**) is a gel made in the lab. Each point is one control sample (•) and one SLE sample (◆). Sample numbers: (**A**) $n = 16$ (control) and 20 (SLE), (**B**) $n = 5$ (control) and 7 (SLE), (**C**) $n = 3$ (control) and 5 (SLE).

5.2.3 **Autophagic flux is impaired in SLE lymphocytes.**

The final stage of autophagosome formation requires LC3-II to integrate in the membrane for closure of the double membrane. Since the ATG5-ATG12 protein complex is essential for LC3-I conversion to LC3-II, I hypothesised that the low expression of this autophagy protein in SLE lymphocytes would ultimately result in the dysfunctional formation of autophagosomes.

The autophagosome-specific dye Cyto-ID® can be used to label and quantify autophagic vacuoles in live cells[369]. As a positive control, I serum-starved healthy donor lymphocytes for 4 h to induce autophagy and treated the cells with the lysosomal protease inhibitors E64d and pepstatin A for the final 2 h to inhibit autophagosome degradation by lysosomes. This allowed the build up of autophagic vacuoles, as can be seen by increased Cyto-ID staining (Figure 5.3.Ai). I then confirmed that baseline autophagy was reduced in SLE lymphocytes (Cyto-ID mean MFI 269) compared to control lymphocytes (Cyto-ID mean MFI 473) (Figure 5.3.Aii-iii).

The amount of LC3-II is correlated with the number of autophagosomes[370]. Therefore, I measured the conversion of LC3-I to LC3-II to determine if the reduced presence of autophagosomes in SLE lymphocytes occurred due to impaired autophagic flux. E64D and pepstatin A were added to the lymphocytes for the final 2 h of the 4 h culture to prevent the degradation of LC3-II on the inner autophagosome membrane and I found by western blotting that LC3-I failed to convert to LC3-II in the SLE lymphocytes (Figure 5.3.Bi). This is more clearly seen when the ratio of LC3-II to LC3-I band densities were quantified using ImageJ software (Figure 5.3.Bii).

5.2.4 **Atg5 gene expression in SLE lymphocytes is normal.**

Since ATG5-ATG12 protein was reduced in SLE lymphocytes, I analysed Atg5 gene expression to ask if less mRNA was transcribed. The results from qPCR showed no significant difference in Atg5 mRNA between SLE and healthy lymphocytes (Figure 5.4.A). As expected, Atg3 gene expression in SLE lymphocytes compared to healthy lymphocytes was also not significantly different (Figure 5.4.B).

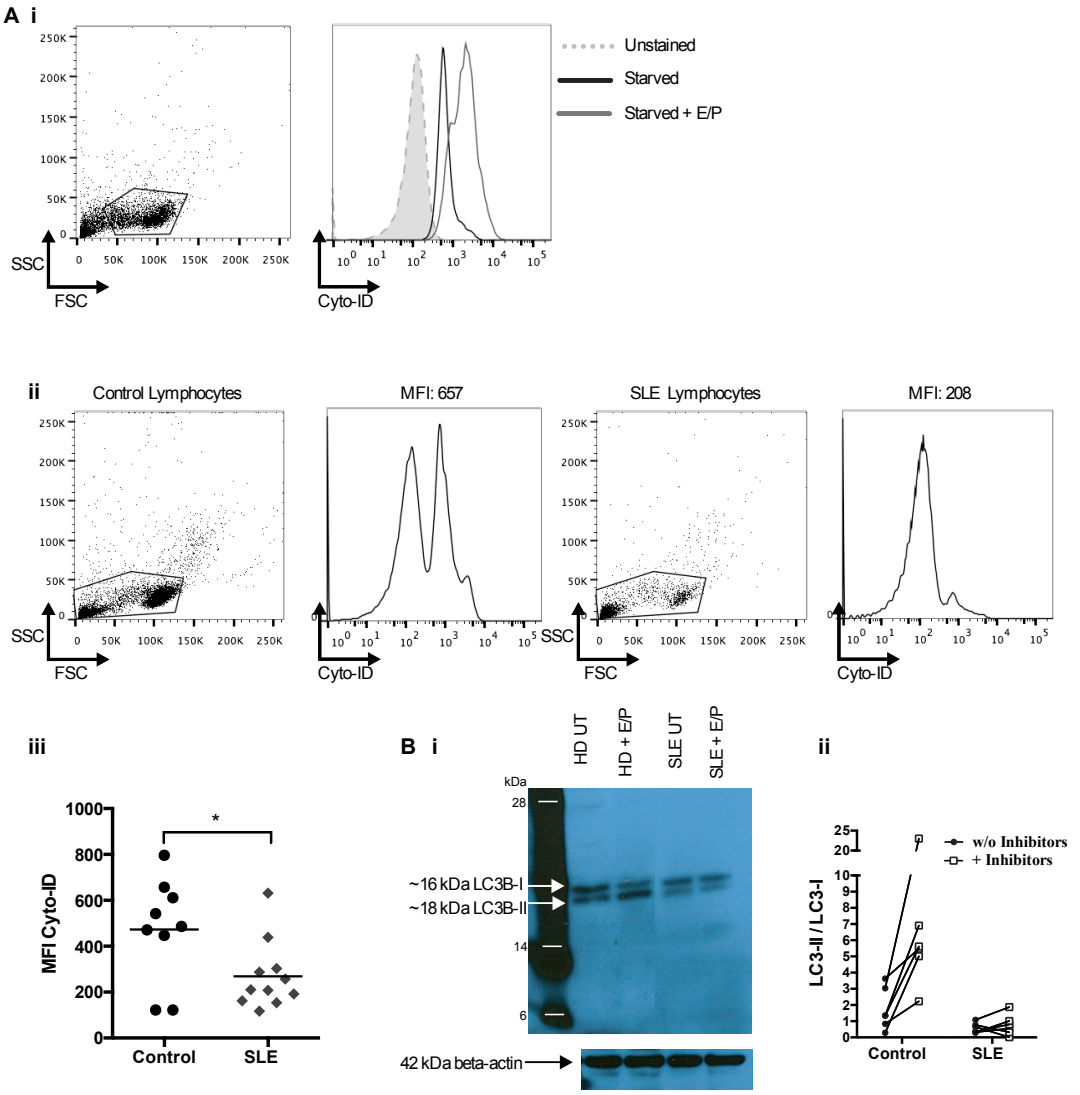

Figure 5.3. LC3-I conversion to LC3-II is impaired in SLE lymphocytes.

(**Ai**) FACS plot of healthy control lymphocytes that were cultured in starvation media for 4 h with (grey line) and without (black line) 2 h treatment with E-64d and pepstatin A (+ E/P) and then stained with Cyto-ID to detect autophagosomes. Untreated and unstained lymphocytes were used as a negative control (grey dashed line). (**Aii**) Representative histograms of control and SLE lymphocytes that were cultured for 4 h then stained with Cyto-ID. (**Aiii**) The mean fluorescence intensity (MFI) of Cyto-ID staining was significantly higher in control lymphocytes compared to SLE lymphocytes ($^{*}P = 0.0342$). Each point is one control sample (•) and one SLE sample (◆). $n = 9$ (control) and 11 (SLE). (**Bi**) Western blot to show LC3B-I (~16 kDa) is not converted to LC3B-II (~18 kDa) when lysosomal proteases are inhibited for 2 h in SLE lymphocytes (+ E/P). β-actin was probed as a loading control. (**Bii**) After normalisation to β-actin, the ratio of the LC3-II density to LC3-I

density was measured in control and SLE lymphocytes without (w/o, •) and with (+, □) lysosomal inhibitors. *n* = 6 (control) and 6 (SLE).

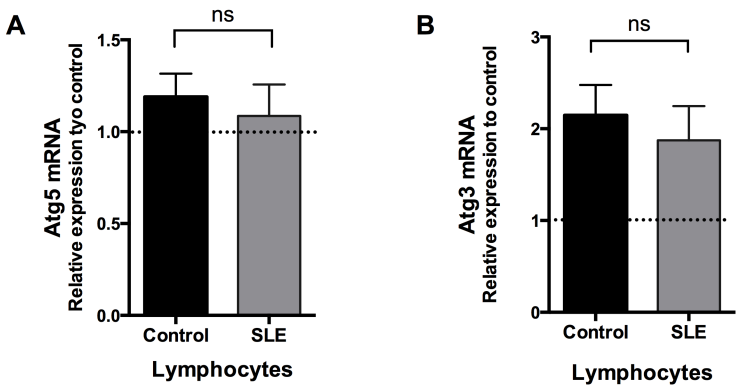

Figure 5.4. Atg5 and Atg3 gene expression in SLE lymphocytes is normal compared to control lymphocytes.

(**A**) Atg5 and (**B**) Atg3 mRNA in control (black bar) and SLE (grey bar) lymphocytes was analysed by real-time PCR and normalised to the house-keeping gene 18S ribosomal RNA. The relative expression in control and SLE samples compared to a control sample that was run on every PCR plate was not statistically significant (ns). Sample numbers: (**A**) *n* = 18 (control) and 19 (SLE), (**B**) *n* = 12 (control) and 12 (SLE).

5.2.5 SNPs in and near the Atg5 gene are not associated with the cohort of SLE samples.

I was interested to determine if variations of SNPs in or near autophagy-related genes differed between controls and the cohort of SLE patients used in this thesis. A total of four SNPs were selected for this analysis. Three SNPs were selected from previous studies showing an association with SLE (ATG5 rs573775[67]; PRDM1-ATG5 rs6568431[67,231]; DRAM-1 rs4622329[233]). The fourth SNP (ATG16L1 rs2241880), was selected as a negative control since it is associated with the chronic inflammatory disorder, Crohn's disease[371], but has not been linked to SLE.

Before performing the SNP genotyping assay, the quality of the samples was assessed using a 2% agarose gel to check the DNA integrity. The absence of ladders indicated that the DNA was intact (Figure 5.5.A).

The genotype frequencies of rs573775, rs6568431, and rs4622329 in the control samples did not deviate significantly from the expected frequencies calculated using the Hardy-Weinberg equation, $p^2 + 2pq + q^2 = 1$, where p represents allele 1 and q represents allele 2 (Table 5.1). However, SNP rs2241880 genotype frequencies in the control samples were significantly different from the expected frequencies calculated using the Hardy-Weinberg equation; therefore this SNP was excluded from further analysis (Table 5.1). Furthermore, the allele clusters generated for rs4622329 were not optimally separated (Figure 5.5.Biv) and for that reason this SNP was also excluded from further analysis.

Using statistical analysis described in the materials and methods, I found that there was no significant difference between the control group and SLE patients in the allele frequency (Table 5.2) and genotype frequency (Table 5.3) of ATG5 (rs573775) and PRDM1-ATG5 (rs6568431), following allelic discrimination (Figure 5.5Bi-ii).

Locus	SNP	Allele p (1)	Allele q (2)	Control	p2	q2	2pq	χ2	P-value
ATG5	rs573775	0.355	0.645		0.126025	0.416025	0.45795	2.304	0.316
				Expected ratio	12.6	41.6	45.8		
				Actual ratio	7.9	36.8	55.3		
PRDM1-ATG5	rs6568431	0.405	0.595		0.164025	0.354025	0.48195	0.6156	0.7351
				Expected ratio	16.4	35.4	48.2		
				Actual ratio	13.5	32.4	54		
ATG16L1	rs2241880	0.419	0.581		0.175561	0.337561	0.486878	19.86	< 0.0001
				Expected ratio	17.6	33.8	48.7		
				Actual ratio	32.4	48.6	18.9		
DRAM-1	rs4622329	0.391	0.609		0.152881	0.370881	0.476238	3.155	0.2065
				Expected ratio	15.3	37.1	47.6		
				Actual ratio	9.4	31.2	59.4		

Table 5.1. Expected genotype frequencies according to the Hardy-Weinberg equation.

Locus	SNP	Allele	Control	SLE	OR (95% CI)	P-value
ATG5	rs573775	A	27	34	1.185 (0.6690-2.099)	0.6622
		G	49	50		
PRDM1-ATG5	rs6568431	A	30	41	1.398 (0.7438-2.629)	0.3379
		C	44	43		

Table 5.2. Allele frequencies of SNPs rs573775 and rs6568431 in control and SLE samples.

Locus	SNP	Genotype	Control (n=38)	SLE (n=42)	X2	P-value
ATG5	rs573775	A/A	3	7	1.463	0.4813
		A/G	21	20		
		G/G	14	15		
			Control (n=37)	**SLE (n=42)**		
PRDM1-ATG5	rs6568431	A/A	5	11	1.967	0.374
		A/C	20	19		
		C/C	12	12		

Table 5.3. Genotype frequencies of SNPs rs573775 and rs6568431 in control and SLE samples.

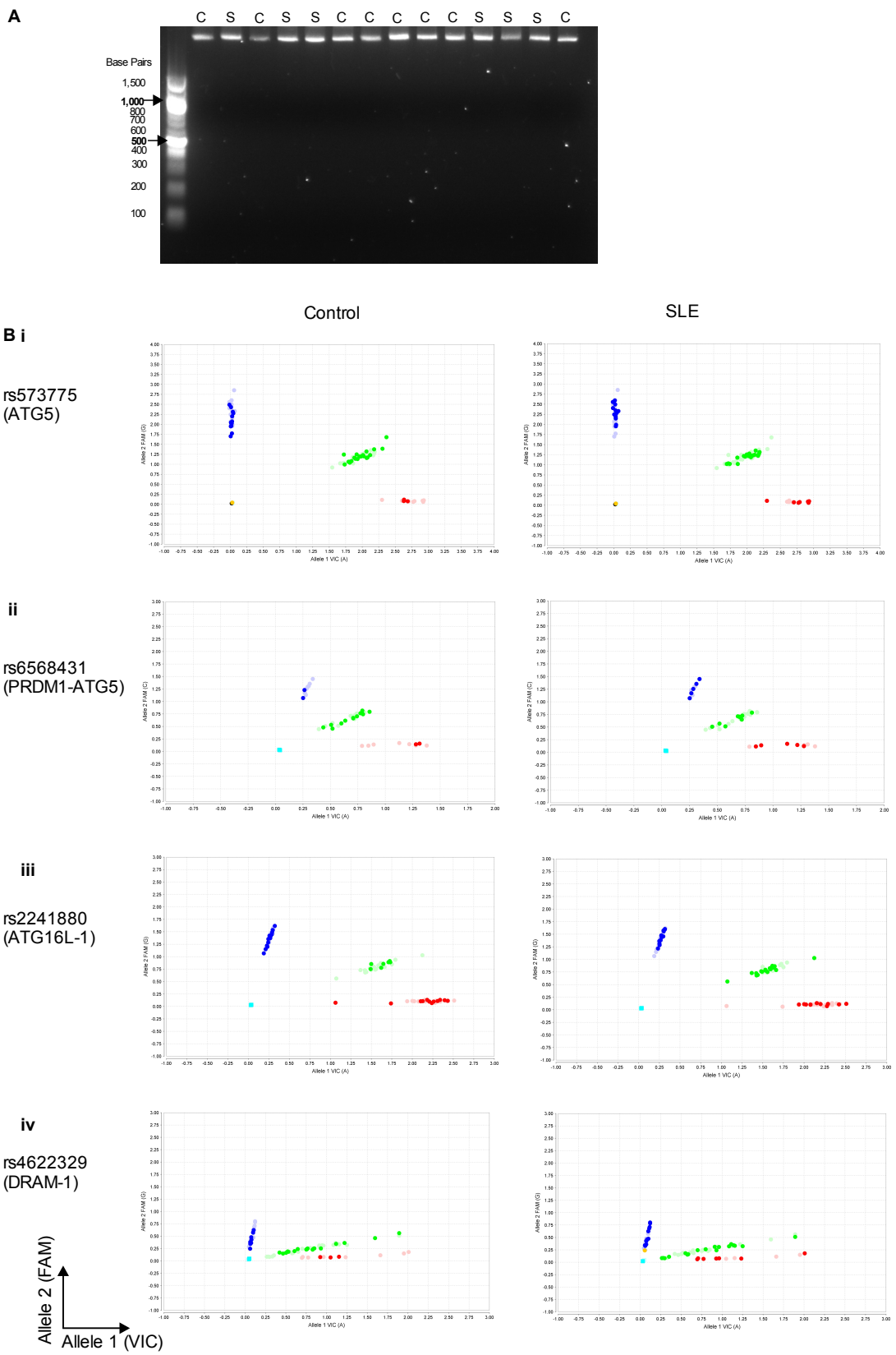

Figure 5.5. SNPs in and near the Atg5 gene are not associated with the cohort of SLE patients.

(**A**) 2% agarose gel to assess integrity of the control (C) and SLE (S) DNA samples. Allelic discrimination plots showing the clustering of homozygotes for allele 1 (red), allele 2 (blue) and heterozygotes (green) for SNPs (**Bi**) rs573775, (**Bii**) rs6568431, (**Biii**) rs2241880, and (**Biv**) rs4622329 in control (left) and SLE (right) DNA samples. Non-template controls are shown in (**Bi**) yellow and (**Bii-iv**) turquoise.

5.2.6 Inhibiting calpain did not significantly restore ATG5-ATG12 protein.

Since SNPs in and near ATG5 were not significantly associated with the SLE patient samples and Atg5 mRNA expression was normal, I wanted to determine if low ATG5-ATG12 protein was caused by rapid degradation of ATG5 in the cytosol. Free ATG5 protein can be cleaved by the non-lysosomal proteases, calpain 1 and calpain 2, following induction of apoptosis in cell types including neutrophils and Jurkat T cells[243]. The 24 kDa cleavage product is translocated to mitochondria, where it further drives apoptotic cell death through inhibition of the anti-apoptotic Bcl-x_L and release of cytochrome *c*[243]. Therefore, I assessed if calpain activity was responsible for the reduced expression of the ATG5-ATG12 complex and the enhanced apoptosis seen in SLE lymphocytes.

There was no significant difference in calpain 1 and calpain 2 mRNA expression in SLE lymphocytes compared to control lymphocytes (Figure 5.6.A). Following 4 h treatment of control and SLE lymphocytes with the calpain-specific inhibitor, calpastatin, ATG5 protein was detected by western blotting. When the ATG5 protein band was analysed by ImageJ software there was a modest increase in ATG5-ATG12 expression when calpain was inhibited, however this did not reach statistical significance (Figure 5.6.Bii). The lymphocytes were also treated with the lysosomal inhibitor HCQ to detect autophagic flux, but even in the presence of calpastatin, LC3-I conversion to LC3-II remained impaired in SLE lymphocytes (Figure 5.6.Bi). Furthermore, the proportion of SLE lymphocytes that became apoptotic (AnV^+ PI^-) and secondarily necrotic (AnV^+ PI^+) following 6 h anti-CD95 treatment was not affected by prior inhibition of calpain for 18 h (Figure 5.6.C).

These findings imply that the calpain-mediated cleavage pathway may not be associated with reduced ATG5-ATG12 in SLE lymphocytes. Nevertheless, it is still possible that ATG5 is proteolytically degraded since treating cells for 2 h with E-64d and pepstatin A resulted in a significant increase in ATG5-ATG12 protein expression in SLE lymphocytes (Figure 5.6D), although it did not restore LC3-I conversion to LC3-II (Figure 5.3.B). In addition to inhibiting calpain, E-64d also inhibits other cysteine proteases.

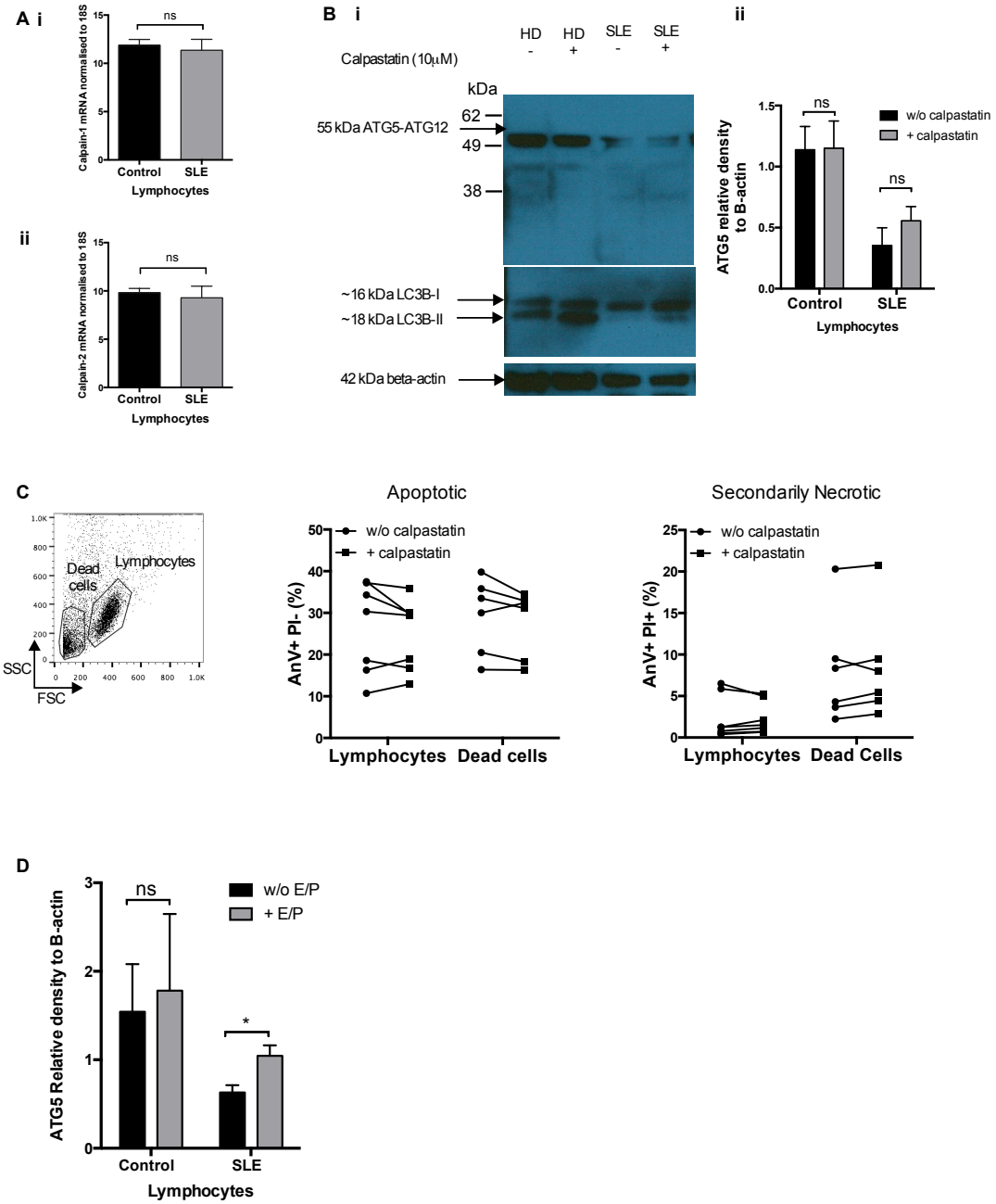

Figure 5.6. Inhibiting calpain did not significantly restore ATG5-ATG12 protein.

There was no significant difference (ns) in (**Ai**) calpain 1 and (**Aii**) calpain 2 gene expression in control (black bar) and SLE (grey bar) lymphocytes, which were analysed by real-time PCR and normalised to the house-keeping gene 18S ribosomal RNA. (**Bi**) Western blot to show that ATG5-ATG12 protein complex was not enhanced and LC3-I did not convert to LC3-II in SLE lymphocytes treated for 4 h with calpastatin (+) and 2 h with HCQ. Healthy donor (HD) lymphocytes were used as a control. (**Bii**) ATG5-ATG12 band density was normalised to β-actin band density using ImageJ software. *n* = 7 (control) and 4 (SLE). (**C**) Lymphocytes and

dead cells were gated on FACS plots and the proportion of apoptotic ($AnV^+ PI^-$) and secondarily necrotic ($AnV^+ PI^+$) cells was analysed in 6 h anti-CD95 SLE samples that had been cultured for 18 h with (■) and without w/o (•) calpastatin. (**D**) Following western blotting the band density of ATG5-ATG12 was normalised to β-actin in control and SLE lymphocytes cultured without E-64d and pepstatin A (w/o E/P, black line) and with E-64d and pepstatin A (+ E/P, grey line). n = 4 (control) and 7 (SLE). Statistical significance was determined by paired t-test; $^*P$=0.0286.

5.2.7 Phagocytosis of apoptotic SLE lymphocytes is impaired.

The increased number of apoptotic cells progressing to secondary necrotic cells seen in patients with SLE is attributed to inefficient phagocytosis caused by lack of opsonisation, such as complement deficiency[361] and reduced phagocytic function of SLE macrophages[77,78]. However, in the absence of SLE serum-influencing factors (such as complement and autoantibodies), I found no significant difference in the mean phagocytic index of monocyte-derived macrophages from controls (mean phagocytic index 64) and SLE patients (mean phagocytic index 54) following 1 h co-culture with UV-irradiated healthy donor apoptotic lymphocytes (Figure 5.7.Ai, Bi, C). This complements previous findings, which used the Jurkat cell line as the apoptotic cell feed[372]. Nevertheless, the phagocytic index of the healthy macrophages responding to healthy apoptotic cells was split into two distinct populations based on the age group of the donors. Macrophages derived from donors that were 25 years old or younger had a higher phagocytic index compared to macrophages from donors that were 30 to 55 years old. It has previously been reported that ageing impairs the phagocytic ability of macrophages (reviewed in reference[373]).

Interestingly, in comparison to healthy apoptotic lymphocytes, when the same number of SLE apoptotic lymphocytes were used the phagocytic index was reduced in both control macrophages (mean phagocytic index 37) and SLE macrophages (mean phagocytic index 26) (Figure 5.7.Aii, Bii, C). This novel finding indicates that SLE macrophages are equally able to phagocytose healthy apoptotic cells. However, like healthy macrophages they are impaired in their ability to ingest apoptotic cells

derived from SLE lymphocytes. This suggests that the apoptotic SLE lymphocytes lack an intrinsic "eat-me" signal.

To further examine if macrophages preferentially engulf healthy apoptotic cells, CM-orange labelled healthy lymphocytes and CM-green labelled SLE lymphocytes induced to die by UV irradiation were co-incubated with control macrophages. After 1 h uptake was measured by flow cytometry, which showed that a mean of 24% macrophages had phagocytosed apoptotic healthy lymphocytes, whereas only 11% and 7% of macrophages were positive for apoptotic SLE lymphocytes or both healthy and SLE lymphocytes, respectively (Figure 5.8).

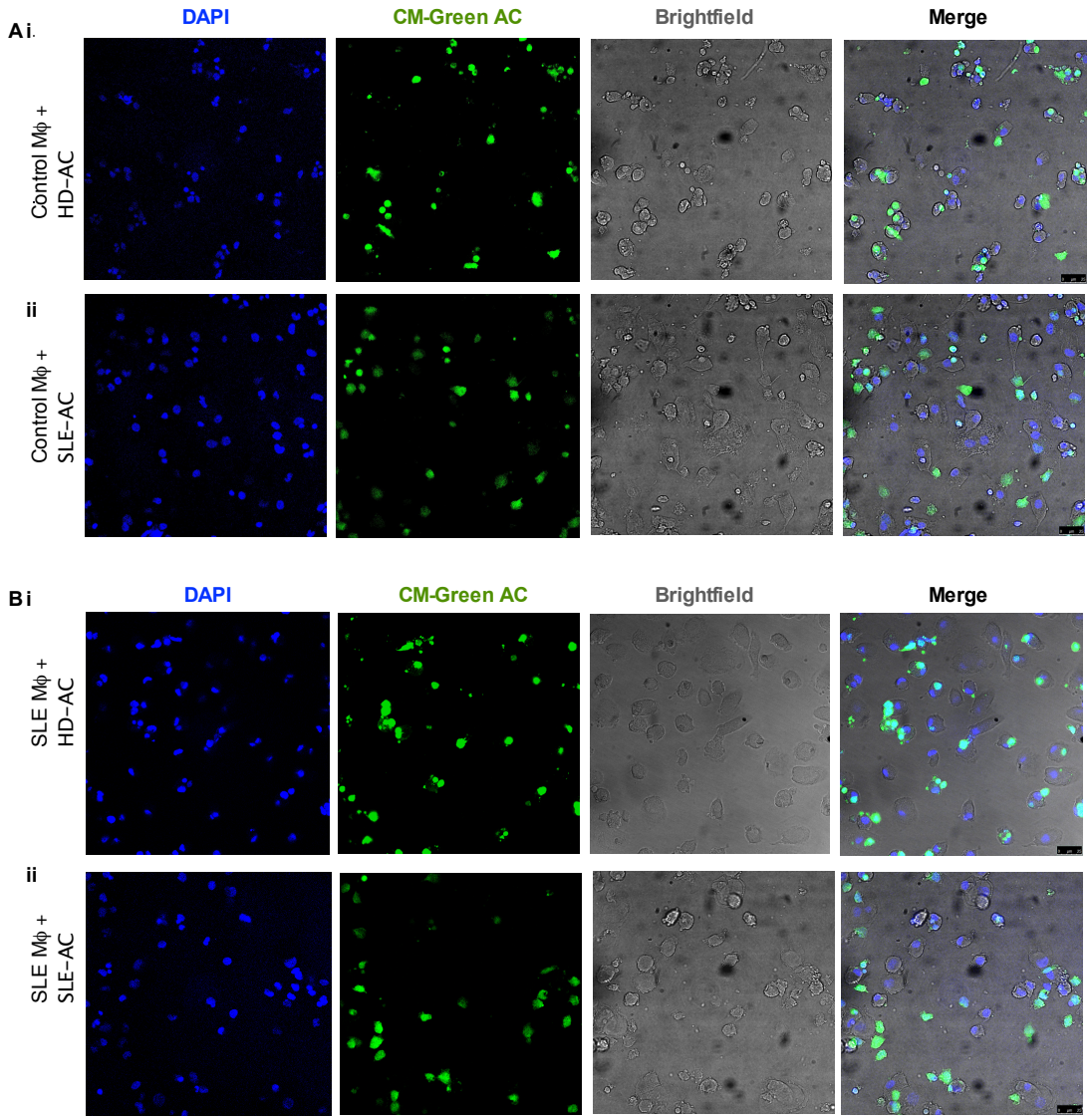

Figure 5.7. Continued overleaf

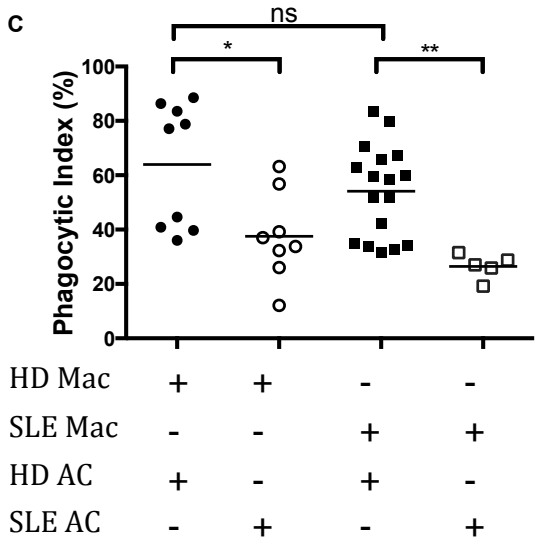

Figure 5.7. Phagocytosis of apoptotic SLE lymphocytes is impaired.

Beginning on the previous page, confocal microscopy images of **(A)** healthy donor macrophages (HD Mϕ) and **(B)** SLE patient macrophages (SLE Mϕ) that were co-cultured for 1 h with 10^6 CM-green labelled UV-irradiated **(i)** healthy donor apoptotic lymphocytes (HD-AC, top row) and **(ii)** SLE apoptotic lymphocytes (SLE-AC, bottom row). **(C)** The number of CM-green apoptotic cells (AC) found in macrophages (depicted by brightfield) was counted, whereas cells lying outside macrophages were ignored. HD Mϕ + HD-AC (•, $n = 9$); HD Mϕ + SLE-AC (∘, $n = 8$); SLE Mϕ + HD-AC (■, $n = 17$); SLE Mϕ + SLE-AC (□, $n = 5$). Scale bar: 25μm. $^{*}P = 0.0160$ and $^{**}P = 0.0019$.

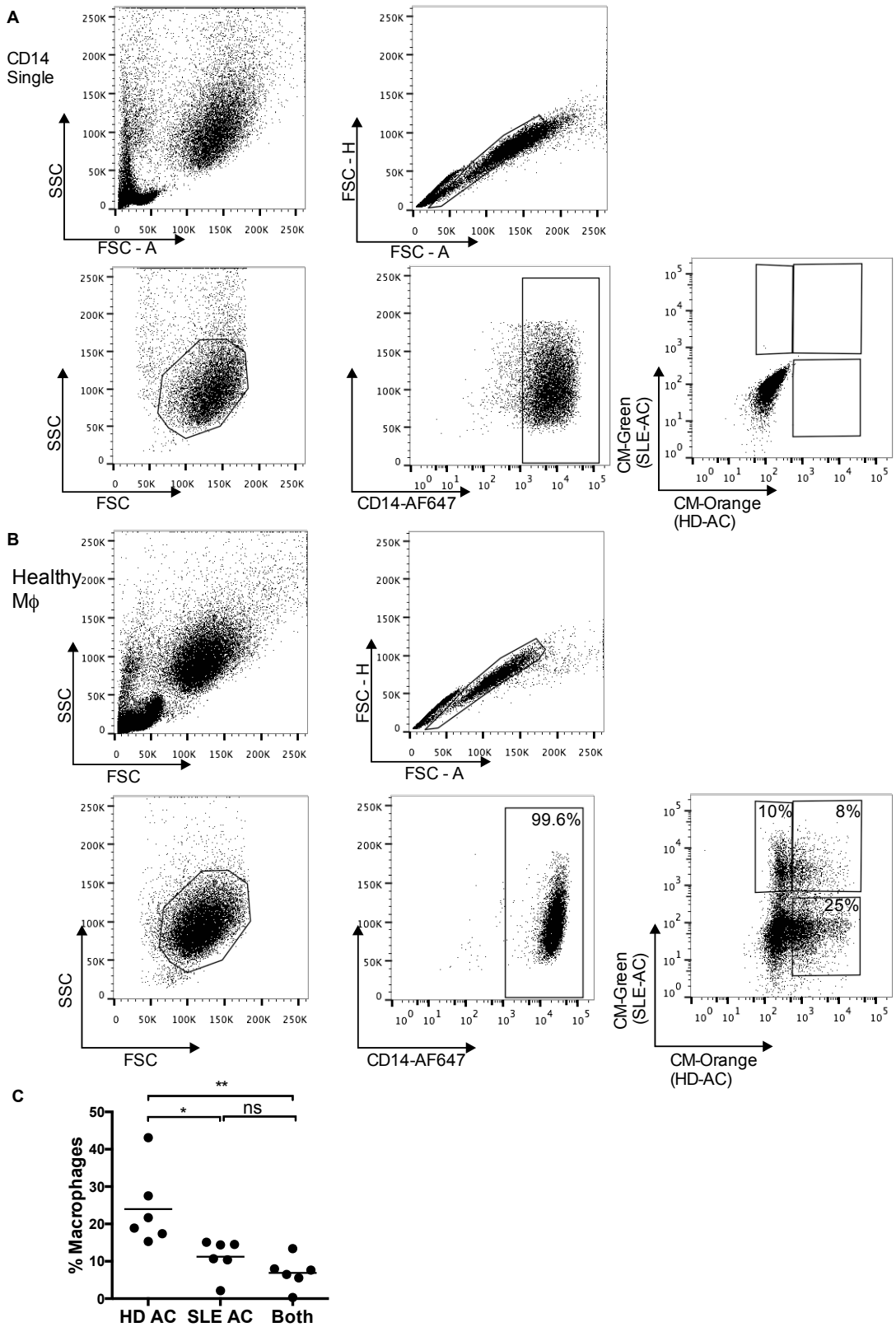

Figure 5.8. Healthy macrophages preferentially phagocytose apoptotic healthy lymphocytes compared to apoptotic SLE lymphocytes.

On the previous page, (**A**) Gates were set on FACS plots using $CD14^+$ macrophages that were cultured alone. (**B**) Representative FACS plots showing $CD14^+$ healthy donor macrophages (HD Mϕ) following 1 h culture with 10^6 CM-orange labelled UV-irradiated healthy donor apoptotic lymphocytes (HD-AC) and 10^6 CM-green labelled UV-irradiated SLE apoptotic lymphocytes (SLE-AC). (**C**) The proportion of macrophages that had taken up HD AC ($CD14^+$ CM-$orange^+$), SLE AC ($CD14^+$ CM-$green^+$), and both HD and SLE AC ($CD14^+$ CM-$orange^+$ CM-$green^+$). n = 6. Statisitcal significance was assessed by one-way ANOVA. $^*P$ = 0.0204 and $^{**}P$ = 0.0037.

5.2.8 Atg5 deficiency does not affect phagocytic uptake of apoptotic cells.

I was interested to determine if low ATG5 protein expression in SLE lymphocytes caused their impaired uptake by asking if autophagy proteins in apoptotic cells are important for their recognition by phagocytes. It was previously considered that autophagy was required for expression of the "eat-me" signal PS on apoptotic embryonic stem (ES) cells[246]. However, the same group have recently published a contradictory report, stating that PS exposure was normal in autophagy-deficient apoptotic cells[248]. Additionally, there is normal PS exposure on apoptotic $Atg5^{-/-}$ iBMKs (Figure 5.1) and SLE lymphocytes (Chapter 4), as indicated by positive AnV binding.

To examine the role of ATG5 in apoptotic cell uptake, mouse BMDMs were cultured with CM-green labelled $Atg5^{+/+}$ or $Atg5^{-/-}$ iBMK cells that were induced to become apoptotic by UV irradiation followed by 6 h incubation. Flow cytometry revealed that Atg5-deficiency did not significantly affect phagocytic uptake of apoptotic iBMK cells (Figure 5.9.A), with an average of 50% and 45% of macrophages positive for $Atg5^{+/+}$ iBMKs and $Atg5^{-/-}$ iBMKs, respectively (Figure 5.9.B).

5.2.9 Apoptotic SLE lymphocytes are pro-inflammatory to macrophages.

Apoptotic cells are known to inhibit TLR-stimulated pro-inflammatory cytokine production by macrophages[45,374], which is reported to require cell contact and is independent of phagocytosis[43]. Therefore, although fewer apoptotic SLE

lymphocytes were phagocytosed by macrophages, I was interested to determine if they could still bestow anti-inflammatory actions on the macrophages.

Monocyte-derived macrophages were stimulated with 5ng/ml LPS, as this concentration induced the most TNF-α production (Appendix D Figure 3A). As expected, I saw a reduction in LPS-induced TNF-α production from healthy donor macrophages when they were co-cultured with healthy donor apoptotic lymphocytes (Figure 5.10.Ai). Conversely, apoptotic SLE lymphocytes significantly enhanced TNF-α production by LPS-stimulated healthy control macrophages (Figure 5.10.Ai). Furthermore, apoptotic SLE lymphocytes augmented secretion of the pro-inflammatory cytokine IL-1β by an average of 13-fold (Figure 5.10.Aii), although this was not statistically significant compared to healthy apoptotic lymphocytes. However, apoptotic SLE lymphocytes did not affect IL-18 (Figure 5.10.C) or IFN-α (Figure 5.10.Ei).

To assess if the increased number of necrotic cells in the SLE lymphocytes were responsible for the increased pro-inflammatory cytokine secretion, LPS-stimulated healthy control macrophages were cultured with healthy donor and SLE patient apoptotic lymphocytes that were made necrotic by freeze-thawing. I was surprised to find that the necrotic cells inhibited LPS-induced TNF-α and IL-1β secretion (Figure 5.10.Bi-ii).

SLE macrophages responded to healthy apoptotic cells in a phlogistic manner, as apoptotic healthy control lymphocytes failed to inhibit TNF-α production by LPS-stimulated macrophages from SLE patients and induced more than double the concentration of TNF-α (Figure 5.10.D). In contrast, IL-1β (Figure 5.10.D) and IFN-α (Figure 5.10.Eii) secretion by SLE macrophages was not enhanced by apoptotic healthy control lymphocytes.

Although I have found no difference in the rate of apoptotic cell death of neutrophils from healthy donors and SLE patients (Chapter 4 Figure 4.9) I was interested to ask

if dying neutrophils from SLE patients were also pro-inflammatory to macrophages since they are associated with inflammation in SLE[93,148,273]. LPS-stimulated control macrophages were co-cultured with neutrophils, which had been induced to die by overnight culture in serum-free conditions. Here I found that apoptotic SLE neutrophils were not pro-inflammatory, as they inhibited LPS-induced TNF-α production by macrophages (Figure 5.11).

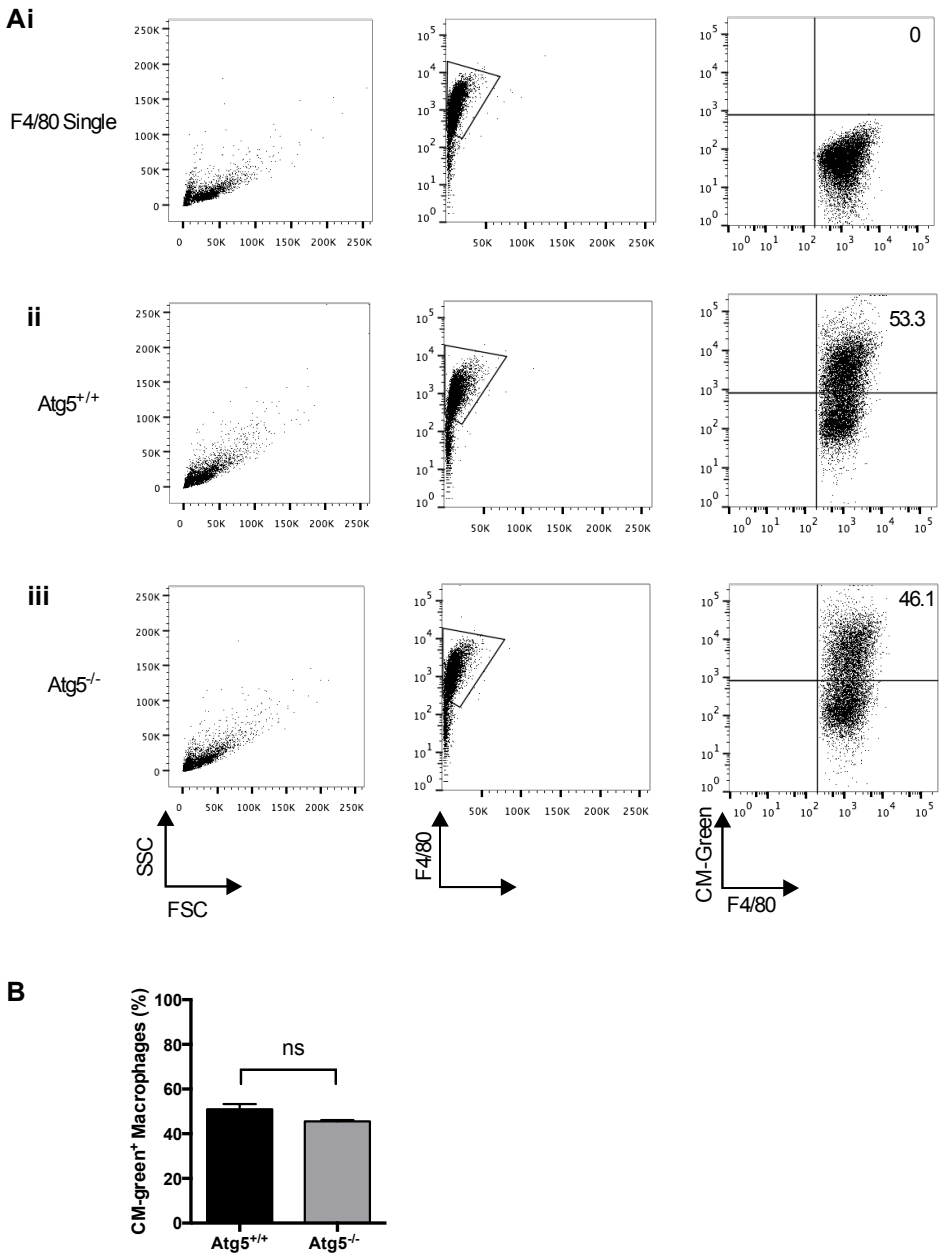

Figure 5.9. Atg5$^{-/-}$ iBMK cells were efficiently phagocytosed by macrophages.

On the previous page, (**Ai**) Gates were set on FACS plots using F4/80^{+} macrophages that were cultured alone. Representative FACS plots of F4/80^{+} mouse macrophages following 1 h culture with CM-green labelled (**Aii**) Atg5$^{+/+}$ and (**Aiii**) Atg5$^{-/-}$ iBMK cells. (**B**) The mean proportion of macrophages from three independent experiments that had phagocytosed apoptotic Atg5$^{+/+}$ (black bar) and Atg5$^{-/-}$ (grey bar) iBMK cells (F4/80^{+} CM-green^{+}). Error bars represent SEM. FACS staining was performed by Katherine Miles.

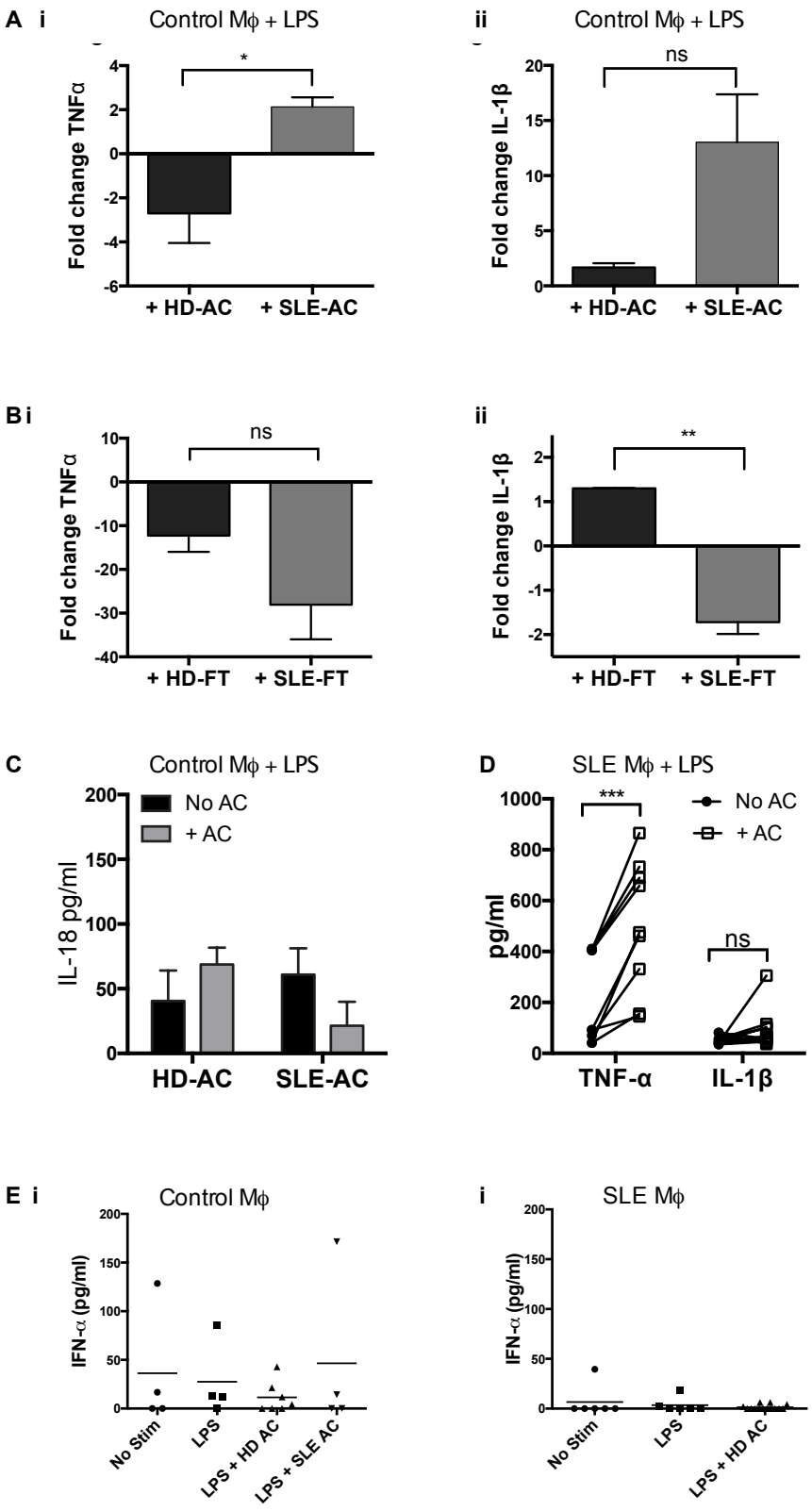

Figure 5.10. Apoptotic SLE lymphocytes induce pro-inflammatory cytokine secretion by control macrophages.

Control macrophages were stimulated with LPS (5ng/ml) and cultured alone and with 10^6 UV-irradiated apoptotic lymphocytes from healthy donors (HD-AC) and SLE patients (SLE-AC). After 18 h, the fold change in (**Ai**) TNF-α (n = 4 (healthy) and 3 (SLE)) and (**Aii**) IL-1β (n = 5 (healthy) and 6 (SLE)) were measured in the cell supernatant. (**B**) Control macrophages were stimulated with LPS (5ng/ml) and cultured alone and with 10^6 UV-irradiated apoptotic lymphocytes that were made necrotic by freezing and thawing (FT) from healthy donors (HD-FT) and SLE patients (SLE-FT). After 18 h, the fold change in (**Bi**) TNF-α (n = 3 (healthy) and 3 (SLE)) and (**Bii**) IL-1β (n = 3 (healthy) and 3 (SLE)) were measured. (**C**) IL-18 was measured in cell supernatants after control macrophages were stimulated with LPS (5ng/ml) and cultured for 18 h alone (No AC, black bar), and with 10^6 control, or 10^6 SLE apoptotic lymphocytes (+ AC, grey bar). (**D**) TNF-α (n = 9) and IL-1β (n = 11) secretion by SLE macrophages was quantified after 18 h stimulation with LPS (5ng/ml) and culture alone (• No AC) and with 10^6 UV-irradiated apoptotic healthy donor lymphocytes (□ + AC). IFN-α secretion by (**Ei**) control and (**Eii**) SLE macrophages was measured in the supernatant following culture as described in A and B. Statistical significance was determined by t-test. $^{*}P = 0.0312$; $^{**}P=0.0077$; $^{***}P = 0.0002$.

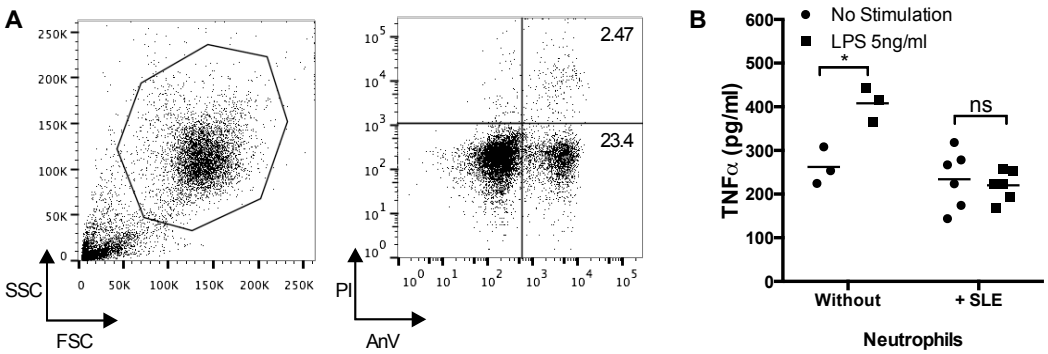

Figure 5.11. Apoptotic SLE neutrophils inhibit LPS-induced TNF-α production by control macrophages.

(**A**) SLE neutrophils were stained for annexin V (AnV) and propidium iodide (PI) after 18 h culture in serum-free media. (**B**) TNF-α was measured in the supernatant of control macrophages that were cultured for 18h with no stimulation (•) and LPS (■) without SLE neutrophils (n = 3) and with apoptotic SLE neutrophils (n = 6). Statistical significance was determined by paired t-test; $^{*}P = 0.0121$.

5.2.10 LC3-associated phagocytosis (LAP) is functional in SLE macrophages.

There was no significant functional defect in the ability of SLE macrophages to phagocytose healthy apoptotic cells (Figure 5.7), but this only measured uptake and

did not determine if they could correctly digest their phagocytic cargo. If apoptotic cells are not efficiently degraded in the phagocyte's lysosomes this can stimulate the production of pro-inflammatory cytokines, including TNF-α[375]. Therefore, since healthy apoptotic lymphocytes enhanced LPS-stimulated TNF-α secretion by SLE macrophages, I hypothesised that SLE macrophages are unable to digest apoptotic cells in the phagolysosome.

Professor Doug Green's lab have shown that LAP is important for the degradation, but not uptake, of apoptotic cells and in the absence of LAP the undigested phagocytic cargo can stimulate pro-inflammatory cytokine release[247,250]. As part of a collaboration with Professor Doug Green and Dr Jennifer Martinez, I co-cultured three-day matured peripheral blood monocytes from healthy controls and SLE patients with Zymosan A (*S. cerevisiae*) bioparticles conjugated to AF594, or CM-green labelled apoptotic healthy donor $CD4^+$ T cells, as described in the materials and methods (page 64). After 1 h, free apoptotic cells were removed, the macrophages were fixed and the phagocytic index was calculated. This confirmed that, compared to healthy macrophages, SLE macrophages are not impaired in their capacity to take up apoptotic cells (Figure 5.13.A-B). Additionally, SLE macrophages and control healthy macrophages had the same ability to engulf killed yeast, with a mean of 4 and 4.5 zymosan bioparticles engulfed per macrophage, respectively (Figure 5.12.A-B). At the same time, the number of apoptotic cells and zymosan bioparticles that were surrounded by a $LC3^+$ phagosome were enumerated. The mean percentage of zymosan bioparticles that were contained within $LC3^+$ phagosomes in control macrophages was half of that counted in SLE macrophages; however this result was not statistically significant possibly due to the spread of the data (Figure 5.12.C). There was also no difference in the percentage of apoptotic T cells that were within $LC3^+$ phagosomes in healthy and SLE macrophages (Figure 5.13.C). These findings suggest that LAP is functioning in SLE macrophages.

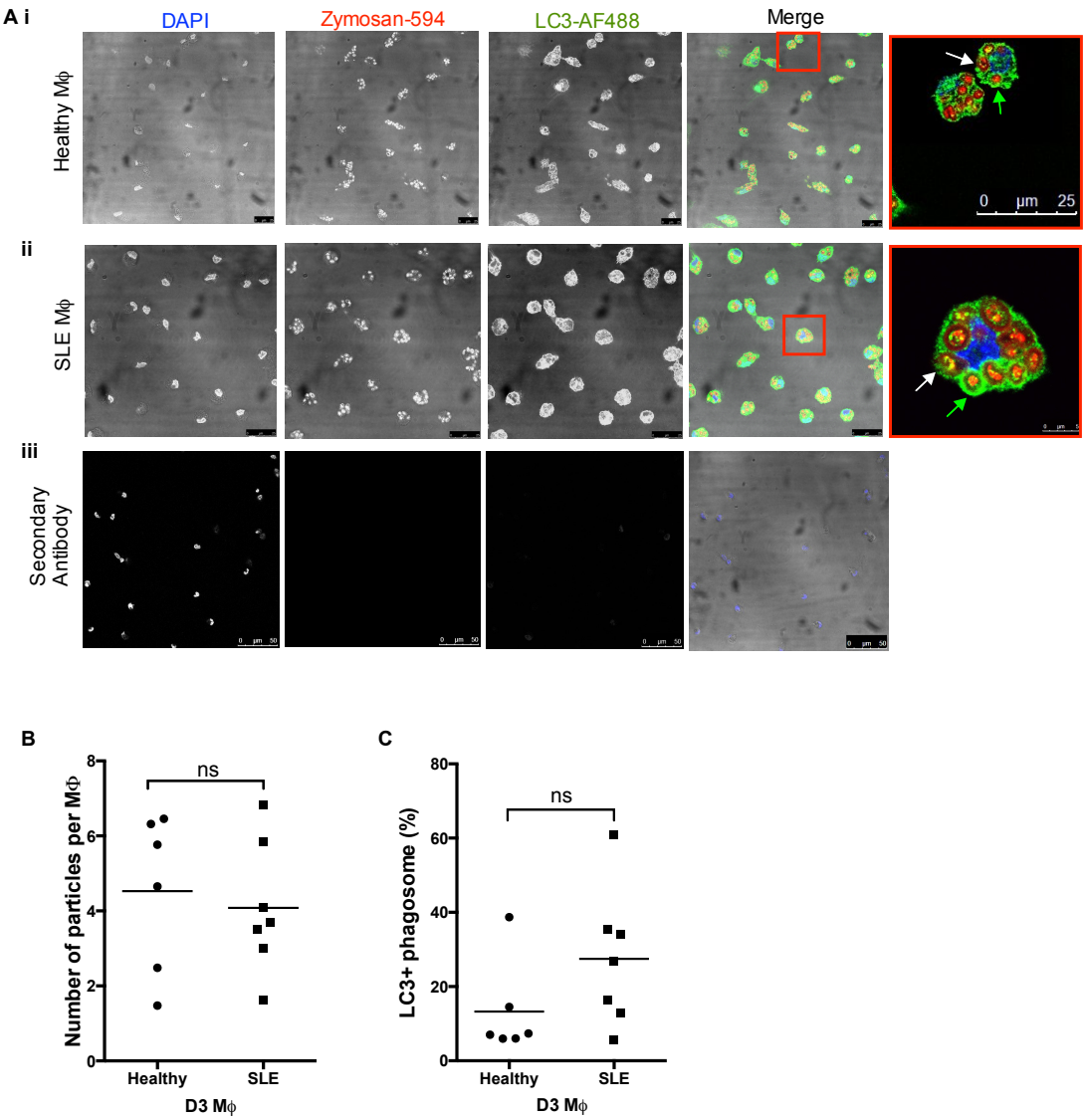

Figure 5.12. SLE macrophages efficiently phagocytose Zymosan A (*S. cerevisiae*) bioparticles by LAP.

Confocal microscopy images of **(Ai)** healthy donor macrophages (HD Mϕ) and **(Aii)** SLE patient macrophages (SLE Mϕ) that were co-cultured for 1 h with zymosan bioparticles conjugated to AF594 (red) at a ratio of 8:1 (8 particles: 1 macrophage). Macrophages were fixed and stained for LC3-associated phagosomes (green) and DNA (DAPI, blue). Green arrows indicate zymosan bioparticles surrounded by $LC3^{+}$ phagosome and white arrows show zymosan bioparticles that were not enclosed within LC3. The red boxes indicate cells that were zoomed in on. Scale bars: 25µm and 5µm. **(Aiii)** Non-specific fluorescence of the secondary antibody goat anti-rabbit AF488 in cells not stained with primary antibody. **(B)** Quantification of the mean number of zymosan bioparticles counted per healthy (•, $n = 6$) and SLE (■, $n = 7$) macrophages. **(C)** The mean proportion of zymosan bioparticles that were surrounded by LC3 in healthy (•, $n = 6$) and SLE (■, $n = 7$) macrophages. No significant difference (ns).

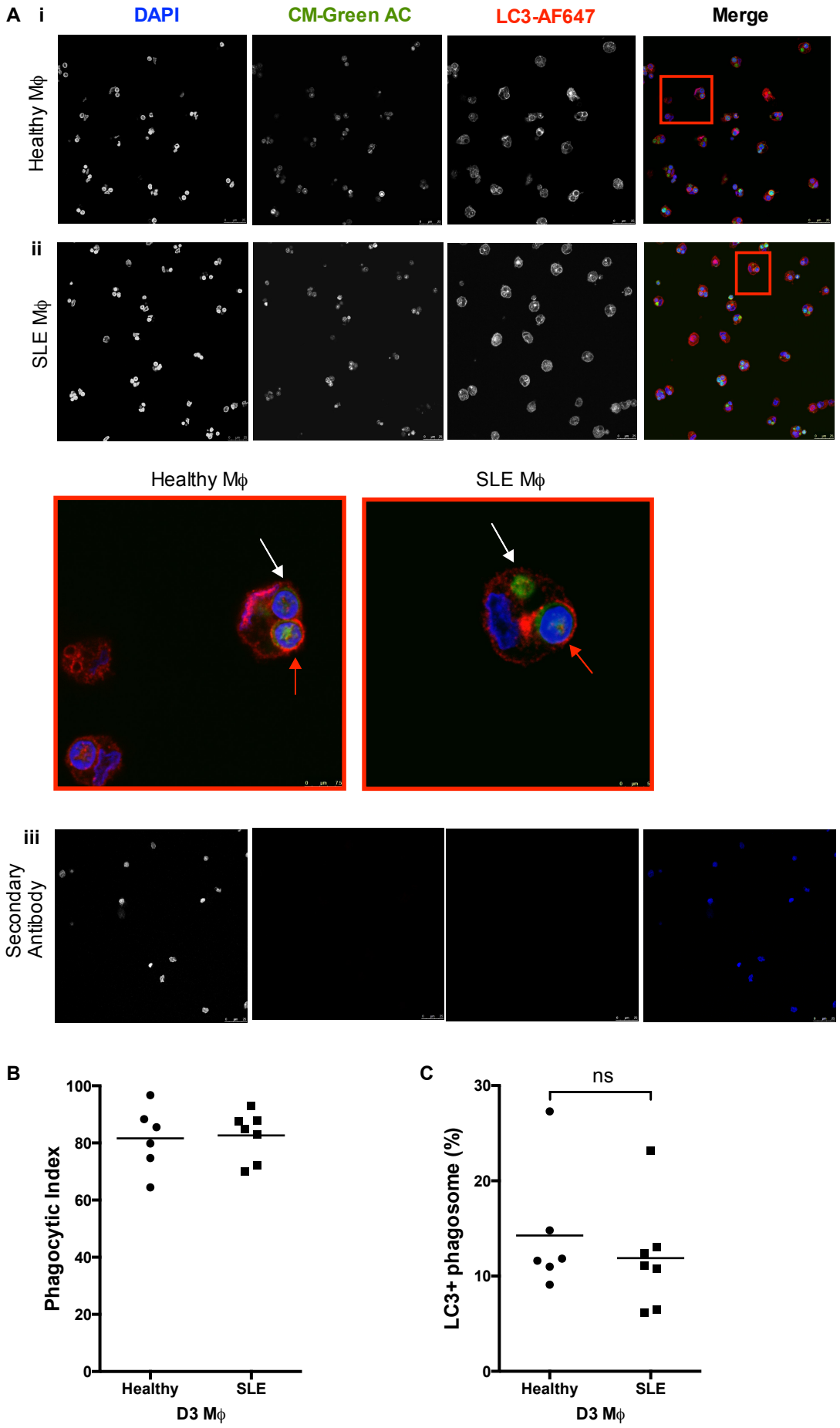
A
i
DAPI
CM-Green AC
LC3-AF647
Merge
Healthy Mϕ
ii
SLE Mϕ
Healthy Mϕ
SLE Mϕ
iii
Secondary Antibody
B
Phagocytic Index
100
80
60
40
20
0
Healthy
SLE
D3 Mϕ
C
ns
LC3+ phagosome (%)
30
20
10
0
Healthy
SLE
D3 Mϕ

Figure 5.13. SLE macrophages efficiciently phagocytose apoptotic healthy $CD4^+$ T cells by LAP.

Beginning on the previous page, confocal microscopy images of **(Ai)** healthy donor macrophages (HD Mϕ) and **(Aii)** SLE patient macrophages (SLE Mϕ) that were co-cultured for 1 h with 10^6 CM-green labelled UV-irradiated healthy donor apoptotic $CD4^+$ T cells (CM-green AC). Macrophages were fixed and stained for LC3-associated phagosomes (red) and DNA (DAPI, blue). Red arrows indicate apoptotic cells surrounded by $LC3^+$ phagosome and white arrows show apoptotic cells that were not enclosed within LC3. The red boxes indicate cells that were zoomed in on. Scale bars: main images 25μm and zoomed images **(Ai)** 7.5μm and **(Aii)** 5μm. **(Aiii)** Non-specific fluorescence of the secondary antibody goat anti-rabbit AF647 in cells not stained with primary antibody. **(B)** The mean phagocytic index of healthy (•, n = 6) and SLE (■, n = 7) macrophages that had engulfed apoptotic cells. **(C)** The mean proportion of apoptotic cells that were surrounded by LC3 in healthy (•, n = 6) and SLE (■, n = 7) macrophages. No significant difference (ns).

5.3 Discussion

Autophagy defects are associated with SLE[67,228-231,366], but it is not clear if autophagy proteins played a role in the aberrant apoptosis and impaired phagocytosis seen in SLE. In this chapter I have presented data to show that SLE lymphocytes have a reduced expression of the ATG5-ATG12 protein complex and defective autophagic flux. Following programmed cell death, apoptotic SLE lymphocytes also underwent more rapid secondary necrosis. Selective ATG5-deficiency in iBMK apoptotic cells also led to enhanced secondary necrosis, yet it did not affect their subsequent uptake by macrophages. In contrast, apoptotic SLE lymphocytes were not efficiently phagocytosed by healthy or SLE macrophages, and they induced phlogistic cytokine responses in these cells. Unexpectedly, SLE macrophages were not impaired in their ability to phagocytose healthy apoptotic cells. Hence the defect in phagocytosis lies not with the SLE macrophage but with an intrinsic defect in apoptotic SLE lymphocytes themselves.

The safe packaging of nuclear constituents in membrane-enclosed apoptotic bodies is essential for promoting anti-inflammatory immune responses. In chapter four it was shown that apoptotic SLE lymphocytes rapidly lost cell membrane integrity compared to healthy donor lymphocytes. In the present chapter I show that SLE

lymphocytes have low ATG5-ATG12 protein expression and similarly to the SLE lymphocytes, a higher proportion of Atg5-deficient iBMK cells became secondarily necrotic following UV irradiation compared to WT iBMK cells. This indicates that functioning autophagy may regulate apoptotic cell membrane integrity, perhaps through the correct formation of apoptotic bodies.

Reduced ATG5-ATG12 protein expression in SLE lymphocytes compared to healthy lymphocytes is a novel finding. Consequently LC3-I failed to convert to LC3-II, which complements previous studies[230,366], but contradicts other published reports that show increased autophagosomes in SLE B cells[229] and an over abundance of autophagic vacuoles in SLE T cells[228]. In the latter study, the number of autophagic vacuoles was potentially overrepresented as they included single-membrane vesicles, whereas autophagic vacuoles are characterised by a double membrane. However, the contrasting findings may be caused by the heterogeneity and disease activity of SLE patients, which emphasises the need for large sample sizes.

SNPs in and near the Atg5 gene have been associated with SLE patients[67,231], yet I found no statistically significant evidence for an association of the ATG5 SNP rs573775 and PRDM1-ATG5 SNP rs6568431 in the SLE patients studied in this thesis. Further analysis of additional SNPs is required to rule out the association of other autophagy-related SNPs. For example, it has been shown that Atg5 gene expression was increased in EBV-transformed B-lymphoblastoid cell lines expressing the PRDM1-ATG5 SNPs rs548234 and rs6937876[232].

SLE lymphocytes are more susceptible to undergoing apoptosis and this is likely caused by their lack of crucial autophagy proteins. Converting LC3I to LC3II is essential to stabilise the autophagosome, yet this process was defective in SLE lymphocytes. Therefore, autophagy cannot occur and the cell cannot survive stress, such as UV irradiation. It was interesting that, despite low ATG5-ATG12 protein, ATG5 mRNA in SLE lymphocytes was comparable to healthy lymphocytes. This suggests that either the mRNA failed to be translated in to protein, or the protein was

rapidly degraded post-translation. The findings using the protease inhibitors calpastatin and E-64d suggest that ATG5 may be targeted for degradation in SLE lymphocytes, which could be clarified utilising a time course of protease inhibition. Pulse-chase experiments with radioactive methionine, followed by immunoprecipitation of ATG5 and SDS-PAGE analysis[376] would also confirm if ATG5 protein turnover is increased in SLE lymphocytes.

Protein degradation is unlikely to occur after ATG5 has conjugated to ATG12 since there is no known enzyme that can break apart the isopeptide bond[377]. ATG7[368] and ATG10[378] are required for the attachment of ATG12 to ATG5. ATG5 also interacts with ATG16 via a non-covalent bond, forming the ATG12-ATG5·ATG16 complex, which localises to the autophagosome outer membrane[379]. Analysing the expression of these other autophagy proteins would determine if it is specifically ATG5 protein that is reduced in SLE lymphocytes. It should be considered that ATG5 might be degraded in SLE lymphocytes if it is not stabilised by ATG12 or ATG16.

Apoptotic SLE lymphocytes and $Atg5^{-/-}$ iBMK cells both expressed the "eat-me" signal PS; hence autophagy machinery is not essential for PS exposure on dying cells. Despite this, apoptotic SLE lymphocytes were not efficiently phagocytosed by healthy or SLE macrophages. In contrast, apoptotic $Atg5^{-/-}$ iBMKs were effectively taken up by mouse macrophages, which supports published data showing PS exposure and uptake of apoptotic corpses in developing *C. elegans* is independent of autophagy protein expression in the apoptotic cell[248]. I have not recapitulated the phagocytosis defect using apoptotic $Atg5^{-/-}$ iBMK cells hence it is likely to be more complicated than reduced ATG5 expression in SLE lymphocytes.

Nevertheless, dysfunctional phagocytosis does seem to be associated with a defect in the dying cell rather than the macrophage, as I found SLE macrophages had the same ability as healthy macrophages to phagocytose apoptotic lymphocytes and zymosan bioparticles. It could be postulated that impaired phagocytosis of SLE lymphocytes was caused by a higher proportion of secondarily necrotic cells; however there was

also 1.5-times more early apoptotic ($AnV^+ PI^-$) SLE cells compared to the healthy apoptotic cell feed (Chapter 4 Figure 4.8). Furthermore, it is reported that necrotic cells are phagocytosed by macrophages [380,381].

The uptake of apoptotic SLE lymphocytes was reduced, rather than completely inhibited; therefore it would be interesting to investigate if the apoptotic SLE lymphocytes that were successfully phagocytosed released a component that switched off additional uptake. It cannot be concluded from my flow cytometry data if apoptotic SLE lymphocytes limited the uptake of apoptotic healthy lymphocytes when they were co-incubated with macrophages, as I did not have a positive control where apoptotic healthy lymphocytes were fed alone. Measuring phagocytic uptake of healthy apoptotic cells, or zymosan bioparticles, by macrophages in the presence and absence of supernatant collected from apoptotic SLE lymphocytes would assess if they secrete an inhibitory factor. Future work to determine why apoptotic SLE lymphocytes are not eaten is discussed more in chapter six.

Despite the reduced uptake of apoptotic SLE lymphocytes, they induced LPS-stimulated macrophages to secrete pro-inflammatory IL-1β. Unlike monocytes, macrophages require two signals to release IL-1β: the first signal (TLR activation) stimulates the production of the IL-1β precursor and the second signal (such as ATP, or LL37) activates the cleavage of pro-IL-1β to make active IL-1β[141]. The cleavage of pro-IL-1β into mature IL-1β is mediated by inflammasome-activated caspase-1 activation[142]. Activated inflammasomes also processes pro-IL-18 to active pro-inflammatory IL-18, but I did not see macrophage production of IL-18 in response to apoptotic SLE lymphocytes. Caspase-1 activity in the macrophages should therefore be measured to confirm if apoptotic SLE lymphocytes activated the inflammasome. It would also be interesting to determine if only the macrophages that have taken up apoptotic SLE lymphocytes secrete the IL-1β. This could be assessed by intracellular IL-1β staining and correlating it with the presence of apoptotic SLE lymphocytes within the macrophage.

The inflammasome is associated with SLE pathogenesis. For example, lupus-like disease is reduced in mouse models deficient in caspase-1 [149] and IL-1β[150]. Additionally, healthy monocytes are stimulated to produce IL-1β in response to NLRP3 inflammasome activation by nuclear constituents, including U1-small nuclear ribonucleoprotein[146] and self-DNA[147], which form immune complexes with antibodies. Apoptotic cells normally inhibit pro-inflammatory cytokine production and inflammasome activation[382] to prevent inflammation, yet I show that apoptotic SLE cells provided a second (danger) signal. Again this may be attributed to the presence of secondarily necrotic cells. However, apoptotic healthy and SLE lymphocytes that were broken apart by freeze-thawing did not induce pro-inflammatory cytokine production. Additionally, late apoptotic (secondarily necrotic) cells induce the same signalling pathway in macrophages as early apoptotic cells[107]. This implies that dying SLE lymphocytes are sensed by the immune system in a different way to healthy apoptotic cells.

It has been shown that increased damaged mitochondrial ROS resulting from autophagy inhibition activates the NLRP3 inflammasome and IL-1β production in THP1 macrophages[383]. Therefore, I hypothesise that the autophagy defect in SLE lymphocytes causes impaired removal of damaged mitochondria (indicated in Chapter 4) and the subsequent ROS production triggers the inflammasome in macrophages that engulf them. Repeating these experiments with primary lymphocytes from autophagy-deficient mice might begin to address this. The potential role of inflammasomes in SLE will be discussed further in chapter six (section 6.1.2).

Healthy apoptotic cells enhanced TNF-α production by LPS-stimulated SLE macrophages, which complements previous findings showing apoptotic cell-derived nucleic acids induced TNF-α secretion by SLE monocytes[384]. Phagosome-lysosome fusion appears normal, as indicated by LC3 association with apoptotic cell-containing phagosomes. This is consistent with a study that recently reported an increase in LC3 mRNA in SLE monocyte-derived macrophages phagocytosing

apoptotic neutrophils[385]. Furthermore, if the SLE macrophages were unable to degrade the apoptotic cell cargo I would expect to see increased IL-1β[247]. Therefore, SLE macrophages appear primed to be pro-inflammatory, even though they express the same amount of TLR4 on their surface as controls[386]. However, SLE monocyte-derived macrophages increase their expression of mRNA for the receptor CD93 following phagocytosis of apoptotic cells, which enhances macrophage sensitivity to TLR stimulation[385]. This susceptibility to being pro-inflammatory would further augment inflammation in patients with SLE.

In summary, this chapter has shown that autophagy is defective in SLE lymphocytes due to reduced expression of the ATG5-ATG12 complex. ATG5-deficiency results in increased secondary necrosis in cells dying by apoptosis. Furthermore, inefficient clearance of apoptotic SLE cells is caused by a defect in the apoptotic cell, rather than the phagocytic cell, and SLE apoptotic lymphocytes are intrinsically pro-inflammatory to macrophages. With these novel findings it may be possible to develop treatments to rectify the defect in leukocyte autophagy, subsequently reducing necrotic cell death and potentially reinstating anti-inflammatory immune responses.

Chapter 6 Overall Discussion

Apoptotic cells in health induce anti-inflammatory immune regulation, even though they express on their surface the autoantigens, DNA, Ro, and RNP, which are associated with SLE[6,73]. The current paradigm of SLE indicates that tolerance is lost to apoptotic cells due to dysfunctional phagocytes and/or loss of opsonisation factors, which allows the progression to secondary necrosis and formation of immune complexes with autoantibodies. However, late apoptotic/secondarily necrotic cells may actually never be inflammatory in a healthy immune system[50,105,387]. Hence, this raises the question, is there something intrinsically different about apoptotic SLE cells that causes inflammation? Chronic inflammation in SLE is associated with IFN-α, and pDCs responding to immune complexes are considered to be the main source due to their specialised ability to secrete this cytokine in response to TLR7 and TLR9 stimulation by nucleic acids. It is now established that pDCs have heterogeneous functions, including an important role in maintaining tolerance through the induction of Tregs. Additionally, TLR9 can no longer simply be viewed as an inflammatory virus receptor, as it protects lupus-prone mice from TLR7-mediated disease[191,192] and also mediates IL-10 secretion by regulatory B cells responding to self-DNA expressed on apoptotic cells[55]. This leads to a second question; do pDCs in health respond to apoptotic cell-derived DNA in a tolerogenic way?

These unresolved questions formed the basis of the main hypothesis of this thesis, that apoptotic cells induce regulation through pDCs in health and an intrinsic defect in SLE apoptotic cells contributes to inflammation. I addressed the hypothesis by studying pDC responses to apoptotic cells in healthy subjects, analysing the cell death kinetics of lymphocytes from SLE patients, and evaluating how B cells and macrophages respond to apoptotic SLE lymphocytes. The following key findings of this study contribute to existing knowledge:

1. In healthy subjects, DNA expressed on apoptotic cells induces anti-inflammatory pDCs, unless they are co-stimulated with a viral mimetic (Chapter 3).

2. Peripheral lymphocytes from SLE patients are susceptible to becoming secondarily necrotic and fail to enhance IL-10 secretion by regulatory B cells (Chapter 4).
3. There is an autophagy defect and an "eat-me" defect in SLE lymphocytes, which are intrinsically pro-inflammatory to macrophages (Chapter 5).

It is important to maintain tolerance to self, in particular apoptotic self, and this is achieved by the well-known anti-inflammatory reactions from professional phagocytes, and regulatory T cells and B cells, discussed in chapter one (section 1.1.3). Here I show for the first time that in health, apoptotic cells control both regulatory and pro-inflammatory responses of pDCs depending on the co-activating TLR stimulus. This confirms that pDCs have heterogeneous functions depending on the microenvironment. This new regulatory function of pDCs may be relevant at homeostatic sites of apoptosis, such as in the thymus, where pDCs are already known to contribute to central tolerance[176-178].

I hypothesised that, like B cells, pDCs are stimulated to make IL-10 by apoptotic DNA/chromatin signalling through TLR9. I confirmed that IL-10 production is dependent on apoptotic DNA/chromatin (Figure 3.9 page 84), but I was surprised to find that the initial secretion of IL-10 is mediated in a TLR9-independent manner (Figure 3.10 page 87). Therefore, against the current thinking, I report that apoptotic cells can induce activated pDCs to secrete IL-10 and promote IL-10-secreting T cells. However, these results do not go as far as to contradict the general consensus that self-DNA is excluded from TLR9 compartments in health to maintain tolerance[161]. The extracellular or intracellular pDC receptor that recognised apoptotic DNA/chromatin is not defined in my study.

For the first time I also demonstrate that apoptotic cells enhance IFN-α production by healthy mouse and human pDCs in the absence of SLE-associated immune complexes (Figures 3.3 page 74; Figure 4.2 page 106). Again this depends on apoptotic DNA/chromatin, and only occurs when pDCs are co-activated with the virus mimetic, CpGA. Therefore, due to the requirement of TLR9 stimulation by

CpGA I was unable to confirm that the apoptotic DNA was sensed by TLR9. A different explanation could be that apoptotic cell DNA enhanced IFN-α produced in the presence of CpGA as a result of entry of more CpGA into the pDC, rather than priming of the cell by the TLR as I suggest. However, this is unlikely since I found that the CpG ODNs still co-localised with the surface of apoptotic cells following the removal of apoptotic DNA (Appendix B Figure 2), and CpG enters pDCs easily[102]. The combination of mammalian DNA and CpGA might form a large complex that gets held up for longer in early endosomes hence results in enhanced IRF7 activation and IFN-α production.

A virus-infected host may benefit from sensing self-DNA in a way that induces IFN-α rather than inducing tolerance, since the local induction of an anti-inflammatory immune response can delay virus clearance[388]. The elevated level of extracellular IFN-α can feedback to augment additional pDC production of IFN-α through the IFNAR[389], thus enhancing anti-viral immunity. It has been shown that cDCs phagocytosing pathogens and apoptotic cells at the same time discriminate between phagosomes containing microbial PAMPs from those containing apoptotic cells[390]. Consequently, cDCs respond to infected apoptotic cells by making TGF-β and IL-6, which together promote a protective Th17 response[391]. However, since virus-infected apoptotic cells cluster self and virus nucleic acids on apoptotic bodies[265], I postulate that they are processed together in pDCs and once the virus particles are no longer co-expressed on apoptotic cells the response by pDCs ceases. This response might trigger autoimmunity in genetically susceptible individuals, as virus infections are associated with SLE[64].

A limitation of the present study is that I did not fully establish how apoptotic cells engage pDCs; although it is likely via interactions with RAGE, the significance of this is still unclear (Figure 3.12 page 92). In pDCs, conventional autophagy is essential for the recognition of ssRNA viruses[253], whereas LAP is required for IRF7 activation in response to DNA-containing immune complexes[254]. Furthermore, the production of IFN-α, but not other inflammatory cytokines, in response to DNA

viruses or CpGA is reduced in mouse pDCs deficient in the essential autophagy proteins ATG5[253] and ATG7[254]. Therefore, in the presence of CpGA, apoptotic cell-derived DNA may be trafficked to TLR9 in autophagosomes. In chapter four I found that SLE pDCs did not make IFN-α in response to co-culture with apoptotic cells and CpGA despite not being completely absent within PBMCs (Figure 4.3 page 109). In chapter five I reported that the essential autophagy protein complex ATG5-ATG12 is reduced in SLE lymphocytes and LC3-I fails to convert to LC3-II (Figure 5.2 page 140; Figure 5.3 page 143). From these results, I hypothesise that, since pDCs can originate from lymphoid progenitors, autophagy is also defective in SLE pDCs, hence IFN-α secretion is reduced and they have an inability to survive. However, diminished numbers of circulating pDCs may indeed be caused by their recruitment to inflammatory sites in the SLE patients[339].

My data provides further evidence to support the literature that reports the non-phlogistic nature of late apoptotic/secondary necrotic cells[105], even when they are left lingering due to deficient phagocytic removal[106]. So could the current paradigm of SLE macrophages being unable to keep up with the number of apoptotic cells thus allowing them to become necrotic and consequently inflammatory be too simple? Indeed in this study I found that, against the existing view, defective phagocytosis is caused by the apoptotic SLE lymphocytes rather than SLE macrophages, which were fully functioning phagocytic cells (Figure 5.7 page 152; Figure 5.13 page 163). Therefore perhaps we need to look at the paradigm of SLE from a different angle; taking into account that impaired uptake of apoptotic lymphocytes is caused by an intrinsic defect in the dying cell. It was suggested many years ago that inflammation observed in phagocyte receptor-deficient mice might not occur as a result of the apoptotic cells progressing to secondary necrosis[387]. Instead, inflammation may reflect the presence of late apoptotic cells in the absence of anti-inflammatory induction through these receptors[387]. Additionally, the autoimmune effect of defective phagocytosis appears to be cell type specific, as C1q-deficient mice develop glomerulonephritis[84], but the removal of apoptotic keratinocytes following UV irradiation is unaffected[392]. It is conceivable that C1q-deficient mice and humans

develop SLE due to downstream effects of the failed clearance of specific apoptotic cells, such as the increased exposure of innate like B cells to apoptotic cell autoantigens in bone marrow. This enhances IgM production by positively selected B1 cells[89] and is supported by my results showing enhanced TLR- and apoptotic cell-induced IL-10 production by B cells isolated from C1q-deficient mice (Figure 3.14 page 95). It is postulated that increased IgM binding to apoptotic cells prevents the exposure of autoantigens that would otherwise induce negative selection of conventional B cells; thus autoreactive B cells escape into the periphery[89].

Despite the contradictory finding, the downstream effect of impaired waste disposal will undoubtedly still be the same, with rapid cell death increasing the availability of autoantigens and cell death-inducing factors provoking flares of disease symptoms. Combined with the fact that apoptotic SLE lymphocytes are inflammatory to macrophages, and they fail to induce immune regulation by B cells, it is not surprising that chronic systemic inflammation occurs. While I found no obvious defect in autophagy proteins, or LAP in SLE monocyte-derived macrophages, they clearly also have an unrelated defect in the handling of phagocytosed apoptotic cells, as indicated by elevated TNF-α (Figure 5.10 page 159). This complements a report that SLE monocyte-derived macrophages upregulate and downregulate different genes compared to healthy macrophages following the phagocytosis of apoptotic cells, although this study used neutrophils as the apoptotic cell feed[385].

Mouse and human pDCs are non-responsive to apoptotic cells that are broken apart by freezing and thawing (Figures 3.5 page 78; figure 4.2 page 106), which I postulate disrupts membrane interactions that are important for recognising DNA/chromatin. Expressing DNA on membrane bound apoptotic bodies is likely a mechanism used by the dying cells to regulate immunity, as apoptotic DNA binds complement[393] hence mediates phagocytosis, and it induces IL-10 secreting B cells[55] and pDCs (chapter 3). Intriguingly, pDCs and B cells make a similar response to apoptotic SLE lymphocytes, as DNase-treated and freeze-thawed healthy apoptotic cells (Figure

4.13 page 128), suggesting that the presentation of apoptotic DNA has gone wrong in SLE.

It is not clearly understood how apoptotic cells create apoptotic bodies. The current assumption is that, as caspase-activated ROCK1 induces the breaking apart of the nucleus, DNA/chromatin passively arrives at the blebbing cell membrane where it is subsequently released as an apoptotic body[16]. Yet, the fundamental process is not known. Our lab has observed that apoptotic $Atg5^{-/-}$ iBMK and MEF cell lines fail to form apoptotic bodies and subsequently break apart (K. Miles, K. Phadwal, J. Simpson and M. Gray, unpublished data), indicating that autophagy proteins are essential for generating apoptotic bodies. The low expression of ATG5-ATG12 in SLE lymphocytes may limit their capacity to make bodies and thus reduce the presentation of membrane-associated DNA. Interestingly, scanning electron microscopy detected fewer bodies in the apoptotic SLE lymphocytes (Figure 4.8 page 120), though it is possible that they were missed due to the cells rapidly progressing through the stages of apoptosis.

6.1 Future work

The results presented in this thesis have, to a certain extent, answered my initial questions, by showing that pDCs do respond to apoptotic cells in health and apoptotic SLE lymphocytes are intrinsically pro-inflammatory. My findings have raised additional interesting questions, which will be investigated in the future.

6.1.1 The role of apoptotic cell-induced regulatory pDCs *in vivo*

One of the limitations of this thesis is that I did not establish how significant the IL-10 produced by pDCs is, as opposed to apoptotic cell-induced IL-10 made by other cells. I reported that pDCs co-cultured with apoptotic cells induce IL-10 secreting T cells *in vitro*, indicating that it is likely that pDCs are important for maintaining regulation to apoptotic cells. The rarity of pDCs means it is difficult to examine pDC-specific responses to apoptotic cells *in vivo* without other immune cells, such as B cells, masking the effect. Therefore, I am commencing a study to determine if

IL10-secreting T cells that are induced by pDCs and apoptotic cells *in vitro* have a regulatory function *in vivo*. This will be achieved using the OVA-peptide system to assess if pDC/apoptotic cell primed T cells, when injected in to mice, suppress antigen-specific T cell proliferation and secretion of pro-inflammatory cytokines.

Additionally, it requires further work to elucidate the signals induced by apoptotic cells that stimulates pDCs to make IL-10. Since the literature states that pDCs do not secrete IL-10 in response to TLR7/9 stimulation due to low ERK1/ERK2 expression[279] and I show that TLR9 is not essential for the initial production of apoptotic cell-induced IL-10 (Figure 3.10 page 87) it suggests that another pathway is triggered within the pDCs. The activation state of pDCs depends accordingly on the TLR ligand used to stimulate them. It is reported that CpGB activates p38 expression by pDCs, whereas IFNα-inducing influenza PR/8 does not[394]. Furthermore, apoptotic cells stimulate IL-10 production in macrophages through p38 and apoptotic cell response elements (ACRE)[395]. It may be that the combined p38-mediated signaling induced by TLR stimulation and apoptotic cells is adequate to induce detectable IL-10 from pDCs.

6.1.2 **The inflammasome and SLE**

In chapter five I discussed the potential role for apoptotic SLE lymphocytes to stimulate the inflammasome in healthy macrophages since I found enhanced IL-1β secretion. Further work is required to elucidate how apoptotic SLE lymphocytes might activate inflammasomes. It is considered that immunogenic cell death cannot occur in the absence of autophagy due to lack of ATP release[396]. However, here I hypothesise that it is SLE DNA that is inflammatory. Oxidised mitochondrial (mt)DNA released following apoptosis induction activates IL-1β through the NLRP3 inflammasome[397]. mtDNA damage is associated with SLE[398,399], and I found that SLE lymphocytes contained an abnormal accumulation of mitochondria (Figure 4.12 page 127), indicating that mtDNA may be inflammatory in SLE. However, I also saw dim TUNEL staining (Figure 4.11 page 124), which implies that nuclear DNA is incompletely fragmented. It is unclear if autophagy is required to regulate DNA fragmentation in mammalian cells, but in Drosophila autophagy degrades the

inhibitor of apoptosis, dBruce, thus permitting CAD-mediated DNA fragmentation[400]. Additionally, the autophagy pathway has recently been reported to play an important role in the degradation of damaged autosomal nuclear DNA partly through the lysosomal nuclease DNase-II[401]. In the absence of autophagy, damaged nuclear DNA initiates inflammation via STING-dependent mechanisms[401]. Impaired DNA degradation is associated with SLE, as indicated by the development of lupus-like disease in DNase-I$^{-/-}$ mice[402]. Yet, the role of autophagy and/or the inflammasome in this process in SLE has not been investigated. Repeating the experiments with DNase added to culture medium to remove SLE DNA would initially determine if this is the inflammatory component.

6.1.3 **Apoptotic SLE lymphocytes lack an "eat-me" signal**

Fewer SLE apoptotic lymphocytes are phagocytosed compared to healthy apoptotic lymphocytes, but there is no clearance defect observed using apoptotic Atg5$^{-/-}$ iBMK cells (Figure 5.9 page 157). Therefore, although ATG5-ATG12 expression is low and autophagy is defective in SLE lymphocytes, the "eat-me" defect appears to be more complex than simply abnormal autophagy. This is supported by the fact that Atg5$^{-/-}$ mice do not develop SLE. We need to find out what is different about the SLE apoptotic cells that prevent them from being removed by macrophages. We know that PS is expressed, but although this is necessary, it is not sufficient for phagocytic uptake of apoptotic cells[387], indicating that other "eat-me" factors are missing. For example, the surface expression of apoptotic DNA acts to stimulate phagocytosis of apoptotic cells (reviewed in reference[403]), but as previously discussed in this chapter, the correct presentation of apoptotic DNA may not occur on apoptotic SLE lymphocytes. Therefore the importance of DNA presentation for the uptake of apoptotic cells remains to be investigated. Retaining surface expression of a "don't eat-me" signal, such as CD47, or CD31, would also prevent the apoptotic cells from being phagocytosed[7]. This will be explored further using the relevant antibodies to detect surface expression of "eat-me" and "don't eat me" factors. Additionally, it still has to be investigated whether complement proteins, such as C1q and C3b, actually bind to the surface of apoptotic SLE lymphocytes to opsonise them. It should also be considered that it is not the effect of a surface receptor, but

the release a factor from apoptotic lymphocytes that inhibits uptake, as discussed in chapter five.

I do not know if the "eat-me" defect is specific to SLE lymphocytes. Exposure to sunlight triggers a photosensitive rash and disease flares in SLE patients; so are non-immune skin epithelial cells keratinocytes that are exposed to UV also unsuccessfully phagocytosed and pro-inflammatory? C1q-deficient mouse studies imply that disposal of apoptotic keratinocytes involves distinct uptake mechanisms compared to other organs, such as the kidneys[392]. The damaging response generated by UV irradiation results in the recruitment of lymphocytes[339], therefore inflammation in the skin might be exemplified when the recruited SLE lymphocytes undergo abnormal apoptosis *in situ*.

6.1.4 Are SLE apoptotic cells intrinsically pro-inflammatory *in vivo*?

I have clearly shown that apoptotic lymphocytes derived from SLE patients exhibit pro-inflammatory actions on macrophages *in vitro*. It is not known though if apoptotic SLE lymphocytes are pro-inflammatory *in vivo*. This could be established by asking if they can confer protection against autoimmunity using *in vivo* mouse models of MS and arthritis, which has been published for healthy apoptotic cells[55,56]. It would also be interesting to determine if the pro-inflammatory effects induced by SLE lymphocytes are resultant from their defect in autophagy. If this were the case then I would expect that autophagy-deficient primary apoptotic cells would not protect mice from *in vivo* autoimmune disease.

6.2 Wider implications

Until now, I have focused on interpreting the meaning of my findings with regards to health and SLE. However, the results presented in this thesis may also have wider implications in other fields, such as tumours and atherosclerosis.

6.2.1 **Tumour immunity**

PDCs infiltrate many solid tumours, such as melanoma[404], breast cancer[405], ovarian carcinoma[406], and head and neck cancer[407]. The recruitment of pDCs is likely mediated by tumour-derived chemokine signals CXCL12 and CCL20, which are recognised by pDC-expressed receptors CXCR4 and CCR6, respectively[408]. It might be expected that pDCs would be detrimental to the tumours that they infiltrate since they are potent producers of IFN-α, which is key in controlling the development of cancer. For example, IFN-α prevents the development of tumour-associated macrophages (TAMs)[409], augments tumour-directed NK cell cytotoxicity, and inhibits the proliferation of tumour cells[410]. However, several studies have reported that the presence of pDCs in tumours is associated with enhanced tumour progression and a negative patient prognosis[405,406,411]. This occurs due to the suppressive tumour microenvironment, which actually prevents IFN-α production by mechanisms including immunosuppressive cytokines TGF-β and IL-10, or ligation of the inhibitory receptor ILT7 by tumour cell-expressed BST2[412]. Consequently, tumour-associated pDCs are tolerogenic and secrete IDO, or express ICOS-L thus inducing IL-10 secreting Tregs[182,185].

Tumour growth, such as B cell (Burkitt's) lymphoma and melanoma, is also accelerated by apoptotic tumour cells, due to the differentiation of TAMs with a pro-angiogenic and matrix remodelling phenotype[58,413]. It could be postulated from the data I presented in chapter three, that tumour-infiltrating pDCs would contribute to the immunosuppressive environment by secreting IL-10 in response to tumour apoptotic cells. Although I failed to induce IL-10 responses using tumour cell lines (Figure 3.8 page 82), pDCs might be stimulated by other infiltrating immune cells that subsequently die *in situ*. My finding that apoptotic tumour cells are not recognised in the same way as healthy apoptotic cells is supported by the report that macrophages develop a distinct phenotype after phagocytosing malignant apoptotic cells compared to non-malignant apoptotic cells[58].

Nevertheless, after anti-cancer chemotherapy and radiotherapy, it is vital to prevent the repopulation of cancer cells, which is dependent on the correct balance between anti-tumour immunity and the immunosuppressive microenvironment generated by apoptotic tumour cells after therapy[396]. IFN-α is ideal for this due to its anti-neoplastic properties. It is important to target IFN-α to the tumour site rather than systemic administration, which comes with adverse effects including depression, fatigue[410], and in certain patients the development of lupus-like disease[110]. Therefore, utilising pDCs as endogenous sources of IFN-α for anti-tumour therapy has recently gained interest[408,412]. Imiquimod, a synthetic TLR7/8 agonist, is already used topically to treat skin cancers. In mice it is reported to work by TLR7-mediated activation of dermal mast cells, which secrete CCL2 to recruit pDCs that are subsequently stimulated through TLR7 to produce IFN-α[414]. The recruitment of peripheral pDCs overcomes the problem that TLR7/9-mediated IFN-α secretion is dysfunctional in pDCs conditioned by the tumour microenvironment. This may also be achieved by combining therapy with inhibitors that restore pDC function[410]. Inducing potent anti-tumour IFN-α secretion by pDCs using CpG ODN nanorings has showed promise in mice[415]. Therefore, my finding that apoptotic cells significantly enhance IFN-α production by pDCs compared to stimulation by CpGA alone could be applied to maximise anti-cancer therapy. Exploiting immune cells as Trojan horses to carry cancer cell-specific lytic virus has proved successful at preventing tumour regrowth after therapy in a mouse model of prostate cancer[416]. Using the same principle, viruses that induce apoptosis of the immune cell at the tumour site would potentially induce effective IFN-α production by pDCs, if I prove the hypothesis that CpGA mimics the co-expression of virus particles on apoptotic bodies with host DNA.

6.2.2 **Atherosclerosis**

Atherosclerosis describes the accumulation of fatty deposits called plaques that build up inside arteries eventually leading to them becoming hard and narrow[417]. Atherosclerosis is the major cause of death in developed countries resulting from myocardial infarction or stroke due to advanced atherosclerotic plaque rupture and thrombosis[417]. The inflammatory immune response to fatty deposits on the arterial

wall involves the infiltration of neutrophils and recruitment of lymphocytes and inflammatory monocytes, which develop into foam macrophages following the engulfment of fat and cholesterol. Macrophages within plaque lesions become apoptotic due to oxidative stress and ER stress triggered by high levels of free cholesterol[418]. As atherosclerosis progresses, inflammation fails to resolve due to the inefficient removal and subsequent accumulation of apoptotic plaque macrophages[419]. Consequently, the apoptotic macrophages progress to secondary necrosis, resulting in the development of a necrotic core that renders the plaque vulnerable to rupturing[419].

Intriguingly, SLE is associated with an increased risk of accelerated atherosclerosis[420]. This may reflect that both diseases share impaired disposal of dying cells. Indeed, C1q-deficiency in low density lipoprotein receptor $(Ldlr)^{-/-}$ mice causes an accumulation of apoptotic cells in early atherosclerotic plaques[421]. It has also recently been demonstrated using a combined model of SLE and atherosclerosis ($Sle16.Ldlr^{-/-}$ mice) that both nephritis and atherosclerosis are accelerated[422]. This was attributed to hyperlipidaemia-mediated elevated pathogenic C3 deposition in the kidneys, resulting in the depletion of protective C3 from atherosclerotic plaques, where complement proteins are important for removing apoptotic cells[422]. Therefore SLE potentially accelerates atherosclerosis by increased complement consumption.

Furthermore, a different study published in the same year reported that defective autophagy may play a role in inefficient removal of apoptotic cells in advanced plaques[423]. A fully functional autophagy pathway is required to protect macrophages from NADPH oxidase-induced oxidative stress and apoptosis, but autophagy activity is reduced in advanced plaques[423]. ATG5-deficient mice had elevated plaque necrosis, but this was not caused by a defect in the phagocytic function of macrophages[423]. Instead, the study reported that the absence of the essential autophagy protein ATG5 in apoptotic macrophages prevented them from being eaten, even though there was no defect in the expression of PS[423]. It is not understood if the reduced autophagy in advanced atherosclerotic plaques is caused

by an intrinsic defect in the macrophages, or as a result of chronic inflammation and this requires further investigation. Nevertheless, the data presented in this thesis using SLE lymphocytes supports the hypothesis generated in this published study on macrophages, that autophagy protects cells from apoptosis-inducing stress and if this fails then autophagy acts to ensure the anti-inflammatory disposal of the dead cells.

Based on the results I present in this thesis, the intrinsic defect in autophagy and reduced ability of apoptotic SLE lymphocytes to be phagocytosed also potentially contribute to accelerated atherosclerosis in SLE patients. It would be interesting to investigate if, like apoptotic SLE lymphocytes, reduced autophagy in atherosclerotic apoptotic cells induces pro-inflammatory responses by macrophages. This might define new inflammatory mechanisms involved in atherosclerosis that are synergistic with SLE.

6.3 Summary and conclusion

It is vital to maintain homeostasis in response to apoptotic cells to prevent autoimmunity. This thesis describes a previously unidentified role for pDCs in contributing to immune tolerance to apoptotic cells in health. It is considered that pDCs only respond to self nucleic acids in SLE due to the formation of immune complexes. However, in this thesis I report that in healthy subjects apoptotic cells boost pro-inflammatory IFN-α in the presence of a virus mimetic. In addition to the novel responses by pDCs, I have found that SLE lymphocytes have reduced expression of the essential autophagy proteins ATG5-ATG12 and consequently cannot convert LC3-I to LC3-II. Therefore, in the absence of functioning autophagy, SLE lymphocytes have a reduced ability to cope with stress, such as UV irradiation, and are subsequently prone to dying by secondary necrosis. SLE is associated with an eating defect, but I propose that this is caused by the apoptotic SLE lymphocytes rather than dysfunctional macrophages. Apoptotic SLE lymphocytes augment inflammatory cytokine production by LPS-stimulated macrophages, and they have a reduced capacity to induce anti-inflammatory cytokine production by B cells. I propose an update to the current paradigm of SLE to include the intrinsic pro-inflammatory role of apoptotic SLE cells (Figure 6.1 and 6.2). In conclusion, the

results presented in this thesis suggest that an intrinsic defect in apoptotic SLE lymphocytes drives inflammation. If we could understand what was causing the lymphocytes to become a danger signal we might have a better handle on new treatments in the future.

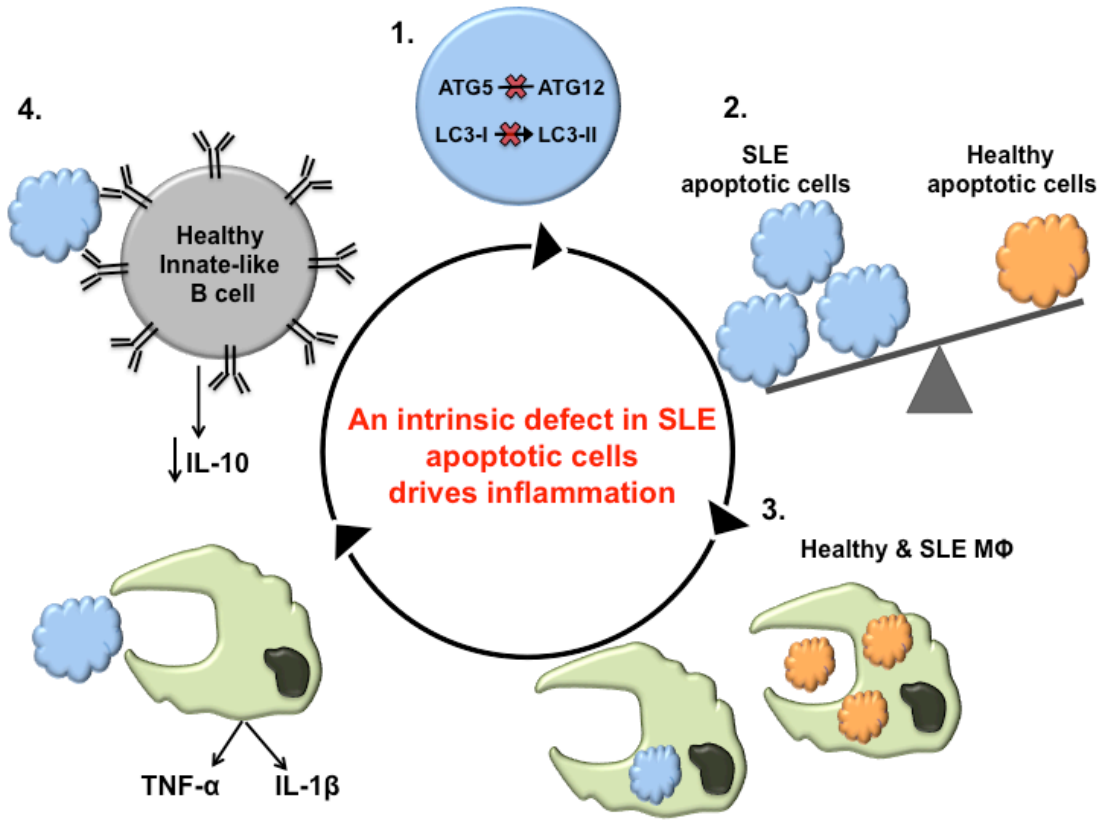

Figure 6.1. An intrinsic defect in SLE apoptotic cells drives inflammation

From the data generated in this thesis my updated hypothesis is that inflammation in SLE is caused by the intrinsic autophagy pathway defect in SLE lymphocytes (1) that leads to their reduced ability to survive stress therefore they are more susceptible to dying (2). I further hypothesise that the incorrect execution of the apoptosis pathway, inefficient uptake by macrophages (3), and induction of pro-inflammatory immunity (4) occurs as a result of dysfunctional autophagy in SLE lymphocytes.

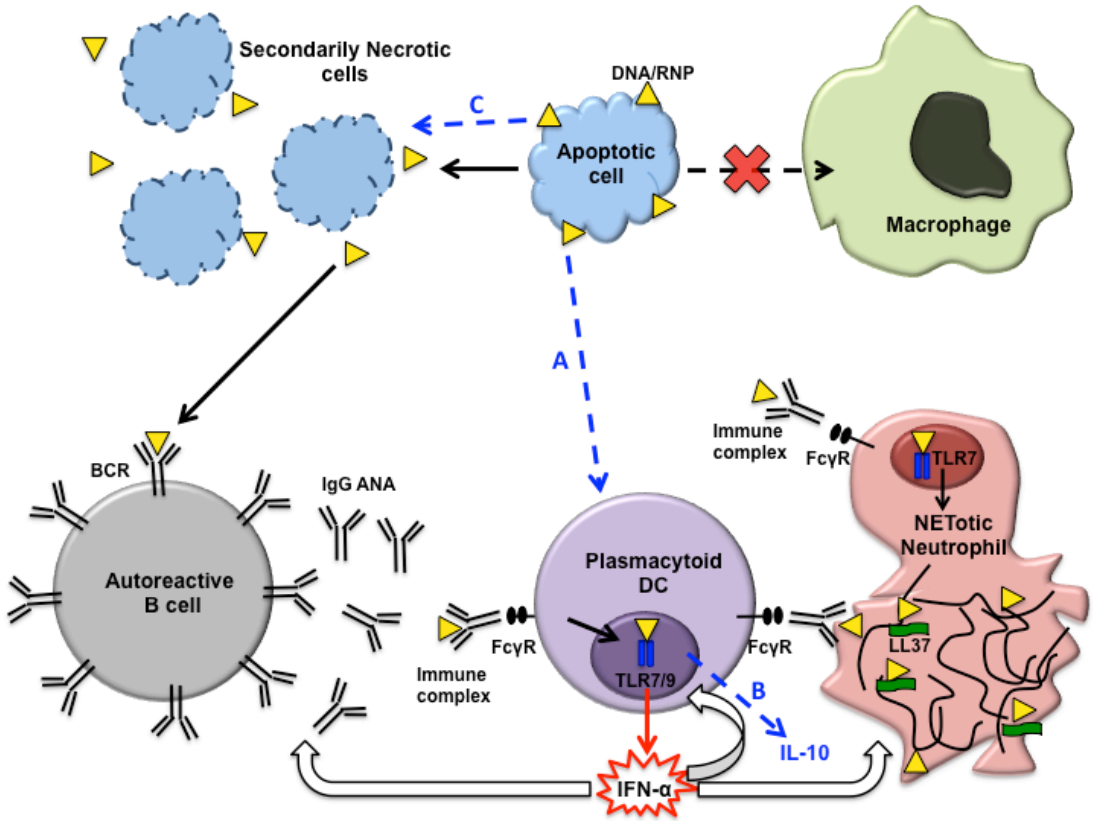

Figure 6.2. The upated paradigm of Systemic Lupus Erythematosus

The paradigm of SLE described in Figure 1.3 can be updated to include the data generated in this thesis (depicted by the blue dashed lines). Whole apoptotic cells are recognised by plasmacytoid DCs in the absence of autoantibody immune complexes (A). Plasmacytoid DCs co-exposed to CpGB/R848 and apoptotic cell-derived DNA are stimulated to secrete IL-10 (B). Lymphocytes from SLE patients are predisposed to becoming apoptotic and rapidly progress to necrosis (C).

Table A.1. SLE patient characteristics

Patient No.	Sex	Age	SELENA-SLEDAI	Antibodies	C3/4	Clinical Features	Medication	Figures
1	F	57	2	Anti-dsDNA	Low	Arthritis, photosensitive rash, ANA	Nil	Figure 4.3A-G, 4.5
2	F	62	2	Anti-dsDNA Anti-Ro Anti-Sm Anti-RNP Anti-cardiolipin (IgG and IgM)	Low	ANA	Pred	Figure 4.3A-G, 4.5
3	F	67	10	Anti-dsDNA Anti-cardiolipin (IgM)	Low	Arthritis, ANA	Aza	Figure 4.3A-G, 4.5, 4.6
4	F	24	0	ND	Normal	ANA	Nil	Figure 4.3A-G, 4.5
5	F	50	6	Anti-Ro Anti-La Anti-cardiolipin	Low	Arthritis, ANA	HCQ	Figure 4.3A-G, 4.5
6	F	71	1	ND	ND		Aza, Pred	Figure 4.3A-G, 4.5
7	F	54	0	Anti-Ro	ND		HCQ, Mtx	Figure 4.3A-G, 4.5
8	F	39	4	Anti-RNP	Normal	Arthritis, ANA, CNS	MMF, Pred	Figure 4.3A-G, 4.5
9	F	22	0	Anti-Ro	ND	ANA	HCQ	Figure 4.3A-G, 4.4, 4.5
10	F	65	3	Anti-dsDNA Anti-cardiolipin (IgG and IgM)	Normal	Arthritis, ANA	HCQ	Figure 4.3A-G, 4.4, 4.5
11	F	20		ND	Normal		HCQ, Pred, Mtx	Figure 4.3A-G, 4.4, 4.5
12	F	19		ND	Normal	ANA	HCQ	Figure 4.3A-F
13	M	21	1	Anti-Ro	Normal	ANA	HCQ, Pred, Mtx	Figure 4.3G

Table A.1. SLE patient characteristics

Patient No.	Sex	Age	SELENA-SLEDAI	Antibodies	C3/4	Clinical Features	Medication	Figures
14	F	65		Anti-Ro Anti-La	Normal	ANA	HCQ, Mtx	Figure 4.3G
15	F	51		Anit-Sm Anti-RNP	Normal	Arthritis, ANA	HCQ	Figure 4.5
16	M	20	1	Anti-Ro	Normal	ANA	HCQ, Pred, MMF	Figure 4.5
17	F	58		Anti-Ro Anti-La	Normal	Arthritis, ANA	HCQ, Pred, Mtx, Rituximab	Figure 4.4, 4.5
18	F	55		ND	ND	ANA	HCQ, Mtx	Figure 4.4, 4.5
19	F	22		ND	Low	ANA	HCQ	Figure 4.4, 4.5
20	F	25	2	Anti-dsDNA	Normal	ANA	HCQ, Pred	Figure 4.4, 4.5, 4.12B-C
21	F	33	2	Anti-dsDNA Anti-cardiolipin	Low	ANA	HCQ	Figure 4.4, 4.5
22	F	65		Anti-Ro Anti-La	Normal	ANA	HCQ, Mtx	Figure 4.4, 4.5
23	M	21	1	Anti-Ro	Normal		HCQ, Pred, MMF	Figure 4.4
24	F	25		Anti-RNP			HCQ	Figure 4.4
25	M	47	4	Anti-dsDNA Anti-Ro Anti-Sm Anti-RNP	Low	Class III Lupus Nephritis, ANA	Nil	Figure 4.6
26	F	59	1	Anti-Ro	Normal		HCQ, Mtx	Figure 4.6
27	F	40	4	ND	Normal	Class III-IV Lupus Nephritis, Arthritis, ANA	HCQ, Aza	Figure 4.6
28	F	42	4	Anti-dsDNA Anti-Ro	Normal		HCQ, Aza, Pred	Figure 4.6
29	F	22	12	Anti-dsDNA	Normal	Lupus Nephritis	HCQ, Aza	Figure 4.6
30	F	20	5	Anti-Sm Anti-RNP	Normal		HCQ	Figure 4.6
31	F	42	4	Anti-dsDNA Anti-Ro Anti-cardiolipin	ND	ANA	Pred, Mtx	Figure 4.6
32	F	66	2	Anti-dsDNA Anti-Ro Anti-	ND	ANA	Aza	Figure 4.6

Table A.1. SLE patient characteristics

				cardiolipin				
Patient No.	**Sex**	**Age**	**SELENA-SLEDAI**	**Antibodies**	**C3/4**	**Clinical Features**	**Medication**	**Figures**
33	F	66	2	Anti-dsDNA	Normal	ANA	HCQ, MMF	Figure 4.6
34	F	24	6	Anti-dsDNA Anti-Sm Anti-RNP Anti-cardiolipin	Normal	ANA	HCQ	Figure 4.6
35	F	37	10	ND	Low	ANA	HCQ, MMF	Figure 4.6
36	M	76	4	Anti-dsDNA Anti-cardiolipin	Normal		Mtx	Figure 4.6, 5.7
37	F	19		Anti-dsDNA	ND		HCQ, Pred, Mtx	Figure 4.6, 5.7
38	F	42	2	Anti-dsDNA Anti-Ro Anti-La	Low	ANA	HCQ	Figure 4.6
39	F	51		Anti-Ro Anti-La	Normal	ANA	Nil	Figure 4.6, 4.12B-C, 5.5
40	F	64		Anti-dsDNA Anti-Ro	Normal	ANA	Nil	Figure 4.6, 5.5
41	F	43		Anti-Ro	Normal	ANA	Pred	Figure 4.6
42	F	26		Anti-dsDNA	Low	ANA	HCQ, Aza, Pred	Figure 4.6
43	F	45	10	Anti-Sm Anti-RNP	Low	Lupus Nephritis	MMF	Figure 4.8A-B, 4.13
44	F	58		Anti-Ro Anti-La	Normal	ANA	HCQ, Mtx, Pred, Rituximab	Figure 4.8A-B, 4.11
45	F	63		ND	Normal		Nil	Figure 4.8A-B
46	F	36		ND	Normal	Alopecia	Nil	Figure 4.8A-B
47	F	56		ND	Normal	Polyarthritis	HCQ	Figure 4.8A-B
48	F	38	8	Anti-dsDNA	Normal	Psoriasis	Mtx, Ustekinumab	Figure 4.8A-B
49	M	65		Anti-dsDNA	Low	Arthritis, Raynaud's	HCQ	Figure 4.8A-B, 5.7
50	F	63		Anti-dsDNA Anti-Ro Anti-Sm Anti-RNP	Low	Photosensitive rash, alopecia	MMF, Pred	Figure 4.8A-B

Table A.1. SLE patient characteristics

				Anti-cardiolipin (IgG and IgM)				
Patient No.	**Sex**	**Age**	**SELENA-SLEDAI**	**Antibodies**	**C3/4**	**Clinical Features**	**Medication**	**Figures**
51	F	66		Anti-Ro Anti-La	ND	Rash	Nil	Figure 4.8A-B, 4.10, 5.2A, 5.3B, 5.5
52	F	22		Anti-Ro Anti-La Anti-Sm Anti-RNP	Low	Rash, arthritis	HCQ, Aza, Pred	Figure 4.8A-B
53	F	45		Anti-dsDNA Anti-Ro Anti-La	ND			Figure 4.8A-B, 5.5
54	F	51		Anti-dsDNA Anti-Ro Anti-Sm	ND			Figure 4.8A-B, 5.7, 5.5
55	F	52		ND	ND			Figure 4.8A-B, 5.5
56	F	62		ND	ND			Figure 4.8A-B
57	F	41	14	Anti-dsDNA Anti-Ro	Normal		HCQ	Figure 4.8A-B, 4.10, 4.13A-B
58	F	66	7	Anti-dsDNA	Normal	Arthritis, ANA	Nil	Figure 4.8A-B, 4.10, 4.13A-B
59	F	53	4	Anti-La Anti-Sm Anti-RNP	ND	ANA	HCQ	Figure 4.8A-B, 4.10, 4.13A-B
60	F	44	2	Anti-dsDNA Anti-Ro Anti-La	Normal		HCQ	Figure 4.8A-B, 4.10, 4.13A-B
61	F	54	5	Anti-dsDNA Anti-Ro	Low	Lupus Nephritis, Arthritis, ANA	HCQ	Figure 4.8A-B, 4.10, 4.13A-B
62	F	38	3	ND	Low	Arthritis, ANA	HCQ, Aza	Figure 4.8A-B, 4.10,

Table A.1. SLE patient characteristics

								4.13A-B
Patient No.	**Sex**	**Age**	**SELENA-SLEDAI**	**Antibodies**	**C3/4**	**Clinical Features**	**Medication**	**Figures**
63	F	46	16	Anti-dsDNA	Low	Lupus Nephritis, Arthritis, Rash, ANA	Rituximab	Figure 4.8A-B, 4.10, 4.13A-B
64	F	74	5	Anti-dsDNA Anti-cardiolipin	Normal	ANA	Nil	Figure 4.8A-B, 4.10, 4.13A-B
65	F	31		Anti-Sm				Figure 4.8A-B, 5.4, 5.5, 5.6A, 5.7
66	M	46	4	Anti-dsDNA Anti-Ro Anti-Sm Anti-RNP	Low	ANA	Nil	Figure 4.8A-D, 5.10A
67	F	45	2	Anti-dsDNA	Normal		Aza, Pred	Figure 4.8A-B, 5.10A
68	F	21	4	Anti-dsDNA Anti-cardiolipin	Normal		HCQ	Figure 4.8A-B, 4.12A, 5.5
69	F	54		Anti-dsDNA	ND			Figure 4.12A, 5.5
70	F	58		Anti-Ro	Normal	ANA	Nil	Figure 4.12A, 5.5
71	F	50		Anti-Ro	Normal	ANA	Aza	Figure 4.12A
72	F	22	16	Anti-dsDNA	Normal	Lupus Nephritis, CNS	HCQ, Aza	Figure 4.12A
73	F	58		Anti-dsDNA Anti-Ro Anti-La Anti-cardiolipin	Normal		HCQ, MMF	Figure 4.12A
74	F	40		Anti-Ro Anti-La Anti-RNP			HCQ	Figure 4.12A, 5.5, 5.7
75	F	40		Anti-dsDNA Anti-Ro Anti-La	Normal	Raynaud's, ANA	HCQ	Figure 4.8C-D, 4.9
76	M	38		Anti-Ro Anti-La	ND			Figure 4.9, 5.6A
77	F	64		Anti-Ro Anti-La			Nil	Figure 4.9

Table A.1. SLE patient characteristics

Patient No.	Sex	Age	SELENA-SLEDAI	Antibodies	C3/4	Clinical Features	Medication	Figures
78	F	27		Anti-dsDNA Anti-Ro Anti-La		ANA	Nil	Figure 4.9
79	M	65	4	Anti-dsDNA	Normal	ANA	HCQ	Figure 4.13A-B, 4.10, 5.8
80	M	21	1	Anti-Ro	Normal		Pred	Figure 4.10, 5.4, 5.5
81	F	33		Anti-Ro Anti-La	Low	Raynaud's	Nil	Figure 4.10, 5.4
82	F	20		Anti-dsDNA	ND	Arthritis, ANA	Nil	Figure 5.2A
83	F	73		Anti-dsDNA	ND		HCQ	Figure 5.2A, 5.3B
84	F	40		Anti-dsDNA	ND	Alopecia, ANA	HCQ	Figure 5.2A, 5.3B, 5.5
85	M	44		Anti-Ro Anti-La			HCQ, MMF previously cyclo-phosphamide	Figure 5.2A, 5.3B
86	F	64		Anti-Ro Anti-La		Lupus Nephritis	Nil	Figure 5.2A-B, 5.4, 5.5
87	F	27		Anti-dsDNA Anti-Ro Anti-La		Rash, ANA	Nil	Figure 5.2A-B, 5.4, 5.5
88	F	42		Anti-Ro Anti-La Anti-Sm Anti-RNP			HCQ, MMF previously cyclo-phosphamide	Figure 5.2A, 5.5
89	F	45		Anti-Ro Anti-La Anti-cardiolipin		Cerebral vasculitis	Nil	Figure 5.2A, 5.4
90	M	49		Anti-dsDNA Anti-Ro Anti-La Anti-RNP				Figure 5.2A-B, 5.3B, 5.4, 5.5, 5.6A-B
91	M	66		Anti-dsDNA Anti-cardiolipin (IgM)	Low		HCQ	Figure 5.2A-B, 5.3B, 5.5, 5.6B-C

Table A.1. SLE patient characteristics

Patient No.	Sex	Age	SELENA-SLEDAI	Antibodies	C3/4	Clinical Features	Medication	Figures
92	F	55		Anti-Ro Anti-La	ND		Nil	Figure 5.2A, 5.4, 5.5
93	F	41		ND	ND	CNS	Mtx, Pred	Figure 5.2A-B, 5.4, 5.5
94	F	51		Anti-Ro	Normal		HCQ, Mtx	Figure 5.2A-B, 5.4, 5.5
95	F	37		ND	ND		Nil	Figure 5.2A, 5.5
96	F	64		Anti-dsDNA Anti-Ro Anti-Sm Anti-RNP	Low		MMF, Pred	Figure 5.2A, 5.5
97	F	34		Anti-dsDNA	Low		Nil	Figure 5.2A, 5.4, 5.5
98	M	22		Anti-Ro	Normal		HCQ, Pred	Figure 5.2A, 5.5
99	F	47		Anti-dsDNA Anti-Ro	Normal		HCQ	Figure 5.2A, 5.5
100	F	35		Anti-dsDNA Anti-RNP	Normal			Figure 5.2A-B, 5.5, 5.6B
101	F	28		Anti-Ro Anti-La			Nil	Figure 5.3A, 5.5, 5.6B, 5.8
102	F	66		Anti-dsDNA				Figure 5.4, 5.5
103	F	54		Anti-RNP		Arthritis, ANA	Pred, MMF	Figure 5.4, 5.5
104	F	51		Anti-Ro Anti-La		ANA	Nil	Figure 5.4
105	F	37		Anti-dsDNA Anti-RNP	Low	ANA	HCQ	Figure 5.4, 5.5
106	M	50		Anti-dsDNA		Arthritis		Figure 5.4, 5.5
107	F	35		Anti-dsDNA Anti-Sm		ANA	Nil	Figure 5.4, 5.5, 5.6A
108	F	77		Anti-Ro Anti-La	Normal	ANA		Figure 5.6A
109	F	53		Anti-Ro Anti-La		Arthritis		Figure 5.5, 5.6B
110	F	46	6		Low	Renal	MMF	Figure

Table A.1. SLE patient characteristics

								5.10A
Patient No.	**Sex**	**Age**	**SELENA-SLEDAI**	**Antibodies**	**C3/4**	**Clinical Features**	**Medication**	**Figures**
111	M	52	13	Anti-dsDNA	Normal		Nil	Figure 5.10A
112	F	75	3	Anti-dsDNA	Normal	ANA	HCQ	Figure 4.13
113	F	53	8	Anti-dsDNA	Low	Renal, arthritis, anti-phospholipid syndrome, ANA	HCQ, Pred	Figure 4.13
114	F	49		Anti-RNP		Photosensitive rash, mouth ulcers, Raynaud's	Nil	Figure 4.11
115	F	34		Anti-dsDNA	Low		HCQ	Figure 5.6C, 5.7
116	F	55		Anti-dsDNA	Low	Anti-phospholipid syndrome, ANA	HCQ	Figure 5.6C
117	F	42		Anti-dsDNA Anti-Ro	Normal		HCQ	Figure 5.6C
118	F	67						Figure 5.6C
119	F	38	4		Low	Arthritis, ANA	HCQ, Aza	Figure 5.8
120	F	50	18	Anti-dsDNA	Low	Arthritis, mouth ulcers, CNS, renal, ANA	Nil	Figure 5.8
121	F	64	8	Anti-Ro Anti-Sm Anti-RNP	Low	Alopecia, Arthralgia, ANA	HCQ	Figure 5.8, 5.10A
122	F	53	13	Anti-dsDNA Anti-Sm Anti-RNP	Low	Arthritis, renal, rash, ANA	Nil	Figure 5.8, 5.10A
123	M	63	5	Anti-dsDNA	Normal	Rash, ANA, interstitial lung disease	HCQ, Pred	Figure 5.10A-C
124	F	28	4	Anti-dsDNA	Normal	Rash, ANA	Mtx, Pred	Figure 5.10A
125	F	29						Figure 5.10B-C
126	F	55						Figure 5.10B-C
127	F	55						Figure

Table A.1. SLE patient characteristics

								5.10B-C
Patient No.	**Sex**	**Age**	**SELENA-SLEDAI**	**Antibodies**	**C3/4**	**Clinical Features**	**Medication**	**Figures**
128	F	37		Anti-dsDNA Anti-Ro			HCQ	Figure 5.11, 5.12
129	F	45		Anti-Ro Anti-RNP			Nil	Figure 5.11, 5.12
130	F	62		Anti-dsDNA	Normal		HCQ	Figure 5.11, 5.12
131	F	56		Anti-Ro Anti-La Anti-RNP		ANA	Nil	Figure 5.11, 5.12
132	F	56		Anti-dsDNA	Normal	ANA	HCQ	Figure 5.11, 5.12
133	F	48	6	Anti-dsDNA Anti-Ro	Normal	ANA	HCQ	Figure 5.11, 5.12
134	F	24	3	Anti-dsDNA	Normal		HCQ, Aza	Figure 5.11, 5.12
135	F	23		Anti-Ro Anti-La Anti-Sm Anti-RNP	Low	Arthritis	HCQ, Aza, Pred	Figure 5.11, 5.12
136	F	47		Anti-dsDNA Anti-Ro Anti-La	Normal	Rash, Raynaud's	HCQ	Figure 5.11, 5.12
137	F	68	14	Anti-dsDNA	Low	Arthritis, renal, Raynaud's	MMF	Figure 5.7
138	M	50		Anti-dsDNA	Low	Anti-phospholipid syndrome		Figure 5.5, 5.7
139	F	77		Anti-dsDNA	Normal	Arthritis	HCQ	Figure 5.7
140	F	64		Anti-dsDNA	Normal	ANA	Nil	Figure 5.7
141	F	62		Anti-dsDNA Anti-Ro Anti-La	Low	Arthritis	HCQ, SSZ	Figure 5.5, 5.7
142	F	53						Figure 5.5
143	F	43		Anti-dsDNA Anti-cardiolipin		Anti-phospholipid syndrome	Nil	Figure 5.5
144	F	37		Anti-dsDNA			Nil	Figure 5.5
145	F	45					Nil	Figure 5.5
146	F	71		Anti-dsDNA	Low	Arthritis, ANA	Pred	Figure 5.5
147	F	67		Anti-dsDNA Anti-Ro Anti-cardiolipin	Normal	Renal, ANA	Pred, MMF	Figure 5.5

Table A.1. SLE patient characteristics

Abbreviations: ANA – antinuclear autoantibodies; Aza – azathioprine; CNS – central nervous system; HCQ – hydroxychloroquine; MMF – micophenolate mofetil; Mtx – methotrexate; ND – not done; Pred – prednisolone; SSZ – sulphasalazine.

Table A.2. Control patient characteristics

Control Patient No.	Sex	Age	Disease	Medication	Figures
1	F	47	Fibromyalgia	Nil	Figure 4.3A-F, 4.4
2	F	64	Rheumatoid arthritis	Nil	Figure 4.3A-F, 4.4
3	F	56	Rheumatoid arthritis	HCQ	Figure 4.5, 4.3
4	F	19	Undifferentiated CTD	Mtx	Figure 4.5
5	F	64	Rheumatoid arthritis	Nil	Figure 4.5
6	F	19	Fibromyalgia, ANA	HCQ	Figure 4.4, 4.3
7	F	25	Fibromyalgia	Nil	Figure 4.4
8	F	49	Raynaud's	Nil	Figure 4.8A-B, 4.10, 5.2A-B
9	F	67	Antiphospholipid syndrome		Figure 4.8A-B, 5.5
10	M	46	Severe pulmonary fibrosis		Figure 5.2A
11	F	57		HCQ	Figure 5.2A
12	F	53	Fibromyalgia, dry eyes		Figure 5.2A, 5.3
13	F	35	Rheumatoid arthritis	Pre-biologic therapy	Figure 4.13C
14	F	49	Rheumatoid arthritis	Biological resistant	Figure 5.4
15	F	56	Rheumatoid arthritis		Figure 5.4
16	F	57		HCQ	Figure 5.4, 5.5
17	F	36	Fatigue	Nil	Figure 5.4, 5.5
18	F	54	Rheumatoid arthritis		Figure 5.4, 5.5
19	F	53	Fibromyalgia		Figure 5.4, 5.5, 5.6
20	M	66			Figure 5.4, 5.5
21	F	77			Figure 5.4, 5.5
22	M	69	Wegener's disease		Figure 5.4
23	F	52	Arthritis	HCQ, Pred	Figure 5.4
24	F	66	Rheumatoid arthritis	Biologic therapy	Figure 5.6, 5.8
25	F	54	Rheumatoid arthritis	Nil	Figure 5.8
26	F	43	Systemic sclerosis		Figure 5.5
27	F	57	Systemic sclerosis		Figure 5.5
28	F	69			Figure 5.5
29	M	64	Swollen joints	Nil	Figure 5.5
30	F	61	Osteoarthritis		Figure 5.5
31	F	45	Undifferentiated CTD, cerebral vasculitis		Figure 5.5
32	F	72			Figure 5.5

Abbreviations: CTD – connective tissue disease; HCQ – hydroxychloroquine; Mtx – methotrexate; Pred – prednisolone.

Appendix B

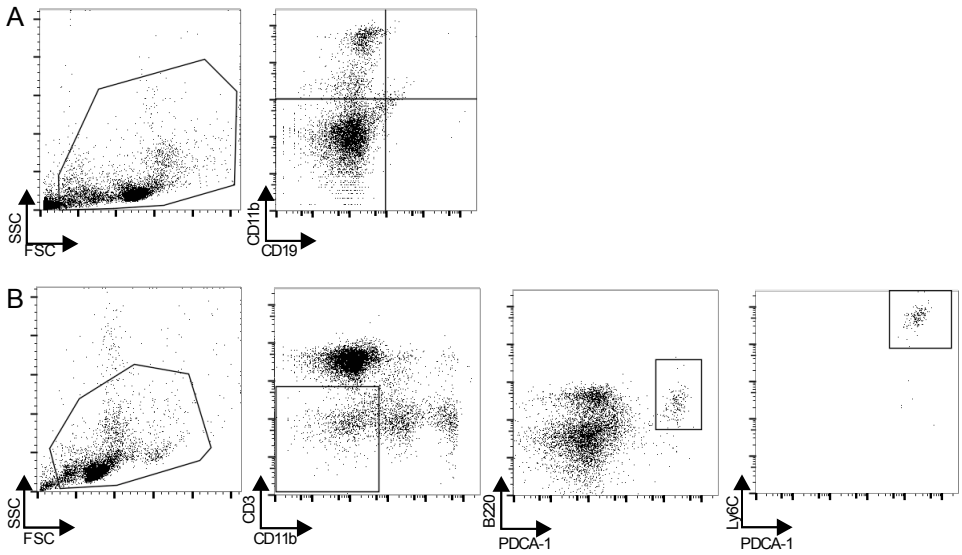

Figure 1. Highly purified mouse pDCs were flow sorted from CD19-negative spleen.

(A) The purity of splenocytes was assessed following the removal of $CD19^+$ B cells by positive bead selection. **(B)** $CD19^-$ splenocytes were flow sorted by first selecting the $CD11b^-$ and $CD3^-$ population to remove monocytes and T cells. The PDCA-1^+ $B220^+$ $Ly6C^+$ population was selected as pDCs, which were routinely more than 99% pure.

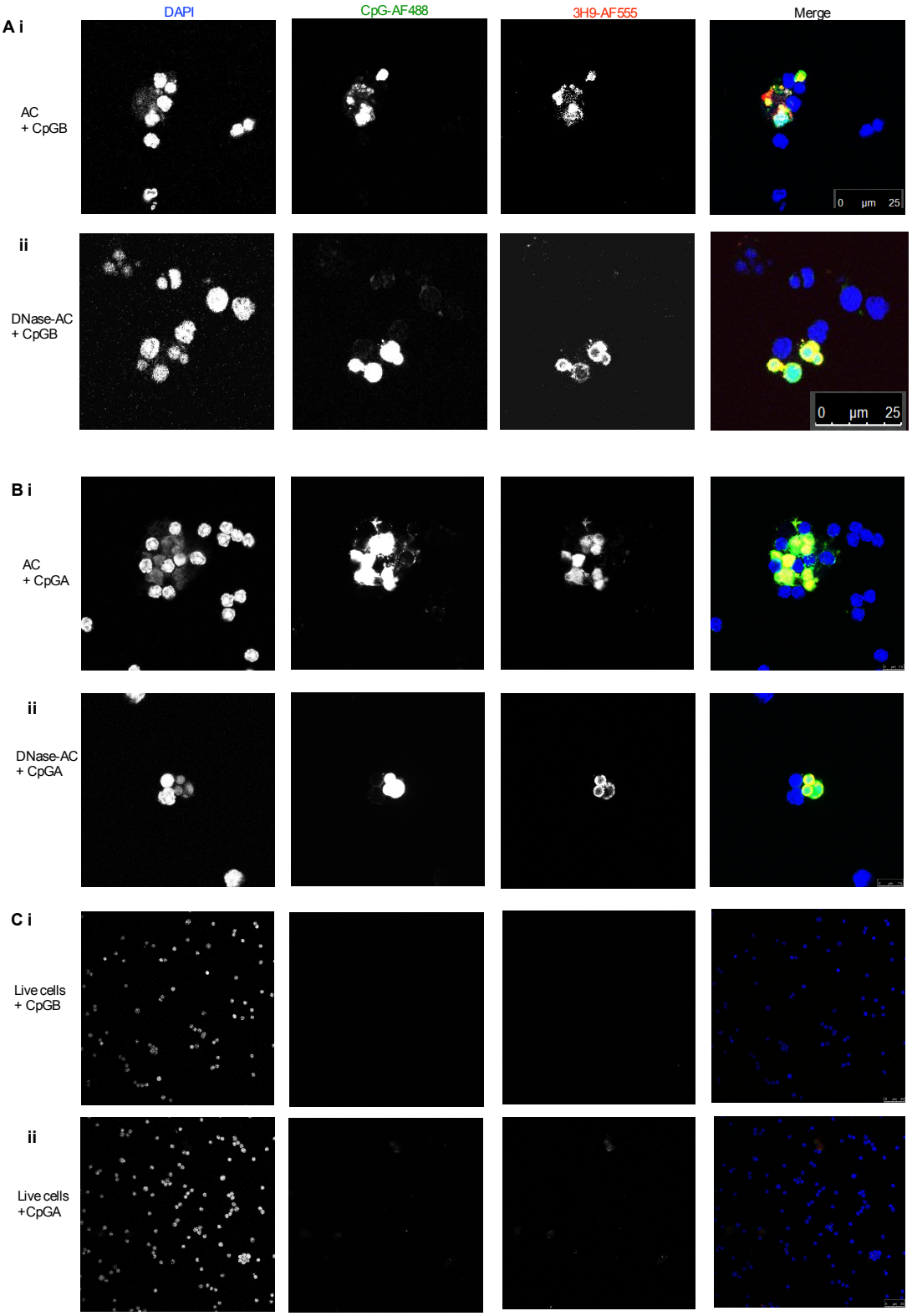
DAPI
CpG-AF488
3H9-AF555
Merge
A i
AC
+ CpGB
0 µm 25
ii
DNase-AC
+ CpGB
0 µm 25
B i
AC
+ CpGA
ii
DNase-AC
+ CpGA
C i
Live cells
+ CpGB
ii
Live cells
+CpGA

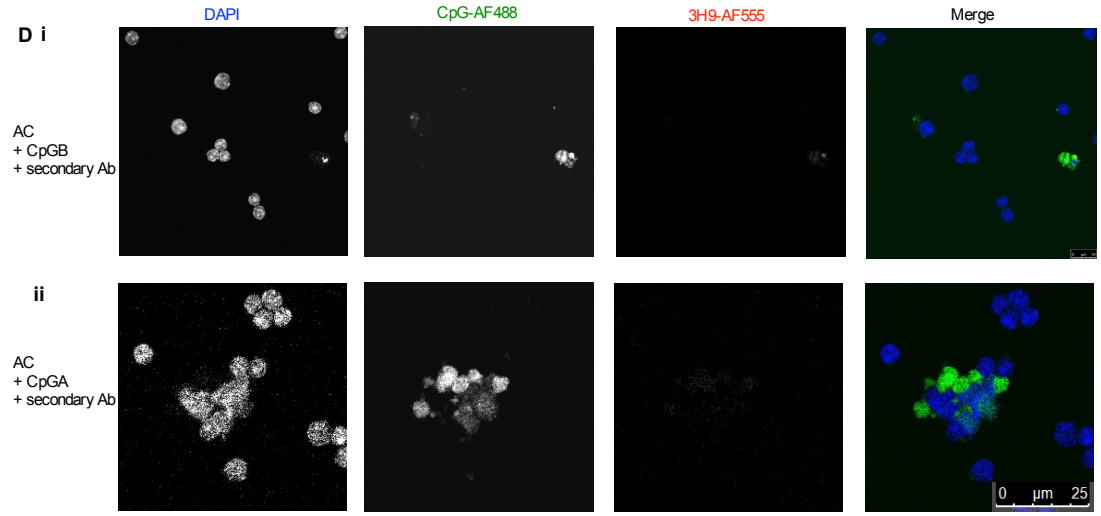

Figure 2. CpG associates with the surface of apoptotic cells.

(**Ai**) UV-irradiated apoptotic thymocytes and (**Aii**) DNase-treated apoptotic thymocytes were cultured for 2 h with CpGB directly conjugated to AF488 (Green). The cells were co-stained for apoptotic DNA and chromatin using the mouse 3H9 antibody and rabbit anti-mouse AF555 (red) and nuclear DNA using DAPI (Blue). (**Bi**) Untreated apoptotic cells and (**Bii**) DNase-treated apoptotic cells were cultured with CpGA-AF488, as described for (A). Freshly isolated live thymocytes were cultured with (**Ci**) CpGB-AF488 and (**Cii**) CpGA-AF488, as described in (A). Apoptotic cells were cultured with (**Di**) CpGB-AF488 and (**Dii**) CpGA-AF488 then stained with goat anti-mouse AF555 to detect non-specific binding of the secondary antibody. Images are representative of three independent experiments and were acquired on a Leica TCS SP5 (Leica Microsystems) confocal laser scanning microscope with a fixed stage inverted microscope DMI6000CS, equipped with a HCX PL APO 63x/1.33 NA oil immersion objective. Images were acquired using LAS AF software (Leica Microsystems) and analysed using ImageJ software.

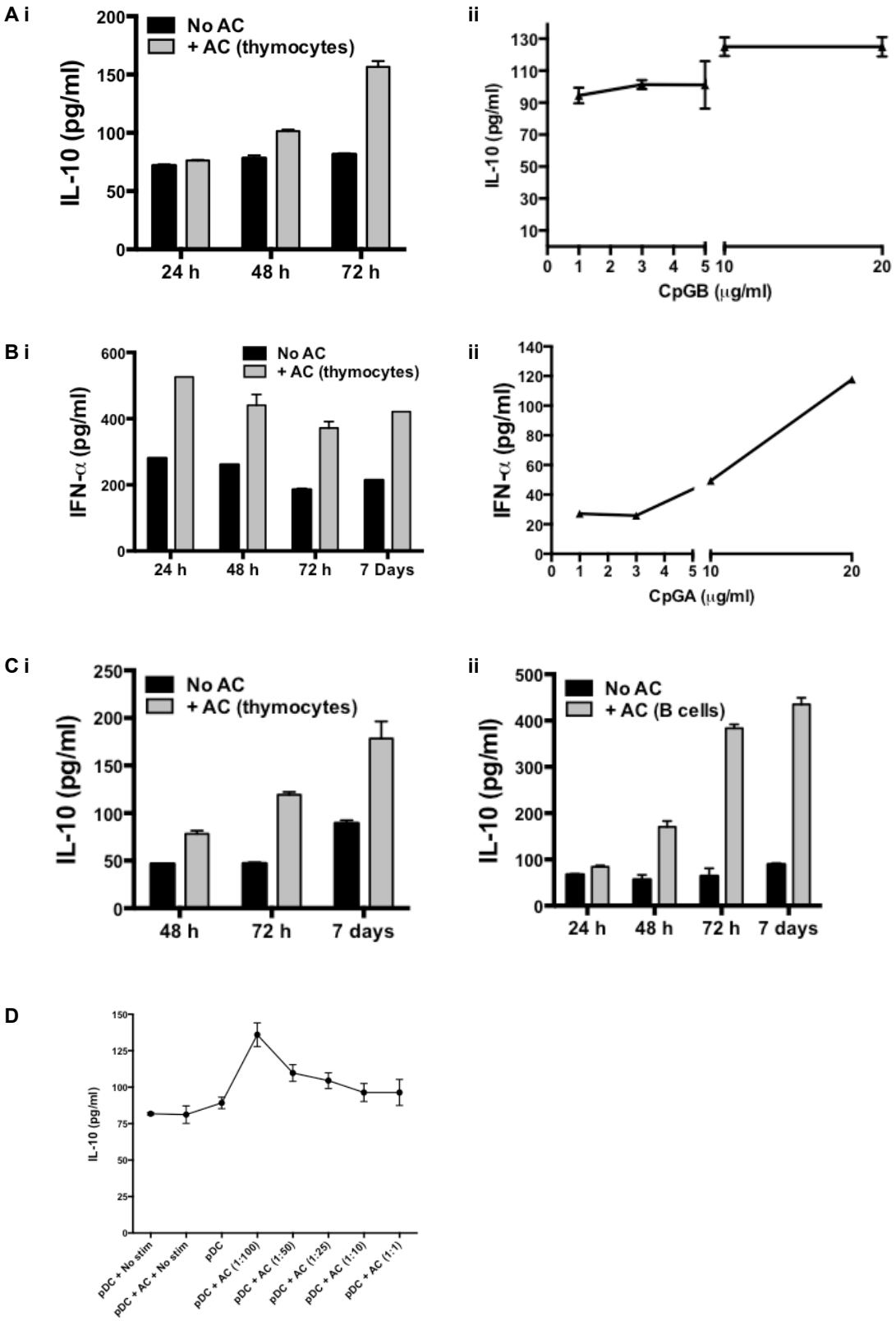

Figure 3. Optimising pDC stimulation by synthetic TLR agonists.

(**Ai**) PDCs were cultured with CpGB (10μg/ml) in the presence (grey bar) and absence (black bar) of apoptotic thymocytes. IL-10 was measured in supernatants

after 24 h, 48 h, and 72 h in culture. (**Aii**) IL-10 in culture supernatants was measured 72 h after pDCs were cultured with apoptotic thymocytes and CpGB at the following concentrations: 1, 3, 5, 10, and 20 μg/ml. (**Bi**) PDCs were cultured with CpGA (20μg/ml) in the presence (grey bar) and absence (black bar) of apoptotic thymocytes. IFN-α was measured in supernatants after 24 h, 48 h, 72 h, and 7 days in culture. (**Bii**) IFN-α in culture supernatants was measured 72 h after pDCs were cultured with apoptotic thymocytes and CpGA at the following concentrations: 1, 3, 10, and 20 μg/ml. PDCs were cultured with R848 (1μg/ml), with (grey bar) and without (black bar) (**Ci**) apoptotic thymocytes and (**Cii**) apoptotic B cells. IL-10 was measured in the culture supernatants at the time points stated. (**D**) IL-10 production by pDCs was measured 72 h after culture with CpGB and apoptotic thymocytes (AC) are the following pDC:AC ratios: 1:1, 1:10, 1:25, 1:50, and 1:100. Results are presented as the mean of two independent experiments, with error bars representing SEM.

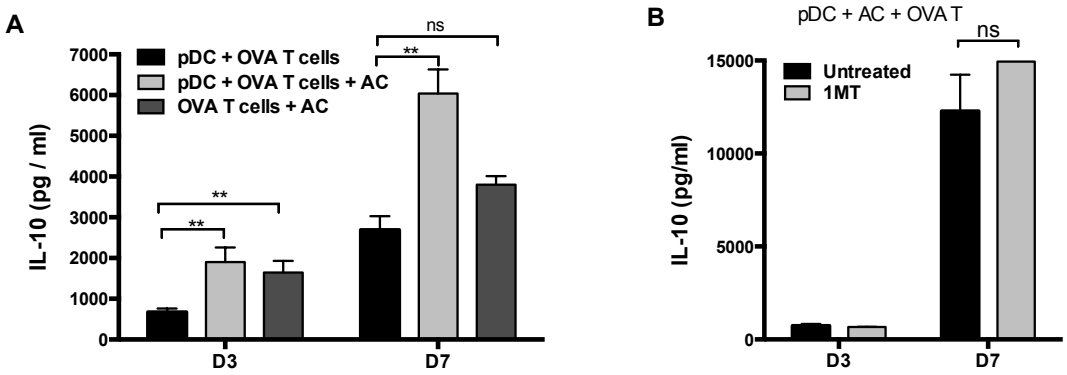

Figure 4. pDCs co-cultured with apoptotic cells induce IL10-secreting OVA peptide-specific T cells independent of IDO.

(**A**) IL-10 protein in cell supernatants was quantified by ELISA three days (D3) and seven days (D7) after DO11.10 OVA-specific T cells ($1x10^5$ /well) and OVA-peptide (2μg/ml) were cultured with BALB/c pDC (black bar), pDC and apoptotic cells (light grey bar), and apoptotic cells (dark grey bar). Results are mean plus or minus SEM of at least four independent experiments. (**B**) OVA-specific T cells were cultured with pDCs, apoptotic cells and OVA-peptide in untreated media, or media treated with 1-methyl-D-tryptophan (1MT 200μM) to inhibit IDO activity. Results are mean plus or minus SEM of three independent experiments. Statistical significance was determined by one-way ANOVA. $^{**}P < 0.01$; ns (not significant).

Appendix C

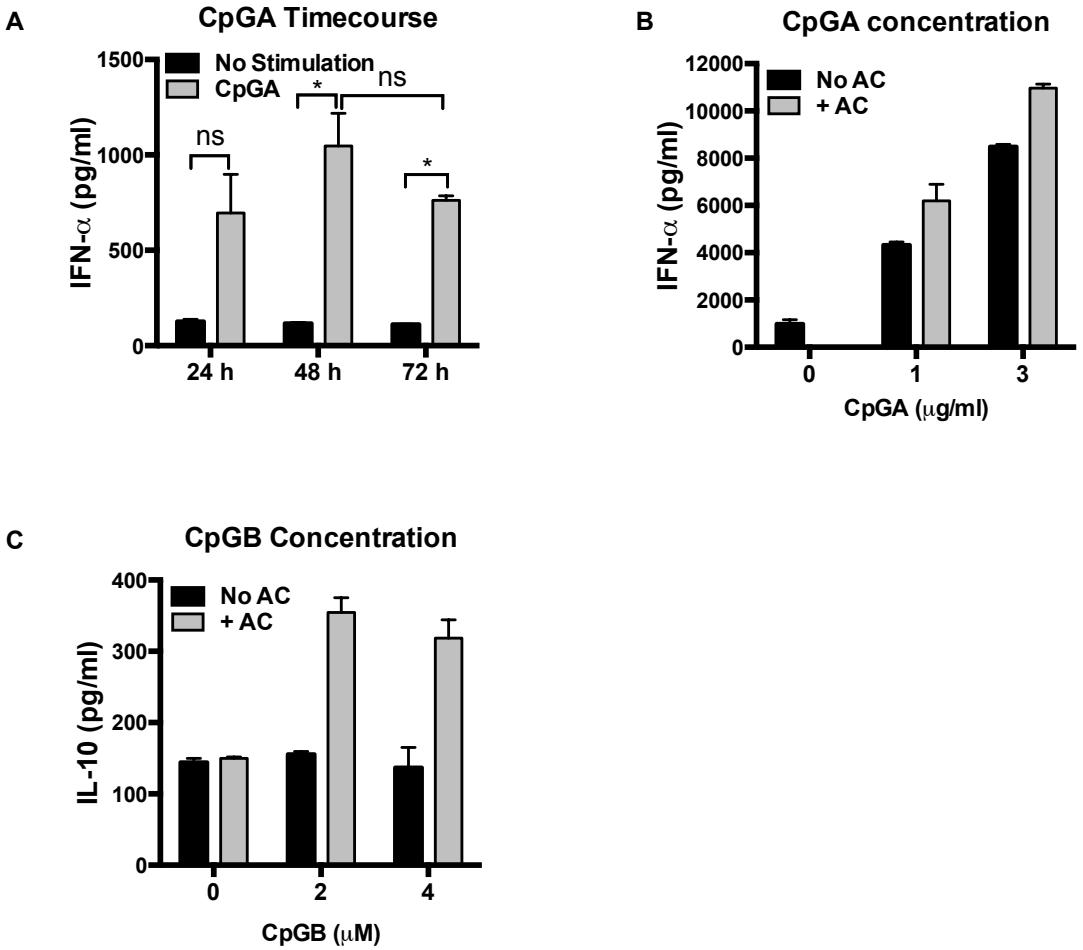

Figure 1. Optimising human CpG stimulation.

(**A**) Healthy PBMCs were cultured alone (No Stimulation) and with CpGA for 24 h, 48 h, and 72 h. IFN-α production was measured by ELISA. (**B**) IFN-α was measured 72 h after healthy PBMCs were cultured with and without apoptotic $CD4^+$ T cells and CpGA at concentrations 0, 1, and 3 μg/ml. (**C**) Healthy B cells were cultured with and without apoptotic $CD4^+$ T cells and CpGB at concentrations 0, 2, and 4 μM. After 72 h IL-10 in culture supernatant was measured by ELISA. Results are presented as mean and SEM of two independent experiments.

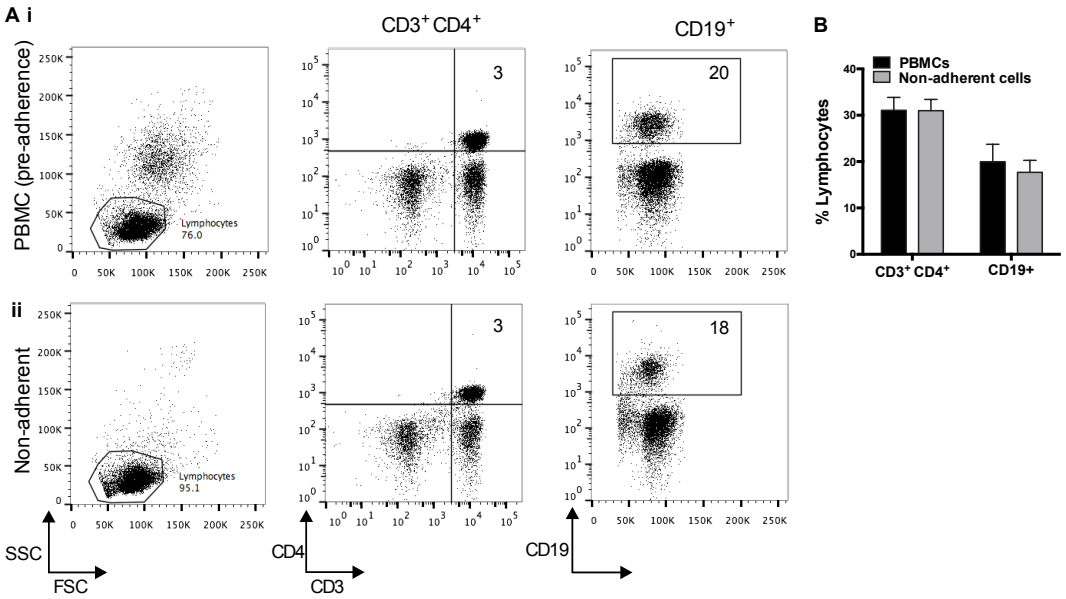

Figure 2. T cell and B cell proportions after adhering monocytes to plastic.

(**A**) $CD3^+CD4^+$ T and $CD19^+$ B lymphocytes were assessed by flow cytometry in (**i**) whole PBMCs and (**ii**) in the non-adherent cell population 1 h after incubation in 24-well culture plates. (**B**) The mean proportion of T and B lymphocytes from four independent experiments. Error bars represent SEM.

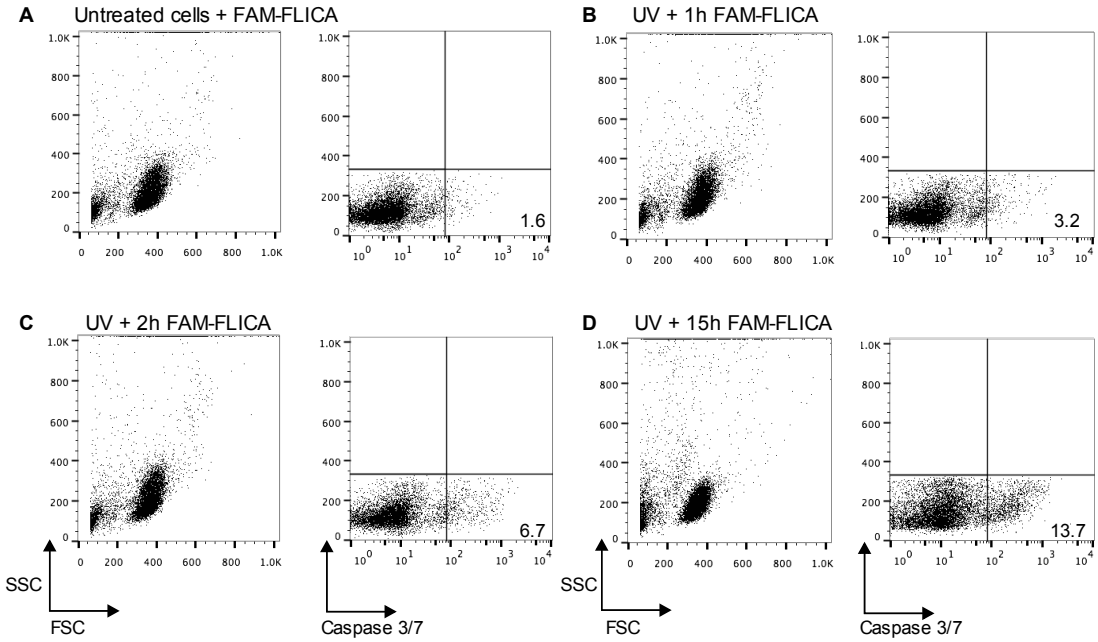

Figure 3. Optimising FAM-FLICA Caspase 3/7 activation kit.

Flow cytometry analysis to assess the proportion of lymphocytes that were positive for active caspases 3 and 7 after FAM-FLICA staining (**A**) untreated cells, and staining UV irradiated cells with FAM-FLICA for (**B**) 1 h, (**C**) 2 h, and (**D**) 15 h.

Appendix D

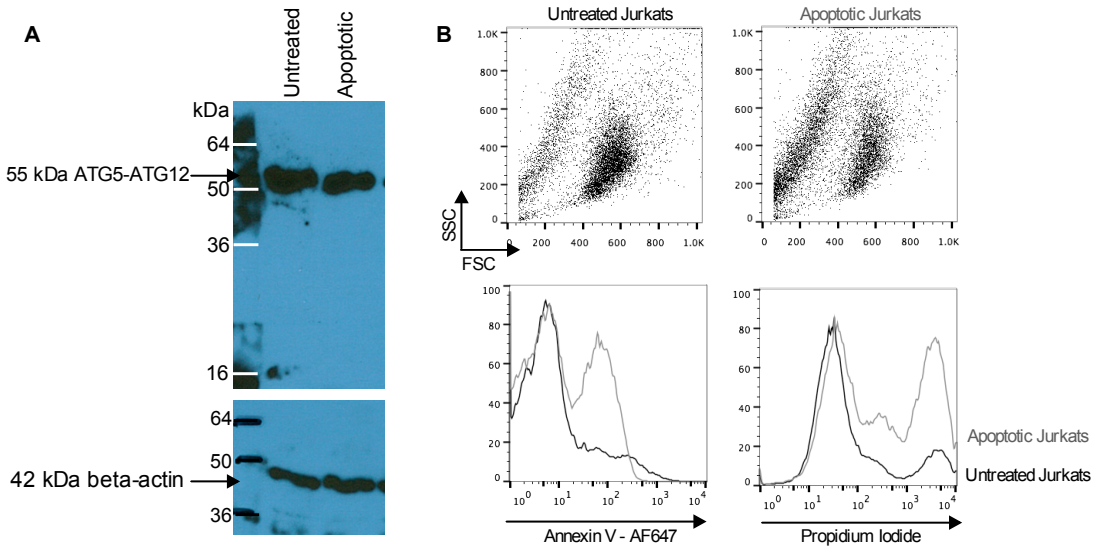

Figure 1. Late apoptotic/secondarily necrotic cells express ATG5-ATG12.

(A) Western blot gel showing 55 kDa ATG5-ATG12 protein expression in untreated and anti-CD95 treated apoptotic Jurkat cells. β-actin was used as the loading control. **(B)** Representative FACS histograms from 1 of 2 independent experiments of untreated and apoptotic Jurkat cells stained with annexin V-AF647 and propidium iodide.

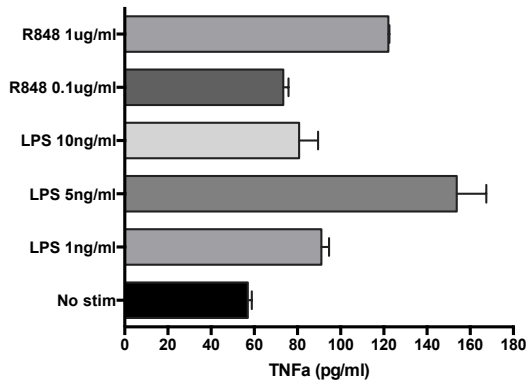

Figure 2. Optimising TLR-stimulation of healthy macrophages.

Control macrophages were culture with no stimulation (No stim) and with LPS (1ng/ml, 5ng/ml, and 10ng/ml), or R848 (0.1μg/ml and 1μg/ml). TNF-α in the cell supernatant was quantified after 18 h.

References

1. Kerr JFR, Wyllie AH, Currie AR. APOPTOSIS - BASIC BIOLOGICAL PHENOMENON WITH WIDE-RANGING IMPLICATIONS IN TISSUE KINETICS. *British Journal of Cancer*. 1972;26(4):239-&.
2. Leist M, Single B, Castoldi AF, Kuhnle S, Nicotera P. Intracellular adenosine triphosphate (ATP) concentration: a switch in the decision between apoptosis and necrosis. *J Exp Med*. 1997;185(8):1481-1486.
3. Eguchi Y, Shimizu S, Tsujimoto Y. Intracellular ATP levels determine cell death fate by apoptosis or necrosis. *Cancer Res*. 1997;57(10):1835-1840.
4. Kass GE, Eriksson JE, Weis M, Orrenius S, Chow SC. Chromatin condensation during apoptosis requires ATP. *Biochem J*. 1996;318 (Pt 3):749-752.
5. Li P, Nijhawan D, Budihardjo I, et al. Cytochrome c and dATP-dependent formation of Apaf-1/caspase-9 complex initiates an apoptotic protease cascade. *Cell*. 1997;91(4):479-489.
6. Casciolarosen LA, Anhalt G, Rosen A. AUTOANTIGENS TARGETED IN SYSTEMIC LUPUS-ERYTHEMATOSUS ARE CLUSTERED IN 2 POPULATIONS OF SURFACE-STRUCTURES ON APOPTOTIC KERATINOCYTES. *Journal of Experimental Medicine*. 1994;179(4):1317-1330.
7. Poon IK, Lucas CD, Rossi AG, Ravichandran KS. Apoptotic cell clearance: basic biology and therapeutic potential. *Nat Rev Immunol*. 2014;14(3):166-180.
8. Tait SW, Green DR. Mitochondria and cell death: outer membrane permeabilization and beyond. *Nat Rev Mol Cell Biol*. 2010;11(9):621-632.
9. Chipuk JE, Moldoveanu T, Llambi F, Parsons MJ, Green DR. The BCL-2 family reunion. *Mol Cell*. 2010;37(3):299-310.
10. Li HL, Zhu H, Xu CJ, Yuan JY. Cleavage of BID by caspase 8 mediates the mitochondrial damage in the Fas pathway of apoptosis. *Cell*. 1998;94(4):491-501.
11. Willis SN, Fletcher JI, Kaufmann T, et al. Apoptosis initiated when BH3 ligands engage multiple Bcl-2 homologs, not Bax or Bak. *Science*. 2007;315(5813):856-859.
12. Fletcher JI, Meusburger S, Hawkins CJ, et al. Apoptosis is triggered when prosurvival Bcl-2 proteins cannot restrain Bax. *Proc Natl Acad Sci U S A*. 2008;105(47):18081-18087.
13. Sakahira H, Enari M, Nagata S. Cleavage of CAD inhibitor in CAD activation and DNA degradation during apoptosis. *Nature*. 1998;391(6662):96-99.
14. Lee N, MacDonald H, Reinhard C, et al. Activation of hPAK65 by caspase cleavage induces some of the morphological and biochemical changes of apoptosis. *Proc Natl Acad Sci U S A*. 1997;94(25):13642-13647.
15. Rudel T, Bokoch GM. Membrane and morphological changes in apoptotic cells regulated by caspase-mediated activation of PAK2. *Science*. 1997;276(5318):1571-1574.
16. Coleman ML, Sahai EA, Yeo M, Bosch M, Dewar A, Olson MF. Membrane blebbing during apoptosis results from caspase-mediated activation of ROCK I. *Nature Cell Biology*. 2001;3(4):339-345.

17. Sebbagh M, Renvoize C, Hamelin J, Riche N, Bertoglio J, Breard J. Caspase-3-mediated cleavage of ROCK I induces MLC phosphorylation and apoptotic membrane blebbing. *Nat Cell Biol*. 2001;3(4):346-352.
18. Ferraro-Peyret C, Quemeneur L, Flacher M, Revillard JP, Genestier L. Caspase-independent phosphatidylserine exposure during apoptosis of primary T lymphocytes. *J Immunol*. 2002;169(9):4805-4810.
19. Segawa K, Kurata S, Yanagihashi Y, Brummelkamp TR, Matsuda F, Nagata S. Caspase-mediated cleavage of phospholipid flippase for apoptotic phosphatidylserine exposure. *Science*. 2014;344(6188):1164-1168.
20. Poon IKH, Chiu Y-H, Armstrong AJ, et al. Unexpected link between an antibiotic, pannexin channels and apoptosis. *Nature*. 2014;507(7492):329-+.
21. Atkin-Smith GK, Tixeira R, Paone S, et al. A novel mechanism of generating extracellular vesicles during apoptosis via a beads-on-a-string membrane structure. *Nat Commun*. 2015;6:7439.
22. Croft DR, Coleman ML, Li S, et al. Actin-myosin-based contraction is responsible for apoptotic nuclear disintegration. *J Cell Biol*. 2005;168(2):245-255.
23. Wickman G, Julian L, Olson MF. How apoptotic cells aid in the removal of their own cold dead bodies. *Cell Death and Differentiation*. 2012;19(5):735-742.
24. Tanaka M, Asano K, Qiu CH. Immune regulation by apoptotic cell clearance. *Clearance of Dying Cells in Healthy and Diseased Immune Systems*. 2010;1209:37-42.
25. Arandjelovic S, Ravichandran KS. Phagocytosis of apoptotic cells in homeostasis. *Nat Immunol*. 2015;16(9):907-917.
26. Elliott MR, Chekeni FB, Trampont PC, et al. Nucleotides released by apoptotic cells act as a find-me signal to promote phagocytic clearance. *Nature*. 2009;461(7261):282-286.
27. Lauber K, Bohn E, Krober SM, et al. Apoptotic cells induce migration of phagocytes via caspase-3-mediated release of a lipid attraction signal. *Cell*. 2003;113(6):717-730.
28. Gude DR, Alvarez SE, Paugh SW, et al. Apoptosis induces expression of sphingosine kinase 1 to release sphingosine-1-phosphate as a "come-and-get-me" signal. *Faseb j*. 2008;22(8):2629-2638.
29. Truman LA, Ford CA, Pasikowska M, et al. CX3CL1/fractalkine is released from apoptotic lymphocytes to stimulate macrophage chemotaxis. *Blood*. 2008;112(13):5026-5036.
30. Chekeni FB, Elliott MR, Sandilos JK, et al. Pannexin 1 channels mediate 'find-me' signal release and membrane permeability during apoptosis. *Nature*. 2010;467(7317):863-867.
31. Buckley CD, Gilroy DW, Serhan CN, Stockinger B, Tak PP. The resolution of inflammation. *Nat Rev Immunol*. 2013;13(1):59-66.
32. Bournazou I, Pound JD, Duffin R, et al. Apoptotic human cells inhibit migration of granulocytes via release of lactoferrin. *J Clin Invest*. 2009;119(1):20-32.
33. Savill J, Dransfield I, Gregory C, Haslett C. A blast from the past: Clearance of apoptotic cells regulates immune responses. *Nature Reviews Immunology*. 2002;2(12):965-975.
34. Hochreiter-Hufford A, Ravichandran KS. Clearing the dead: apoptotic cell sensing, recognition, engulfment, and digestion. *Cold Spring Harb Perspect Biol*. 2013;5(1):a008748.

35. Korb LC, Ahearn JM. C1q binds directly and specifically to surface blebs of apoptotic human keratinocytes: complement deficiency and systemic lupus erythematosus revisited. *J Immunol*. 1997;158(10):4525-4528.
36. Martin M, Leffler J, Blom AM. Annexin A2 and A5 Serve as New Ligands for C1q on Apoptotic Cells. *Journal of Biological Chemistry*. 2012;287(40):33733-33744.
37. Nauta AJ, Trouw LA, Daha MR, et al. Direct binding of C1q to apoptotic cells and cell blebs induces complement activation. *Eur J Immunol*. 2002;32(6):1726-1736.
38. Chen Y, Park YB, Patel E, Silverman GJ. IgM antibodies to apoptosis-associated determinants recruit C1q and enhance dendritic cell phagocytosis of apoptotic cells. *J Immunol*. 2009;182(10):6031-6043.
39. Kinchen JM, Ravichandran KS. Phagosome maturation: going through the acid test. *Nat Rev Mol Cell Biol*. 2008;9(10):781-795.
40. Baudino L, Sardini A, Ruseva MM, et al. C3 opsonization regulates endocytic handling of apoptotic cells resulting in enhanced T-cell responses to cargo-derived antigens. *Proc Natl Acad Sci U S A*. 2014;111(4):1503-1508.
41. Peng Y, Elkon KB. Autoimmunity in MFG-E8-deficient mice is associated with altered trafficking and enhanced cross-presentation of apoptotic cell antigens. *J Clin Invest*. 2011;121(6):2221-2241.
42. Gregory CD, Pound JD. Microenvironmental influences of apoptosis in vivo and in vitro. *Apoptosis*. 2010;15(9):1029-1049.
43. Lucas M, Stuart LM, Zhang A, et al. Requirements for apoptotic cell contact in regulation of macrophage responses. *Journal of Immunology*. 2006;177(6):4047-4054.
44. Hart SP, Dransfield I, Rossi AG. Phagocytosis of apoptotic cells. *Methods*. 2008;44(3):280-285.
45. Fadok VA, Bratton DL, Konowal A, Freed PW, Westcott JY, Henson PM. Macrophages that have ingested apoptotic cells in vitro inhibit proinflammatory cytokine production through autocrine/paracrine mechanisms involving TGF-beta, PGE2, and PAF. *Journal of Clinical Investigation*. 1998;101(4):890-898.
46. Henson PM, Bratton DL. Antiinflammatory effects of apoptotic cells. *J Clin Invest*. 2013;123(7):2773-2774.
47. Sanjabi S, Zenewicz LA, Kamanaka M, Flavell RA. Anti-inflammatory and pro-inflammatory roles of TGF-beta, IL-10, and IL-22 in immunity and autoimmunity. *Curr Opin Pharmacol*. 2009;9(4):447-453.
48. Sauter B, Albert ML, Francisco L, Larsson M, Somersan S, Bhardwaj N. Consequences of cell death: exposure to necrotic tumor cells, but not primary tissue cells or apoptotic cells, induces the maturation of immunostimulatory dendritic cells. *J Exp Med*. 2000;191(3):423-434.
49. Ravishankar B, Liu H, Shinde R, et al. Tolerance to apoptotic cells is regulated by indoleamine 2,3-dioxygenase. *Proc Natl Acad Sci U S A*. 2012;109(10):3909-3914.
50. Miles K, Clarke DJ, Lu W, et al. Dying and necrotic neutrophils are anti-inflammatory secondary to the release of alpha-defensins. *J Immunol*. 2009;183(3):2122-2132.

51. Ding Q, Yeung M, Camirand G, et al. Regulatory B cells are identified by expression of TIM-1 and can be induced through TIM-1 ligation to promote tolerance in mice. *Journal of Clinical Investigation*. 2011;121(9):3645-3656.
52. Yeung MY, Ding Q, Brooks CR, et al. TIM-1 signaling is required for maintenance and induction of regulatory B cells. *Am J Transplant*. 2015;15(4):942-953.
53. Xiao S, Brooks CR, Sobel RA, Kuchroo VK. Tim-1 is essential for induction and maintenance of IL-10 in regulatory B cells and their regulation of tissue inflammation. *J Immunol*. 2015;194(4):1602-1608.
54. Mauri C, Menon M. The expanding family of regulatory B cells. *Int Immunol*. 2015;27(10):479-486.
55. Miles K, Heaney J, Sibinska Z, et al. A tolerogenic role for Toll-like receptor 9 is revealed by B-cell interaction with DNA complexes expressed on apoptotic cells. *Proc Natl Acad Sci U S A*. 2012;109(3):887-892.
56. Gray M, Miles K, Salter D, Gray D, Savill J. Apoptotic cells protect mice from autoimmune inflammation by the induction of regulatory B cells. *Proc Natl Acad Sci U S A*. 2007;104(35):14080-14085.
57. Gray M, Gray D. Regulatory B cells mediate tolerance to apoptotic self in health: implications for disease. *Int Immunol*. 2015;27(10):505-511.
58. Ford CA, Petrova S, Pound JD, et al. Oncogenic properties of apoptotic tumor cells in aggressive B cell lymphoma. *Curr Biol*. 2015;25(5):577-588.
59. Hodge S, Hodge G, Scicchitano R, Reynolds PN, Holmes M. Alveolar macrophages from subjects with chronic obstructive pulmonary disease are deficient in their ability to phagocytose apoptotic airway epithelial cells. *Immunology and Cell Biology*. 2003;81(4):289-296.
60. Orbai AM, Truedsson L, Sturfelt G, et al. Anti-C1q antibodies in systemic lupus erythematosus. *Lupus*. 2015;24(1):42-49.
61. Trendelenburg M, Lopez-Trascasa M, Potlukova E, et al. High prevalence of anti-C1q antibodies in biopsy-proven active lupus nephritis. *Nephrol Dial Transplant*. 2006;21(11):3115-3121.
62. Siegert C, Daha M, Westedt ML, van der Voort E, Breedveld F. IgG autoantibodies against C1q are correlated with nephritis, hypocomplementemia, and dsDNA antibodies in systemic lupus erythematosus. *J Rheumatol*. 1991;18(2):230-234.
63. Rahman A, Isenberg DA. Mechanisms of disease: Systemic lupus erythematosus. *New England Journal of Medicine*. 2008;358(9):929-939.
64. Poole BD, Scofield RH, Harley JB, James JA. Epstein-Barr virus and molecular mimicry in systemic lupus erythematosus. *Autoimmunity*. 2006;39(1):63-70.
65. Ghodke-Puranik Y, Niewold TB. Immunogenetics of systemic lupus erythematosus: A comprehensive review. *J Autoimmun*. 2015;64:125-136.
66. Mohan C, Putterman C. Genetics and pathogenesis of systemic lupus erythematosus and lupus nephritis. *Nat Rev Nephrol*. 2015;11(6):329-341.
67. Harley JB, Alarcon-Riquelme ME, Criswell LA, et al. Genome-wide association scan in women with systemic lupus erythematosus identifies susceptibility variants in ITGAM, PXK, KIAA1542 and other loci. *Nature Genetics*. 2008;40(2):204-210.

68. Bernal CB, Zamora LD, Navarra SV. Biologic therapies in systemic lupus erythematosus. *Int J Rheum Dis*. 2015;18(2):146-153.
69. Navarra SV, Guzman RM, Gallacher AE, et al. Efficacy and safety of belimumab in patients with active systemic lupus erythematosus: a randomised, placebo-controlled, phase 3 trial. *Lancet*. 2011;377(9767):721-731.
70. Furie R, Petri M, Zamani O, et al. A phase III, randomized, placebo-controlled study of belimumab, a monoclonal antibody that inhibits B lymphocyte stimulator, in patients with systemic lupus erythematosus. *Arthritis Rheum*. 2011;63(12):3918-3930.
71. Ota M, Duong BH, Torkamani A, et al. Regulation of the B cell receptor repertoire and self-reactivity by BAFF. *J Immunol*. 2010;185(7):4128-4136.
72. Manzi S, Sanchez-Guerrero J, Merrill JT, et al. Effects of belimumab, a B lymphocyte stimulator-specific inhibitor, on disease activity across multiple organ domains in patients with systemic lupus erythematosus: combined results from two phase III trials. *Ann Rheum Dis*. 2012;71(11):1833-1838.
73. Radic M, Marion T, Monestier M. Nucleosomes are exposed at the cell surface in apoptosis. *J Immunol*. 2004;172(11):6692-6700.
74. Casciola-Rosen L, Rosen A, Petri M, Schlissel M. Surface blebs on apoptotic cells are sites of enhanced procoagulant activity: implications for coagulation events and antigenic spread in systemic lupus erythematosus. *Proc Natl Acad Sci U S A*. 1996;93(4):1624-1629.
75. Bigler C, Schaller M, Perahud I, Osthoff M, Trendelenburg M. Autoantibodies against complement C1q specifically target C1q bound on early apoptotic cells. *J Immunol*. 2009;183(5):3512-3521.
76. Munoz LE, Lauber K, Schiller M, Manfredi AA, Herrmann M. The role of defective clearance of apoptotic cells in systemic autoimmunity. *Nature Reviews Rheumatology*. 2010;6(5):280-289.
77. Ren Y, Tang J, Mok MY, Chan AW, Wu A, Lau CS. Increased apoptotic neutrophils and macrophages and impaired macrophage phagocytic clearance of apoptotic neutrophils in systemic lupus erythematosus. *Arthritis Rheum*. 2003;48(10):2888-2897.
78. Tas SW, Quartier P, Botto M, Fossati-Jimack L. Macrophages from patients with SLE and rheumatoid arthritis have defective adhesion in vitro, while only SLE macrophages have impaired uptake of apoptotic cells. *Annals of the Rheumatic Diseases*. 2006;65(2):216-221.
79. Hom G, Graham RR, Modrek B, et al. Association of systemic lupus erythematosus with C8orf13-BLK and ITGAM-ITGAX. *N Engl J Med*. 2008;358(9):900-909.
80. Nath SK, Han S, Kim-Howard X, et al. A nonsynonymous functional variant in integrin-alpha(M) (encoded by ITGAM) is associated with systemic lupus erythematosus. *Nat Genet*. 2008;40(2):152-154.
81. Fossati-Jimack L, Ling GS, Cortini A, et al. Phagocytosis is the main CR3-mediated function affected by the lupus-associated variant of CD11b in human myeloid cells. *PLoS One*. 2013;8(2):e57082.
82. Potter PK, Cortes-Hernandez J, Quartier P, Botto M, Walport MJ. Lupus-prone mice have an abnormal response to thioglycolate and an impaired clearance of apoptotic cells. *J Immunol*. 2003;170(6):3223-3232.

83. Mevorach D, Zhou JL, Song X, Elkon KB. Systemic exposure to irradiated apoptotic cells induces autoantibody production. *Journal of Experimental Medicine*. 1998;188(2):387-392.
84. Botto M, Dell'Agnola C, Bygrave AE, et al. Homozygous C1q deficiency causes glomerulonephritis associated with multiple apoptotic bodies. *Nature Genetics*. 1998;19(1):56-59.
85. Bygrave AE, Rose KL, Cortes-Hernandez J, et al. Spontaneous autoimmunity in 129 and C57BL/6 mice-implications for autoimmunity described in gene-targeted mice. *PLoS Biol*. 2004;2(8):E243.
86. Lewis MJ, Botto M. Complement deficiencies in humans and animals: Links to autoimmunity. *Autoimmunity*. 2006;39(5):367-378.
87. Sang A, Zheng YY, Morel L. Contributions of B cells to lupus pathogenesis. *Mol Immunol*. 2014;62(2):329-338.
88. Jacobi AM, Mei H, Hoyer BF, et al. HLA-DRhigh/CD27high plasmablasts indicate active disease in patients with systemic lupus erythematosus. *Ann Rheum Dis*. 2010;69(1):305-308.
89. Ferry H, Potter PK, Crockford TL, et al. Increased positive selection of B1 cells and reduced B cell tolerance to intracellular antigens in C1q-deficient mice. *Journal of Immunology*. 2007;178(5):2916-2922.
90. Silva MT. Secondary necrosis: the natural outcome of the complete apoptotic program. *FEBS Lett*. 2010;584(22):4491-4499.
91. Sarma JV, Ward PA. The complement system. *Cell Tissue Res*. 2011;343(1):227-235.
92. Walport MJ. Complement and systemic lupus erythematosus. *Arthritis Res*. 2002;4 Suppl 3:S279-293.
93. Garcia-Romo GS, Caielli S, Vega B, et al. Netting Neutrophils Are Major Inducers of Type I IFN Production in Pediatric Systemic Lupus Erythematosus. *Science Translational Medicine*. 2011;3(73):11.
94. Fuchs TA, Abed U, Goosmann C, et al. Novel cell death program leads to neutrophil extracellular traps. *J Cell Biol*. 2007;176(2):231-241.
95. Brinkmann V, Reichard U, Goosmann C, et al. Neutrophil extracellular traps kill bacteria. *Science*. 2004;303(5663):1532-1535.
96. Hakkim A, Furnrohr BG, Amann K, et al. Impairment of neutrophil extracellular trap degradation is associated with lupus nephritis. *Proc Natl Acad Sci U S A*. 2010;107(21):9813-9818.
97. Vallin H, Blomberg S, Alm GV, Cederblad B, Ronnblom L. Patients with systemic lupus erythematosus (SLE) have a circulating inducer of interferon-alpha (IFN-alpha) production acting on leucocytes resembling immature dendritic cells. *Clinical and Experimental Immunology*. 1999;115(1):196-202.
98. Vallin H, Perers A, Alm GV, Ronnblom L. Anti-double-stranded DNA antibodies and immunostimulatory plasmid DNA in combination mimic the endogenous IFN-alpha inducer in systemic lupus erythematosus. *Journal of Immunology*. 1999;163(11):6306-6313.
99. Batteux F, Palmer P, Daeron M, Weill B, Lebon P. FC gamma RII (CD32)-dependent induction of interferon-alpha by serum from patients with lupus erythematosus. *European Cytokine Network*. 1999;10(4):509-513.
100. Bave U, Magnusson M, Eloranta ML, Perers A, Alm GV, Ronnblom L. Fc gamma RIIa is expressed on natural IFN-alpha-producing cells (plasmacytoid

dendritic cells) and is required for the IFN-alpha production induced by apoptotic cells combined with lupus IgG. *Journal of Immunology*. 2003;171(6):3296-3302.
101. Means TK, Latz E, Hayashi F, Murali MR, Golenbock DT, Luster AD. Human lupus autoantibody-DNA complexes activate DCs through cooperation of CD32 and TLR9. *Journal of Clinical Investigation*. 2005;115(2):407-417.
102. Swiecki M, Colonna M. The multifaceted biology of plasmacytoid dendritic cells. *Nat Rev Immunol*. 2015;15(8):471-485.
103. Chen Z, Moyana T, Saxena A, Warrington R, Jia Z, Xiang J. Efficient antitumor immunity derived from maturation of dendritic cells that had phagocytosed apoptotic/necrotic tumor cells. *Int J Cancer*. 2001;93(4):539-548.
104. Scaffidi P, Misteli T, Bianchi ME. Release of chromatin protein HMGB1 by necrotic cells triggers inflammation. *Nature*. 2002;418(6894):191-195.
105. Ren Y, Stuart L, Lindberg FP, et al. Nonphlogistic clearance of late apoptotic neutrophils by macrophages: efficient phagocytosis independent of beta 2 integrins. *J Immunol*. 2001;166(7):4743-4750.
106. Devitt A, Parker KG, Ogden CA, et al. Persistence of apoptotic cells without autoimmune disease or inflammation in CD14(-/-) mice. *Journal of Cell Biology*. 2004;167(6):1161-1170.
107. Patel VA, Longacre A, Hsiao K, et al. Apoptotic cells, at all stages of the death process, trigger characteristic signaling events that are divergent from and dominant over those triggered by necrotic cells - Implications for the delayed clearance model of autoimmunity. *Journal of Biological Chemistry*. 2006;281(8):4663-4670.
108. Lopez de Padilla CM, Niewold TB. The type I interferons: Basic concepts and clinical relevance in immune-mediated inflammatory diseases. *Gene*. 2016;576(1 Pt 1):14-21.
109. Niewold TB, Swedler WI. Systemic lupus erythematosus arising during interferon-alpha therapy for cryoglobulinemic vasculitis associated with hepatitis C. *Clin Rheumatol*. 2005;24(2):178-181.
110. Rönnblom LE, Alm GV, Oberg KE. Possible induction of systemic lupus erythematosus by interferon-alpha treatment in a patient with a malignant carcinoid tumour. *J Intern Med*. 1990;227(3):207-210.
111. Thomas C, Moraga I, Levin D, et al. Structural linkage between ligand discrimination and receptor activation by type I interferons. *Cell*. 2011;146(4):621-632.
112. Baechler EC, Batliwalla FM, Karypis G, et al. Interferon-inducible gene expression signature in peripheral blood cells of patients with severe lupus. *Proceedings of the National Academy of Sciences of the United States of America*. 2003;100(5):2610-2615.
113. Bennett L, Palucka AK, Arce E, et al. Interferon and granulopoiesis signatures in systemic lupus erythematosus blood. *Journal of Experimental Medicine*. 2003;197(6):711-723.
114. Yao Y, Liu Z, Jallal B, Shen N, Ronnblom L. Type I interferons in Sjogren's syndrome. *Autoimmun Rev*. 2013;12(5):558-566.
115. Raterman HG, Vosslamber S, de Ridder S, et al. The interferon type I signature towards prediction of non-response to rituximab in rheumatoid arthritis patients. *Arthritis Res Ther*. 2012;14(2):R95.

116. Wright HL, Thomas HB, Moots RJ, Edwards SW. Interferon gene expression signature in rheumatoid arthritis neutrophils correlates with a good response to TNFi therapy. *Rheumatology (Oxford)*. 2015;54(1):188-193.
117. Toro-Dominguez D, Carmona-Saez P, Alarcon-Riquelme ME. Shared signatures between rheumatoid arthritis, systemic lupus erythematosus and Sjogren's syndrome uncovered through gene expression meta-analysis. *Arthritis Res Ther*. 2014;16(6):489.
118. Blanco P, Palucka AK, Gill M, Pascual V, Banchereau J. Induction of dendritic cell differentiation by IFN-alpha in systemic lupus erythematosus. *Science*. 2001;294(5546):1540-1543.
119. Jego G, Palucka AK, Blanck JP, Chalouni C, Pascual V, Banchereau J. Plasmacytoid dendritic cells induce plasma cell differentiation through type I interferon and interleukin 6. *Immunity*. 2003;19(2):225-234.
120. Schneider WM, Chevillotte MD, Rice CM. Interferon-stimulated genes: a complex web of host defenses. *Annu Rev Immunol*. 2014;32:513-545.
121. Hron JD, Peng SL. Type I IFN protects against murine lupus. *J Immunol*. 2004;173(3):2134-2142.
122. Santiago-Raber ML, Baccala R, Haraldsson KM, et al. Type-I interferon receptor deficiency reduces lupus-like disease in NZB mice. *J Exp Med*. 2003;197(6):777-788.
123. Thibault DL, Graham KL, Lee LY, Balboni I, Hertzog PJ, Utz PJ. Type I interferon receptor controls B-cell expression of nucleic acid-sensing Toll-like receptors and autoantibody production in a murine model of lupus. *Arthritis Res Ther*. 2009;11(4):R112.
124. Zhuang H, Szeto C, Han S, Yang L, Reeves WH. Animal Models of Interferon Signature Positive Lupus. *Front Immunol*. 2015;6:291.
125. Lee PY, Weinstein JS, Nacionales DC, et al. A novel type I IFN-producing cell subset in murine lupus. *J Immunol*. 2008;180(7):5101-5108.
126. Stohl W. Future prospects in biologic therapy for systemic lupus erythematosus. *Nat Rev Rheumatol*. 2013;9(12):705-720.
127. Petri M, Wallace DJ, Spindler A, et al. Sifalimumab, a human anti-interferon-alpha monoclonal antibody, in systemic lupus erythematosus: a phase I randomized, controlled, dose-escalation study. *Arthritis Rheum*. 2013;65(4):1011-1021.
128. Kalunian KC, Merrill JT, Maciuca R, et al. A Phase II study of the efficacy and safety of rontalizumab (rhuMAb interferon-alpha) in patients with systemic lupus erythematosus (ROSE). *Ann Rheum Dis*. 2016;75(1):196-202.
129. Lauwerys BR, Hachulla E, Spertini F, et al. Down-regulation of interferon signature in systemic lupus erythematosus patients by active immunization with interferon alpha-kinoid. *Arthritis Rheum*. 2013;65(2):447-456.
130. Chiche L, Jourde-Chiche N, Whalen E, et al. Modular transcriptional repertoire analyses of adults with systemic lupus erythematosus reveal distinct type I and type II interferon signatures. *Arthritis Rheumatol*. 2014;66(6):1583-1595.
131. Rosser EC, Oleinika K, Tonon S, et al. Regulatory B cells are induced by gut microbiota-driven interleukin-1beta and interleukin-6 production. *Nat Med*. 2014;20(11):1334-1339.
132. Cash H, Relle M, Menke J, et al. Interleukin 6 (IL-6) deficiency delays lupus nephritis in MRL-Faslpr mice: the IL-6 pathway as a new therapeutic target in

treatment of autoimmune kidney disease in systemic lupus erythematosus. *J Rheumatol*. 2010;37(1):60-70.
133. 2014 ACR/ARHP Annual Meeting Abstract Supplement. *Arthritis Rheumatol*. 2014;66 Suppl 10:S1-s1402.
134. Martin JC, Baeten DL, Josien R. Emerging role of IL-17 and Th17 cells in systemic lupus erythematosus. *Clin Immunol*. 2014;154(1):1-12.
135. Geginat J, Paroni M, Maglie S, et al. Plasticity of human CD4 T cell subsets. *Front Immunol*. 2014;5:630.
136. Yu CF, Peng WM, Oldenburg J, et al. Human plasmacytoid dendritic cells support Th17 cell effector function in response to TLR7 ligation. *J Immunol*. 2010;184(3):1159-1167.
137. Isaksson M, Ardesjo B, Ronnblom L, et al. Plasmacytoid DC promote priming of autoimmune Th17 cells and EAE. *Eur J Immunol*. 2009;39(10):2925-2935.
138. Villanueva E, Yalavarthi S, Berthier CC, et al. Netting neutrophils induce endothelial damage, infiltrate tissues, and expose immunostimulatory molecules in systemic lupus erythematosus. *J Immunol*. 2011;187(1):538-552.
139. Lin AM, Rubin CJ, Khandpur R, et al. Mast cells and neutrophils release IL-17 through extracellular trap formation in psoriasis. *J Immunol*. 2011;187(1):490-500.
140. Nestle FO, Conrad C, Tun-Kyi A, et al. Plasmacytoid predendritic cells initiate psoriasis through interferon-alpha production. *Journal of Experimental Medicine*. 2005;202(1):135-143.
141. Netea MG, Nold-Petry CA, Nold MF, et al. Differential requirement for the activation of the inflammasome for processing and release of IL-1 beta in monocytes and macrophages. *Blood*. 2009;113(10):2324-2335.
142. Martinon F, Burns K, Tschopp J. The inflammasome: A molecular platform triggering activation of inflammatory caspases and processing of proIL-beta. *Molecular Cell*. 2002;10(2):417-426.
143. Kahlenberg JM, Kaplan MJ. The inflammasome and lupus: another innate immune mechanism contributing to disease pathogenesis? *Current Opinion in Rheumatology*. 2014;26(5):475-481.
144. Benoit ME, Clarke EV, Morgado P, Fraser DA, Tenner AJ. Complement protein C1q directs macrophage polarization and limits inflammasome activity during the uptake of apoptotic cells. *J Immunol*. 2012;188(11):5682-5693.
145. Asgari E, Le Friec G, Yamamoto H, et al. C3a modulates IL-1beta secretion in human monocytes by regulating ATP efflux and subsequent NLRP3 inflammasome activation. *Blood*. 2013;122(20):3473-3481.
146. Shin MS, Kang Y, Lee N, et al. U1-Small Nuclear Ribonucleoprotein Activates the NLRP3 Inflammasome in Human Monocytes. *Journal of Immunology*. 2012;188(10):4769-4775.
147. Shin MS, Kang Y, Lee N, et al. Self Double-Stranded (ds) DNA Induces IL-1 beta Production from Human Monocytes by Activating NLRP3 Inflammasome in the Presence of Anti-dsDNA Antibodies. *Journal of Immunology*. 2013;190(4):1407-1415.
148. Kahlenberg JM, Carmona-Rivera C, Smith CK, Kaplan MJ. Neutrophil Extracellular Trap-Associated Protein Activation of the NLRP3 Inflammasome Is Enhanced in Lupus Macrophages. *Journal of Immunology*. 2013;190(3):1217-1226.

149. Kahlenberg JM, Yalavarthi S, Zhao W, et al. An Essential Role of Caspase 1 in the Induction of Murine Lupus and Its Associated Vascular Damage. *Arthritis & Rheumatology*. 2014;66(1):152-162.
150. Voronov E, Dayan M, Zinger H, et al. IL-1 beta-deficient mice are resistant to induction of experimental SLE. *European Cytokine Network*. 2006;17(2):109-116.
151. Colonna M, Trinchieri G, Liu YJ. Plasmacytoid dendritic cells in immunity. *Nature Immunology*. 2004;5(12):1219-1226.
152. Fitzgeraldbocarsly P. HUMAN NATURAL INTERFERON-ALPHA PRODUCING CELLS. *Pharmacology & Therapeutics*. 1993;60(1):39-62.
153. Vollenweider R, Lennert K. PLASMACYTOID T-CELL CLUSTERS IN NON-SPECIFIC LYMPHADENITIS. *Virchows Archiv B-Cell Pathology Including Molecular Pathology*. 1983;44(1):1-14.
154. Siegal FP, Kadowaki N, Shodell M, et al. The nature of the principal type 1 interferon-producing cells in human blood. *Science*. 1999;284(5421):1835-1837.
155. Sathe P, Vremec D, Wu L, Corcoran L, Shortman K. Convergent differentiation: myeloid and lymphoid pathways to murine plasmacytoid dendritic cells. *Blood*. 2013;121(1):11-19.
156. Ishikawa F, Niiro H, Iino T, et al. The developmental program of human dendritic cells is operated independently of conventional myeloid and lymphoid pathways. *Blood*. 2007;110(10):3591-3660.
157. Cisse B, Caton ML, Lehner M, et al. Transcription factor E2-2 is an essential and specific regulator of plasmacytoid dendritic cell development. *Cell*. 2008;135(1):37-48.
158. Nagasawa M, Schmidlin H, Hazekamp MG, Schotte R, Blom B. Development of human plasmacytoid dendritic cells depends on the combined action of the basic helix-loop-helix factor E2-2 and the Ets factor Spi-B. *Eur J Immunol*. 2008;38(9):2389-2400.
159. Grouard G, Rissoan MC, Filgueira L, Durand I, Banchereau J, Liu YJ. The enigmatic plasmacytoid T cells develop into dendritic cells with interleukin (IL)-3 and CD40-ligand. *Journal of Experimental Medicine*. 1997;185(6):1101-1111.
160. Banchereau J, Briere F, Caux C, et al. Immunobiology of dendritic cells. *Annual Review of Immunology*. 2000;18:767-+.
161. Gilliet M, Cao W, Liu YJ. Plasmacytoid dendritic cells: sensing nucleic acids in viral infection and autoimmune diseases. *Nature Reviews Immunology*. 2008;8(8):594-606.
162. Guery L, Hugues S. Tolerogenic and activatory plasmacytoid dendritic cells in autoimmunity. *Front Immunol*. 2013;4:59.
163. Di Pucchio T, Chatterjee B, Smed-Sorensen A, et al. Direct proteasome-independent cross-presentation of viral antigen by plasmacytoid dendritic cells on major histocompatibility complex class I. *Nat Immunol*. 2008;9(5):551-557.
164. Janeway CA, Medzhitov R. Innate immune recognition. *Annual Review of Immunology*. 2002;20:197-216.
165. O'Neill LA, Golenbock D, Bowie AG. The history of Toll-like receptors - redefining innate immunity. *Nat Rev Immunol*. 2013;13(6):453-460.
166. Barton GM, Kagan JC, Medzhitov R. Intracellular localization of Toll-like receptor 9 prevents recognition of self DNA but facilitates access to viral DNA. *Nature Immunology*. 2006;7(1):49-56.

167. Uematsu S, Akira S. Toll-like receptors and Type I interferons. *J Biol Chem*. 2007;282(21):15319-15323.
168. Uematsu S, Akira S. Toll-like receptors and innate immunity. *Journal of Molecular Medicine-Jmm*. 2006;84(9):712-725.
169. Kim YM, Brinkmann MM, Paquet ME, Ploegh HL. UNC93B1 delivers nucleotide-sensing toll-like receptors to endolysosomes. *Nature*. 2008;452(7184):234-U280.
170. Latz E, Schoenemeyer A, Visintin A, et al. TLR9 signals after translocating from the ER to CpG DNA in the lysosome. *Nature Immunology*. 2004;5(2):190-198.
171. Ewald SE, Lee BL, Lau L, et al. The ectodomain of Toll-like receptor 9 is cleaved to generate a functional receptor. *Nature*. 2008;456(7222):658-U688.
172. Haas T, Metzger J, Schmitz F, et al. The DNA sugar backbone 2' deoxyribose determines toll-like receptor 9 activation. *Immunity*. 2008;28(3):315-323.
173. Dai J, Megjugorac NJ, Amrute SB, Fitzgerald-Bocarsly P. Regulation of IFN regulatory factor-7 and IFN-alpha production by enveloped virus and lipopolysaccharide in human plasmacytoid dendritic cells. *J Immunol*. 2004;173(3):1535-1548.
174. Ciancanelli MJ, Huang SX, Luthra P, et al. Infectious disease. Life-threatening influenza and impaired interferon amplification in human IRF7 deficiency. *Science*. 2015;348(6233):448-453.
175. Davidson S, Crotta S, McCabe TM, Wack A. Pathogenic potential of interferon alphabeta in acute influenza infection. *Nat Commun*. 2014;5:3864.
176. Martin-Gayo E, Sierra-Filardi E, Corbi AL, Toribio ML. Plasmacytoid dendritic cells resident in human thymus drive natural Treg cell development. *Blood*. 2010;115(26):5366-5375.
177. Hanabuchi S, Ito T, Park WR, et al. Thymic stromal lymphopoietin-activated plasmacytoid dendritic cells induce the generation of FOXP3+ regulatory T cells in human thymus. *J Immunol*. 2010;184(6):2999-3007.
178. Hadeiba H, Lahl K, Edalati A, et al. Plasmacytoid dendritic cells transport peripheral antigens to the thymus to promote central tolerance. *Immunity*. 2012;36(3):438-450.
179. Ochando JC, Homma C, Yang Y, et al. Alloantigen-presenting plasmacytoid dendritic cells mediate tolerance to vascularized grafts. *Nature Immunology*. 2006;7(6):652-662.
180. de Heer HJ, Hammad H, Soullie T, et al. Essential role of lung plasmacytoid dendritic cells in preventing asthmatic reactions to harmless inhaled antigen. *Journal of Experimental Medicine*. 2004;200(1):89-98.
181. Chen W, Liang XQ, Peterson AJ, Munn DH, Blazar BR. The indoleamine 2,3-dioxygenase pathway is essential for human plasmacytoid dendritic cell-induced adaptive T regulatory cell generation. *Journal of Immunology*. 2008;181(8):5396-5404.
182. Munn DH, Sharma MD, Hou D, et al. Expression of indoleamine 2,3-dioxygenase by plasmacytoid dendritic cells in tumor-draining lymph nodes. *J Clin Invest*. 2004;114(2):280-290.
183. Sharma MD, Baban B, Chandler P, et al. Plasmacytoid dendritic cells from mouse tumor-draining lymph nodes directly activate mature Tregs via indoleamine 2,3-dioxygenase. *Journal of Clinical Investigation*. 2007;117(9):2570-2582.

184. Swiecki M, Colonna M. Unraveling the functions of plasmacytoid dendritic cells during viral infections, autoimmunity, and tolerance. *Immunological Reviews*. 2010;234:142-162.
185. Ito T, Yang M, Wang YH, et al. Plasmacytoid dendritic cells prime IL-10-producing T regulatory cells by inducible costimulator ligand. *J Exp Med*. 2007;204(1):105-115.
186. Jongbloed SL, Benson RA, Nickdel MB, Garside P, McInnes LB, Brewer JM. Plasmacytoid Dendritic Cells Regulate Breach of Self-Tolerance in Autoimmune Arthritis. *Journal of Immunology*. 2009;182(2):963-968.
187. Kavousanaki M, Makrigiannakis A, Boumpas D, Verginis P. Novel Role of Plasmacytoid Dendritic Cells in Humans Induction of Interleukin-10-Producing Treg Cells by Plasmacytoid Dendritic Cells in Patients With Rheumatoid Arthritis Responding to Therapy. *Arthritis and Rheumatism*. 2010;62(1):53-63.
188. Bonnefoy F, Perruche S, Couturier M, et al. Plasmacytoid dendritic cells play a major role in apoptotic leukocyte-induced immune modulation. *J Immunol*. 2011;186(10):5696-5705.
189. Moseman EA, Liang XQ, Dawson AJ, et al. Human plasmacytoid dendritic cells activated by CpG oligodeoxynucleotides induce the generation of CD4(+)CD25(+) regulatory T cells. *Journal of Immunology*. 2004;173(7):4433-4442.
190. Wingender G, Garbi N, Schumak B, et al. Systemic application of CpG-rich DNA suppresses adaptive T cell immunity via induction of IDO. *European Journal of Immunology*. 2006;36(1):12-20.
191. Christensen SR, Shupe J, Nickerson K, Kashgarian M, Flavell RA, Shlomchik MJ. Toll-like receptor 7 and TLR9 dictate autoantibody specificity and have opposing inflammatory and regulatory roles in a murine model of lupus. *Immunity*. 2006;25(3):417-428.
192. Nickerson KM, Christensen SR, Shupe J, et al. TLR9 Regulates TLR7-and MyD88-Dependent Autoantibody Production and Disease in a Murine Model of Lupus. *Journal of Immunology*. 2010;184(4):1840-1848.
193. Nickerson KM, Cullen JL, Kashgarian M, Shlomchik MJ. Exacerbated Autoimmunity in the Absence of TLR9 in MRL.Fas(lpr) Mice Depends on Ifnar1. *Journal of Immunology*. 2013;190(8):3889-3894.
194. Izui S, Iwamoto M, Fossati L, Merino R, Takahashi S, Ibnouzekri N. THE YAA GENE MODEL OF SYSTEMIC LUPUS-ERYTHEMATOSUS. *Immunological Reviews*. 1995;144:137-156.
195. Pisitkun P, Deane JA, Difilippantonio MJ, Tarasenko T, Satterthwaite AB, Bolland S. Autoreactive B cell responses to RNA-related antigens due to TLR7 gene duplication. *Science*. 2006;312(5780):1669-1672.
196. Shen N, Fu Q, Deng Y, et al. Sex-specific association of X-linked Toll-like receptor 7 (TLR7) with male systemic lupus erythematosus. *Proc Natl Acad Sci U S A*. 2010;107(36):15838-15843.
197. Ewald SE, Engel A, Lee J, Wang M, Bogyo M, Barton GM. Nucleic acid recognition by Toll-like receptors is coupled to stepwise processing by cathepsins and asparagine endopeptidase. *J Exp Med*. 2011;208(4):643-651.
198. Kumagai Y, Kumar H, Koyama S, Kawai T, Takeuchi O, Akira S. Cutting Edge: TLR-Dependent viral recognition along with type I IFN positive feedback

signaling masks the requirement of viral replication for IFN-{alpha} production in plasmacytoid dendritic cells. *J Immunol*. 2009;182(7):3960-3964.
199. Takahashi K, Asabe S, Wieland S, et al. Plasmacytoid dendritic cells sense hepatitis C virus-infected cells, produce interferon, and inhibit infection. *Proceedings of the National Academy of Sciences of the United States of America*. 2010;107(16):7431-7436.
200. Dreux M, Garaigorta U, Boyd B, et al. Short-range exosomal transfer of viral RNA from infected cells to plasmacytoid dendritic cells triggers innate immunity. *Cell Host Microbe*. 2012;12(4):558-570.
201. Feng Z, Li Y, McKnight KL, et al. Human pDCs preferentially sense enveloped hepatitis A virions. *J Clin Invest*. 2015;125(1):169-176.
202. Hoeffel G, Ripoche AC, Matheoud D, et al. Antigen crosspresentation by human plasmacytoid dendritic cells. *Immunity*. 2007;27(3):481-492.
203. Chappell CP, Giltiay NV, Draves KE, et al. Targeting antigens through blood dendritic cell antigen 2 on plasmacytoid dendritic cells promotes immunologic tolerance. *J Immunol*. 2014;192(12):5789-5801.
204. Loschko J, Heink S, Hackl D, et al. Antigen targeting to plasmacytoid dendritic cells via Siglec-H inhibits Th cell-dependent autoimmunity. *J Immunol*. 2011;187(12):6346-6356.
205. Cao W, Rosen DB, Ito T, et al. Plasmacytoid dendritic cell-specific receptor ILT7-Fc epsilonRI gamma inhibits Toll-like receptor-induced interferon production. *J Exp Med*. 2006;203(6):1399-1405.
206. Popovic PJ, DeMarco R, Lotze MT, et al. High mobility group B1 protein suppresses the human plasmacytoid dendritic cell response to TLR9 agonists. *Journal of Immunology*. 2006;177(12):8701-8707.
207. Sims GP, Rowe DC, Rietdijk ST, Herbst R, Coyle AJ. HMGB1 and RAGE in inflammation and cancer. *Annu Rev Immunol*. 2010;28:367-388.
208. Ma W, Rai V, Hudson BI, Song F, Schmidt AM, Barile GR. RAGE binds C1q and enhances C1q-mediated phagocytosis. *Cell Immunol*. 2012;274(1-2):72-82.
209. He M, Kubo H, Morimoto K, et al. Receptor for advanced glycation end products binds to phosphatidylserine and assists in the clearance of apoptotic cells. *EMBO Rep*. 2011;12(4):358-364.
210. Tian J, Avalos AM, Mao SY, et al. Toll-like receptor 9-dependent activation by DNA-containing immune complexes is mediated by HMGB1 and RAGE. *Nature Immunology*. 2007;8(5):487-496.
211. Bastos-Amador P, Perez-Cabezas B, Izquierdo-Useros N, et al. Capture of cell-derived microvesicles (exosomes and apoptotic bodies) by human plasmacytoid dendritic cells. *Journal of Leukocyte Biology*. 2012;91(5):751-758.
212. Xiao S, Zhu B, Jin H, et al. Tim-1 stimulation of dendritic cells regulates the balance between effector and regulatory T cells. *Eur J Immunol*. 2011;41(6):1539-1549.
213. Feng Y, He D, Yao Z, Klionsky DJ. The machinery of macroautophagy. *Cell Res*. 2014;24(1):24-41.
214. Li WW, Li J, Bao JK. Microautophagy: lesser-known self-eating. *Cell Mol Life Sci*. 2012;69(7):1125-1136.
215. Cuervo AM, Wong E. Chaperone-mediated autophagy: roles in disease and aging. *Cell Res*. 2014;24(1):92-104.

216. Nazio F, Strappazzon F, Antonioli M, et al. mTOR inhibits autophagy by controlling ULK1 ubiquitylation, self-association and function through AMBRA1 and TRAF6. *Nat Cell Biol*. 2013;15(4):406-416.
217. Kroemer G, Marino G, Levine B. Autophagy and the integrated stress response. *Mol Cell*. 2010;40(2):280-293.
218. Russell RC, Tian Y, Yuan H, et al. ULK1 induces autophagy by phosphorylating Beclin-1 and activating VPS34 lipid kinase. *Nat Cell Biol*. 2013;15(7):741-750.
219. Hayashi-Nishino M, Fujita N, Noda T, Yamaguchi A, Yoshimori T, Yamamoto A. A subdomain of the endoplasmic reticulum forms a cradle for autophagosome formation. *Nat Cell Biol*. 2009;11(12):1433-1437.
220. Yla-Anttila P, Vihinen H, Jokitalo E, Eskelinen EL. 3D tomography reveals connections between the phagophore and endoplasmic reticulum. *Autophagy*. 2009;5(8):1180-1185.
221. Ravikumar B, Moreau K, Jahreiss L, Puri C, Rubinsztein DC. Plasma membrane contributes to the formation of pre-autophagosomal structures. *Nat Cell Biol*. 2010;12(8):747-757.
222. Hailey DW, Rambold AS, Satpute-Krishnan P, et al. Mitochondria supply membranes for autophagosome biogenesis during starvation. *Cell*. 2010;141(4):656-667.
223. Hanada T, Noda NN, Satomi Y, et al. The Atg12-Atg5 conjugate has a novel E3-like activity for protein lipidation in autophagy. *Journal of Biological Chemistry*. 2007;282(52):37298-37302.
224. McEwan DG, Popovic D, Gubas A, et al. PLEKHM1 regulates autophagosome-lysosome fusion through HOPS complex and LC3/GABARAP proteins. *Mol Cell*. 2015;57(1):39-54.
225. Itakura E, Kishi-Itakura C, Mizushima N. The hairpin-type tail-anchored SNARE syntaxin 17 targets to autophagosomes for fusion with endosomes/lysosomes. *Cell*. 2012;151(6):1256-1269.
226. Jiang P, Nishimura T, Sakamaki Y, et al. The HOPS complex mediates autophagosome-lysosome fusion through interaction with syntaxin 17. *Mol Biol Cell*. 2014;25(8):1327-1337.
227. Weissmann G. LYSOSOMES AUTOIMMUNE PHENOMENA + DISEASES OF CONNECTIVE TISSUE. *Lancet*. 1964;2(737):1373-&.
228. Gros F, Arnold J, Page N, et al. Macroautophagy is deregulated in murine and human lupus T lymphocytes. *Autophagy*. 2012;8(7):1113-1123.
229. Clarke AJ, Ellinghaus U, Cortini A, et al. Autophagy is activated in systemic lupus erythematosus and required for plasmablast development. *Annals of the Rheumatic Diseases*. 2015;74(5):912-920.
230. Alessandri C, Barbati C, Vacirca D, et al. T lymphocytes from patients with systemic lupus erythematosus are resistant to induction of autophagy. *Faseb Journal*. 2012;26(11):4722-4732.
231. Gateva V, Sandling JK, Hom G, et al. A large-scale replication study identifies TNIP1, PRDM1, JAZF1, UHRF1BP1 and IL10 as risk loci for systemic lupus erythematosus. *Nature Genetics*. 2009;41(11):1228-U1293.
232. Zhou XJ, Lu XL, Lv JC, et al. Genetic association of PRDM1-ATG5 intergenic region and autophagy with systemic lupus erythematosus in a Chinese population. *Annals of the Rheumatic Diseases*. 2011;70(7):1330-1337.

233. Yang W, Tang H, Zhang Y, et al. Meta-analysis Followed by Replication Identifies Loci in or near CDKN1B, TET3, CD80, DRAM1, and ARID5B as Associated with Systemic Lupus Erythematosus in Asians. *American Journal of Human Genetics*. 2013;92(1):41-51.
234. Crighton D, Wilkinson S, O'Prey J, et al. DRAM, a p53-induced modulator of autophagy, is critical for apoptosis. *Cell*. 2006;126(1):121-134.
235. Debnath J, Mills KR, Collins NL, Reginato MJ, Muthuswamy SK, Brugge JS. The role of apoptosis in creating and maintaining luminal space with normal and oncogene-expressing mammary acini. *Cell*. 2002;111(1):29-40.
236. Leist M, Jaattela M. Four deaths and a funeral: From caspases to alternative mechanisms. *Nature Reviews Molecular Cell Biology*. 2001;2(8):589-598.
237. Marino G, Niso-Santano M, Baehrecke EH, Kroemer G. Self-consumption: the interplay of autophagy and apoptosis. *Nature Reviews Molecular Cell Biology*. 2014;15(2):81-94.
238. Pattingre S, Tassa A, Qu XP, et al. Bcl-2 antiapoptotic proteins inhibit Beclin 1-dependent autophagy. *Cell*. 2005;122(6):927-939.
239. Rubinstein AD, Eisenstein M, Ber Y, Bialik S, Kimchi A. The Autophagy Protein Atg12 Associates with Antiapoptotic Bcl-2 Family Members to Promote Mitochondrial Apoptosis. *Molecular Cell*. 2011;44(5):698-709.
240. Oral O, Oz-Arslan D, Itah Z, et al. Cleavage of Atg3 protein by caspase-8 regulates autophagy during receptor-activated cell death. *Apoptosis*. 2012;17(8):810-820.
241. Norman JM, Cohen GM, Bampton ETW. The in vitro cleavage of the hAtg proteins by cell death proteases. *Autophagy*. 2010;6(8):1042-1056.
242. Wirawan E, Vande Walle L, Kersse K, et al. Caspase-mediated cleavage of Beclin-1 inactivates Beclin-1-induced autophagy and enhances apoptosis by promoting the release of proapoptotic factors from mitochondria. *Cell Death & Disease*. 2010;1.
243. Yousefi S, Perozzo R, Schmid I, et al. Calpain-mediated cleavage of Atg5 switches autophagy to apoptosis. *Nature Cell Biology*. 2006;8(10):1124-U1146.
244. Laussmann MA, Passante E, Duessmann H, et al. Proteasome inhibition can induce an autophagy-dependent apical activation of caspase-8. *Cell Death and Differentiation*. 2011;18(10):1584-1597.
245. Young MM, Takahashi Y, Khan O, et al. Autophagosomal Membrane Serves as Platform for Intracellular Death-inducing Signaling Complex (iDISC)-mediated Caspase-8 Activation and Apoptosis. *Journal of Biological Chemistry*. 2012;287(15):12455-12468.
246. Qu X, Zou Z, Sun Q, et al. Autophagy gene-dependent clearance of apoptotic cells during embryonic development. *Cell*. 2007;128(5):931-946.
247. Martinez J, Almendinger J, Oberst A, et al. Microtubule-associated protein 1 light chain 3 alpha (LC3)-associated phagocytosis is required for the efficient clearance of dead cells. *Proceedings of the National Academy of Sciences of the United States of America*. 2011;108(42):17396-17401.
248. Huang S, Jia K, Wang Y, Zhou Z, Levine B. Autophagy genes function in apoptotic cell corpse clearance during C. elegans embryonic development. *Autophagy*. 2013;9(2):138-149.

249. Li W, Zou W, Yang Y, et al. Autophagy genes function sequentially to promote apoptotic cell corpse degradation in the engulfing cell. *Journal of Cell Biology*. 2012;197(1):27-35.
250. Martinez J, Malireddi RKS, Lu Q, et al. Molecular characterization of LC3-associated phagocytosis reveals distinct roles for Rubicon, NOX2 and autophagy proteins. *Nature Cell Biology*. 2015;17(7):893-906.
251. Sanjuan MA, Dillon CP, Tait SW, et al. Toll-like receptor signalling in macrophages links the autophagy pathway to phagocytosis. *Nature*. 2007;450(7173):1253-1257.
252. Levine B, Mizushima N, Virgin HW. Autophagy in immunity and inflammation. *Nature*. 2011;469(7330):323-335.
253. Lee HK, Lund JM, Ramanathan B, Mizushima N, Iwasaki A. Autophagy-dependent viral recognition by plasmacytoid dendritic cells. *Science*. 2007;315(5817):1398-1401.
254. Henault J, Martinez J, Riggs JM, et al. Noncanonical Autophagy Is Required for Type I Interferon Secretion in Response to DNA-Immune Complexes. *Immunity*. 2012;37(6):986-997.
255. Chaturvedi A, Dorward D, Pierce SK. The B cell receptor governs the subcellular location of Toll-like receptor 9 leading to hyperresponses to DNA-containing antigens. *Immunity*. 2008;28(6):799-809.
256. Deretic V, Kimura T, Timmins G, Moseley P, Chauhan S, Mandell M. Immunologic manifestations of autophagy. *J Clin Invest*. 2015;125(1):75-84.
257. van der Burgh R, Nijhuis L, Pervolaraki K, et al. Defects in mitochondrial clearance predispose human monocytes to interleukin-1beta hypersecretion. *J Biol Chem*. 2014;289(8):5000-5012.
258. Shi CS, Shenderov K, Huang NN, et al. Activation of autophagy by inflammatory signals limits IL-1beta production by targeting ubiquitinated inflammasomes for destruction. *Nat Immunol*. 2012;13(3):255-263.
259. Remijsen Q, Vanden Berghe T, Wirawan E, et al. Neutrophil extracellular trap cell death requires both autophagy and superoxide generation. *Cell Res*. 2011;21(2):290-304.
260. Romao S, Gasser N, Becker AC, et al. Autophagy proteins stabilize pathogen-containing phagosomes for prolonged MHC II antigen processing. *J Cell Biol*. 2013;203(5):757-766.
261. Cooney R, Baker J, Brain O, et al. NOD2 stimulation induces autophagy in dendritic cells influencing bacterial handling and antigen presentation. *Nat Med*. 2010;16(1):90-97.
262. Nedjic J, Aichinger M, Emmerich J, Mizushima N, Klein L. Autophagy in thymic epithelium shapes the T-cell repertoire and is essential for tolerance. *Nature*. 2008;455(7211):396-400.
263. Pengo N, Scolari M, Oliva L, et al. Plasma cells require autophagy for sustainable immunoglobulin production. *Nat Immunol*. 2013;14(3):298-305.
264. Frenz T, Graalmann L, Detje CN, et al. Independent of Plasmacytoid Dendritic Cell (pDC) infection, pDC Triggered by Virus-Infected Cells Mount Enhanced Type I IFN Responses of Different Composition as Opposed to pDC Stimulated with Free Virus. *Journal of Immunology*. 2014;193(5):2496-2503.
265. Rosen A, Casciola-Rosen L, Ahearn J. Novel packages of viral and self-antigens are generated during apoptosis. *J Exp Med*. 1995;181(4):1557-1561.

266. Honda K, Ohba Y, Yanai H, et al. Spatiotemporal regulation of MyD88-IRF-7 signalling for robust type-I interferon induction. *Nature*. 2005;434(7036):1035-1040.
267. Guiducci C, Ott G, Chan JH, et al. Properties regulating the nature of the plasmacytoid dendritic cell response to Toll-like receptor 9 activation. *Journal of Experimental Medicine*. 2006;203(8):1999-2008.
268. Blasius AL, Beutler B. Intracellular toll-like receptors. *Immunity*. 2010;32(3):305-315.
269. Kawai T, Akira S. Toll-like receptors and their crosstalk with other innate receptors in infection and immunity. *Immunity*. 2011;34(5):637-650.
270. Colonna M, Trinchieri G, Liu YJ. Plasmacytoid dendritic cells in immunity. *Nat Immunol*. 2004;5(12):1219-1226.
271. Sozzani S, Vermi W, Del Prete A, Facchetti F. Trafficking properties of plasmacytoid dendritic cells in health and disease. *Trends Immunol*. 2010;31(7):270-277.
272. Lovgren T, Eloranta ML, Bave U, Alm GV, Ronnblom L. Induction of interferon-a production in plasmacytoid dendritic cells by immune complexes containing nucleic acid released by necrotic or late anoptotic cells and lupus IgG. *Arthritis and Rheumatism*. 2004;50(6):1861-1872.
273. Lande R, Ganguly D, Facchinetti V, et al. Neutrophils Activate Plasmacytoid Dendritic Cells by Releasing Self-DNA-Peptide Complexes in Systemic Lupus Erythematosus. *Science Translational Medicine*. 2011;3(73).
274. Ohlsson M, Jonsson R, Brokstad KA. Subcellular redistribution and surface exposure of the Ro52, Ro60 and La48 autoantigens during apoptosis in human ductal epithelial cells: A possible mechanism in the pathogenesis of Sjogren's syndrome. *Scandinavian Journal of Immunology*. 2002;56(5):456-469.
275. Lui G, Manches O, Angel J, Molens JP, Chaperot L, Plumas J. Plasmacytoid dendritic cells capture and cross-present viral antigens from influenza-virus exposed cells. *PLoS One*. 2009;4(9):e7111.
276. Hoeffel G, Ripoche AC, Matheoud D, et al. Antigen crosspresentation by human plasmacytoid dendritic cells. *Immunity*. 2007;27(3):481-492.
277. Chen M, Huang L, Shabier Z, Wang J. Regulation of the lifespan in dendritic cell subsets. *Molecular Immunology*. 2007;44(10):2558-2565.
278. Asselin-Paturel C, Boonstra A, Dalod M, et al. Mouse type IIFN-producing cells are immature APCs with plasmacytoid morphology. *Nature Immunology*. 2001;2(12):1144-1150.
279. Boonstra A, Rajsbaum R, Holman M, et al. Macrophages and myeloid dendritic cells, but not plasmacytoid dendritic cells, produce IL-10 in response to MyD88- and TRIF-dependent TLR signals, and TLR-independent signals. *Journal of Immunology*. 2006;177(11):7551-7558.
280. Lamb RA, Zebedee SL, Richardson CD. INFLUENZA VIRUS-M2 PROTEIN IS AN INTEGRAL MEMBRANE-PROTEIN EXPRESSED ON THE INFECTED-CELL SURFACE. *Cell*. 1985;40(3):627-633.
281. Wu X, Peng SL. Toll-like receptor 9 signaling protects against murine lupus. *Arthritis Rheum*. 2006;54(1):336-342.
282. Christensen SR, Kashgarian M, Alexopoulou L, Flavell RA, Akira S, Shlomchik MJ. Toll-like receptor 9 controls anti-DNA autoantibody production in murine lupus. *J Exp Med*. 2005;202(2):321-331.

283. Christensen SR, Shlomchik MJ. Regulation of lupus-related autoantibody production and clinical disease by Toll-like receptors. *Semin Immunol*. 2007;19(1):11-23.
284. Stott K, Tang GSF, Lee KB, Thomas JO. Structure of a complex of tandem HMG boxes and DNA. *Journal of Molecular Biology*. 2006;360(1):90-104.
285. Rovere-Querini P, Capobianco A, Scaffidi P, et al. HMGB1 is an endogenous immune adjuvant released by necrotic cells. *Embo Reports*. 2004;5(8):825-830.
286. Bell CW, Jiang WW, Reich CF, Pisetsky DS. The extracellular release of HMGB1 during apoptotic cell death. *American Journal of Physiology-Cell Physiology*. 2006;291(6):C1318-C1325.
287. Yamada Y, Fujii T, Ishijima R, et al. The release of high mobility group box 1 in apoptosis is triggered by nucleosomal DNA fragmentation. *Archives of Biochemistry and Biophysics*. 2011;506(2):188-193.
288. Schiller M, Heyder P, Ziegler S, et al. During apoptosis HMGB1 is translocated into apoptotic cell-derived membraneous vesicles. *Autoimmunity*. 2013;46(5):342-346.
289. Korb LC, Ahearn JM. C1q binds directly and specifically to surface blobs of apoptotic human keratinocytes - Complement deficiency and systemic tapes erythematosus revisited. *Journal of Immunology*. 1997;158(10):4525-4528.
290. Lood C, Gullstrand B, Truedsson L, et al. C1q Inhibits Immune Complex-Induced Interferon-alpha Production in Plasmacytoid Dendritic Cells A Novel Link Between C1q Deficiency and Systemic Lupus Erythematosus Pathogenesis. *Arthritis and Rheumatism*. 2009;60(10):3081-3090.
291. Santer DM, Hall BE, George TC, et al. C1q Deficiency Leads to the Defective Suppression of IFN-alpha in Response to Nucleoprotein Containing Immune Complexes. *Journal of Immunology*. 2010;185(8):4738-4749.
292. Son M, Santiago-Schwarz F, Al-Abed Y, Diamond B. C1q limits dendritic cell differentiation and activation by engaging LAIR-1. *Proceedings of the National Academy of Sciences of the United States of America*. 2012;109(46):E3160-E3167.
293. Triantafyllopoulou A, Moutsopoulos H. Persistent viral infection in primary Sjogren's syndrome: review and perspectives. *Clin Rev Allergy Immunol*. 2007;32(3):210-214.
294. Boettler T, von Herrath M. Protection against or triggering of Type 1 diabetes? Different roles for viral infections. *Expert Rev Clin Immunol*. 2011;7(1):45-53.
295. Yu XL, Cheng YM, Shi BS, et al. Measles Virus Infection in Adults Induces Production of IL-10 and Is Associated with Increased CD4(+)CD25(+) Regulatory T Cells. *Journal of Immunology*. 2008;181(10):7356-7366.
296. Brockman MA, Kwon DS, Tighe DP, et al. IL-10 is up-regulated in multiple cell types during viremic HIV infection and reversibly inhibits virus-specific T cells. *Blood*. 2009;114(2):346-356.
297. Grouard G, Rissoan MC, Filgueira L, Durand I, Banchereau J, Liu YJ. The enigmatic plasmacytoid T cells develop into dendritic cells with interleukin (IL)-3 and CD40-ligand. *J Exp Med*. 1997;185(6):1101-1111.
298. Kazama H, Ricci J-E, Herndon JM, Hoppe G, Green DR, Ferguson TA. Induction of immunological tolerance by apoptotic cells requires caspase-dependent oxidation of high-mobility group box-1 protein. *Immunity*. 2008;29(1):21-32.

299. Ma WC, Rai V, Hudson BI, Song F, Schmidt AM, Barile GR. RAGE binds C1q and enhances C1q-mediated phagocytosis. *Cellular Immunology*. 2012;274(1-2):72-82.
300. He M, Kubo H, Morimoto K, et al. Receptor for advanced glycation end products binds to phosphatidylserine and assists in the clearance of apoptotic cells. *Embo Reports*. 2011;12(4):358-364.
301. Iparraguirre A, Tobias JW, Hensley SE, et al. Two distinct activation states of plasmacytoid dendritic cells induced by influenza virus and CpG 1826 oligonucleotide. *Journal of Leukocyte Biology*. 2008;83(3):610-620.
302. Klaschik S, Tross D, Shirota H, Klinman DM. Short- and long-term changes in gene expression mediated by the activation of TLR9. *Molecular Immunology*. 2010;47(6):1317-1324.
303. Paludan SR, Bowie AG. Immune Sensing of DNA. *Immunity*. 2013;38(5):870-880.
304. Kim T, Pazhoor S, Bao M, et al. Aspartate-glutamate-alanine-histidine box motif (DEAH)/RNA helicase A helicases sense microbial DNA in human plasmacytoid dendritic cells. *Proceedings of the National Academy of Sciences of the United States of America*. 2010;107(34):15181-15186.
305. Tedder TF. B10 Cells: A Functionally Defined Regulatory B Cell Subset. *Journal of Immunology*. 2015;194(4):1395-1401.
306. Pelayo R, Hirose J, Huang JX, et al. Derivation of 2 categories of plasmacytoid dendritic cells in murine bone marrow. *Blood*. 2005;105(11):4407-4415.
307. Bjoerck P, Leong HX, Engleman EG. Plasmacytoid Dendritic Cell Dichotomy: Identification of IFN-alpha Producing Cells as a Phenotypically and Functionally Distinct Subset. *Journal of Immunology*. 2011;186(3):1477-1485.
308. Csomor E, Bajtay Z, Sandor N, et al. Complement protein C1q induces maturation of human dendritic cells. *Mol Immunol*. 2007;44(13):3389-3397.
309. Dhir V, Singh AP, Aggarwal A, Naik S, Misra R. Increased T-lymphocyte apoptosis in lupus correlates with disease activity and may be responsible for reduced T-cell frequency: a cross-sectional and longitudinal study. *Lupus*. 2009;18(9):785-791.
310. Emlen W, Niebur J, Kadera R. ACCELERATED IN-VITRO APOPTOSIS OF LYMPHOCYTES FROM PATIENTS WITH SYSTEMIC LUPUS-ERYTHEMATOSUS. *Journal of Immunology*. 1994;152(7):3685-3692.
311. Bijl M, Horst G, Limburg PC, Kallenberg CG. Fas expression on peripheral blood lymphocytes in systemic lupus erythematosus (SLE): relation to lymphocyte activation and disease activity. *Lupus*. 2001;10(12):866-872.
312. Manea ME, Mueller RB, Dejica D, et al. Increased expression of CD154 and FAS in SLE patients' lymphocytes. *Rheumatol Int*. 2009;30(2):181-185.
313. Xue C, Lan-Lan W, Bei C, Jie C, Wei-Hua F. Abnormal Fas/FasL and caspase-3-mediated apoptotic signaling pathways of T lymphocyte subset in patients with systemic lupus erythematosus. *Cell Immunol*. 2006;239(2):121-128.
314. Lam GK, Petri M. Assessment of systemic lupus erythematosus. *Clin Exp Rheumatol*. 2005;23(5 Suppl 39):S120-132.
315. Jin O, Sun LY, Zhou KX, et al. Lymphocyte apoptosis and macrophage function: correlation with disease activity in systemic lupus erythematosus. *Clinical Rheumatology*. 2005;24(2):107-110.

316. Lande R, Gregorio J, Facchinetti V, et al. Plasmacytoid dendritic cells sense self-DNA coupled with antimicrobial peptide. *Nature*. 2007;449(7162):564-U566.
317. Ganguly D, Chamilos G, Lande R, et al. Self-RNA-antimicrobial peptide complexes activate human dendritic cells through TLR7 and TLR8. *Journal of Experimental Medicine*. 2009;206(9):1983-1994.
318. Barrat FJ, Meeker T, Gregorio J, et al. Nucleic acids of mammalian origin can act as endogenous ligands for Toll-like receptors and may promote systemic lupus erythematosus. *J Exp Med*. 2005;202(8):1131-1139.
319. Krug A, Rothenfusser S, Hornung V, et al. Identification of CpG oligonucleotide sequences with high induction of IFN-alpha/beta in plasmacytoid dendritic cells. *European Journal of Immunology*. 2001;31(7):2154-2163.
320. Hornung V, Rothenfusser S, Britsch S, et al. Quantitative expression of toll-like receptor 1-10 mRNA in cellular subsets of human peripheral blood mononuclear cells and sensitivity to CpG oligodeoxynucleotides. *J Immunol*. 2002;168(9):4531-4537.
321. Eloranta ML, Lovgren T, Finke D, et al. Regulation of the Interferon-alpha Production Induced by RNA-Containing Immune Complexes in Plasmacytoid Dendritic Cells. *Arthritis and Rheumatism*. 2009;60(8):2418-2427.
322. Rönnblom L, Alm GV. Systemic lupus erythematosus and the type I interferon system. *Arthritis Res Ther*. 2003;5(2):68-75.
323. Kuznik A, Bencina M, Svajger U, Jeras M, Rozman B, Jerala R. Mechanism of endosomal TLR inhibition by antimalarial drugs and imidazoquinolines. *J Immunol*. 2011;186(8):4794-4804.
324. Blair PA, Norena LY, Flores-Borja F, et al. CD19(+)CD24(hi)CD38(hi) B Cells Exhibit Regulatory Capacity in Healthy Individuals but Are Functionally Impaired in Systemic Lupus Erythematosus Patients. *Immunity*. 2010;32(1):129-140.
325. Courtney PA, Crockard AD, Williamson K, Irvine AE, Kennedy RJ, Bell AL. Increased apoptotic peripheral blood neutrophils in systemic lupus erythematosus: relations with disease activity, antibodies to double stranded DNA, and neutropenia. *Ann Rheum Dis*. 1999;58(5):309-314.
326. Carli L, Tani C, Vagnani S, Signorini V, Mosca M. Leukopenia, lymphopenia, and neutropenia in systemic lupus erythematosus: Prevalence and clinical impact-A systematic literature review. *Semin Arthritis Rheum*. 2015;45(2):190-194.
327. Scheel-Toellner D, Wang K, Craddock R, et al. Reactive oxygen species limit neutrophil life span by activating death receptor signaling. *Blood*. 2004;104(8):2557-2564.
328. Dorward DA, Lucas CD, Alessandri AL, et al. Technical advance: autofluorescence-based sorting: rapid and nonperturbing isolation of ultrapure neutrophils to determine cytokine production. *J Leukoc Biol*. 2013;94(1):193-202.
329. Lakhani SA, Masud A, Kuida K, et al. Caspases 3 and 7: key mediators of mitochondrial events of apoptosis. *Science*. 2006;311(5762):847-851.
330. Korytowski W, Basova LV, Pilat A, Kernstock RM, Girotti AW. Permeabilization of the mitochondrial outer membrane by Bax/truncated Bid (tBid) proteins as sensitized by cardiolipin hydroperoxide translocation: mechanistic implications for the intrinsic pathway of oxidative apoptosis. *J Biol Chem*. 2011;286(30):26334-26343.

331. Metivier D, Dallaporta B, Zamzami N, et al. Cytofluorometric detection of mitochondrial alterations in early CD95/Fas/APO-1-triggered apoptosis of Jurkat T lymphoma cells. Comparison of seven mitochondrion-specific fluorochromes. *Immunology Letters*. 1998;61(2-3):157-163.
332. Kagan VE, Tyurin VA, Jiang J, et al. Cytochrome c acts as a cardiolipin oxygenase required for release of proapoptotic factors. *Nat Chem Biol*. 2005;1(4):223-232.
333. Schiller M, Parcina M, Heyder P, et al. Induction of Type I IFN Is a Physiological Immune Reaction to Apoptotic Cell-Derived Membrane Microparticles. *The Journal of Immunology*. 2012;189(4):1747-1756.
334. Poth JM, Coch C, Busch N, et al. Monocyte-Mediated Inhibition of TLR9-Dependent IFN-alpha Induction in Plasmacytoid Dendritic Cells Questions Bacterial DNA as the Active Ingredient of Bacterial Lysates. *Journal of Immunology*. 2010;185(12):7367-7373.
335. Migita K, Miyashita T, Maeda Y, et al. Reduced blood BDCA-2+ (lymphoid) and CD11c+ (myeloid) dendritic cells in systemic lupus erythematosus. *Clin Exp Immunol*. 2005;142(1):84-91.
336. Blomberg S, Eloranta ML, Magnusson M, Alm GV, Ronnblom L. Expression of the markers BDCA-2 and BDCA-4 and production of interferon-alpha by plasmacytoid dendritic cells in systemic lupus erythematosus. *Arthritis Rheum*. 2003;48(9):2524-2532.
337. Wu P, Wu J, Liu S, et al. TLR9/TLR7-triggered downregulation of BDCA2 expression on human plasmacytoid dendritic cells from healthy individuals and lupus patients. *Clin Immunol*. 2008;129(1):40-48.
338. Jin O, Kavikondala S, Sun L, et al. Systemic lupus erythematosus patients have increased number of circulating plasmacytoid dendritic cells, but decreased myeloid dendritic cells with deficient CD83 expression. *Lupus*. 2008;17(7):654-662.
339. Meller S, Winterberg F, Gilliet M, et al. Ultraviolet radiation-induced injury, chemokines, and leukocyte recruitment: An amplification cycle triggering cutaneous lupus erythematosus. *Arthritis Rheum*. 2005;52(5):1504-1516.
340. Pau E, Cheung YH, Loh C, Lajoie G, Wither JE. TLR tolerance reduces IFN-alpha production despite plasmacytoid dendritic cell expansion and anti-nuclear antibodies in NZB bicongenic mice. *PLoS One*. 2012;7(5):e36761.
341. Ding C, Cai Y, Marroquin J, Ildstad ST, Yan J. Plasmacytoid Dendritic Cells Regulate Autoreactive B Cell Activation via Soluble Factors and in a Cell-to-Cell Contact Manner. *Journal of Immunology*. 2009;183(11):7140-7149.
342. Sigurdsson S, Goring HH, Kristjansdottir G, et al. Comprehensive evaluation of the genetic variants of interferon regulatory factor 5 (IRF5) reveals a novel 5 bp length polymorphism as strong risk factor for systemic lupus erythematosus. *Hum Mol Genet*. 2008;17(6):872-881.
343. Berggren O, Alexsson A, Morris DL, et al. IFN-alpha production by plasmacytoid dendritic cell associations with polymorphisms in gene loci related to autoimmune and inflammatory diseases. *Hum Mol Genet*. 2015;24(12):3571-3581.
344. Niewold TB, Kelly JA, Flesch MH, Espinoza LR, Harley JB, Crow MK. Association of the IRF5 risk haplotype with high serum interferon-alpha activity in systemic lupus erythematosus patients. *Arthritis Rheum*. 2008;58(8):2481-2487.

345. Rowland SL, Riggs JM, Gilfillan S, et al. Early, transient depletion of plasmacytoid dendritic cells ameliorates autoimmunity in a lupus model. *J Exp Med*. 2014;211(10):1977-1991.
346. Lindau D, Mussard J, Rabsteyn A, et al. TLR9 independent interferon alpha production by neutrophils on NETosis in response to circulating chromatin, a key lupus autoantigen. *Ann Rheum Dis*. 2014;73(12):2199-2207.
347. Palanichamy A, Bauer JW, Yalavarthi S, et al. Neutrophil-mediated IFN activation in the bone marrow alters B cell development in human and murine systemic lupus erythematosus. *J Immunol*. 2014;192(3):906-918.
348. Zykova SN, Seredkina N, Benjaminsen J, Rekvig OP. Reduced fragmentation of apoptotic chromatin is associated with nephritis in lupus-prone (NZB x NZW)F-1 mice. *Arthritis and Rheumatism*. 2008;58(3):813-825.
349. Jog NR, Frisoni L, Shi Q, et al. Caspase-activated DNase is required for maintenance of tolerance to lupus nuclear autoantigens. *Arthritis Rheum*. 2012;64(4):1247-1256.
350. Gergely P, Grossman C, Niland B, et al. Mitochondrial hyperpolarization and ATP depletion in patients with systemic lupus erythematosus. *Arthritis and Rheumatism*. 2002;46(1):175-190.
351. Leishangthem BD, Sharma A, Bhatnagar A. Role of altered mitochondria functions in the pathogenesis of systemic lupus erythematosus. *Lupus*. 2015.
352. Fan H, Liu F, Dong G, et al. Activation-induced necroptosis contributes to B-cell lymphopenia in active systemic lupus erythematosus. *Cell Death Dis*. 2014;5:e1416.
353. Caza TN, Fernandez DR, Talaber G, et al. HRES-1/Rab4-mediated depletion of Drp1 impairs mitochondrial homeostasis and represents a target for treatment in SLE. *Ann Rheum Dis*. 2014;73(10):1888-1897.
354. Lemasters JJ. Selective mitochondrial autophagy, or mitophagy, as a targeted defense against oxidative stress, mitochondrial dysfunction, and aging. *Rejuvenation Res*. 2005;8(1):3-5.
355. Stephenson LM, Miller BC, Ng A, et al. Identification of Atg5-dependent transcriptional changes and increases in mitochondrial mass in Atg5-deficient T lymphocytes. *Autophagy*. 2009;5(5):625-635.
356. Dalgaard J, Beckstrom KJ, Jahnsen FL, Brinchmann JE. Differential capability for phagocytosis of apoptotic and necrotic leukemia cells by human peripheral blood dendritic cell subsets. *J Leukoc Biol*. 2005;77(5):689-698.
357. Cocca BA, Cline AM, Radic MZ. Blebs and apoptotic bodies are B cell autoantigens. *J Immunol*. 2002;169(1):159-166.
358. Sims GP, Ettinger R, Shirota Y, Yarboro CH, Illei GG, Lipsky PE. Identification and characterization of circulating human transitional B cells. *Blood*. 2005;105(11):4390-4398.
359. Sim JH, Kim HR, Chang SH, Kim IJ, Lipsky PE, Lee J. Autoregulatory function of interleukin-10-producing pre-naive B cells is defective in systemic lupus erythematosus. *Arthritis Res Ther*. 2015;17:190.
360. Salmon JE, Kimberly RP, Gibofsky A, Fotino M. DEFECTIVE MONONUCLEAR PHAGOCYTE FUNCTION IN SYSTEMIC LUPUS-ERYTHEMATOSUS - DISSOCIATION OF FC RECEPTOR-LIGAND BINDING AND INTERNALIZATION. *Journal of Immunology*. 1984;133(5):2525-2531.

361. Walport MJ, Davies KA, Botto M. Clq and systemic lupus erythematosus. *Immunobiology*. 1998;199(2):265-285.
362. Radic M, Marion T, Monestier M. Nucleosomes are exposed at the cell surface in apoptosis. *Journal of Immunology*. 2004;172(11):6692-6700.
363. Casciola-Rosen LA, Anhalt G, Rosen A. Autoantigens targeted in systemic lupus erythematosus are clustered in two populations of surface structures on apoptotic keratinocytes. *J Exp Med*. 1994;179(4):1317-1330.
364. Gray M, Miles K, Salter D, Gray D, Savill J. Apoptotic cells protect mice from autoimmune inflammation by the induction of regulatory B cells. *Proc Natl Acad Sci U S A*. 2007;104(35):14080-14085.
365. Stuart LM, Takahashi K, Shi L, Savill J, Ezekowitz RAB. Mannose-binding lectin-deficient mice display defective apoptotic cell clearance but no autoimmune phenotype. *Journal of Immunology*. 2005;174(6):3220-3226.
366. Colasanti T, Vomero M, Alessandri C, et al. Role of alpha-synuclein in autophagy modulation of primary human T lymphocytes. *Cell Death & Disease*. 2014;5.
367. Maiuri MC, Zalckvar E, Kimchi A, Kroemer G. Self-eating and self-killing: crosstalk between autophagy and apoptosis. *Nature Reviews Molecular Cell Biology*. 2007;8(9):741-752.
368. Mizushima N, Noda T, Yoshimori T, et al. A protein conjugation system essential for autophagy. *Nature*. 1998;395(6700):395-398.
369. Chan LL, Shen D, Wilkinson AR, et al. A novel image-based cytometry method for autophagy detection in living cells. *Autophagy*. 2012;8(9):1371-1382.
370. Mizushima N, Yoshimori T. How to interpret LC3 immunoblotting. *Autophagy*. 2007;3(6):542-545.
371. Duraes C, Machado JC, Portela F, et al. Phenotype-Genotype Profiles in Crohn's Disease Predicted by Genetic Markers in Autophagy-Related Genes (GOIA Study II). *Inflammatory Bowel Diseases*. 2013;19(2):230-239.
372. Bijl M, Reefman E, Horst G, Limburg PC, Kallenberg CGM. Reduced uptake of apoptotic cells by macrophages in systemic lupus erythematosus: correlates with decreased serum levels of complement. *Annals of the Rheumatic Diseases*. 2006;65(1):57-63.
373. Solana R, Pawelec G, Tarazona R. Aging and innate immunity. *Immunity*. 2006;24(5):491-494.
374. Lucas M, Stuart LM, Savill J, Lacy-Hulbert A. Apoptotic cells and innate immune stimuli combine to regulate macrophage cytokine secretion. *Journal of Immunology*. 2003;171(5):2610-2615.
375. Nagata S, Hanayama R, Kawane K. Autoimmunity and the Clearance of Dead Cells. *Cell*. 2010;140(5):619-630.
376. Jansens A, Braakman I. Pulse-chase labeling techniques for the analysis of protein maturation and degradation. *Methods in molecular biology (Clifton, NJ)*. 2003;232:133-145.
377. Geng JF, Klionsky DJ. The Atg8 and Atg12 ubiquitin-like conjugation systems in macroautophagy. *Embo Reports*. 2008;9(9):859-864.
378. Shintani T, Mizushima N, Ogawa Y, Matsuura A, Noda T, Ohsumi Y. Apg10p, a novel protein-conjugating enzyme essential for autophagy in yeast. *Embo Journal*. 1999;18(19):5234-5241.

379. Matsushita M, Suzuki NN, Obara K, Fujioka Y, Ohsumi Y, Inagaki F. Structure of Atg5 center dot Atg16, a complex essential for autophagy. *Journal of Biological Chemistry*. 2007;282(9):6763-6772.
380. Brouckaert G, Kalai M, Krysko DV, et al. Phagocytosis of necrotic cells by macrophages is phosphatidylserine dependent and does not induce inflammatory cytokine production. *Molecular Biology of the Cell*. 2004;15(3):1089-1100.
381. Bottcher A, Gaipl US, Furnrohr BG, et al. Involvement of phosphatidylserine, alpha v beta 3, CD14, CD36, and complement C1q in the phagocytosis of primary necrotic lymphocytes by macrophages. *Arthritis and Rheumatism*. 2006;54(3):927-938.
382. Grau A, Tabib A, Grau I, Reiner I, Mevorach D. Apoptotic Cells Induce NF-kappa B and Inflammasome Negative Signaling. *Plos One*. 2015;10(3).
383. Zhou R, Yazdi AS, Menu P, Tschopp J. A role for mitochondria in NLRP3 inflammasome activation. *Nature*. 2011;469(7329):221-225.
384. Sule S, Rosen A, Petri M, Akhter E, Andrade F. Abnormal Production of Pro- and Anti-Inflammatory Cytokines by Lupus Monocytes in Response to Apoptotic Cells. *Plos One*. 2011;6(3).
385. Majai G, Kiss E, Tarr T, et al. Decreased apopto-phagocytic gene expression in the macrophages of systemic lupus erythematosus patients. *Lupus*. 2014;23(2):133-145.
386. Migita K, Miyashita T, Maeda Y, et al. Toll-like receptor expression in lupus peripheral blood mononuclear cells. *Journal of Rheumatology*. 2007;34(3):493-500.
387. Gregory CD, Devitt A. The macrophage and the apoptotic cell: an innate immune interaction viewed simplistically? *Immunology*. 2004;113(1):1-14.
388. Iwasaki A, Pillai PS. Innate immunity to influenza virus infection. *Nat Rev Immunol*. 2014;14(5):315-328.
389. Liao AP, Salajegheh M, Morehouse C, et al. Human plasmacytoid dendritic cell accumulation amplifies their type 1 interferon production. *Clin Immunol*. 2010;136(1):130-138.
390. Blander JM, Medzhitov R. Toll-dependent selection of microbial antigens for presentation by dendritic cells. *Nature*. 2006;440(7085):808-812.
391. Torchinsky MB, Garaude J, Martin AP, Blander JM. Innate immune recognition of infected apoptotic cells directs T(H)17 cell differentiation. *Nature*. 2009;458(7234):78-82.
392. Pickering MC, Fischer S, Lewis MR, Walport MJ, Botto M, Cook HT. Ultraviolet-radiation-induced keratinocyte apoptosis in C1q-deficient mice. *J Invest Dermatol*. 2001;117(1):52-58.
393. Paidassi H, Tacnet-Delorme P, Lunardi T, Arlaud GJ, Thielens NM, Frachet P. The lectin-like activity of human C1q and its implication in DNA and apoptotic cell recognition. *FEBS Lett*. 2008;582(20):3111-3116.
394. Iparraguirre A, Tobias JW, Hensley SE, et al. Two distinct activation states of plasmacytoid dendritic cells induced by influenza virus and CpG 1826 oligonucleotide. *J Leukoc Biol*. 2008;83(3):610-620.
395. Chung EY, Liu J, Homma Y, et al. Interleukin-10 expression in macrophages during phagocytosis of apoptotic cells is mediated by homeodomain proteins Pbx1 and Prep-1. *Immunity*. 2007;27(6):952-964.
396. Kroemer G, Galluzzi L, Kepp O, Zitvogel L. Immunogenic cell death in cancer therapy. *Annu Rev Immunol*. 2013;31:51-72.

397. Shimada K, Crother TR, Karlin J, et al. Oxidized mitochondrial DNA activates the NLRP3 inflammasome during apoptosis. *Immunity*. 2012;36(3):401-414.
398. Lopez-Lopez L, Nieves-Plaza M, Castro Mdel R, et al. Mitochondrial DNA damage is associated with damage accrual and disease duration in patients with systemic lupus erythematosus. *Lupus*. 2014;23(11):1133-1141.
399. Lee HM, Sugino H, Aoki C, Nishimoto N. Underexpression of mitochondrial-DNA encoded ATP synthesis-related genes and DNA repair genes in systemic lupus erythematosus. *Arthritis Res Ther*. 2011;13(2):R63.
400. Nezis IP, Shravage BV, Sagona AP, Johansen T, Baehrecke EH, Stenmark H. Autophagy as a trigger for cell death: autophagic degradation of inhibitor of apoptosis dBruce controls DNA fragmentation during late oogenesis in Drosophila. *Autophagy*. 2010;6(8):1214-1215.
401. Lan YY, Londono D, Bouley R, Rooney MS, Hacohen N. Dnase2a deficiency uncovers lysosomal clearance of damaged nuclear DNA via autophagy. *Cell Rep*. 2014;9(1):180-192.
402. Napirei M, Karsunky H, Zevnik B, Stephan H, Mannherz HG, Moroy T. Features of systemic lupus erythematosus in Dnase1-deficient mice. *Nature Genetics*. 2000;25(2):177-181.
403. Poon IK, Hulett MD, Parish CR. Molecular mechanisms of late apoptotic/necrotic cell clearance. *Cell Death Differ*. 2010;17(3):381-397.
404. Charles J, Di Domizio J, Salameire D, et al. Characterization of circulating dendritic cells in melanoma: role of CCR6 in plasmacytoid dendritic cell recruitment to the tumor. *J Invest Dermatol*. 2010;130(6):1646-1656.
405. Sisirak V, Faget J, Gobert M, et al. Impaired IFN-alpha production by plasmacytoid dendritic cells favors regulatory T-cell expansion that may contribute to breast cancer progression. *Cancer Res*. 2012;72(20):5188-5197.
406. Labidi-Galy SI, Treilleux I, Goddard-Leon S, et al. Plasmacytoid dendritic cells infiltrating ovarian cancer are associated with poor prognosis. *Oncoimmunology*. 2012;1(3):380-382.
407. Hartmann E, Wollenberg B, Rothenfusser S, et al. Identification and functional analysis of tumor-infiltrating plasmacytoid dendritic cells in head and neck cancer. *Cancer Res*. 2003;63(19):6478-6487.
408. Lombardi VC, Khaiboullina SF, Rizvanov AA. Plasmacytoid dendritic cells, a role in neoplastic prevention and progression. *Eur J Clin Invest*. 2015;45 Suppl 1:1-8.
409. U'Ren L, Guth A, Kamstock D, Dow S. Type I interferons inhibit the generation of tumor-associated macrophages. *Cancer Immunol Immunother*. 2010;59(4):587-598.
410. Zitvogel L, Galluzzi L, Kepp O, Smyth MJ, Kroemer G. Type I interferons in anticancer immunity. *Nat Rev Immunol*. 2015;15(7):405-414.
411. Jensen TO, Schmidt H, Moller HJ, et al. Intratumoral neutrophils and plasmacytoid dendritic cells indicate poor prognosis and are associated with pSTAT3 expression in AJCC stage I/II melanoma. *Cancer*. 2012;118(9):2476-2485.
412. Di Domizio J, Demaria O, Gilliet M. Plasmacytoid dendritic cells in melanoma: can we revert bad into good? *J Invest Dermatol*. 2014;134(7):1797-1800.
413. Lauber K, Herrmann M. Tumor biology: with a little help from my dying friends. *Curr Biol*. 2015;25(5):R198-201.

414. Drobits B, Holcmann M, Amberg N, et al. Imiquimod clears tumors in mice independent of adaptive immunity by converting pDCs into tumor-killing effector cells. *J Clin Invest*. 2012;122(2):575-585.
415. Gungor B, Yagci FC, Tincer G, et al. CpG ODN nanorings induce IFNalpha from plasmacytoid dendritic cells and demonstrate potent vaccine adjuvant activity. *Sci Transl Med*. 2014;6(235):235ra261.
416. Muthana M, Rodrigues S, Chen YY, et al. Macrophage delivery of an oncolytic virus abolishes tumor regrowth and metastasis after chemotherapy or irradiation. *Cancer Res*. 2013;73(2):490-495.
417. Weber C, Noels H. Atherosclerosis: current pathogenesis and therapeutic options. *Nat Med*. 2011;17(11):1410-1422.
418. Tabas I. Macrophage death and defective inflammation resolution in atherosclerosis. *Nat Rev Immunol*. 2010;10(1):36-46.
419. Chinetti-Gbaguidi G, Colin S, Staels B. Macrophage subsets in atherosclerosis. *Nat Rev Cardiol*. 2015;12(1):10-17.
420. Roman MJ, Shanker BA, Davis A, et al. Prevalence and correlates of accelerated atherosclerosis in systemic lupus erythematosus. *N Engl J Med*. 2003;349(25):2399-2406.
421. Bhatia VK, Yun S, Leung V, et al. Complement C1q reduces early atherosclerosis in low-density lipoprotein receptor-deficient mice. *Am J Pathol*. 2007;170(1):416-426.
422. Lewis MJ, Malik TH, Fossati-Jimack L, et al. Distinct roles for complement in glomerulonephritis and atherosclerosis revealed in mice with a combination of lupus and hyperlipidemia. *Arthritis Rheum*. 2012;64(8):2707-2718.
423. Liao X, Sluimer JC, Wang Y, et al. Macrophage autophagy plays a protective role in advanced atherosclerosis. *Cell Metab*. 2012;15(4):545-553.